SYNTHESIS OF NOVEL CONJUGATED POLYMERS AND COPOLYMERS

Matthew Robert Cottle

A dissertation submitted to the faculty of the University of North Carolina at Chapel Hill in partial fulfillment of the requirements for the degree of Doctor of Philosophy in the Department of Chemistry.

Chapel Hill
2008

Approved by

Advisor: Dr. Valerie Sheares Ashby

Reader: Dr. Sergei S. Sheiko

Reader: Dr. Maurice S. Brookhart

Reader: Dr. Wei You

Reader: Dr. Andrew M. Moran

ABSTRACT

MATTHEW R. COTTLE: SYNTHESIS OF NOVEL CONJUGATED POLYMERS AND COPOLYMERS

(Under the direction of Dr. Valerie V. Sheares Ashby)

Conjugated polymers have found many uses as high-strength materials in the automotive and aerospace industries as well as the active components in thin film transistors, light emitting diodes and solar cell devices. There are few pathways to the synthesis of soluble conjugated polymers and side reactions or stringent polymerization conditions are prevalent in many of them. This work describes the synthesis of several conjugated polymers via Ni(0)-catalyzed coupling or Stille coupling. First, poly(2,5-benzophenone) macroinitiators are synthesized via Ni(0)-catalyzed coupling and incorporated, as the middle block, into coil-rod-coil triblock copolymers with poly(lactide). The study of the effects of ligand type, solvent type, reaction temperature, and reaction time in the Ni(0)-catalyzed coupling of 2-benzenesulfonyl-1,4-dichlorobenzene are then presented. Next, the synthesis of poly(paraphenylene) containing a thermally removable solubilizing group is shown. The optical bandgap was shown to decrease as the solubilizing group undergoes two thermolysis steps to afford native poly(paraphenylene). Furthering this work, alternating donor-acceptor polymers are synthesized via Stille coupling that also contain thermally removable solubilizing groups. These materials are characterized by NMR, GPC, DSC, TGA, and UV-vis.

This work is dedicated to my wife Kari for loving, supporting and putting up with me always, and my family, Bob Cottle, Cathy Cottle, Jessica Oliver and Steven Cottle for their constant support. I would also like to thank my colleagues Dr. Jinrong Liu, Dr. Ben Pierce, Dr. Andy Brown, Peter Uthe, Jake Sprague and Sean Hemp for their friendships and advice.

TABLE OF CONTENTS

LIST OF TABLES

Table

LIST OF FIGURES

Figure

LIST OF ABBREVIATIONS

Bipy	2,2'-bipyridyl
DMAc	*N*,*N*-dimethylacetamide
DSC	Dynamic Scanning Calorimetry
EDOT	3,4-ethylenedioxythiophene
GPC	Gel Permeation Chromatography
HDPE	High Density Polyethylene
HOMO	Highest Occupied Molecular Orbital
LUMO	Lowest Unoccupied Molecular Orbital
MDMO-PPV	Poly[2-methoxy-5-(3,7-dimethyloctyloxy)-1,4-phenylen]-*alt*-(vinylene)]
MEH-PPV	Poly[2-methoxy-5-(2'-ethylhexoxy)-1,4-phenylenevinylene
Methoxy bipy	4,4'-dimethoxy-2,2'-bypiridine
Methyl bipy	4,4'-dimethyl-2,2'-dipyridyl
NMR	Nuclear Magnetic Resonance Spectroscopy
P3HT	Poly(3-hexylthiophene)
PBP	Poly(2,5-benzophenone)
PCBM	[6,6]-phenyl-C_{61}-butyric acid methyl ester
PDLLA	Poly(D,L-lactide)
PDTFE	Poly[[1,1'-biphenyl]-4,4'-diyl[2,2,2-trifluoro-1-(tifluoromethyl)ethylidene]]
PEDOT	Poly(3,4-ethylenedioxythiophene)
PLLA	Poly(L-lactide)

PPE	Poly(phenyleneethenylene)
PPP	Poly(paraphenylene)
PPV	Poly(phenylenvinylene)
t-butyl bipy	4,4'-di-*tert*-butyl-2,2'-dipyridyl
THF	Tetrahydrofuran
TGA	Thermogravimetric analysis
TPP	Triphenylphosphine
$Sn(Oct)_2$	Stannous 2-ethylhexanoate
UV-vis	Ultra violet-visible spectroscopy

LIST OF SYMBOLS

EQE	External Quantum Efficiency
I_{SC}	Short Circuit Current
λ_{max}	wavelength of maximum absorption
$<M_n>$	Number average molecular weight
PDI	Polydispersity Index
T_g	Glass transition temperature
V_{OC}	Open Circuit Voltage

Chapter 1

LITERATURE REVIEW OF CURRENT ADVANCES IN NI(0)-CATALYZED COUPLING POLYMERIZATIONS AND CONJUGATED POLYMERS FOR SOLAR CELLS

1.1 High Performance Polymers

The synthesis of high performance polymers continues to receive much interest as the demand for polymers with outstanding physical, chemical, and electrical properties grows. High performance polymers have found increasing use in the automotive, aerospace, construction, and electronics industries. For high strength applications such as airplane bodies, polymers have a higher strength to weight ratio than their metallic counterparts. In the electronics industry, plastics are much easier and cheaper to process into working devices than are the high purity metals that must be used. The synthesis and development of new polymeric materials remains an industrially and scientifically important process. The ability to understand the structure-property relationship of polymer systems allows polymer chemists to tailor materials for specific applications. Two avenues for the development of new polymeric materials are the synthesis of copolymers and the synthesis of novel polymers.

The simple blending of two polymers to achieve a novel material can be hampered by polymer-polymer immiscibility. Most polymers are immiscible in other polymers and, when blended, will tend to completely phase separate due to insignificant enthalpies of mixing and small entropies of mixing. This limitation can be overcome through the synthesis of copolymers. Copolymers can be synthesized in a variety of ways and result in an assortment of copolymer architectures including random, alternating, tapered, block, and graft (**Figure 1)**. Phase separation does not occur with random or alternating copolymers, but is a factor with the others. The polymer segments can no longer totally phase separate due to the covalent bonding between the polymer segments. The result is microphase separation that is controlled by the volume fraction of the components, molecular weight of the segments, and

degree of phase separation (χ). These factors result in an array of morphologies that, with increasing volume fraction of one component, follow the pattern of spheroids, cylinders, lamellae, inverse cylinders, and inverse spheroids. Other, less common, morphologies can be achieved through the synthesis of special rod-coil copolymers such as zigzags, arrowheads, and mushrooms.[1]

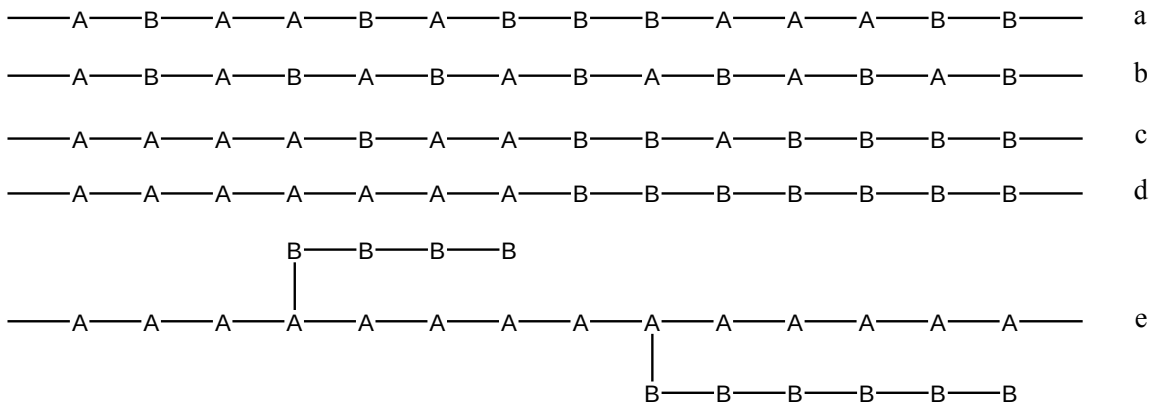

Figure 1.1 Copolymer architectures, a) random b) alternating c) tapered d) block e) graft.

Another method for tailoring material properties is the design and synthesis of novel polymers. Seemingly slight changes to a polymer structure can lead to vast property differences. For example, high-density polyethylene (HDPE) and poly(tetrafluoroethylene) (commonly known as Teflon®) are both made from analogous monomers but exhibit stark differences in their properties. Both polymers are tough, semicrystalline polymers but, because of the fluorine functionality, Teflon® has a very low dielectric constant, surface energy and coefficient of friction while also possessing good thermal properties. Teflon is used as a non-stick coating on cookware while HDPE has poorer thermal stability and is used primarily as an impact resistant material.

The understanding of polymer structure-property relationships has led to the advancement of high-performance polymers and, in particular, poly(*p*-phenylene)s (PPP)s.

Poly(*p*-phenylene) has remarkable thermal stability, mechanical properties, and can be conductive if doped. PPP's have been considered for use in composites, lubricant additives, and thermoset precursors for high-performance aerospace material applications. A major challenge with PPP synthesis is that the polymer has poor solubility in organic solvents due to its rigid backbone, which causes it to precipitate from solution during polymerization resulting in low molecular weight material. Lateral substitution has been used to increase solubility of PPPs. The most successful methods of PPP synthesis have been the Suzuki[2] and the Colon[3] methods, both of which use transition metal catalysts (**Scheme 1**). The pendant aliphatic chain, in the Suzuki method, increases the solubility of the polymer but decreases the mechanical and thermal properties.

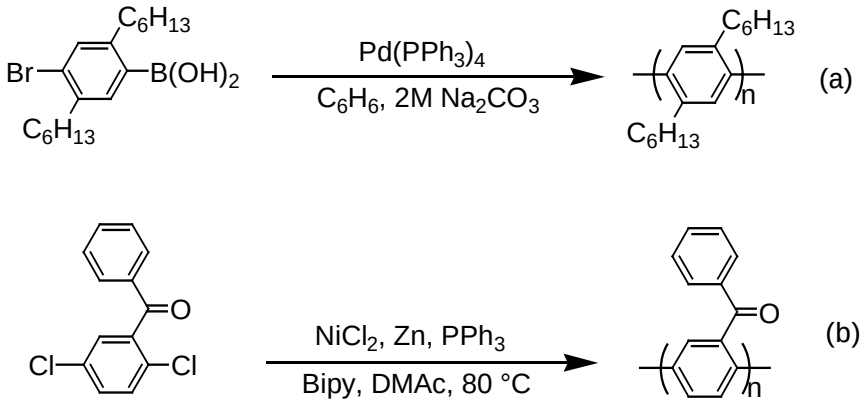

Scheme 1.1 Synthesis of PPP via a) the Suzuki method and b) the Colon Method

1.2 Ni(0)-Catalyzed Coupling Polymerizaton

In 1985, researchers at Union Carbide developed a process for coupling aryl chlorides by nickel and reducing metals.[1] Colon and Kelsey were able to show these reactions to proceed quickly and in very high yields under mild conditions in the presence of catalytic nickel reagent (generated *in situ*) and excess reducing metal (zinc, magnesium or

manganese). This method of synthesizing carbon-carbon aryl bonds is attractive due to the ability to use catalytic amounts of air-stable nickel(II) reagent and the ability to use aryl chlorides instead of the more expensive aryl bromide and iodide analogues. This chemistry is also very tolerant of functional groups, excluding nitro groups and acidic substituents.

Expanding the scope of the Colon method to aryl dichlorides allows for the synthesis of various polyphenylenes. Poly(*p*-phenylene) (PPP) exhibits remarkable thermal stability and have been considered for uses in numerous materials including composites, lubricant additives and thermoset precursors for high-performance aerospace material applications.

PX-1000™, poly(benzoyl-1,4-phenylene), created by Maxdem Inc. is a transparent, amorphous polymer that showed very unique properties including an unprecedented isotropic tensile modulus of over 10 GPa.[2] PX-1000 could also be injection molded and solvent cast into strong films. PX-1000 is harder than any other unfilled thermoplastic and has comparable yield strength to high-grade aluminum. The materials had $<M_n>$ = 14.0-18.0 x 10^3 g/mol and a T_g of 140-150 °C.

Phillips employed Ni(0)-coupling to polymerize isomeric dichlrobenzophenones.[3] To synthesize poly(4,4'-dichlorobenzophenone) an imine-functionalized dichloride monomer was synthesized by the treatment of 4,4'-dichlorobenzophenone with aniline. Post-polymerization hydrolysis of the amorphous material led to a completely insoluble material presumably due to high levels of crystallinity. The 5% weight loss temperatures in air and nitrogen were 510 and 560 °C, respectively. Changing the monomer to 2,5-dichlorobenzophenone led to the synthesis of a substituted PPP that was totally amorphous and soluble common organic solvents. The reaction proceeded to high conversion with a

$<M_n>$ of 26.7 x 10^3 g/mol, a T_g = 206 °C and 5% weight loss temperatures in air and in nitrogen of 496 and 495 °C, respectively.

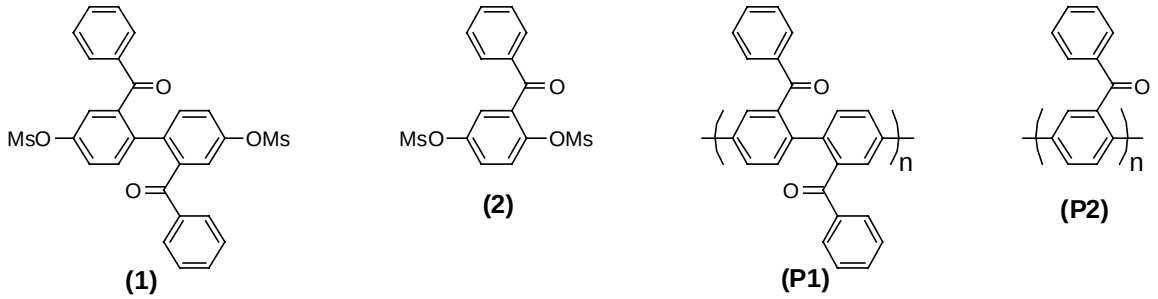

Figure 1.2. Monomers (1 and 2) and polymers (P1 and P2) used to study effects of regioregularity on ultimate polymer properties.

Percec *et. al.* studied the effects of regioregularity on the properties of PPPs synthesized from arylene bismesylates via Ni(0)-coupling polymerization (**Figure 2**).[4] HH-TT regioregular PPPs (**P1**) were synthesized from the polymerization of 2,2'-disubstituted 4,4'-bis[(methylsulfonyl)oxy]biphenyl. This monomer has no *ortho* substituents and was expected to participate in the Ni(0)-catalyzed homocoupling reaction more rapidly and with fewer side reactions than the corresponding polymerization of 2,5-bis[(methylsulfonyl)oxy]benzophenone (**P2**). The regioregularity of **P1** resulted in insoluble crystalline PPPs. Adding a 4-*tert*-butylbenzoyl substituent broke up the crystallinity and resulted in and amorphous and soluble material (**P3**) that resulted in a higher $<M_n>$ than **P2**. This result showed that the Ni(0)-catalyzed homocoupling of **1** was more efficient than **2**, but the solubility of the resulting PPP controls the $<M_n>$. Copolymerization of **1** and **2** resulted in PPPs of significantly higher molecular weight than that of the homopolymers. The highest $<M_n>$ was achieved with a 1:1 of **1** and **2** because the number of reactions involving *ortho* substituents was reduced while enough regioirregularity was introduced to keep the polymer amorphous and soluble.

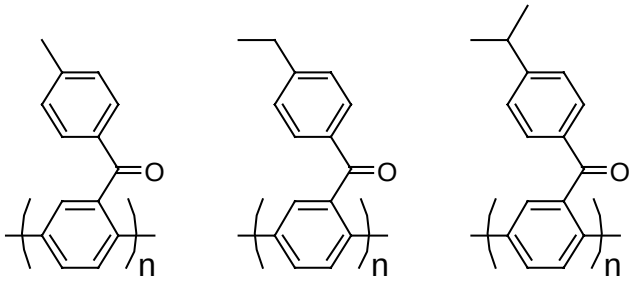

(P3) **(P4)** **(P5)**

Figure 1.3. Alkyl substituted poly(2,5-benzophenone)s

A series of alkyl-substituted 2,5-dichlorobenzophenones were polymerized via Ni(0)-coupling polymerization and blended in attempts to control the thermal properties of the blends (**Figure 3**).[5] Three poly(2,5-benzophenone) analogues were synthesized with methyl, ethyl, or isopropyl groups substituted at the 4'-position with T_g's of 223, 173 and 208 °C, respectively. Equimolar blends were made of **P4**, **P5** and **P6**. The T_g of the **P4-P5** blend was 198 °C, the **P4-P6** blend was 217 °C and the **P5-P6** was 191 °C. The polymers showed good miscibility with one another and the **P4-P5** has the potential to tune the glass transition temperature over a 50 °C range.

Wang and Sheares attempted to extend the Ni(0)-coupling methodology to the synthesis of polythiophene based materials with the synthesis of 3-benzoyl-2,5-dichlorothiophene and its *para*-substituted analogues.[6] A $<M_n>$ range of 0.8-1.7 x 10^5 g/mol was achieved for these polymers with T_g's ranging from 137-167 °C. The resulting polymers were soluble in common organic solvents and showed good thermal stability with 10% weight loss greater than 400 °C and showed ultraviolet absorption maxima of approximately 470 nm.

Poly[[1,1'-biphenyl]-4,4'-diyl[2,2,2-trifluoro-1-(trifluoromethyl)ethylidene]] (PDTFE) is another high-performance polymer that utilized Ni(0)-coupling polymerization.[7]

The introduction of the fluorinated isopropylidene linkage acted to breakup any crystallinity in the polymer as well as impart good thermal properties, a low dielectric constant, low moisture absorption, and excellent flame retardance. The reaction proceeded in high yield with an $<M_n>$ of 19.2 x 10^3 g/mol, a T_g of 255 °C, and 5% weight loss of 515 °C. PDTFE showed very high gas permeability for an aromatic, glassy polymer and good selectivity for O_2/N_2 and CO_2/CH_4 gas pairs.

An easily functionalizable PPP derivative was synthesized from 4'-fluoro-2,5-dichlorodiphenyl sulfone.[8] This method took advantage of the fact that aromatic fluorides are unreactive to this method of Ni(0)-coupling. This method resulted in polymers with pendant aryl fluorides that can be displaced via nucleophilic aromatic substitution in post-polymerization reactions. A variety of nucleophiles were substituted onto the polymer backbones resulting in a wide variety of glass transition temperatures. Poly(ethylene oxide) and poly(arylene ether ketone) were also substituted onto the poly(2,5-diphenyl sulfone) to make highly branched copolymers. Crosslinked PPPs were synthesized by using a multifunctional nucleophile that resulted in an insoluble material with low solvent uptake and a T_g = 240 °C.

Expanding on the use of fluorine containing monomers as reactive sites in post-polymerization nucleophilic aromatic substitutions Bloom and Sheares developed a new methodology for synthesizing PPP macromonomers and multiblock copolymers.[9] Using 4-chloro-4'-fluorobenzophenone as an end-capping agent for the polymerization of 4-methyl-2,5-dichlorobenzophenone, macromonomers were synthesized with $<M_n>$ ranging from 1.58 x 10^3 with 0.25 mol fraction of end-capping agent to 3.96 x 10^3 with a 0.05 mol fraction of end-capping agent. The fluorine functionalized macromonomer ($<M_n>$ = 1.91 x 10^3) was

then reacted with a dihydroxy-terminated poly(arylene ether ketone) ($<M_n> = 4.50 \times 10^3$) via nucleophilic aromatic substitution to afford a multiblock copolymer ($<M_n> = 19.5 \times 10^3$). The resulting copolymer, unlike the macromonomers, formed transparent, flexible films that could be creased.

Following the macromonomer approach to block copolymers, coil-rod-coil triblock copolymers were synthesized with poly(2,5-benzophenone) as the rod block and polystyrene as the coil blocks.[10] Poly(2,5-benzophenone) macroinitiators were synthesized utilizing 4-chloro-4'-isopropylbenzophenone as an end-capping agent. Phase transfer chlorination was used to chlorinate the chain ends, creating initiation sites for the atom transfer radical polymerization of styrene. Macroinitiators from $<M_n>$ of 1.7 – 3.3 x 10^3 g/mol were synthesized. Triblocks ranged from a $<M_n>$ of 7.9 - 42.0 x 10^3 g/mol with PDI's all below 2.0. Triblocks with a rod volume fraction smaller than 10% produced a morphology of uniformly sized poly(2,5-benzophenone) spheroids in a polystyrene matrix.

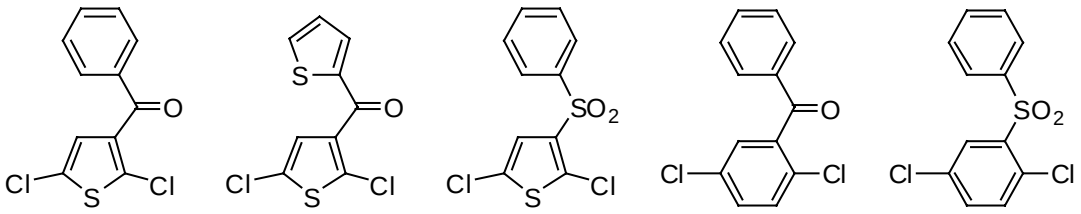

Figure 1.4. Monomers used to study the effects of thiophene and sulfone units on Ni(0)-coupling polymerizations.

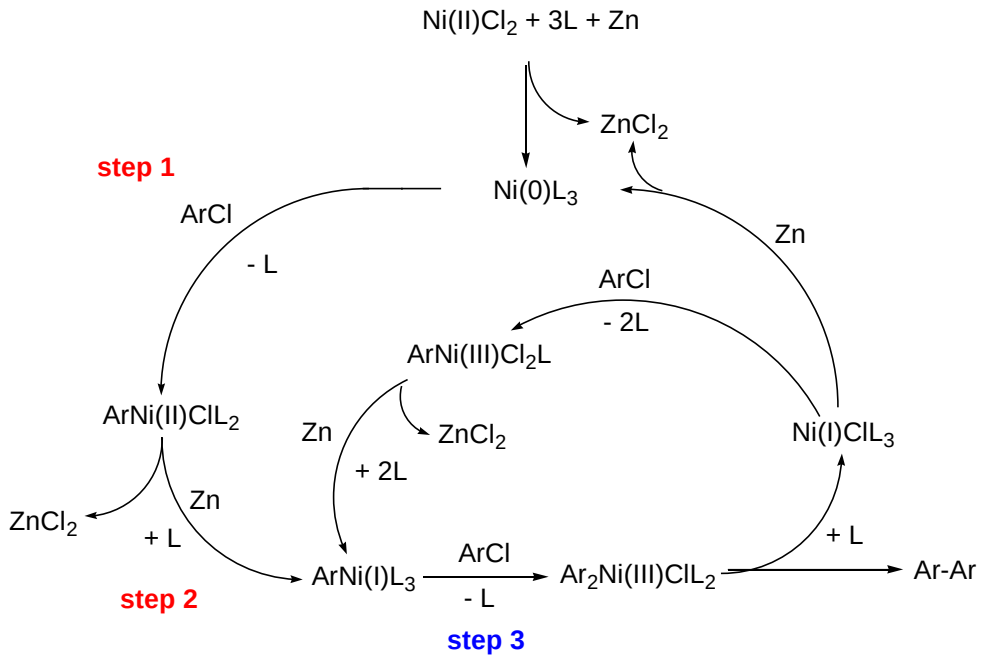

Scheme 1.2. Proposed Ni(0)-catalyzed coupling catalytic cycle.

Work studying the effects of solvent and monomer structure on Ni(0)-coupling polymerization showed dramatic effects on the catalyst system and final polymer.[11] Studying the polymerization of monomers in **Figure 4**, reactions run in *N*,*N*-dimethylacetamide (DMAc) resulted in side reactions, such as degradation of the thiophene polymers and reduction of the carbonyl groups. Using tetrahydrofuran (THF) as the solvent for the polymerizations of monomers **4** and **6** resulting in high molecular weight polymers with no observed side reactions. Reactions with monomers containing a sulfone (**5** and **7**) resulted in oligomeric materials. It was reasoned from these results that in Ni(0)-catalyzed polymerization there is a window of electron-withdrawing ability that meet the criteria to accelerate the reaction. Carbonyl-containing pendant groups meet these criteria whereas

sulfone-containing pendant groups have an increased electron-withdrawing ability and slow the reaction due to deactivation of the $ArNi(I)L_3$ reactive intermediate for oxidative addition.

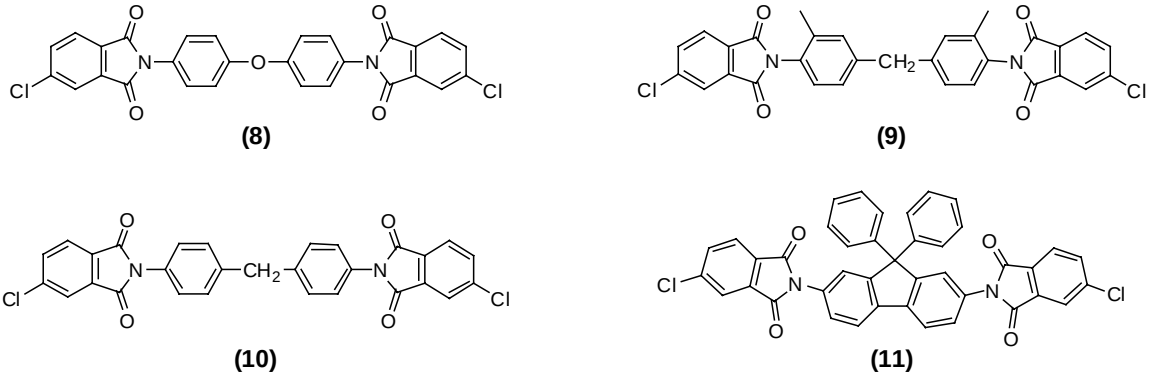

Figure 1.5. Imide containing aromatic chlorides for the synthesis of copoly(phenylene-imide)s.

Copoly(phenylene-imide)s have also been synthesized via Ni(0)-coupling polymerization of aromatic dichlorides containing imide structure and 2,5-dichlorobenzophenone (**Figure 5**).[12] Homopolymerization of **8** led only to oligomeric material, introduction of 2,5-dichlorobenzophenone as a copolymer led to higher molecular weight polymers due to the bulky lateral group imparting better solubility into the copolymer. Copolymers were synthesized combining each monomer (**8-10**) with an equimolar amount of 2,5-dichlorobenzophenone. Two copolymers of **9** with 20 mole % and 90 mole % of 2,5-dichlorobenzophenone were also synthesized. All copolymers except the one containing monomer **10** formed solvent cast films with enough mechanical integrity to be tested using a dynamic mechanical thermal analyzer. Glass-transition temperatures ranged from 209 °C – 319 °C with tensile moduli ranging from 1.6 – 3.6 GPa and 10% weight-loss temperatures exceeded 500 °C for all copolymers.

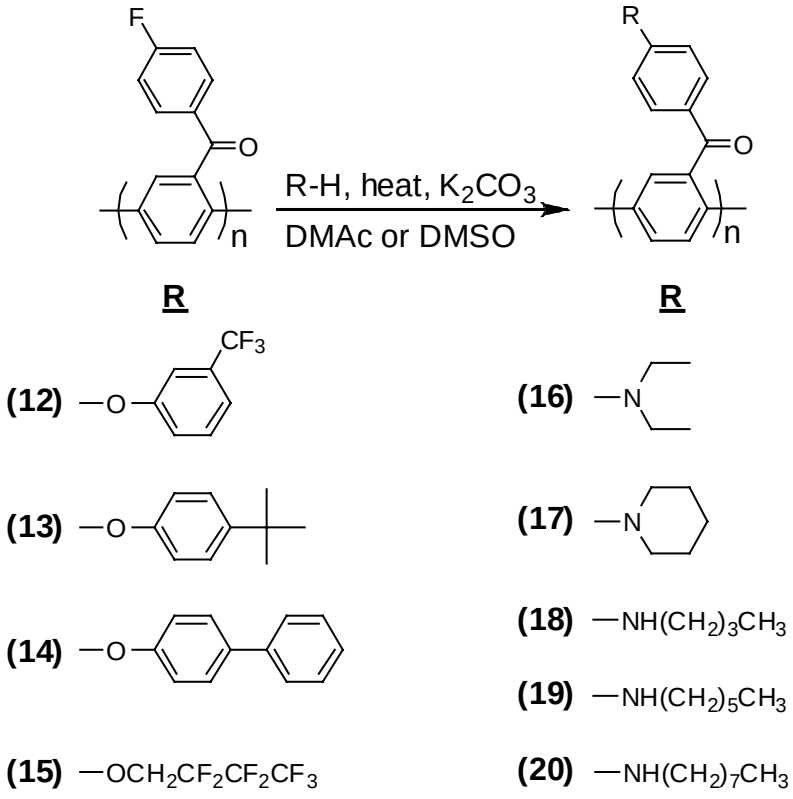

Scheme 1.3. Nucleophilic aromatic substitution of poly(4'-fluoro-2,5-benzophenone) with various nucleophiles

Expanding on previous work,[8] Bloom developed a method for facile synthesis of functionalized poly(2,5-benzophenone)s using poly(4'-fluoro-2,5-benzophenone) as a substrate for nucleophilic aromatic substitution (**Scheme 3**).[13] Using an identical precursor ($<M_n>$ = 1.66 x 10^4), nine different substituted poly(2,5-benzophenone)s were synthesized. All substitutions proceeded in high yield, with the lowest being 74% substitution for diethylamine due to the inability to run the reaction at high temperature due to the low boiling point of diethylamine. The unsubstituted material had a T_g = 167 °C and the substituted polymers had T_g's ranging from 123 – 225 °C for polymers **12** and **17**, respectively. All materials except for **15** were amorphous polymers. **12-14** formed flexible, transparent films while **15** and all the amine-substituted derivatives produced brittle films.

The previous sections described the current state of Ni(0)-catalyzed coupling polymerizations used to synthesize soluble, functionalized PPP derivatives. Although many quality materials have demonstrated good mechanical strength and thermal stability, there are areas that still need to be addressed. Namely, the synthesis of PPP derivatives that can be cast into tough films or molded materials as well as further elucidation of the limitations of this polymerization technique with regards to monomer structure.

1.3 Conjugated Polymers

1.3.1 Theory

Initially it was thought that π-bonding in a conjugated polymer, like polyacetylene, would produce bonds of equal length. Thus, the p_z orbital of each carbon would overlap equally with both of its neighbors, resulting in a π-electron wavefunction extending over the whole polymer chain. Therefore, a chain of polyacetylene with N carbon atoms has N closely spaced energy levels. The Pauli exclusion principal allows each level to take two electrons of opposite spin so that only the bottom N/2 energy levels are occupied. Therefore it appears, in theory, that polyacetylene has a half-filled band and should behave as a metal. In reality, Peierl's distortion, or bond alternation, occurs and this alternation of bond lengths lowers the energy level of the HOMO and raises the energy level of the LUMO creating an energy gap in the electron density of states (**Figures 1 and 2**). The presence of this energy gap turns polyacetylene, and other conjugated polymers, into semiconductors.

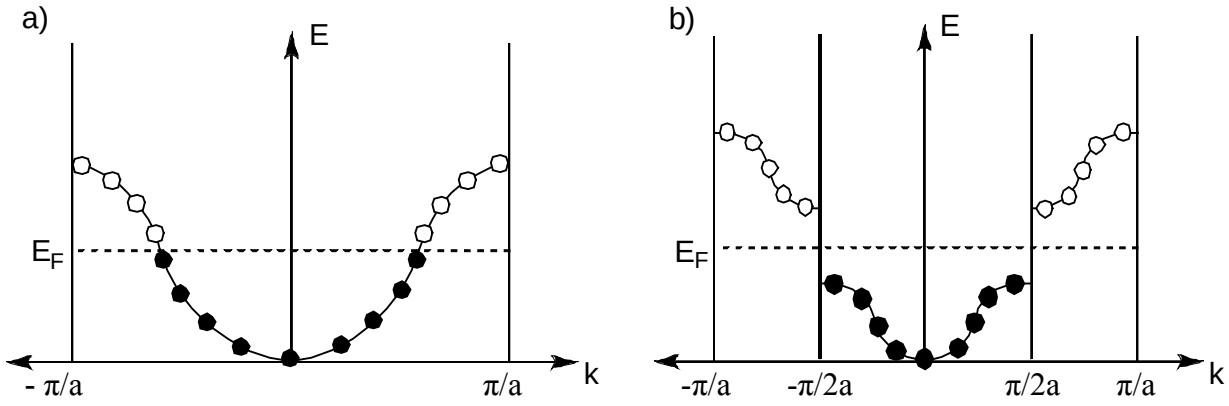

Figure 1.6. Energy diagram of theoretical (left) and actual (right) energy levels for polyacetylene. The bandgap appears due to bond alternation along the backbone of the conjugated polymer

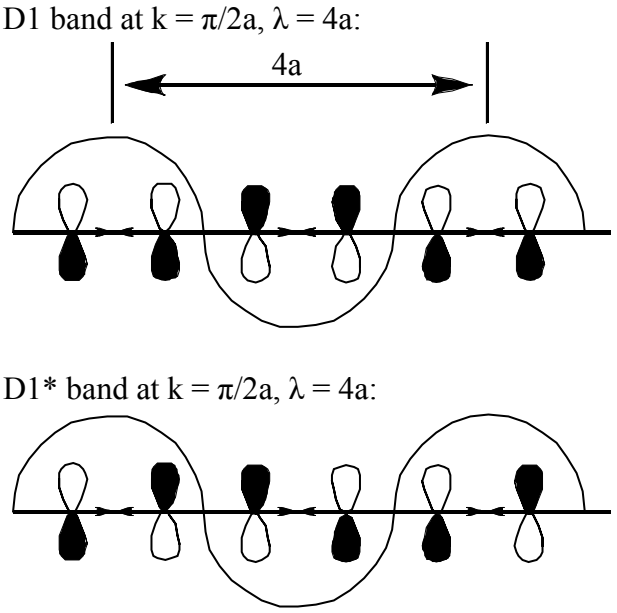

Figure 1.7. Representation of the effect of Pierl's distortion on D1 (top) and D1* (bottom) energy bands. In the D1 band (top) the bonding orbitals are brought closer together and the anti-bonding orbitals are separated lowering the energy. In the D1* band (bottom) the anti-bonding orbitals are brought closer together and the bonding orbitals are separated increasing the energy

1.3.2 Solar Cells

The unique ability of these organic materials to act as semiconductors has led to intensive research into a number of applications including organic thin film transistors, organic light emitting diodes, and organic solar cells.[14-16] Organic solar cells are of extreme interest due to the anticipated future problems associated with energy supply, energy security, and high levels of atmospheric CO_2. Current global energy consumption is about 13 TW per year with a projected rise to around 28 TW per year by 2050.

One promising strategy to meet growing energy demands is taking advantage of solar energy. Current commercial solar cell technology is based on inorganic silicon solar cells. These solar panels operate at 12% efficiency and cost around $\$350/m^2$. This results in an average cost of \$0.20/kW-hr for electricity produced by a solar cell versus \$0.06/kW-hr provided by grid electricity. Solar cells have a lifetime of approximately 30 years. Since solar cells use no fuel, the primary investment is capital cost. Increasing the efficiency of the solar cell would directly impact the overall electricity cost, because higher-efficiency cells will produce more electrical energy per unit of cell area over the cell lifetime. Another way to decrease the cost of solar electricity is by decreasing the manufacturing cost of solar cells. Manufacturing costs for solar cells have historically followed what is termed an "80% learning curve." That is to say, for every doubling in solar cell production, manufacturing costs decrease by 20%. The emergence of polymeric solar cells could greatly reduce the manufacturing cost of these systems. Most solar cells are produced using vapor deposition of silicon, which is an expensive and wasteful process. Polymeric systems allow manufacturers to take advantage of spin coating and solution-casting technologies that are low cost and simple compared to the current methods.

1.3.3 Device Architectures

Organic photovoltaic cells were first designed 22 years ago (**Figure 3**).[17] During the mid-1990s a 2.9% -efficient solar cell was produced using a bulk heterojunction approach with a semi-conductive polymer donor matrix and a C_{60} based acceptor (**Figure 4**).[18] Over the next decade, improvements in materials, device engineering, and better understanding of the underlying physics have produced solar cells with efficiency greater than 5%.

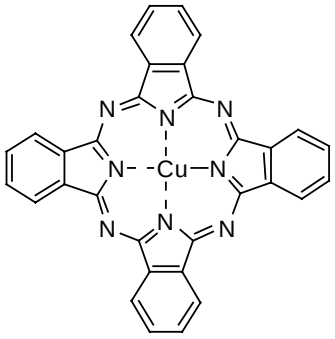

Copper Pthalocyanine

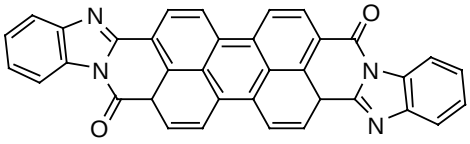

Perylene Tetracaroxylic Derivative

Figure 1.8. Materials used in the first bilayer organic solar cell

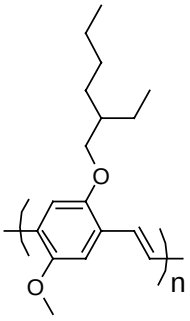

MEH-PPV

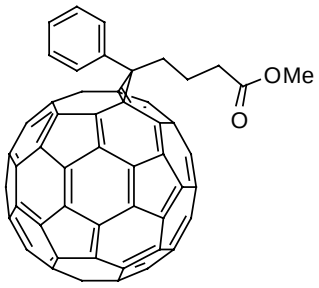

PCBM

Figure 1.9. Materials used to produce bulk heterojunction solar cells (MEH-PPV = poly[2-methoxy-5-(2'-ethylhexoxy)-1,4-phenylenevinylene], PCBM = [6,6]-phenyl-C_{61} butyric acid methyl ester)

There are a number of strategies for producing organic solar cells. Single layer semiconductor organic solar cells are the most basic devices. These consist of a single organic semiconductor layer sandwiched between the two electrodes. These devices were

improved upon with the introduction of bilayer solar cells. In a bilayer device there is an electron-donor layer, usually a semiconducting polymer, and an electron-accepting layer, usually a metal oxide, small molecule, or a semiconducting polymer. Bilayer devices are able to effectively split electron-hole exciton pairs at the interface of the two layers as well as use the differing bandgaps of the two layers to absorb a broader range of light. Due to the fact that most semiconducting polymers have a bandgap around 2.0 eV, the layers must be ~100-200 nm thick to effectively absorb photons. Unfortunately, the diffusion length of excitons in most polymers is only ~20 nm. This means that excitons formed more than 20 nm from the interface usually never make it to the interface and, instead of undergoing electron transfer, recombine.

Bulk-heterojunction devices are designed to greatly increase the interfacial area between the donor and acceptor materials. The state-of-the-art in this field is based on donor polymers blended with the electron accepting fullerene derivative [6,6]-phenyl-C61-butyric acid methyl ester (PCBM). Fullerenes are the best currently available acceptor material for photovoltaic devices due to their high electron affinity and superior ability to transport charge.

1.3.4 Optimizaton

In order to optimize the performance of organic solar cells, it is imperative to understand the four fundamental steps in which light energy is converted into electrical energy in these devices: 1) absorption of light and generation of excitons, 2) diffusion of the excitons, 3) dissociation of the excitons with generation of charge, and 4) charge transport and collection (**Scheme 1**).[19] The active layer donor-acceptor interaction controls all aspects of this mechanism. Also, the open circuit voltage (V_{oc}) is governed by the energetic

relationship between the donor and the acceptor. The energy difference between the HOMO of the donor and the LUMO of the acceptor has been found to correlate closely with the V_{oc} value.[20,21]

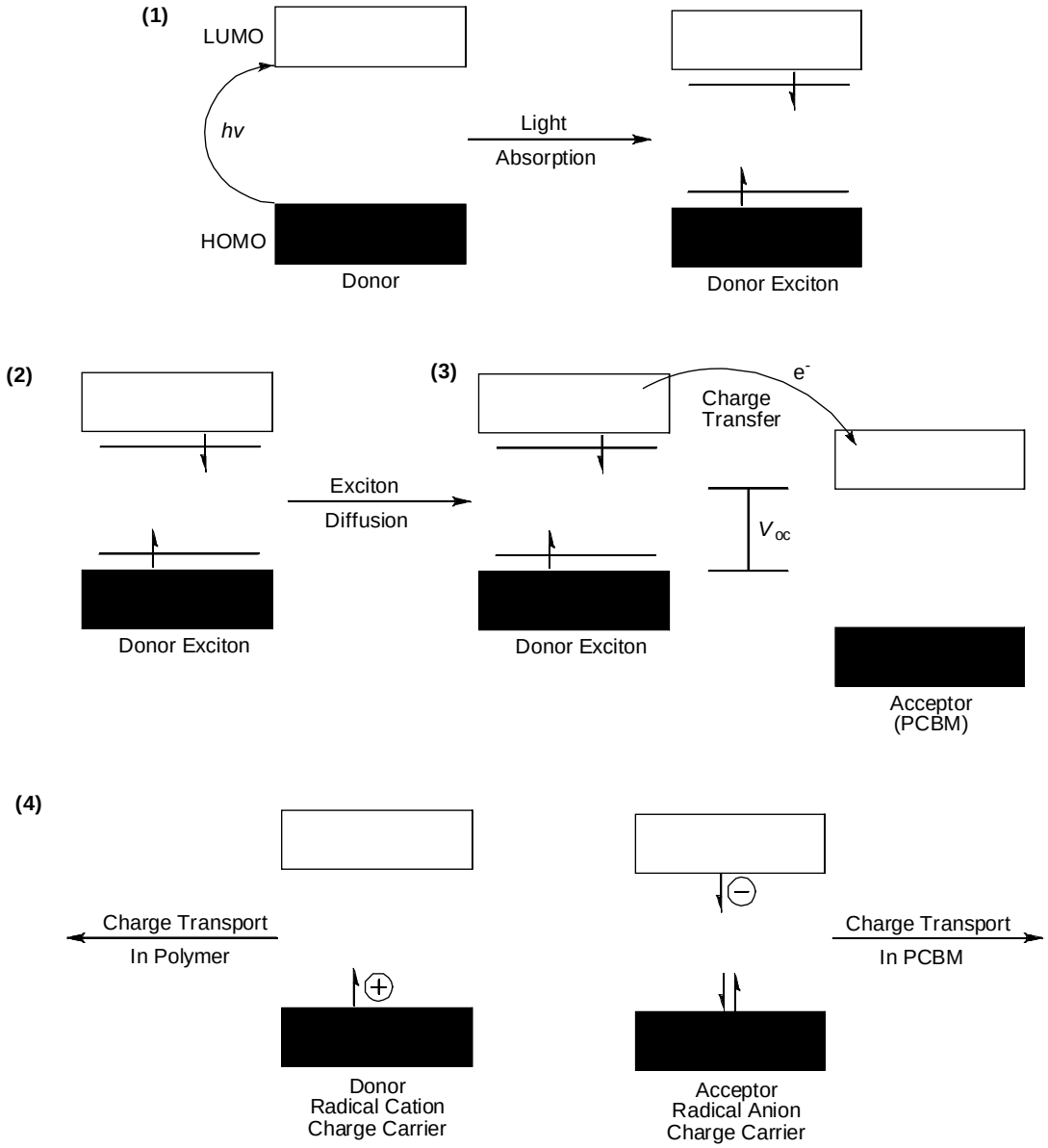

Scheme 1.4. General mechanism for photoenergy conversion in excitonic solar cells

Optimizing polymer-fullerene solar cells is based on fine-tuning the electronic properties and interactions of the donor and acceptor components with the goal to absorb the most light and generate the greatest number of free charges with minimal concomitant loss of

energy, and transport the charges to the respective electrodes at a maximum rate and with a minimum of recombination.[22] Fullerenes are considered to be ideal acceptors for organic solar cells because they have a deep-lying LUMO imparting a high electron affinity,[23] they can be reversibly reduced with up to six electrons,[24] and they have shown very high electron mobility.[25]

If fullerenes are to be used as the acceptor material, then the donor material must be tuned for maximum compatibility. A downhill energetic driving force is necessary for the charge transfer process to be favorable and the driving force must exceed the exciton binding energy (typically estimated to be 0.4-0.5 eV).[26] The overall energetic driving force for an electron transfer from the donor to the acceptor is represented by the difference between the LUMOs of the donor and acceptor. It has been shown that a minimum energy difference of 0.3 eV is required to effectively cause exciton splitting and charge dissociation.[27] PCBM has been the most commonly used soluble fullerene derivative and has a LUMO of 4.2 eV. Therefore, the ideal polymeric donor would have a LUMO around 3.9 eV.

The HOMO of the donor polymer must also be considered. The desired HOMO level is determined by taking into consideration the bandgap of the polymer, which controls the absorption of light and impacts the V_{oc}. Lowering the HOMO level increases the bandgap of the polymer. The maximum theoretical V_{oc} increases with an increasing bandgap, but the larger the bandgap, the poorer the spectral overlap with the photon flux from the sun. The photon flux from the sun has a maximum at 1.8 eV (~ 700 nm). A bandgap of 1.5 eV is an optimal value for a polymer absorber.[28] This would give an ideal HOMO energy of 5.4 eV and a V_{oc} of 1.2 V. The optimal bandgap value was determined through a detailed analysis that balances the attainable V_{oc} and the donor bandgap.[29]

The morphology of bulk-heterojunction devices is an extremely important factor in device performance and extensive studies have been conducted on solvent effects, thermal annealing, molecular weight, regioregularity, and polymer:PCBM ratio but goes beyond the scope of this review.

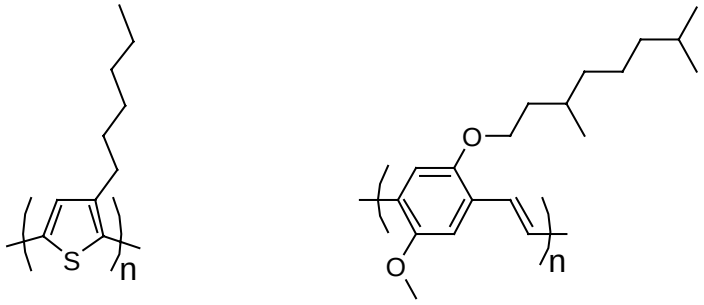

P3HT **MDMO-PPV**

Figure 1.10. Poly(3-hexylthiophene) (P3HT) and poly[2-methoxy-5-(3,7-dimethyloctyloxy)-1,4-phenylen]-*alt*-(vinylene)] (MDMO-PPV)

Poly(3-hexylthiophene) (P3HT) and poly[2-methoxy-5-(3,7-dimethyloctyloxy)-1,4-phenylen]-*alt*-(vinylene)] (MDMO-PPV) are the two most commonly used donor polymers (**Figure 5**). While much information has been gleaned from these systems, neither MDMO-PPV (E_g = 2.2 eV) nor P3HT (E_g = 1.9 eV) can effectively harvest photons from the solar spectrum, and they do not match up efficiently with the bandgap of PCBM (**Figure 6**). It is calculated that P3HT is only capable of absorbing 46% of the available solar photons.[28] New materials are needed that extend the overlap with the solar spectrum while retaining high absorption coefficients and suitable energy levels for interaction with PCBM.

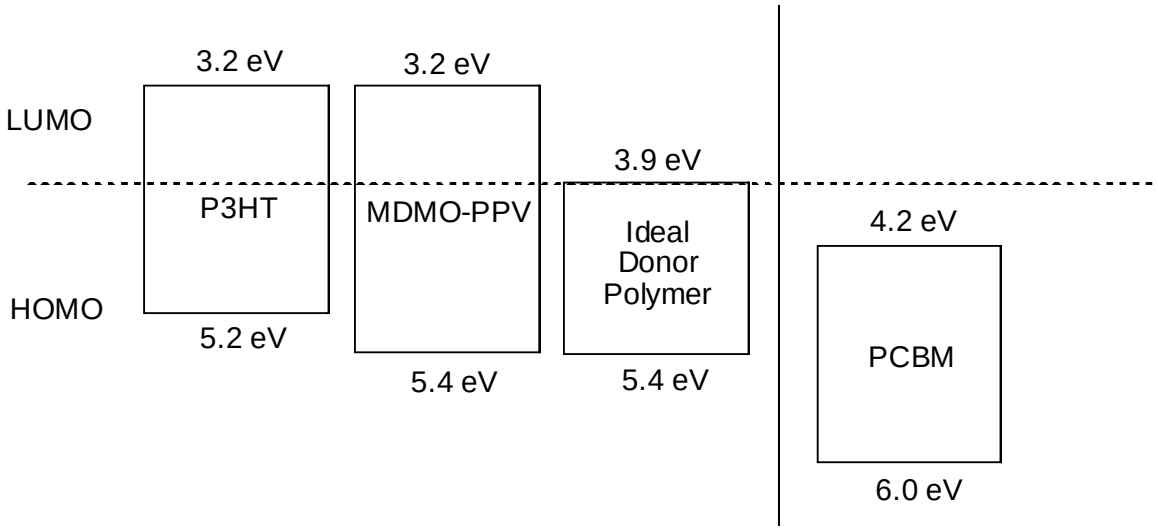

Figure 1.11. Band structure diagram comparing the HOMO and LUMO energies of P3HT, MDMO-PPV, and an ideal donor relative to the band structure of PCBM

1.3.5 Donor-Acceptor Low-Bandgap Polymers

The most common approach to increasing the spectral breadth of absorbed photons is the use of low-bandgap polymers.[30] Low-bandgap polymers are generally considered to be any polymer that has a bandgap less than that of P3HT (< 1.9 eV). The alternating donor-acceptor approach is the most popular technique for synthesizing low-bandgap polymers.[31]

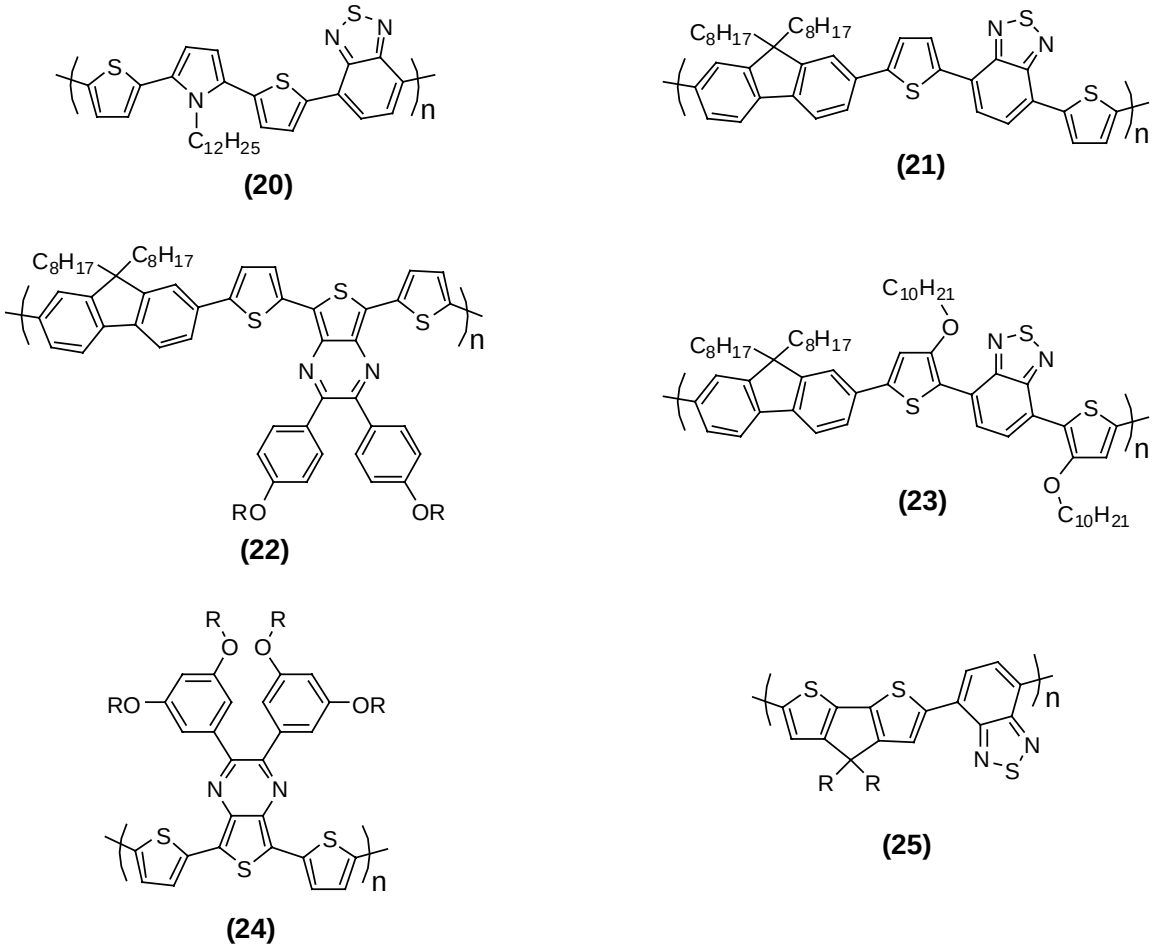

Figure 1.12. Alternating donor-accepter low-bandgap polymers utilizing benzothiadiazole (or analogues)

Polymers utilizing benzothiadiazole (or analogues) as the acceptor have shown promising results (**Figure 7**). Polymer **20** showed a bandgap around 1.6 eV.[27] When blended with PCBM in a 1:3 polymer to PCBM ratio, an efficiency of 1 % was achieved. These devices were able to extend the photocurrent out to nearly 800 nm but the blends gave external quantum efficiency (EQE) values, the ratio (in %) of electrons harvested to incident photons at a single wavelength) of only 20 % at the λ_{max} value of 550 nm.

Polymer **21** introduces the popular dialkylfluorene donor monomer to afford poly[{2,7-(9,9-dialkylfluorene)}-*alt*-{5,5-(2,4-di-2'-thienyl-2,1,3-benzothiadiazole)}].[32]

Efficiencies as high as 2.8% were achieved with EQE values greater than 50% in the 350-600 nm range. The bandgap is still approximately 1.9 eV, so the high performance cannot be solely attributed to an increase in absorption.

A variation of polymer **21** is APFO-Green 5 (polymer **22**). A much stronger acceptor thienopyrazine lowers the bandgap to 1.6 eV.[33] Efficiencies of 2.2% were measured in 1:3 blends with PCBM, and EQE values of 40 % were measured at 700 nm. The V_{oc} is lowered due to the smaller bandgap to 0.6 V from 1.0 V for polymer **2**.

Polymer **23** uses electron-rich 3-alkoxythiophene units to create stronger donor-acceptor interactions than polymer **21**. This affords a lower bandgap of 1.78 eV and efficiencies of 1.6 % for 1:4 blends with PCBM.[34] This polymer exemplifies how a seemingly small change in polymer structure can have a major effect on the bandgap of the polymer system.

The lowest bandgap polymer, to date, that has an efficiency of more than 1% also takes advantage of a thienopyrazine unit (polymer **24**).[35] Wienk *et. al.* reported this polymer to have a bandgap of 1.2 eV and manufactured devices that operated at about 1.1% efficiency in 1:4 blends with PCBM. More importantly, the authors were able to achieve a 0.7 eV reduction in bandgap relative to P3HT while only reducing the V_{oc} value by 0.05 V by carefully engineering the HOMO and LUMO levels of the polymer.

Polymer **25** has proven to be the most efficient low-bandgap polymer to date. Its bandgap was measured to be 1.45 eV and devices made of a 1:1 blend with PCBM showed efficiencies of 2.7% and V_{oc} of 0.65 V.[28,36] Using a C_{70} PCBM derivative resulted in efficiencies as high as 3.5% due mainly to the greater absorbance of C_{70} relative to C_{60}.

1.3.6 Stability

It has been shown that many good candidates for the donor material in polymer:PCBM bulk-heterojunction devices have utilized the thienopyrazine moiety. When considering the use of solar cell technology as a replacement for current power supplies and inorganic-based solar cells, one must take into consideration the longevity of these devices. The photodegradation of copolymers and oligomers containing thienopyrazine has been recently studied.[37] The thienopyrazine moiety was found to rapidly photodegrade upon UV irradiation in air. This degradation led to undesirable changes in the absorption, photoluminescence, and electroluminescence. NMR and FTIR studies show a break down of the C=N bonds in the thienopyrazine ring to form secondary amines. The intramolecular charge transfer absorption band at ~550 nm is completely quenched after 1 h of irradiation at 365 nm showing that the thienopyrazine moiety might not be suitable for stable and durable photovoltaic devices.

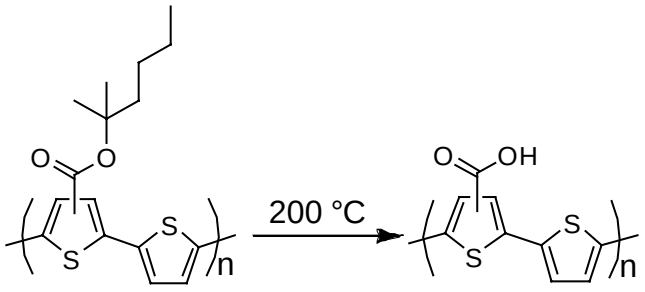

Scheme 1.5. Thermal cleavage of tertiary ester bearing polythiophene

Liu *et. al.* synthesized a polythiophene with thermocleavable side groups on every second thiophene ring.[38] They took advantage of the facile cleavage of a tertiary ester around 190-210 °C (S**cheme 2**). This material, after cleavage of the alkyl chain, showed very good stability compared to the non-cleaved material as well as polythiophenes and poly(phenylene vinylene)s possessing solubilizing alkyl side chains.[39] One possible explanation for the

increased lifetime and thermal stability is that the rigidity and density of the film increases after cleavage making diffusion of the aluminum from the electrode much slower, decreasing the amount of photoreduction occurring in the material.

This material was later shown, upon heating to ~300 °C, to lose carbon dioxide resulting in a route to polythiophene by solution processing.[40] This polymer is unique in that it is possible to "switch off" the solubility by thermal cleavage of the tertiary ester leaving a carboxylic acid pendant group. Removal of the solubilizing group increases the stability by increasing the glass transition temperature of the polymer through hydrogen bonding of the carboxylic acid moieties.[41] Also, further cleavage of the carboxylic acid affords native polythiophene. This is the first solution processable approach to unsubstituted polythiophene.

1.3.7 3,4-Ethylenedioxythiophene Containing Polymers

Poly(3,4-ethylenedioxythiophene) (PEDOT) is the most produced electrically conducting organic polymer (**Figure 8**). PEDOT is widely studied due to its low ionization potential, high conductivity when doped and good stability.[42,43] PEDOT homopolymer is widely used as a conducting and hole-injecting electrode in organic light emitting diodes,[44,45] as a component in electrochromic displays[46-48] and as an electrode in solar cells.[49-51]

Figure 8 shows a number of EDOT based donor-acceptor conjugated polymers. All of these polymers showed an optical or electrochemical band gap of 1.0 eV or less, making them promising materials as transparent conductors or in electrochromic applications. To be used in photovoltaic devices, the bandgap would ideally be increased over these examples.[52-56]

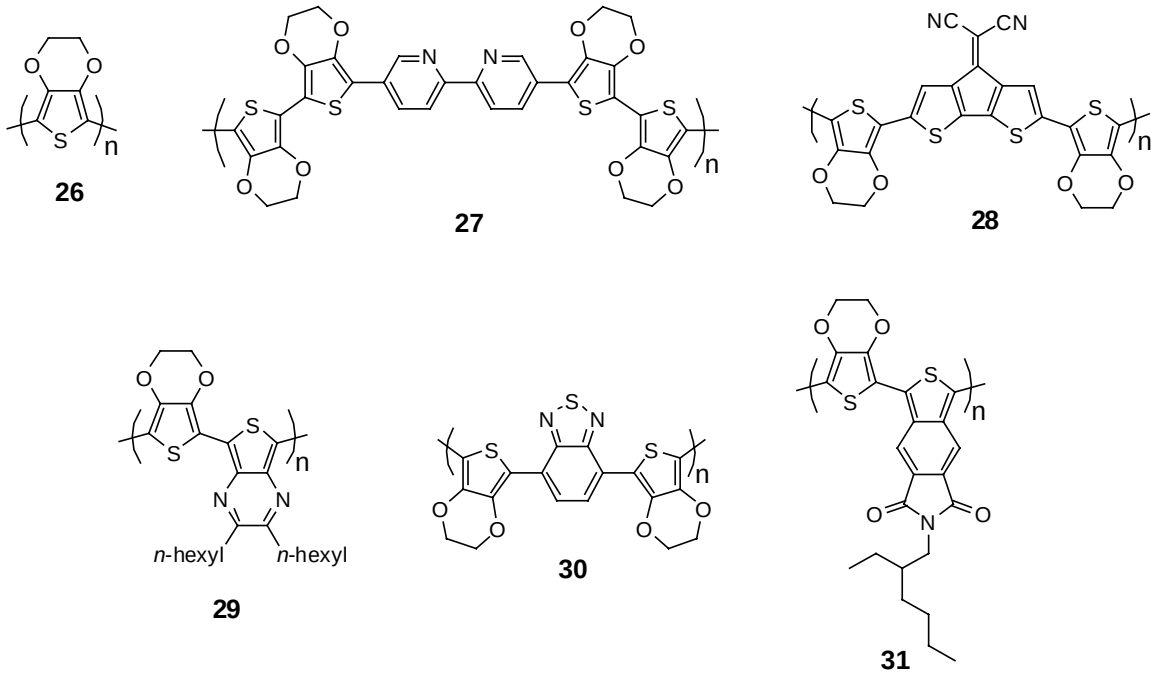

Figure 1.13. (26) Poly(3,4-ethylenedioxythiophene) (PEDOT) (27) PEDOT-pyridine (28) PEDOT-(4-dicyanomethylene-4H-cyclopenta[2,1-b;3,4-b']dithiophene) (29) PEDOT-thienopyrazine (30) PEDOT-benzothiadiazole (31) PEDOT-(N'2'-ethylene-4,5-dicarboxylic imide benzothiophene

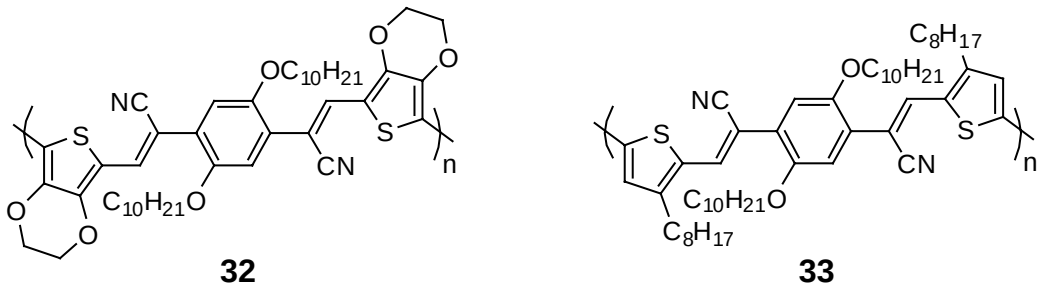

Figure 1.14. Low bandgap copolymers based on EDOT (32) and a long alkyl side chain containing thiophene (33)

Comparisons between an EDOT containing low bandgap copolymer and a copolymer with a long alkyl side chain on the thiophene ring were recently studied (**Figure 9**).[57] The optical bandgap of **32** was ~1.5 eV and the bandgap of **33** was ~2.1 eV. The two copolymers had similar LUMO levels but **32**'s HOMO level was measured to be ~0.65 eV higher than

the HOMO of **33**. As expected, the V_{OC} of **32** was lower than that of **33** due to the difference in bandgaps. **32** showed a significantly higher I_{SC} than **33** (1.87 mA/cm^2 vs. 0.50 mA/cm^2). Solar cells fabricated with both materials showed similar device efficiencies between 0.15 and 0.19 %.

The previous sections described the current state of donor-acceptor conjugated polymers used in organic solar cell devices. There have been significant advancements in the understanding of these devices that has led to better fabrication techniques and targeted photoelectronic properties. The need for better performing materials is apparent. Bandgap control and device stability are two pressing issues that are being widely researched.

1.4 Dissertation Organization

This dissertation is organized into six parts. Chapter 1 is a general discussion in two parts. The first part discusses high performance polymers synthesized via Ni(0)-catalyzed coupling polymerization, while the second part reviews conjugated polymers used in organic solar cell devices. Chapter 2 discusses the synthesis of novel coil-rod-coil triblock copolymers with poly(lactide) as the coil block and poly(2,5-benzophenone) as the rod block. Chapter 3 describes research conducted on the effects of the reaction conditions on the synthesis of poly(2-benzenesulfonyl-1,4-benzene) via the Ni(0)-catalyzed coupling of 2-benzenesulfonyl-1,4-dichlorobenzene. Chapter 4 discusses the synthesis and characterization of a soluble tertiary ester-functionalized PPP via Ni(0)-catalyzed coupling, which undergoes two separate thermolysis events to form native poly(paraphenylene). Chapter 5 describes the synthesis and characterization of alternating donor-acceptor conjugated polymers synthesized via Stille coupling for use in photovoltaic devices. Chapter 6 discusses continuing

experiments and future research directions. Supplemental data for Chapters 2 through 5 is presented in the appendices. Chapters 4 and 5 will be submitted for publication.

1.5 References

1. Colon, I and Kelsey, D. R. *J. Org. Chem.* **1986**, *51*, 2627-2637.

2. Marroco, M.; Trimmer, M. S.; Hsu, L. C.; Gagne, R. R. *SAMPE Proc.*, **1994**, *39*, 1063.

3. Phillips, R. W.; Sheares, V. V.; Samulski, E. T.; DeSimone, J. M. *Macromolecules*, **1994**, *27*, 2354-2356.

4. Percec, V.; Zhao, M.; Bae, J-Y.; Hill, D. H. *Macromolecules*, **1996**, *29*, 3727-3735.

5. Pasquale, A. J. and Sheares, V. V. *J. Polym. Sci., Part A: Polym. Chem.*, **1998**, *36*, 2611-2618.

6. Wang, J. and Sheares, V. V. *Macromolecules*, **1998**, *31*, 6769-6775.

7. Havelka-Rivard, P. A.; Nagai, K; Freeman, B. D.; Sheares, V. V. *Macromolecules*, **1999**, *32*, 6428-6424.

8. Bloom, P. D. and Sheares, V. V. *Macromolecules*, **2001**, *34*, 1627-1633.

9. Bloom, P. D. and Sheares, V. V. *J. Polym. Sci., Part A: Polym. Chem.*, **2001**, *39*, 3505-3512.

10. Hagberg, E. C.; Goodridge, B.; Ugurlu, O.; Chumbley, S.; Sheares, V. V. *Macromolecules*, **2004**, *37*, 3642-3650.

11. Hagberg, E. C.; Olson, D. A.; Sheares, V. V. *Macromolecules*, **2004**, *37*, 4748-4754.

12. Wu, S.; Zhang, S.; Li, W. *Polymer*, **2005**, *46*, 8396-8402.

13. Bloom, P. D.; Jones III, C. A.; Sheares, V. V. *Macromolecules*, **2005**, *38*, 2159-2166.

14. (a) Kraft, A.; Grimsdale, A. C.; Holmes, A. B. *Angew. Chem., Int. Ed.* **1998**, *37*, 402. (b) Mitschke, U.; Bauerle, P. *J. Mater. Chem.* **2000**, *10*, 1471. (c) Sheats, J. R.; Antoniadis, H.; Hueschen, M.; Leonard, W.; Miller, J.; Moon, R.; Roitman, D.; Stocking, A. *Science* **1996**, *273*, 884. (d) Kulkarni, A. P.; Tonzola, C. J.; Babel, A.; Jenekhe, S. A. *Chem. Mater.* **2004**, *16*, 4556. (e) Forrest, S. R. *Nature* **2004**, *428*, 911. (f) Aziz, H.; Popovic, Z. D. *Chem. Mater.* **2004**, *16*, 4522.

15. (a) Hoppe, H.; Sariciftci, N. S. *J. Mater. Res.* **2004**, *19*, 1924. (b) Peumans, P.; Yakimov, A.; Forrest, S. R. *J. Appl. Phys.* **2003**, *93*, 3693. (c) Coakley, K. M.; McGehee, M. D. *Chem. Mater.* **2004**, *16*, 4533. (d) Alam, M. M.; Jenekhe, S. A. *Chem. Mater.* **2004**, *16*, 4647. (e) Ma, W.; Yang, C.; Gong, X.; Lee, K.; Heeger, A. J. *Adv. Funct. Mater.* **2005**, *15*, 1617.

16. (a) Dimitrakopoulos, C. D.; Malenfant, P. R. L. *Adv. Mater.* **2002**, *14*, 99. (b) Horowitz, G. *J. Mater. Chem.* **2004**, *19*, 1946. (c) Babel, A.; Jenekhe, S. A. *J. Am. Chem. Soc.* **2003**, *125*, 13656. (d) Yoon, M.-H.; Facchetti, A.; Stern, C. E.; Marks, T. J. *J. Am. Chem. Soc.* **2006**, *128*, 5792. (e) Briseno, A. L.; Tseng, R. J.; Ling, M.-M.; Falcao, E. H. L.; Yang, Y.; Wudl, F.; Bao, *Z. Adv. Mater.* **2006**, *18*, 2320.

17. C. W. Tang *Appl. Phys. Lett.* **1986**, *48*, 183-185.

18. Yu, G.; Gao, J.; Hummelen, J. C.; Wudl, F.; Heeger, A. J. *Science*, **1995**, *270*, 1789-1791.

19. Brabec, C. J.; Sariciftci, N. S.; Hummelen, J. C. *Adv. Funct. Mater.* **2001**, *11*, 15-26.

20. Brabec, C. J.; Cravino, A.; Meissner, D.; Sariciftci, N. S.; Fromherz, T.; Rispens, M. T.; Sanchez, L.; Hummelen, J. C. *Adv. Funct. Mater.* **2001**, *11*, 374-380.

21. Gadisa, A.; Svensson, M.; Andersson, M.R.; Inganas, O. *Appl. Phys. Lett.* **2004**, *84*, 1609-1611.

22. Thompson, B. C.; Fréchet, J. M. J. *Angew. Chem. Int. Ed.* **2008**, *47*, 58-77.

23. Allemand, P. –M.; Koch, A.; Wudl, F. *J. Am. Chem. Soc.* **1991**, *113*, 1050-1051.

24. Gunes, S.; Neugebauer, H.; Sariciftci, N. S. *Chem. Rev.* **2007**, *107*, 1324-1338.

25. Singh, T. B.; Marjanovic, N.; Matt, G. J.; Gunes, S.; Sariciftci, N. S.; Ramil, A. M.; Andreev, A.; Sitter, H.; Schwodiauer, R.; Bauer, S. *Org. Electron.* **2005**, *6*, 105-110
.
26. Arkhipov, V. I.; Bassler, H. *Phys. Status Solidi A* **2004**, *201*, 1152-1187.

27. Brabec, C. J.; Winder, C.; Sariciftci, N. S.; Hummelen, J. C.; Dhanabalan, A.; van Hal, P. A.; Janssen, R. A. J. *Adv. Funct. Mater.* **2002**, *12*, 709-712.

28. Soci, C.; Hwang, I., -W.; Moses, D.; Zhu, Z.; Waller, D.; Guadiana, R.; Brabec, C. J.; Heeger, A. J. *Adv. Funct. Mater.* **2007**, *17*, 632-636.

29. Scharber, M. C.; Muhlbacher, D.; Koppe, M.; Denk, P.; Waldauf, C.; Heeger, A. J.; Brabec, C. J. *Adv. Funct. Mater.* **2006**, *18*, 789-794.

30. Winder, C.; Sariciftci, N. S. *J. Mater. Chem.* **2004**, *14*, 1077-1086.

31. van Mullekom, H. A. M.; Vekemans, J. A. J. M.; Havinga, E. E.; Meijer, E. W. *Mater. Sci. Eng. R* **2001**, *32*, 1-40.

32. Zhang, F.; Jespersen, K. G.; Björström, C.; Svensson, M.; Andersson, M. R.; Sundström, V.; Magnusson, K.; Moons, E.; Yartsev, A.; Inganäs, O. *Adv. Funct. Mater.* **2006**, *16*, 667-674.

33. Zhang, F.; Mammo, W.; Andersson, L. M.; Admassie, S.; Andersson, M. R.; Inganäs, O. *Adv. Mater.* **2006**, *18*, 2169-2173.

34. Shi, C.; Yao, Y.; Yang, Y.; Pei, Q. *J. Am. Chem. Soc.* **2006**, *128*, 8980-8986.

35. Wienk, M. M.; Turbiez, M. G. R.; Struijk, M. P.; Fonrodona, M.; Janssen, R. A. J. *Appl. Phys. Lett.* **2006**, *88*, 153511.

36. Mühlbacher, D.; Scharber, M.; Morana, M.; Zhu, Z.; Waller, D.; Gaudiana, R.; Brabec, C. *Adv. Mater.* **2006**, *18*, 2884-2889.

37. Kulkarni, A. P.; Zhu, Y.; Jenekhe, S. A. *Macromolecules* **2008**, *41*, 339-345.

38. Liu, J. S.; Kadnikova, E. N.; Liu, Y. X.; McGehee, M. D.; Fréchet, J. M. J. *J. Am. Chem. Soc.* **2004**, *126*, 9486-9487.

39. Krebs, F. C. and Spanggaard, H. *Chem. Mater.* **2005**, *17*, 5235-5237.

40. Bjerring, M.; Nielsen, J. S.; Nielsen, N. C.; Krebs, F. C. *Macromolecules* **2007**, *40*, 6012-6013.

41. Bjerring, M.; Nielsen, J. S.; Siu, A.; Nielsen, N. C.; Krebs, F. C. *Sol. Energy Mater. Sol. Cells* **2008**, *92*, 772-784.

42. Groenendaal, L. B.; Jonas, F.; Greitag, D.; Pielartzik, H.; Reynolds, J. R. *Adv. Mater.* **2000**, *12*, 481-494.

43. Groenendaal, L. B.; Zotti, G.; Aubert, P. H.; Waybright, S. M.; Reynolds, J. R. *Adv. Mater.* **2003**, *15*, 855-879.

44. Thompson, B. C.; Madrigal, L. G.; Pinto, M. R.; Kang, T. S.; Schanze, K. S.; Reynolds, J. R. *J. Polym. Sci. Part A: Polym. Chem.* **2005**, *43*, 1417-1431.

45. Kulkarni, A. P.; Zhu, Y.; Jenekhe, S. A. *Macromolecules* **2005**, *38*, 1553-1563.

46. Heuer, H. W.; Wehrmann, R.; Kirchmeyer, S. *Adv. Funct. Mater.* **2002**, *12*, 89-94.

47. Cutler, C. A.; Bouguettaya, M.; Reynolds, J. R. *Adv. Mater.* **2002**, *14*, 684-688.

48. Sapp, S. A.; Sotzing, G. A.; Reynolds, J. R. *Chem. Mater.* **1998**, *10*, 2101-2108.

49. Arias, A. C.; Granström, M.; Thomas, D. S.; Petritsch, K.; Friend, R. H. *Phys. Rev. B* **1999**, *60*, 1854-1860.

50. Dhanabalan, A.; van Duren, J. K. J.; van Hal, P. A.; van Dongen, J. L. J.; Janssen, R. A. J. *Adv. Funct. Mater.* **2001**, *11*, 255-262.

51. Huynh, W. U.; Dittmer, J. J.; Alivisatos, A. P. *Science* **2002**, *295*, 2425-2427.

52. Zhu, S. S. and Swager, T. M. *J. Am. Chem. Soc.* **1997**, *119*, 12568-12577.

53. Berlin, A. and Zanelli, A. *Chem. Mater.* **2004**, *14*, 3667-3676.

54. Perepichka, I. F.; Levillain, E.; Roncali, J. *J. Mater. Chem.* **2004**, *14*, 1679-1681.

55. Raimundo, J. M.; Blanchard, P.; Brisset, H.; Akoudad, S.; Roncali, J. *Chem. Commun.* **2000**, *11*, 939-940.

56. Meng, H.; Tucker, D.; Chaffins, S.; Chen, Y.; Helgeson, R.; Dunn, B.; Wudl, F. *Adv. Mater.* **2003**, *15*, 146-149.

57. Nguyen, L. H.; Günes, S.; Neugebauer, H.; Sariciftci, N. S.; Colladet, K.; Fourier, S.; Cleij, T. J.; Lutsen, L.; Gelan, J.; Vanderzande, D. *Eur. Phys. J. Appl. Phys.* **2007**, *36*, 219-223.

Chapter 2

THE SYNTHESIS OF POLYLACTIDE-POLY(2,5-BENZOPHENONE)-POLYLACTIDE COIL-ROD-COIL TRIBLOCK COPOLYMERS

2.1 Introduction

2.1.1 General Introduction

The understanding of polymer structure-property relationships has led to the advancement of high-performance polymers and, in particular, poly(*p*-phenylene)s (PPP)'s. Poly(*p*-phenylene) has remarkable thermal stability, mechanical properties, and can be conductive if doped. PPP's have been considered for use in composites, lubricant additives, and thermoset precursors for high-performance aerospace material applications. A major challenge with PPP synthesis is that the polymer has poor solubility in organic solvents due to its rigid backbone, which causes it to precipitate from solution during polymerization. Lateral substitution has been used to increase solubility of PPP's. The most successful methods of PPP synthesis have been the Suzuki[1] and the Colon[2] methods, both of which use transition metal catalysts (**Scheme 1**). The pendant aliphatic chain, in the Suzuki method, increases the solubility of the polymer but decreases the mechanical and thermal properties. High molecular weight amorphous poly(2,5-benzophenone) has been synthesized, without sacrificing physical properties, up to 2.5 x 10^4 g/mol,[3] following the Colon method, and 5.8 x 10^4 g/mol with slight modifications to the Colon method.[4]

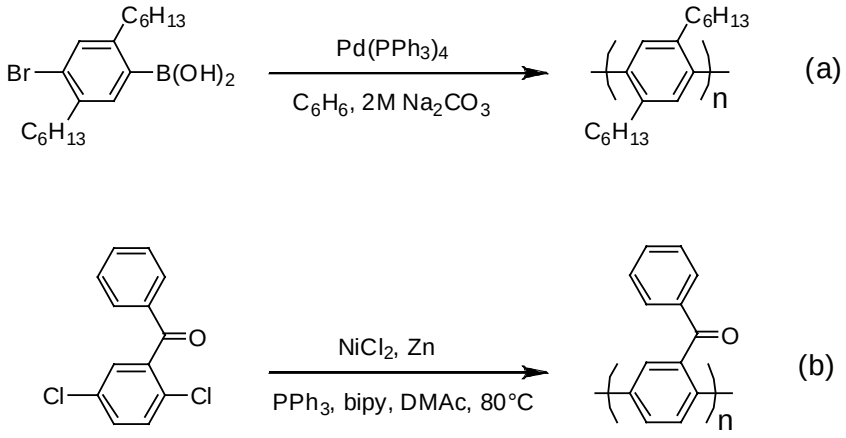

Scheme 2.1. Synthesis of PPP via a) the Suzuki method and b) the Colon Method

Since its development by Colon and Kelsey, nickel(0)-catalyzed coupling has proven to be a powerful method for the synthesis of carbon-carbon aryl bonds. A wide range of monomeric materials can be utilized by this Ni(0)-coupling process, including aryl chlorides[4], mesylates[5-6], and the bromide, iodide, and triflate derivatives.[7-9] It has been shown that the presence of an electron-withdrawing group ortho or para to the reactive site increases the reaction rate by activating that site to oxidative addition by the Ni(0) complex.[10] Poly(2,5-benzophenone) and its derivatives have been synthesized successfully with Ni(0)-catalyzed coupling.[4,11-13]

Roid-coil and coil-rod-coil block copolymers are a unique and interesting new class of materials. The combination of the flexible random coil segments with rigid rod blocks gives rise to many potential applications including opto-electronic devices, nano-patterning and mechanical reinforcing agents. The utility of these materials arises from the block copolymer architecture. The inherent incompatibility resulting from entropic factors between the rigid rod-like block and the flexible random coil block leads to phase separation at much lower molecular weights than coil-coil systems.[14] The flexible coil-like blocks also increase the solubility and processibility of the copolymer over that of the rod-like homopolymer. Rod-coil block copolymers containing materials such as polyphenylenevinylene (PPV),[15,16] polyphenyleneethylene (PPE)[17] and PPP[18] have been synthesized.

Ordered, phase separated structures with dimensions as small as 10 nm have been constructed. The ability to pattern materials such as PPV, PPE and PPP on nm scales leads to potential utility in the electronics industry. For example, coil-rod-coil block copolymers have exhibited narrowed emission spectra over that of the rod homopolymer due to isolated

domains of the optically active material.[19] Furthermore, the high modulus of the rigid backbones has been exploited through the use of these materials to construct nanocomposites.[20]

Narrow overall polydispersity is generally considered a prerequisite for the formation of ordered structures from most block copolymers consisting of two coil blocks. However, the importance of polydispersity in systems containing a polydisperse rod block has never fully been explored. Due to the incompatibility of the rod block in the random coil phase, phase separation is expected, but the degree of control of the resulting morphology is not known.[14]

The primary challenge in working with rod-coil block copolymers lies in the synthesis of rods with controlled polydispersity and controlled functionality at the chain end. The difficulties arise from the long stepwise syntheses necessary to build functionalized rods of useful molecular weight. Poly(ethylene oxide)-*b*-poly(phenylenevinylene)-*b*-poly(ethylene oxide) is a good example.[15] This material, containing monodisperse rod and coil blocks, exhibits interesting self-assembly in solution, but requires seven separate synthetic steps to produce triblock copolymers containing PPV eightmers. When not a requirement for the desired application, removal of the narrow polydispersity constraint upon the rod block expands the possible synthetic pathways. By the addition of molecules monofunctional with respect to the polymerization conditions, chain end functionalized rod-like polymers can be synthesized in a single step. Polymerizaton methods such as this eliminate the necessity for long, laborious, step-wise synthetic methods. The resulting materials can be converted to the desired block copolymers by grafting or by using them as macroinitiators.

2.1.2 Specific Aims

Poly(2,5-benzophenone) is a rigid, amorphous high-performance thermoplastic with excellent thermal stability and a tensile modulus 2-4 times greater than other high performance polymers, such as poly(phenylene sulfide) and poly(ether ether ketone).[13] While poly(2,5-benzophenone) has many excellent physical properties it also has areas of weakness that prevent its commercial use, which are poor solubility of the polymer, inability to form flexible films, and a lack of functionality. One way to approach solving these issues is the formation of copolymers that will add solubility and flexibility. It is difficult to make copolymers using Ni(0)-catalyzed coupling due to the fact that different monomers tend to only homopropagate due to differences in the electronics of the monomers. So, as has been demonstrated before functionality can be added by introducing a fluorinated monomer (**Scheme 2**).[12,21,22] Aromatic fluoride is unreactive in the Ni(0)-coupling reaction. These sites, when activated by an electron-withdrawing group, can be used for post-polymerization functionalization, which can lead to graft, triblock, and multiblock copolymers.[12,22]

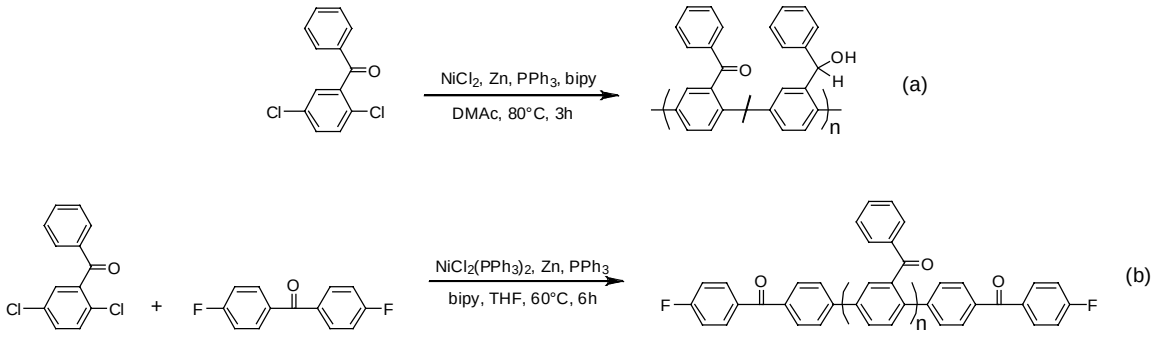

Scheme 2.2. Synthesis of poly(2,5-benzophenone) with a) reactive sites along backbone and b) reactive sites at chain ends

To expand on this method, a novel poly(L-lactide)-poly(2,5-benzophenone)-poly(L-lactide) triblock copolymer will be synthesized from commercially available starting material

to yield a polymer that can take advantage of the physical strength of poly(2,5-benzophenone) (PBP) and the flexible film-forming ability of poly(L-lactide) (PLLA). PLLA is a versatile, biodegradable, aliphatic polyester that is derived from 100% renewable resources in the form of corn and sugar beets. PLLA can be synthesized by the direct condensation of lactic acid or by the ring-opening polymerization of L-lactide. The ring-opening method is usually preferred due to the ease with which high molecular weight polymer is achieved. Stannous 2-ethylhexanoate ($Sn(Oct)_2$) is the most commonly used catalyst due to its high reaction rate, the low degree of product racemization, and its acceptance by the FDA. Along with $Sn(Oct)_2$, alcohols can be used as co-initiators. According to recent results, $Sn(Oct)_2$ first reacts with compounds containing hydroxyl groups to form a tin alkoxide that acts as an initiator in the polymerization, and the propagation stops via chain transfer with another alcohol molecule, yielding hydroxyl-terminated poly(lactide).[23] This leads to the approach of performing a nucleophilic aromatic substitution on fluorine functionalized PBP with the diol Bisphenol A in order to obtain PBP with functional hydroxyl groups that can serve as initiation sites for the ring opening polymerization of lactide (**Scheme 3**).

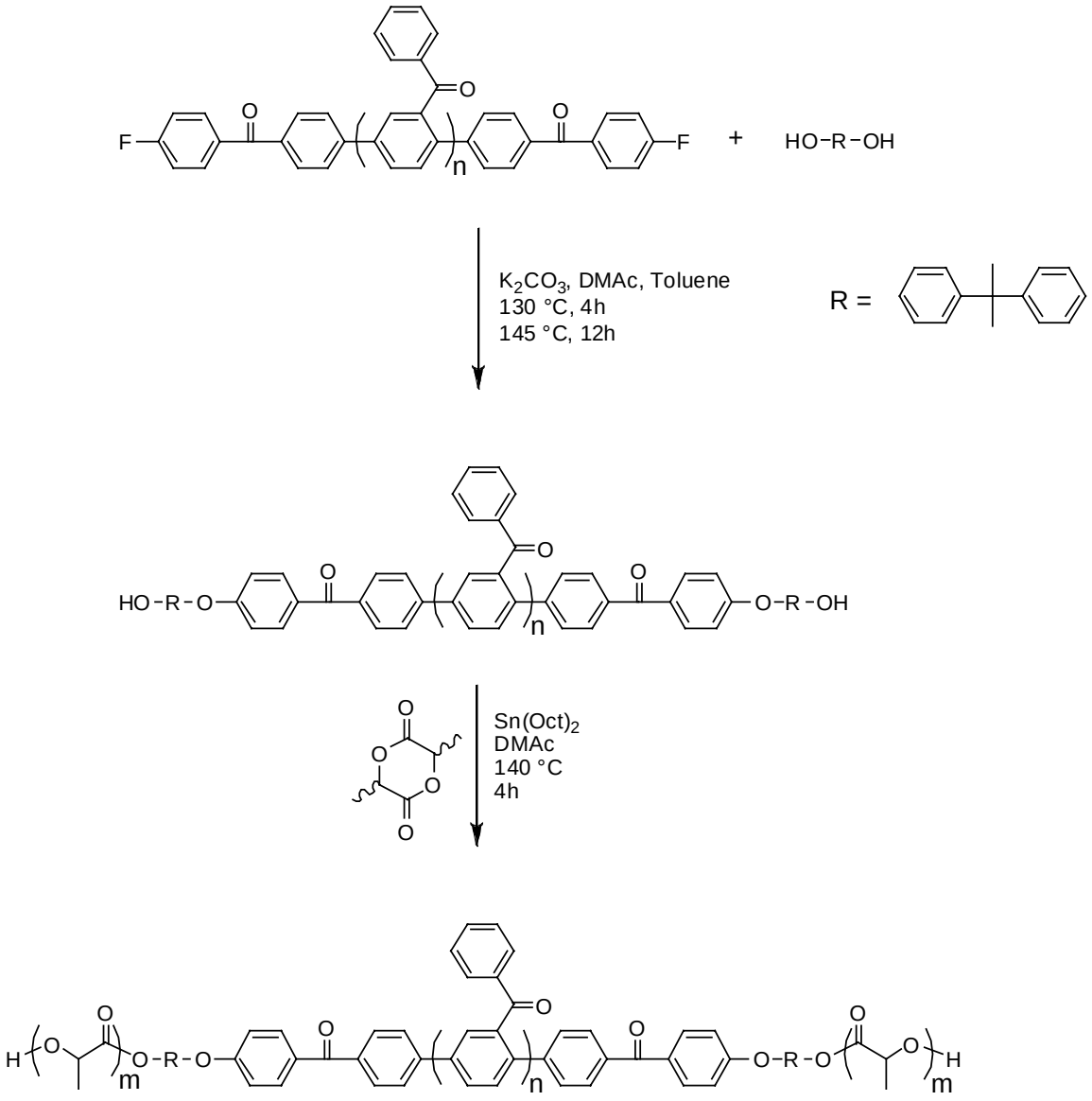

Scheme 2.3. Polymerizing lactide with hydroxyl endcapped PBP as co-initiator

2.2 Experimental

2.2.1 Materials

All reagents were purchased from Aldrich and used as received, unless otherwise noted. 2,5-dichlorobenzophenone was provided by Bayer and was recrystallized from ethanol and carbon black. Triphenylphosphine (TPP) and 2,2'-dipyridyl (bipy) were recrystallized from ethanol. L-lactide and D,L-lactide were recrystallized from acetone. *N*,*N*'-

dimethylacrylamide (Fisher) and toluene (Fisher) were distilled *in vacuo* from sodium. Potassium carbonate (Fisher) was dried at 120 °C for 24h prior to use.

2.2.2 Monomer Synthesis

4-chloro-4'-fluorobenzophenone

4-chlorobenzoyl chloride (1 equiv.), fluorobenzene (1.2 equiv.), and nitromethane (mL NO_2CH_3 < mL fluorobenzene) were stirred in a 500 mL round-bottom flask. $AlCl_3$ (1 equiv.) was added to the stirring solution that was then placed in an ice bath and allowed to stir for 24h under nitrogen. The resulting slurry was precipitated by pouring it into acidic ice water and allowed to stir for 24h. The white crystals were recrystallized in ethanol, filtered, and dried before characterization to give a 60% yield. ^{1}H-NMR (CD_2Cl_2): δ (ppm) = 7.19 (t, 2H), 7.49 (d, 2H), 7.72 (d, 2H), 7.81 (dd, 2H).

2.2.3 Polymer Synthesis

Poly(2,5-benzophenone) with fluorine endcap

Dichlorobis(triphenylphosphine)nickel(II) (0.1 equiv.), zinc (3.1 equiv.), triphenylphosphine (0.2 equiv.), and bipy (0.1 equiv); in a drybox, were added to a flask equipped with an overhead stirrer and a nitrogen inlet. Tetrahydrofuran (THF) (10 equiv.) was added via syringe and allowed to stir at 60 °C until a deep red color was observed. 4-chloro-4'-fluoro-benzophenone (0.005-0.20 equiv.) and 2,5-dichlorobenzophenone (0.995-0.80 equiv.) were added and allowed to react for 6h. The polymer was precipitated in a 4:1 methanol:hydrochloric acid mixture, filtered and washed with aqueous sodium bicarbonate and methanol. The resulting yellow powder was then purified by soxhlet extraction with chloroform. The organic solution was concentrated and the polymer was precipitated into methanol. The polymer was characterized by ^{1}H-NMR, ^{19}F-NMR, GPC, DSC, and TGA.

2.2.4 Macromonomer Substitution

Poly(2,5-benzophenone) with hydroxyl endcap

This is an example for one reaction, amounts vary based on the molecular weight of the polymer chain.

The fluorine endcapped poly(2,5-benzophenone) (1g, 3.22 x 10^{-4} mol), bisphenol A (10 equiv.) and anhydrous potassium carbonate (20 equiv.) were added to a flask equipped with an overhead stirrer, Dean-Stark trap and condenser, and a nitrogen inlet. DMAc (10 mL) and toluene (20 mL) were added and the solution was dehydrated at 130 °C for 4h and then raised to 145 °C and allowed to react for 12h. The solution changed from a peach-bronze color to a dark brown. The solution was precipitated into methanol and the yellow precipitate was collected by filtration. The polymer was characterized by ^{1}H-NMR, ^{19}F-NMR, GPC, DSC, TGA, and IR.

2.2.5 Triblock Poly(lactide)-Poly(2,5-benzophenone)-Poly(lactide)

Hydroxyl endcapped poly(2,5-benzophenone) and either L-lactide or D,L-lactide (varying amounts) were dissolved in DMAc in a flask equipped with an overhead stirrer and a nitrogen inlet and heated to 140 °C. Stannous(II) 2-ethylhexanoate ($Sn(Oct)_2$) (.01 equiv.) was added to the stirring solution which was then allowed to react for 4h. After 4h the reaction was allowed to cool and was then precipitated into cold methanol (0 °C). The precipitate was isolated by filtration and characterized by ^{1}H-NMR, GPC, DSC, TGA, and IR.

2.2.6 Characterization

^{1}H-NMR spectra were acquired in deuterated methylene chloride or deuterated chloroform on a Bruker 400 AVANCE. ^{19}F-NMR spectra were acquired in deuterated

methylene chloride on a Bruker 400 DRX with chlorotrifluoromethane as an internal standard. Molecular weights, relative to narrow polystyrene standards, were measured using a Waters GPC system using RI detection. Glass transition temperatures and melting points were measured on a Seiko 220C DSC using the second heat at a heating rate of 10 °C/min. Weight loss data was collected on a Perkin-Elmer Pyris 1 TGA with a heating rate of 10 °C/min.

2.3 Results and Discussion

2.3.1 Macromonomer Synthesis

Fluorine-endcapped poly(2,5-benzophenone) (PBP-F) was prepared at different molecular weights by varying the ratio of 2,5-dichlorobenzophenone and 4-chloro-4'-fluorobenzophenone. This approach has been taken before, but high molecular weight fluorine-endcapped poly(2,5-benzophenone) was unattainable since DMAc was used as the solvent in the Ni(0)-coupling catalyst system.[21] When run in DMAc, the carbonyl of the benzophenone is reduced which decreases the reactivity of the molecule. In this work, THF was used as the reaction solvent which eliminates the reduction of the carbonyl and has afforded PBP homopolymer of higher molecular weight than that which is attainable when DMAc is used as the reaction solvent. The amount of endcapping agent was varied between 20 and 0.5 mol % resulting in polymer from 2-12 kg/mol (**Table 1**). We believe the increasing PDI to be due to impurities in the endcapping monomer that will be studied shortly. ^{19}F-NMR of the endcapped polymer shows the presence of aryl fluoride (**Figure 1**).

Sample	Endcap mol %	$<M_n>$ x 10^{-3} g/mol	PDI	T_g (°C)
1	20	2.0	1.6	130
2	10	3.5	2.0	140
3	1	8.0	3.7	153
4	0.5	12.3	4.7	162

Table 2.1. Effect of endcap mol % on M_n of F-endcapped poly(2,5-benzophenone)

Once the PBP-F was prepared, nucleophilic aromatic substitution was performed with bisphenol A to give hydroxy-endcapped poly(2,5-benzophenone) (OH-endcapped PBP). ^{19}F-NMR was used to determine full conversion of the chain ends. **Figure 2** shows that, after the substitution, no aryl-fluoride is detectable. Infrared spectroscopy was also used to determine the presence of hydroxyl groups. **Figure 3** marks the appearance of a signal attributed to the presence of hydroxyl groups after the substitution has been conducted. As expected, the GPC's taken of the F- and OH- endcapped PBP showed them to be identical with no degradation of the polymer chains.

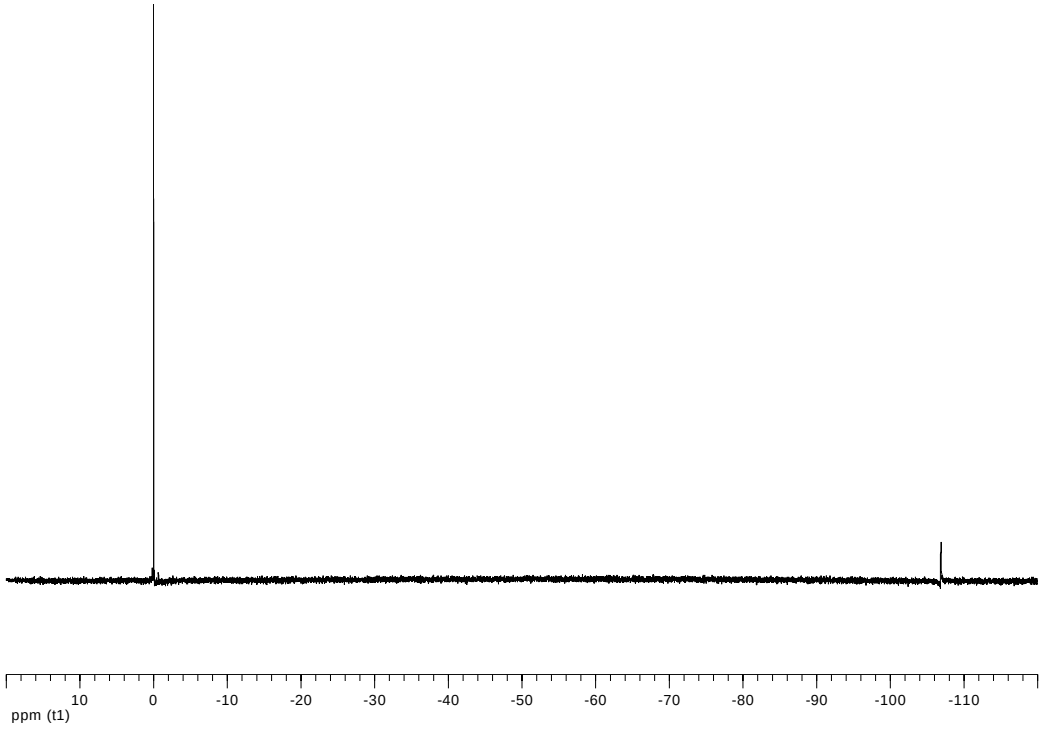

Figure 2.1. ^{19}F-NMR of F-endcapped PBP

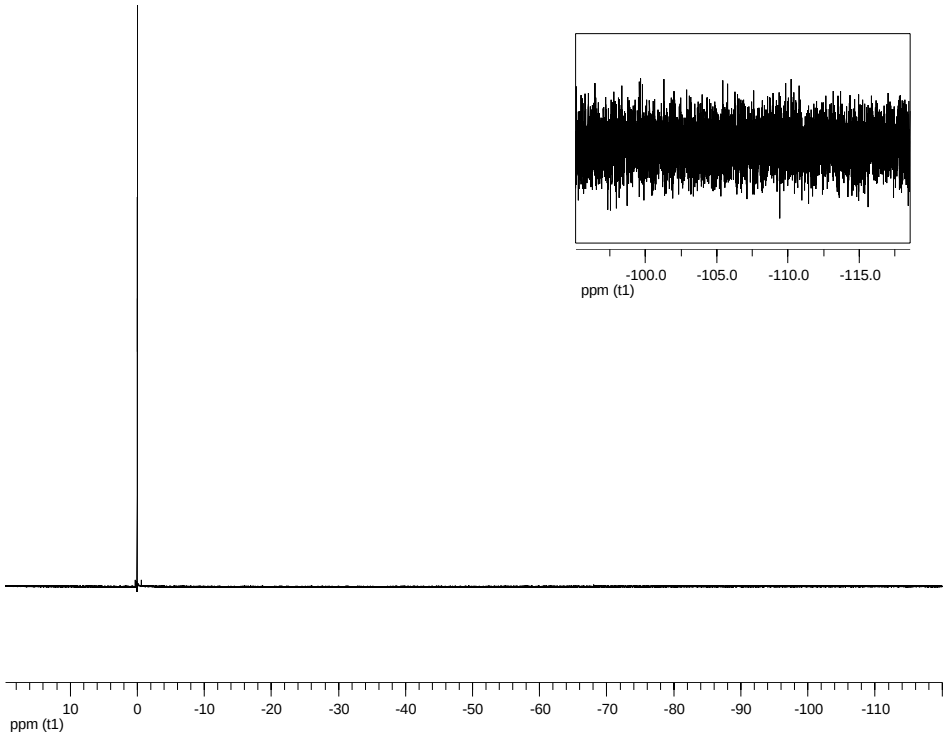

Figure 2.2. ^{19}F-NMR of OH-endcapped PBP

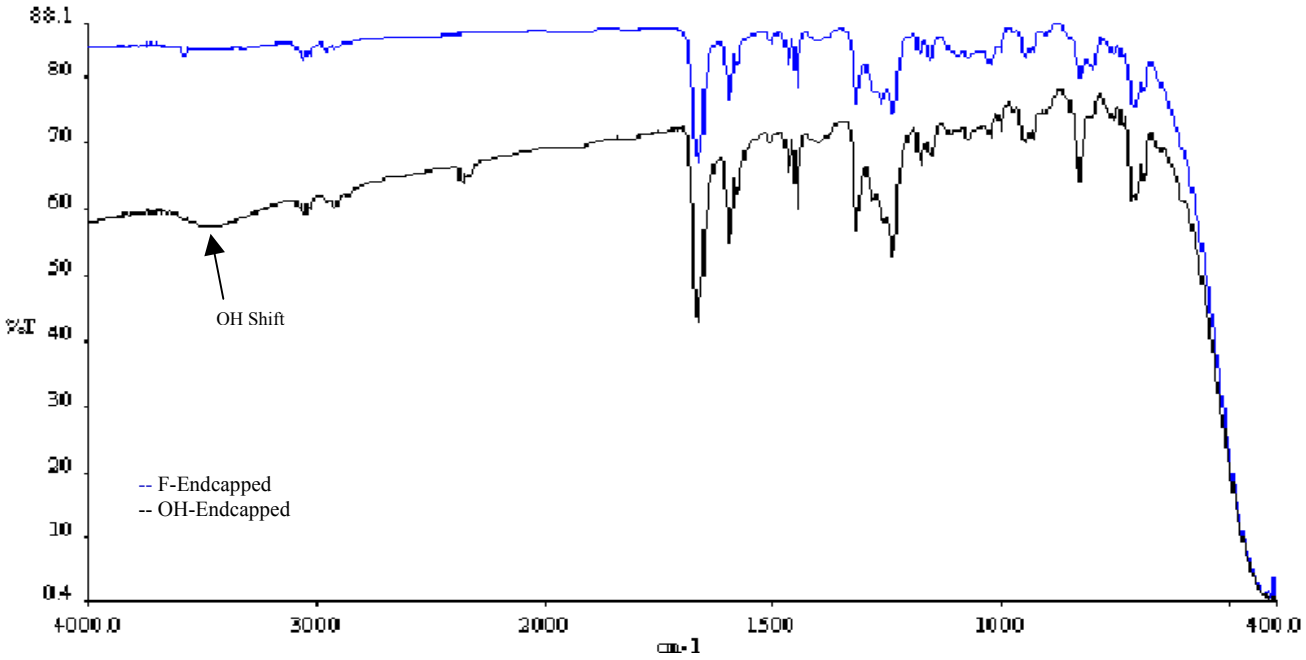

Figure 2.3. IR Spectra of F-endcapped PBP and OH-endcapped PBP

2.3.2 Triblock Copolymer Synthesis

2.3.2.1 Poly(L-Lactide)-*b*-Poly(2,5-benzophenone)-*b*-Poly(L-Lactide)

Poly(L-lactide) (PLLA) chains were grown from OH-endcapped PBP to produce PLLA-PBP-PLLA triblock copolymers. The copolymer's GPC data shows a molecular weight increase from the macromonomer that is monomodal. The ^{1}H-NMR shows the aromatic peaks of PBP (7-8ppm), the backbone hydrogen of PLLA (5.2ppm), and the methyl hydrogens of PLLA (1.5ppm) (**Figure 4**). Four copolymers were synthesized with varying ratios of macromonomer to L-lactide (**Table 2**). Unfortunately, solvent cast films formed from these materials were too brittle to perform mechanical testing.

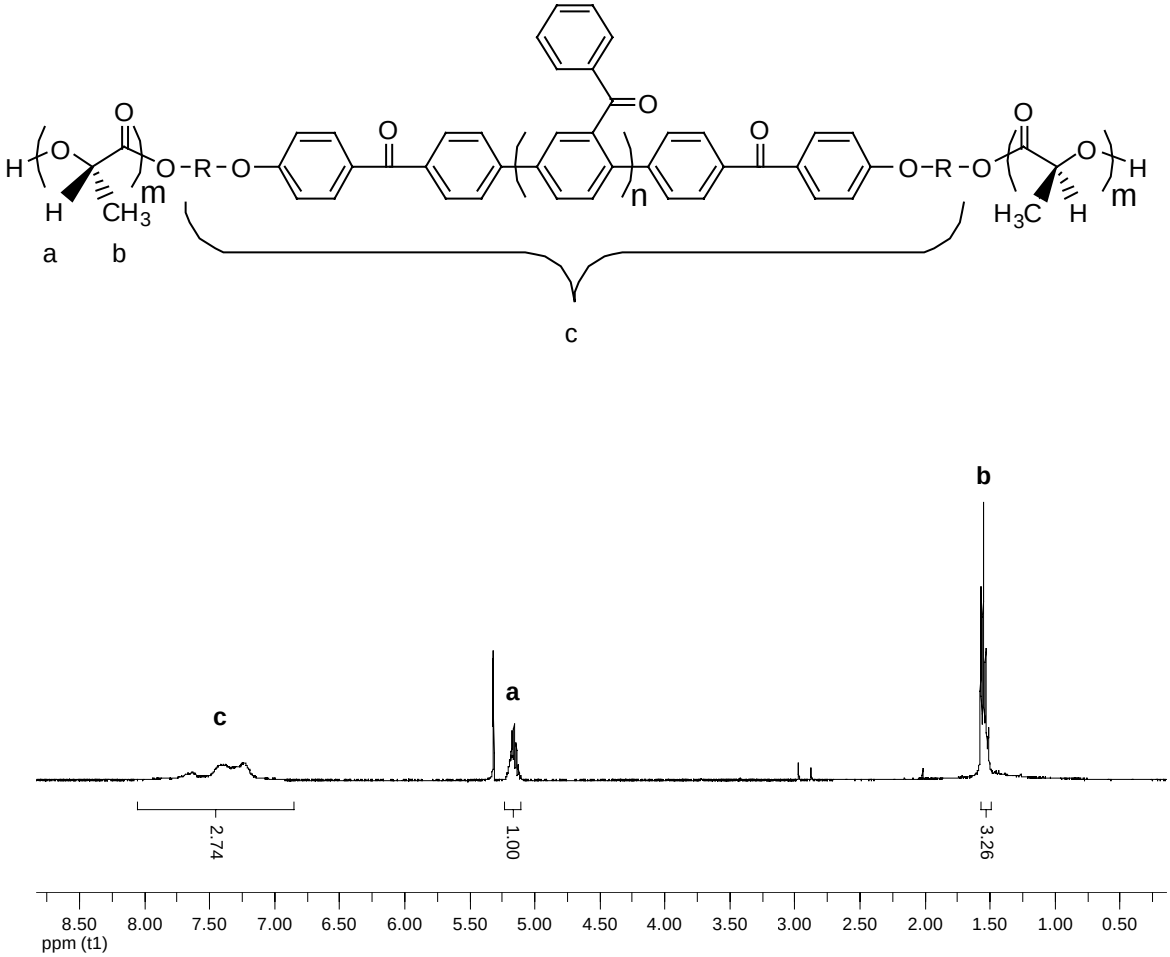

Figure 2.4. ^{1}H-NMR of Sample 5 PLLA-PBP-PLLA triblock copolymer

Sample	$\langle M_n \rangle \times 10^{-3}$ PBP (g/mol)	PDI PBP	$\langle M_n > \times 10^{-3}$ Triblock (g/mol)	PDI Triblock
5	3.1	2.4	12.2	2.1
6	3.5	2.0	5.9	2.5
7	8.1	3.3	20.3	2.2
8	2.7	2.0	26.4	1.6

Table 2.2. Molecular weight data of PLLA-PBP-PLLA triblock copolymers

2.3.2.2 Poly(D,L-lactide)-b-Poly(2,5-benzophenone)-b-Poly(D,L-lactide)

Poly(D,L-lactide) (PDLLA) chains were grown from HO-PBP-OH to produce PDLLA-PBP-PDLLA triblock copolymers. The reason for using poly(D,L-lactide) is that it is amorphous and should result in a less brittle material than the triblocks containing semi-crystalline poly(L-lactide). The GPC data shows a molecular weight increase from the macroinitiator that is monomodal. Four copolymers were synthesized with varying HO-PBP-OH macroinitiator molecular weights (**Table 3**). The resulting triblock copolymers also formed films that were too brittle to be testsed mechanically.

Sample	$\langle M_n \rangle \times 10^{-3}$ PBP (g/mol)	PDI PBP	$\langle M_n > \times 10^{-3}$ Triblock (g/mol)	PDI Triblock
9	2.7	2.0	28.0	1.6
10	2.7	2.0	15.8	1.4
11	5.8	2.5	9.7	1.5
12	5.8	2.5	6.8	2.0

Table 2.3. Molecular weight data of PDLLA-PBP-PDLLA triblock copolymers

2.4 Conclusions

ABA triblock materials utilizing poly(2,5-benzophenone) as the B block and polylactide as the A block were synthesized by ring opening polymerization of lactide from end-functionalized poly(2,5-benzophenone) macromonomers. An increase in the mechanical properties over those of polylactide homopolymers was not observed. Not shown, the feed ratio of lactide monomer and incorporation into the polymer chain correlated poorly. Use of an alternate catalyst system, such as 1,5,7-triazabicyclo-[4.4.0]dec-5-ene,[24] may improve control over the reaction and subsequently allow for better study of how molecular weight ratio of the different blocks affects the mechanical properties.

2.5 Acknowledgments

We would like to acknowledge funding from Chevron-Phillips and UNC-Chapel Hill Startup Funds. Also we would like to thank Dr. Erik Hagberg for useful discussions regarding polymer synthesis.

2.6 References

(1) Rehahn, M.; Schluter, A. D.; Wegner, G.; Feast, W. J. *Polymer*, **1989**, *30*, 1060.

(2) Marrocco, M. L.; Gagne, R. R. U. S. Patent 5,227,457, 1993.

(3) Phillips, R. W.; Sheares, V. V.; Samulski, E.T.; DeSimone, J. M. *Macromolecules* **1994**, *27*, 2354.

(4) Hagberg, E. C.; Olson, D. A.; Sheares, V. V. *Macromolecules* **2004**, *37*, 4748.

(5) Percec, V.; Bae, J. Y.; Zhao, M.; Hill, D. H. *J. Org. Chem.* **1995**, *60*, 176.

(6) Grob, M. C.; Feiring, A. E.; Auman, B. C.; Percec, V.; Zhao, M.; Hill, D. H. *Macromolecules* **1996**, *29*, 7284.

(7) Percec, V.; Okita, S.; Weiss, R. *Macromolecules* **1992**, *25*, 1816.

(8) Colon, I.; Kelsey, D. R. *J. Org. Chem.* **1986**, 51, 2627.

(9) Pei, J.; Yu, W. -L.; Ni, J.; Lai, Y., -H.; Huang. W.; Heeger, A. J. *Macromolecules* **2001**, *34*, 7241.

(10) Stille, J. K.; Lau, K. S. U. *Acc. Chem. Res.* **1977**, *10*, 434.

(11) Pasquale, A. J.; Sheares, V. V. *J. Polym. Sci., Part A: Polym. Chem.* **1998,** *36*, 2611.

(12) Bloom, P. D.; Jones, C. A., III; Sheares, V. V. *Macromolecules* **2005**, *38*, 2159.

(13) Marrocco, M. L.; Gagne, R. R.; Trimmer, M. S.; Hsu, L. C. *SAMPE Proc.* **1994**, *39*, 1063.

(14) Klok, H.; Lecommandoux, S. *Adv. Mater.* **2001**, *13*, 1217.

(15) Wang, H.; Wang, H. A.; Urban, V. S.; Littrell, K. C.; Thiyagarajan, P.; Yu, L. *J. Amer. Chem. Soc.* **2000**, *122*, 6855.

(16) Tew, G. N.; Pralle, M. U.; Stupp, S. I. *J. Amer. Chem. Soc.* **1999**, *121*, 9852.

(17) Huang, W. Y.; Matsuoka, S.; Kwei, T. K.; Okamoto, Y.; Hu, X.; Rafailovich, M. H.; Sokolov, J. S. *Macromolecules* **2001**, *34*, 7809.

(18) Tsolakis, P. K.; Koulouri, E. G.; Kallitis, J. K. *Macromolecules* **1999**, *32*, 9054

(19) Marsitzky, D.; Klapper, M.; Mullen, K. *Macromolecules* **1999**, *32*, 8685.

(20) Pae, Y.; Harris, F. W. *J. Polym. Sci. Pt. A Polym. Chem.* **2000**, *38*, 4247.

(21) Bloom, P. D.; Sheares, V. V. Journal of Polymer Science, Part A: Polymer Chemistry **2001**, 39, 3505.

(22) Hagberg, E. C.; Goodridge, B.; Ugurlu, O.; Chumbley, S.; Sheares, V. V. *Macromolecules* **2004**, *37*, 3642.

(23) Korhonen, H.; Helminen, A.; Seppälä, J. K. *Polymer* **2001**, *42*, 7541.

(24) Pratt, R. C.; Lohmeijer, B. G. G.; Long, D. A.; Waymouth, R. M.; Hedrick, J. L. *J. Amer. Chem. Soc.* **2006**, *128*, 4556.

Chapter 3

EFFECTS OF LIGAND AND SOLVENT TYPE ON THE SYNTHESIS OF POLY(2-BENZENESULFONYL-1,4-BENZENE) VIA NI(0)-CATALYZED COUPLING

3.1 Introduction

Since its development by Colon and Kelsey, nickel(0)-catalyzed coupling has proven to be a powerful synthetic method for the formation of carbon-carbon aryl bonds. The reaction conditions tolerate many functionalities with the only known exceptions being protic, nitro, and amine containing substituents. A wide range of polymeric materials have been synthesized from inexpensive arylene chlorides[1] and mesylates[2,3] as well as the bromide, iodide, and triflate derivatives.[4-6] The mechanism of the reaction has been of great interest, and many advances have been made in understanding the role of ligands, temperature and reducing metal on the polymerization.[7]

Our interests are in the synthesis of polyphenylenes substituted with electron-withdrawing substituents. The presence of electron-withdrawing groups ortho or para to the reactive site accelerates the reaction rate by activating the site to oxidative addition by the Ni(0) complex.[8] Substituents such as the benzoyl and benzenesulfonyl pendant group have been shown to exhibit many additional beneficial properties. The benzoyl pendant is known to increase the solubility of the wholly aromatic polyphenylene material, while maintaining the outstanding thermal and mechanical properties of the conjugated backbone.[9] The benzene-sulfonyl pendant imparts very high thermal stability with 10% weight loss temperatures for oligomeric materials near 500 ºC.[10]

In our work with polypenylenes we noted the excellent reactivity of benzophenone derivatives. Materials with number-average molecular weights of up to 25 x 10^3 g/mol with outstanding mechanical and thermal properties were synthesized, but these polymers formed brittle films.[11] The formation of flexible films is a requirement for many of the potential applications of this material, such as separation membranes and organic electronics. Also,

reduction of nearly 15% of the carbonyl group was observed.[12] When the carbonyl group was replaced with a sulfone functionality, only oligomeric materials were synthesized.[10]

The choice of solvent and the monomer structure have been shown to be key considerations in the Ni(0) polymerization of arylene dichloride monomers containing electron-withdrawing substituents. Polymerization in *N*,*N*-dimethylacetamide (DMAc) results in side reactions, such as degradation of thiophene rings in the reaction mixture and reduction of the carbonyl groups, which limits the material's utility. Using tetrahydrofuran (THF) as solvent, high molecular weight poly[3-(2'-thiophenecarbonyl)-2,5-thiophene] and poly(2,5-benzophenone) were synthesized with no side reactions being observed. Although the exact cause of the differing results was not found, drastic differences in the catalytic environments in the two solvents were observed by NMR. While high molecular weight materials from monomers containing carbonyl functionalities were obtained, substitution with a sulfone resulted in oligomeric material. Analysis of the results and consideration of the mechanism has shown that in Ni(0)-catalyzed polymerization there is a window of electron-withdrawing ability for which functionalities such as carbonyl-containing pendants meet the criteria and greatly accelerate the reaction. Increasing the electron-withdrawing ability by substitution with a sulfone slows the reaction due to the stabilization of a reactive intermediate.[13]

In this paper, the synthesis of poly(2-benzenesulfonyl-1,4-benzene) via the Ni(0)-catalyzed coupling of 2-benzenesulfonyl-1,4-dichlorobenzene is presented. Reaction conditions were varied and analyzed to address the limitations presented above. Factors considered are type of ligand present in the reaction, solvent type and reaction time.

Materials were analyzed by gel permeation chromatography (GPC), thermogravimetric analysis (TGA) and differential scanning calorimetry (DSC).

3.2 Experimental

3.2.1 Materials

All reagents were purchased from Aldrich, unless otherwise noted, and used without further purification. *N,N*-dimethylacetamide (DMAc) was dried over CaH_2 and vacuum distilled before use. Tetrahydrofuran (THF) was dried over sodium and benzophenone and vacuum distilled before use. 2,2'-bipyridine (bipy), 4,4'-di-*tert*-butyl-2,2'-dipyridyl (*t*-butyl bipy), 4,4'-dimethyl-2,2'-dipyridyl (methyl bipy) and 4,4'-dimethoxy-2,2'-bypyridine (methoxy bipy) were purified by recrystallization from ethanol. Triphenylphosphine (TPP) was purified by recrystallization from cyclohexane.

3.2.2 Monomer Synthesis

2-benzenesulfonyl-1,4-dichlorobenzene. Aluminum chloride (1 equiv.) was added to a stirring mixture of 1,4-dichlorobenzenesulfonyl chloride (1 equiv.) and benzene (1.2 equiv.) in nitromethane (5 equiv.) at 0 °C. The reaction was allowed to warm to room temperature and stir for 24 h. The reaction was stopped by pouring the solution into acidic ice water. The crude solid was isolated by filtration. The crude product was treated with activated carbon in boiling ethyl acetate/heptane (1:8) and filtered. The resulting white crystals were isolated by filtration and dried under vacuum. The product was recovered in 58% yield and had an observed melting point of 135 °C. ^{1}H-NMR: δ (ppm) = 7.38 (d, 1H), 7.50 (d, 1H), 7.54 (dd, 2H), 7.65 (t, 1H), 7.95 (d, 2H), 8.33 (d, 1H).

3.2.3 Polymer Synthesis

Bis(triphenylphosphine)nickel(II) dichloride (0.1 equiv.), zinc (3.1 equiv.), TPP (0.2 equiv.) and bipy, *t*-butyl bipy, methyl bipy, or methoxy bipy (0.1 equiv) were added to a flask equipped with an overhead stirrer and a nitrogen inlet. Solvent (10 equiv.) was added via syringe and the mixture was stirred at 60 °C (in THF) or 80 °C (for DMAc). Upon addition of solvent the mixture turned green, indicating the presence of Ni(II). Once the mixture became a deep red, indication of Ni(0), monomer was added and allowed to react for a specified amount of time. The polymer was then precipitated in hydrochloric acid and methanol (1:4), filtered, and washed on a glass frit. A Soxhlet extraction was performed with chloroform on the collected polymer. The organic solution was then concentrated and the polymer was precipitated into stirring methanol. The polymer was collected via filtration and dried under vacuum. Yields for all polymerizations were greater than 90 %.

3.2.4 Characterization

^{1}H and ^{13}C NMR spectra were acquired in deuterated solvents on a Bruker 400 AVANCE spectrometer. Molecular weights, relative to narrow polystyrene standards, were measured using a Waters GPC system using RI detection. The measurements were taken at 35 °C with THF as the mobile phase on three columns (Waters Styragel HR2, HR4, HR5). Thermal transitions were measured with a Seiko 220C DSC on the second heat with a heating rate of 10 °C/min. Glass transitions were determined at the inflection point of the endotherm. Thermogravimetric analysis was carried out using a Perkin Elmer TGA with a heating rate of 10 °C/min in a N_2 atmosphere.

3.3 Results and Discussion

In previous work with the 2-benzenesulfonyl-1,4-dichlorobenzene monomer, only oligomeric materials were able to be synthesized.[12,13] It was hypothesized that there is a window of electron-withdrawing ability for which functionalities such as carbonyl containing pendants meet the criteria and greatly accelerate the reaction. Increasing the electron-withdrawing ability by substitution with a sulfone slows the reaction due to deactivation of the $ArNi(I)L_3$ reactive intermediate for oxidative addition (step 3 on scheme 1).

To understand the role of monomer structure in the reaction, the mechanism was considered. The catalytic cycle proposed by Colon and Kelsey contains three steps in which the structure of the monomer could possibly play a role (Scheme 1).[5] These steps were oxidative addition of Ni(0) across the aryl chloride bond (step 1), reduction resulting in an arylnickel(I) species (step 2) and oxidative addition of the arylnickel(I) species to a second aryl chloride (step 3). The first two steps were shown to be accelerated by the presence of an electron-withdrawing substituent on the aryl chloride.[8] In the third step, the presence of an electron-withdrawing group *ortho* to the Ni-C bond would be expected to increase the stability of the electron-rich $ArNi(I)L_3$ complex and thus slow the oxidative addition reaction of this complex with a second aryl chloride. Colon and Kelsey proposed that early in the reaction (conversions less than 80%) the reaction was pseudo-zero-order in aryl chloride and the reduction of the $ArNi(II)ClL_2$ (step 2) was the rate-determining step. As the concentration of the aryl chloride approaches that of nickel, the oxidative addition of $ArNi(I)L_3$ (step 3) becomes the rate-determining step. Oligomers of 10 repeat units previously synthesized with sulfone containing materials equate to a conversion of 90%

owing to the fact that this polymerization proceeds under step-growth kinetics and it follows that DP = 1/(1-ρ), where DP is the degree of polymerization and ρ is the conversion. Sulfonyl groups are stronger withdrawing groups than ketones and thus deactivate the $ArNi(I)L_3$ complex for oxidative addition to a greater extent.[13]

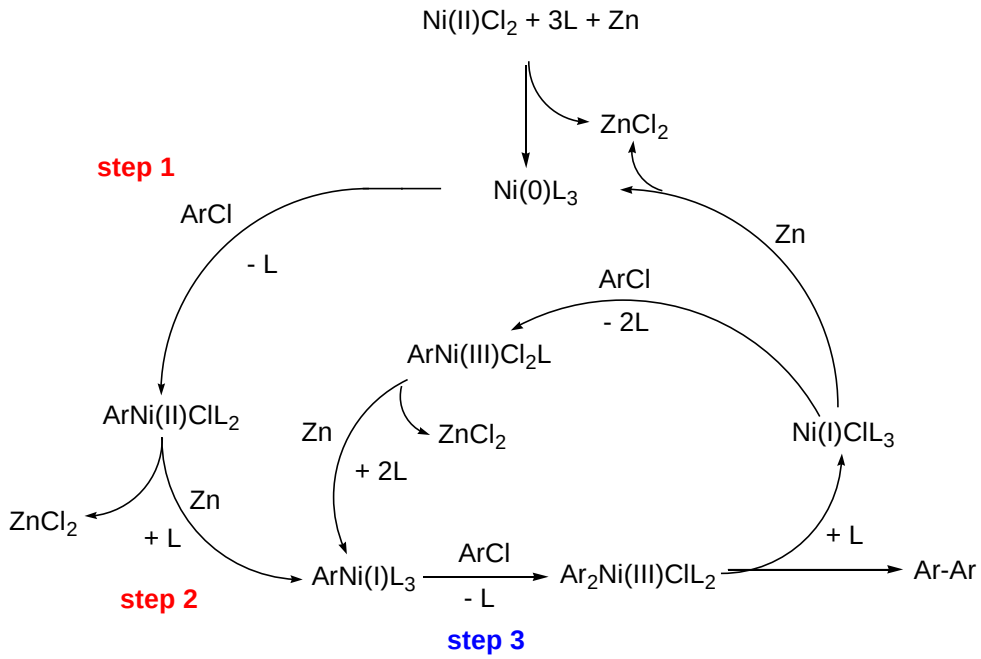

Scheme 3.1. Proposed Ni(0)-catalyzed coupling catalytic cycle

The next step was to examine the polymerization behavior by changing the ligand type while also varying solvent type and reaction time (**Scheme 2**). The general procedure for Ni(0)-catalyzed coupling involves the use of bipyridine. This bidentate ligand is believed to force the diarylnickel(II) complex into a *cis* aryl geometry and shows a rate enhancement over polymerization conditions where only triphenylphosphine is used as the ligand.[5] Therefore, a series of bipyridine based ligands containing electron-donating groups were used to offset the strong electron-withdrawing sulfonyl group on the aryl chloride (**Figure 1**).

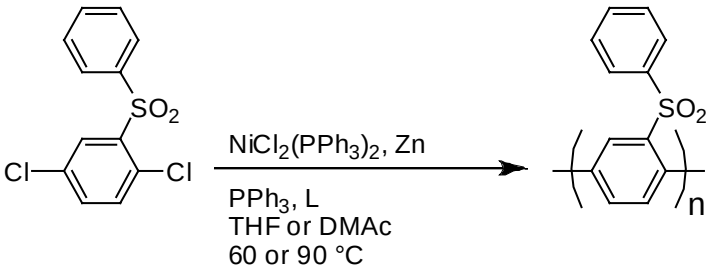

L = bipy, *t*-butyl bipy, methyl bipy, or methoxy bipy

Scheme 3.2. Reaction conditions for the synthesis of poly(2-benzenesulfonyl-1,4-benzene)

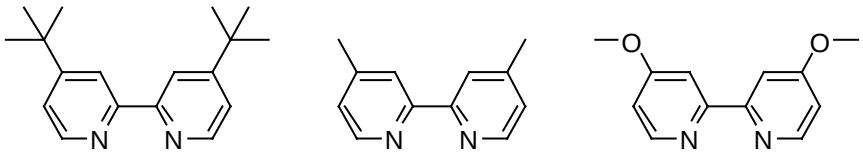

Figure 3.1. 2,2'-bipyridine ligands containing electron-donating substituents. 4,4'-*t*-butyl-2,2'-dipyridyl (left), 4,4'-dimethyl-2,2'-dipyridyl (center), 4,4'-dimethoxy-2,2'-bipyridine (right)

The results of the polymerization studies are shown in **Table 1**. For comparative purposes, sample **1** was synthesized using standard reaction conditions. As expected, oligomeric material was produced which showed good thermal stability (10% weight loss = 466 °C) and a glass-transition temperature of 129 °C. All polymerization conditions produced product with significant insoluble fractions (≥ 50%) after Soxhlet extraction with chloroform. For all samples except **2** the insoluble fraction was discarded and not analyzed. Sample **2a** was the insoluble fraction of the polymerization run in THF for 6 h with *t*-butyl bipy as the coordinating ligand, and **2b** was the soluble fraction. The thermal stability of the soluble and insoluble fractions were very similar with 10% weight loss values of 533 and 534 °C, respectively. **2b** showed a glass-transition at 159 °C while for **2a** no thermal transitions were observed in a range of 25 – 300 °C. While sample **2b** showed a significant increase in the glass-transition temperature versus **1**, the molecular weight showed only a slight increase.

Sample **3** used the same reaction conditions as sample **2** except the reaction time was increased from 6 to 24 hours. The resulting material did not differ in any significant way from when the reaction was run for 6 hours.

With the reaction conditions for samples **2** and **3** still providing only oligomeric material, the reaction solvent was changed to DMAc for samples **4-6**. The soluble fractions of samples **1-3** were more readily soluble in DMAc than in THF, so it was thought that running the reaction in DMAc might keep the polymer from precipitating from the solution during the reaction. Samples **4-6** did not show any increase in molecular weight from the samples synthesized in THF, the T_gs were similar to the THF samples and ranged from 138-159 °C but the thermal stabilities were slightly lower. Increasing the reaction temperature (**5**) and the reaction time (**6**) resulted in lower T_gs but similar thermal stabilities.

Samples **7-9** were synthesized using methyl bipy as the coordinating ligand. This ligand would have similar electron-donating capacity as the *t*-butyl bipy, but possesses less steric bulk. The materials synthesized with methyl bipy as the ligand showed similar properties to those materials synthesized with *t*-butyl bipy as the ligand. The T_gs of the three materials ranged from 148-156 °C**,** matching samples **2-6**. Materials synthesized in DMAc again showed slightly lower thermal stability than those synthesized in THF.

The alkyl-substituted bipyridines showed a negligible effect on the molecular weight of the final product, so methoxy bipy was used since it possessed the much stronger donating methoxy groups. Samples **10** and **11** were synthesized using the methoxy bipy ligand in THF and DMAc, respectively. As before, no significant change in molecular weight was observed with these samples. Thermal stability for the two samples was similar, but no T_g was observed for sample **10**, while sample **11** showed a T_g of 150 °C**.**

Table 3.1. Conditions and results for the polymerization of poly(2-benzensulfonyl-1,4-benzene)

Sample	Time (h)	Temp (°C)	Solvent Type	Ligand Type	$<M_n>x10^{-3}$ (g/mol)[a]	PDI[a]	T_g (°C)[b]	5% Wt. Loss (°C)[c]	10% Wt. Loss (°C)[c]
1	6	90	DMAc	Bipy	0.97	1.2	129	405	466
2a[d]	6	60	THF	*t*-butyl bipy	--	--	--[h]	505	534
2b[e]	6	60	THF	*t*-butyl bipy	1.45	1.2	159	475	533
3	24	60	THF	*t*-butyl bipy	1.24[f]	--[g]	160	517	529
4	6	60	DMAc	*t*-butyl bipy	1.19	1.3	159	395	453
5	6	90	DMAc	*t*-butyl bipy	1.11	1.3	146	434	470
6	24	90	DMAc	*t*-butyl bipy	1.30	1.3	138	400	487
7	6	60	THF	Methyl bipy	1.13	1.2	154	487	516
8	6	60	DMAc	Methyl bipy	1.11	1.2	148	433	494
9	6	90	DMAc	Methyl bipy	1.28	1.4	156	431	464
10	6	60	THF	Methoxy bipy	1.28[f]	--[g]	--[h]	500	519
11	6	90	DMAc	Methoxy bipy	1.35	1.3	150	460	500

DMAc = *N*,*N*-dimethylacetamide, THF = tetrahydrofuran. [a]Determined by GPC with THF mobile phase. [b]Determined by DSC with a heating rate of 10 °C/min. [c]Determined by TGA with a heating rate of 10 °C/min. [d]Insoluble fraction for sample 2 after Soxhlet extraction with chloroform. [e]Soluble fraction for sample 2 after Soxhlet extraction with chloroform. [f]M_p according to GPC (M_n could not be quantitated). [g]Unable to quantitate by GPC. [h]No glass-transition endotherm observed in a range of 25 – 300 °C

It was apparent that changing the structure of the bipyridine ligand had no appreciable effect on the final molecular weight of the materials but, by grouping the data into categories of solvent type and ligand type, general trends for the thermal properties of the materials could be observed (**Table 2**). Materials synthesized in the presence of bipyridine ligands with electron-donating substituents showed fairly identical T_gs and thermal stability. The only real difference comes in comparing materials synthesized in THF versus those materials synthesized in DMAc. Materials synthesized in THF showed an average T_g of 157 °C while materials synthesized in DMAc showed an average T_g of 146 °C. There is an even more drastic difference in the thermal stability of the materials. Five percent weight loss values for materials synthesized in THF were, on average, 72 °C higher than materials synthesized in DMAc and the 10% weight loss values were 48 °C higher.

Table 3.2. Thermal properties of soluble fractions of poly(2-benzensulfonyl-1,4-benzene) synthesized under various conditions

Property	Solvent Used		Ligand Used			
	THF	DMAc	Bipy	*t*-Butyl Bipy	Methyl Bipy	Methoxy Bipy
Tg (°C)[a]	157	146	129	152	152	150
5% Wt. Loss (°C)[b]	494	422	405	444	450	480
10 % Wt. Loss (°C)[b]	524	476	466	494	491	509

DMAc = *N*,*N*-dimethylacetamide, THF = tetrahydrofuran. [a]Determined by DSC with a heating rate of 10 °C/min. [b]Determined by TGA with a heating rate of 10 °C/min

3.4 Conclusions

It was shown that the addition of electron-donating groups onto the bipyridine ligand had little to no effect on the molecular weight of poly(2-benzenesulfonyl-1,4-benzene). Bipy, *t*-butyl bipy, methyl bipy and methoxy bipy were all used as coordinating ligands in the

Ni(0)-catalyzed coupling of 2-benzenesulfonyl-1,4-dichlorobenzene, and only oligomeric material with $<M_n>$ up to 1450 g/mol was observed. Altering the solvent, temperature and reaction times also had no effect on the molecular weight of the final product. It appears that the structure of the monomer is the dominating factor in the ability to achieve high molecular weight material in this system. Materials synthesized in THF versus those synthesized in DMAc showed higher T_gs and thermal stability. Also, all polymerizations produced insoluble fractions that were similar in appearance to the soluble portions and showed similar thermal stability but no apparent thermal transitions. Altering the monomer structure to include an electron-donating substituent at the 4'-position may help to offset the strong electron-withdrawing sulfonyl group.

3.5 Acknowledgements

We would like to thank Chevron-Phillips and UNC-Chapel Hill Startup Funds for funding of this research.

3.6 References

1. Phillips, R. W.; Sheares, V. V.; Samulski, E. T.; DeSimone, J. M. *Macromolecules* **1994**, *27*, 2354.

2. Percec, V.; Bae, J. Y.; Zhao, M.; Hill, D. H. *J. Org. Chem.* **1995**, *60*, 176.

3. Grob, M. C.; Feiring, A. E.; Auman, B. C.; Percec, V.; Zhao, M.; Hill, D. H. *Macromolecules* **1996**, *29*, 7284.

4. Percec, V.; Okita, S.; Weiss, R. *Macromolecules* **1992**, *25*, 1816.

5. Colon, I.; Kelsey, D. R. *J. Org. Chem.* **1986**, *51*, 2627.

6. Pei, J. Yu, W. –L.; Ni, J.; Lai, Y. –H.; Huang, W.; Heeger, A. J. *Macromolecules* **2001**, *34*, 7241.

7. Wang, Y.; Quirk, R. P. *Macromolecules* **1995**, *28*, 3495.

8. Stille, J. K.; Lau, K. S. Y. *Acc. Chem. Res.* **1977**, *10*, 434.

9. Marrocco, M. L.; Gange, R. R. U.S. Patent 5,27,457, 1993.

10. Bloom, P. D.; Sheares, V. V. *Macromolecules*, **2001**, *34*, 1627.

11. Pasquale, A. J.; Sheares, V. V. *J. Polym. Sci., Part A: Polym. Chem.* **1998**, *36*, 2611.

12. Bloom, P. D.; Jones III, C. A.; Sheares V. V. *Macromolecules* **2005**, *38*, 2159.

13. Hagberg, E. C.; Olson, D. A.; Sheares, V. V. *Macromolecules* **2004**, *37*, 4748.

CHAPTER 4

SYNTHESIS OF POLY(PARAPHENYLENE) CONTAINING THERMALLY REMOVABLE SOLUBILIZING GROUPS

4.1 Introduction

4.1.1 General Introduction

The synthesis of new high-performance polymeric materials continues to receive much interest as the demand for materials with outstanding physical, thermal and chemical properties increases. The automotive, aerospace, construction and electronics industries rely more on polymeric materials than ever before. Compared to their metallic counterparts, polymeric materials offer higher strength-to-weight ratios. This allows plastics to serve as replacements for heavier metallic parts for overall energy conversation. In addition to weight reduction other beneficial properties of polymeric materials include chemical resistance, lubricity, abrasion resistance, optical clarity and general ease of processing.[1]

Poly(paraphenylene)s are a popular class of high performance thermoplastic polymers due to their outstanding physical and thermal properties. Poly(paraphenylene) (PPP) itself has very low solubility in organic solvents. PPP has been produced by the Kovacic method shown in **Scheme 1**.[2] Unfortunately, this reaction leads to an insoluble and intractable product with low molecular weight and irregular structure. This approach with other aromatics, including biphenyl, *p*-terphenyl, and naphthalene, produced similar results.[3] Percec *et al.*[4] produced oligo-1,4-phenylenes via Ni(0)-catalyzed coupling of isomeric 4,4'''-dichloroquaterphenyls (**Scheme 2**). Again, only low molecular weight materials with irregular structure were produced. Thermal aromatization of poly(1,3-cyclohexadiene)s has also been attempted (**Scheme 3**).[5] The free radical polymerization technique used for this polymerization produced a fair amount of 1,2 coupling. The actual structure produced was a series of cyclohexene-interrupted PPP oligomers.

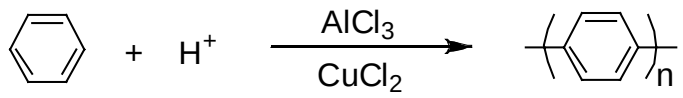

Scheme 4.1. Synthesis of PPP via the Kovacic method

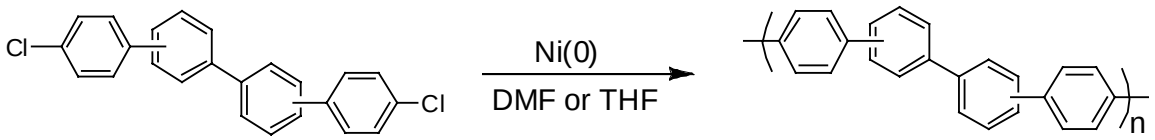

Scheme 4.2. Synthesis of PPP via Ni(0) coupling method

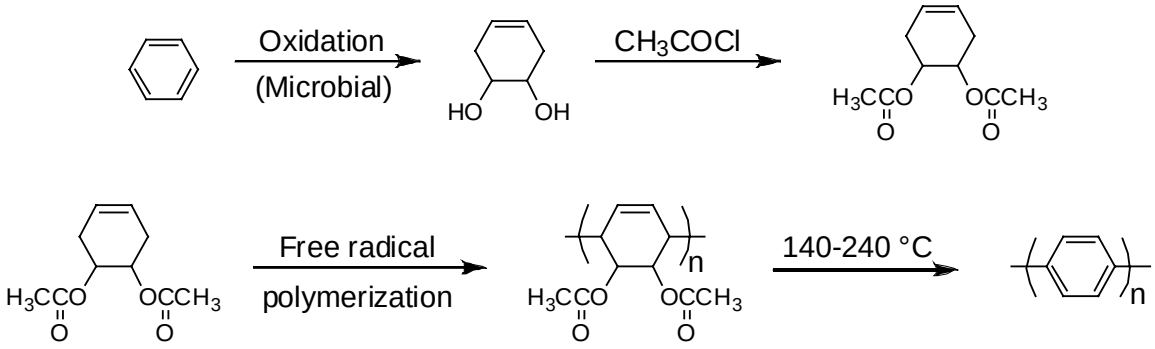

Scheme 4.3. Synthesis of PPP via aromatization of a poly(cyclohexadiene) precursor

Pendant groups have been used to improve PPP solubility (**Scheme 4**).[6-8] Specifically, the use of benzoyl pendant groups attached to phenylene monomers improved solubility of growing chains during polymerization and allowed for the production of high molecular weight material (**Scheme 4C**).[8] While addition of pendant groups onto the PPP backbone increases the solubility of the polymers and allows them to achieve high molecular weights, these groups either decrease the mechanical and thermal stability of the polymers when compared to native PPP or, in the case of poly(2,5-benzophenone), result in materials that are still too brittle to produce tough films or molded materials.

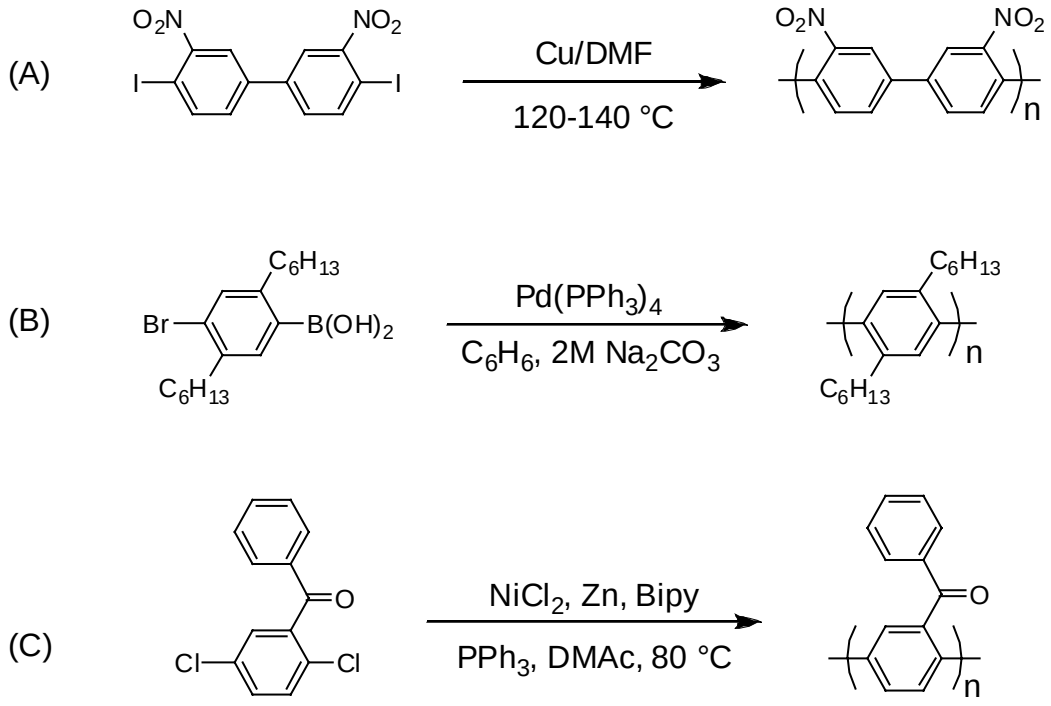

Scheme 4.4. Synthetic methods for the production of high molecular weight PPPs containing solubilizing pendant groups. (A) Ullman method[6] (B) Suzuki method[7] (C) Colon method[8]

Synthesis of solution-processable conjugated polymers is also key in the development of low-cost solar cells.[9] To make conjugated polymers solution-processable, the addition of solubilizing side groups is usually necessary. The introduction of these groups tends to interrupt orderly stacking of polymer chains and results in a decrease in the density of chromophores. However, using thermally removable solubilizing groups has been shown to cause an enhancement in the photocurrent of photovoltaic devices.[10]

4.1.2 Specific Aims

Herein, we describe the synthesis of a PPP derivative synthesized via Ni(0)-catalyzed coupling polymerization containing tertiary ester pendant groups (**Scheme 5**). The presence of the pendant groups causes the polymer to be soluble in common organic solvents and solvent cast into films. The ester groups can also be thermally-cleaved at moderate

temperatures to afford a poly(2,5-benzoic acid). This carboxylic acid functionalized polymer can be further heated and converted to native poly(paraphenylene) via decarboxylation (**Scheme 6**).

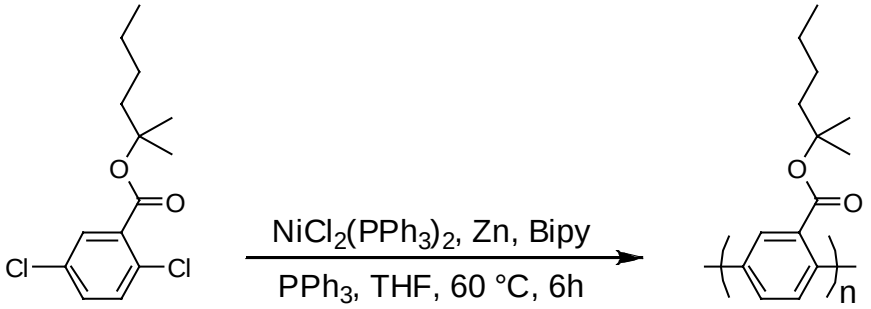

Scheme 4.5. Synthesis of ester-functionalized PPP via Ni(0) coupling method

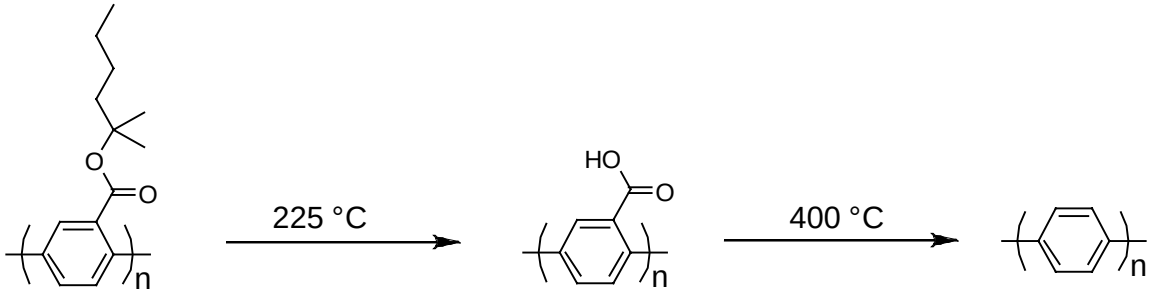

Scheme 4.6. Thermal cleavage of ester-functionalized PPP to acid-functionalized PPP to native PPP

4.2 Experimental

4.2.1 Materials. All reagents were purchased from Aldrich and used without further purification unless otherwise noted. Tetrahydrofuran (THF) was refluxed over sodium and benzophenone, distilled before use, and stored over 4 Å molecular sieves. 2,2'-Bipyridyl

(Bipy) and triphenylphosphine (PPh_3) were purified by recrystallization from ethanol and *n*-heptane, respectively.

4.2.2 Instrumentation. ^1H and ^{13}C NMR spectra were acquired in deuterated solvents on a Bruker 400 AVANCE spectrometer. Molecular weights, relative to narrow polystyrene standards, were measured using a Waters GPC system using RI detection. The measurements were taken at 35 °C with THF as the mobile phase on three columns (Waters Styragel HR2, HR4, HR5). Thermal transitions were measured with a Seiko 220C DSC on the second heat with a heating rate of 10 °C/min. Thermogravimetric analysis was carried out using a Perkin Elmer TGA with a heating rate of 10 °C/min or 50 °C/min in a N_2 atmosphere. UV-vis spectra were recorded using a Shimadzu UV-2401PC spectrophotometer. For the measurements of thin films, polymers were spin-coated onto precleaned quartz slides from 10 mg/mL polymer solutions in chlorobenzene.

4.2.3 Synthesis of 2-Methyl-2-hexyl-2,5-dichlorobenzene-2-carboxylate. To a mixture of 2,5-dichlorobenzoic acid (15.0 mmol) and 2-chloro-3,5-dinitropyridine (15.0 mmol) in pyridine (30 mL) was added 2-methyl-2-hexanol (19.5 mmol). The mixture was refluxed under N_2 at 115 °C for 1 h. The reaction mixture was allowed to cool to room temperature and poured into 6% aqueous $NaHCO_3$ (300 mL) and extracted with diethyl ether. The combined organic phases were washed with water then dried over anhydrous Na_2SO_4. The solvent was removed and the dark orange residue was purified by column chromatography (SiO_2) using ethyl acetate/hexane (1:7) as eluent. The desired product was obtained as a light yellow oil (32 % recovery). ^1H-NMR: δ (ppm) = 0.91 (t, 3H), 1.35 (m, 4H), 1.56 (s, 6H), 1.88 (t, 2H), 7.68 (s, 1H), 7.36 (overlap of 2 singlets, 2H).

4.2.4 Polymer Synthesis. In a glove box in an argon atmosphere, bis(triphenylphosphine)nickel(II) dichloride (0.1 equiv.), zinc (3.1 equiv.), TPP (0.2 equiv.) and bipy, (0.1 equiv) were added to a flask equipped with an overhead stirrer. The reaction vessel was then removed from the glove box and evacuated and refilled three times with nitrogen. THF (10 equiv.) was added via syringe and the mixture was stirred at 60 °C. Upon addition of solvent the mixture turned green, indicating the presence of Ni(II). Once the mixture became a deep red, indication of Ni(0), monomer (1.0 equiv.) was added and allowed to react for a specified amount of time. The polymer was then precipitated in hydrochloric acid and methanol (1:8), filtered, and washed with methanol. A Soxhlet extraction was performed with chloroform on the collected polymer. The organic solution was then concentrated and the polymer was precipitated into stirring methanol. The polymer was collected via filtration and dried under vacuum (86% recovery). ^{1}H-NMR: δ (ppm) = 0.75-2.00 (broad, 15H), 7.25-8.00 (broad, 3H).

4.3 Results and Discussion

4.3.1 Monomer Synthesis

The synthesis of 2-methyl-2-hexyl-2,5-dichlorobenzene-2-carboxylate was conducted based on the synthesis of 2-methyl-2-hexyl-2-5-dibromothiophene-3-carboxylate.[10] The structure of this monomer was chosen because the tertiary ester group allows for thermal cleavage at a relatively low temperature and the branched nature of the ester group contributes to higher solubility of the polymer. The esterification of 2,5-dichlorobenzoic acid was carried out using 2-chloro-2,5-dinitropyridine as a condensing agent in pyridine at 115 °C for 1 hour to afford the desired product as a light yellow oil in 32 % yield following extraction and column chromatography.

4.3.2 Polymer Synthesis and Characterization

The ester-functionalized PPP (**P1**) was synthesized utilizing Ni(0)-catalyzed coupling of the aryl dihalide monomer (**Scheme 5**). Conditions similar to those that had been previously optimized for similar monomer systems were used.[11] **P1** was synthesized with an $<M_n>$ of 4.0 kg/mol with a PDI of 1.8 as measured by GPC. The resulting polymer was a slightly yellow, soft tacky material that showed a broad glass-transition around –4 °C.

Thermogravimetric analysis (TGA) showed two distinct weight-loss phenomena (**Figure 1**). Using a fast temperature ramp of 50 °C/min a rapid weight-loss event occurs ~200 °C leveling off between 55 and 60 % of the original mass. We believe this corresponds with elimination of 2-methyl-2-hexene, which accounts for 45% of the total polymer weight. Upon further heating, a second rapid weight-loss event occurs ~400 °C leveling off between 35 and 40 % of the original mass. The molar masses for the repeat unit of carboxylic acid functionalized PPP (120 g/mol) and native PPP (76 g/mol) are 55 and 35 % of the molar mass of the **P1** repeat unit (218 g/mol). These calculated figures correlate extremely well with the TGA data obtained for this polymer system.

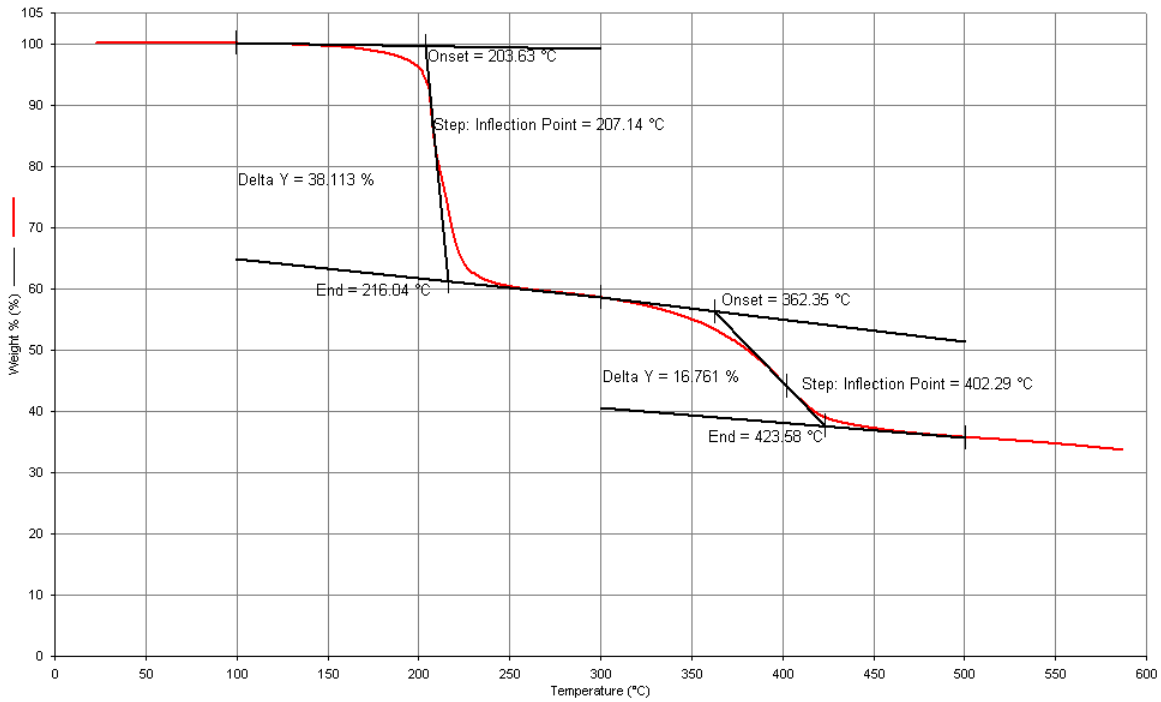

Figure 4.1. TGA curve of ester-functionalized PPP at a temperature ramp of 50 °C/min

4.3.3 Photophysics

We were interested in studying how these thermolysis events affected the bandgap of the materials. Freshly spin-coated samples were left at room temperature or annealed at approximately 225 °C or 400 °C for 5 minutes. After annealing, it was possible to visually see the color change of the films. The samples left at room temperature were clear and colorless, the samples annealed at 225 °C were slightly yellow and the samples annealed at 400 °C were reddish-orange. **Figure 2** shows the results of UV-vis analysis of **P1** annealed at different temperatures.

Optical bandgaps were calculated from the onset of absorption of the UV-vis spectrum. Unannealed **P1** shows a bandgap ~3.5 eV while the sample annealed at 225 °C is slightly red-shifted and has a bandgap ~3.4 eV. The sample annealed at 400 °C shows a drastic change in the photophysical properties. The absorption spectrum is extremely red-

shifted compared to the other samples and there is a drastic decrease in the bandgap to ~2.3 eV.

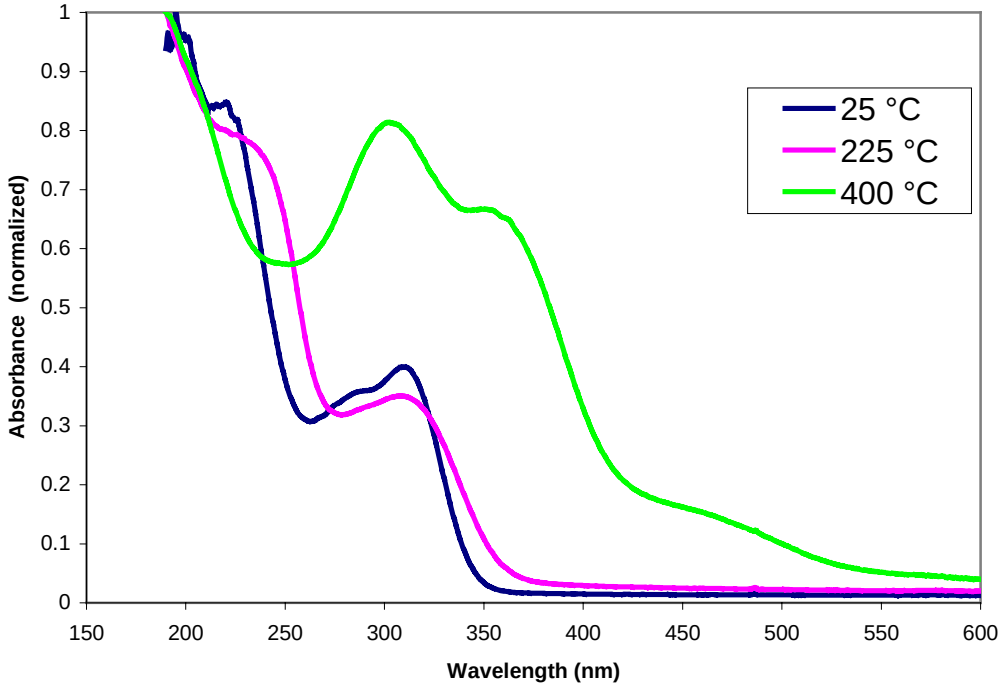

Figure 4.2. UV-Vis spectra of spin-coated films on quartz slides and annealed at three different temperatures (25, 225 and 400 °C)

4.4 Conclusions

We have shown a simple method for synthesizing a soluble ester-functionalized PPP derivative that can be processed into carboxylic acid-functionalized PPP and native PPP through a simple thermal treatment. Upon heating the bulk material, it goes from a soluble, soft and malleable material to an intractable powdery solid. A significant change in the photophysical properties was observed in the spin-coated films upon annealing with a decrease in the measured bandgap of 1.2 eV from the ester-functionalized PPP to native PPP.

The fact that these polymers have tunable solubility and electronic properties makes them promising interface materials in solution-processed multiplayer solar cells. Also, the fact that the ester-functionalized polymer is easily malleable could lead it to be used as a precursor for molding shapes that could then be heated to produce molded poly(paraphenylene).

4.5 Acknowledgement.

We would like to thank ACS PRF for funding of this research.

4.6 References

1. Rosato, D.V.; Di Mattia, D. P.; Rosato, D. V. *Designing with Plastics and Composites, a Handbook*. Van Nostrand Reinhold: New York, 1991, p. 1-9.

2. Kovacic, P. and Kyriakis, A. *J. Org. Chem.* **1963**, *29*, 100.

3. Odian, G. *Principles of Polymerization*, 3rd edition; Wiley-Interscience: New York, 1991, p. 175.

4. Percec, V. and Okita, S. *J. Polym. Sci. Pt. A: Polym. Chem.* **1993**, *31*, 877.

5. Ballard, D. G. H.; Courtis, A.; Shirley, I. M.; Taylor, S. C. *J. Chem. Soc., Chem. Commun.* **1983**, *17*, 954.

6. Wirth, H. O.; Muller, R.; Kern, W. *Makromol. Chem.* **1964**, *77*, 90.

7. Rehahn, M.; Schluter, A. D.; Wegner, G.; Feast, W. J. *Polymer* **1989**, *30*, 1060.

8. Phillips, R. W.; Sheares, V. V.; Samulski, E. T.; DeSimone, J. M. *Macromolecules* **1994**, *27*, 2354.

9. Padinger, F.; Rittberger, R. S.; Sariciftci, N. S. *Adv. Funct. Mater.* **2003**, 85.

10. Liu, J.; Kadnikova, E. N.; Liu, Y.; McGehee, M. D.; Fréchet, J. M. J. *J. Am. Chem. Soc.* **2004**, *126*, 9486.

11. Hagberg, E. C.; Olson, D. A.; Sheares, V. V. *Macromolecules*, **2004**, *37*, 4748-4754.

CHAPTER 5

ALTERNATING DONOR-ACCEPTOR COPOLYMERS CONTAINING THERMALLY REMOVABLE SOLUBILIZING GROUPS

5.1 Introduction

5.1.1 General Introduction

Conjugated polymer based solar cells are a promising alternative to inorganic semiconductor photovoltaic devices. Synthesis of a solution-processable conjugated polymer is key in the development of low-cost solar cells.[1] To make conjugated polymers solution-processable, the addition of solubilizing side groups is usually necessary. The introduction of these groups tends to interrupt orderly stacking of polymer chains and results in a decrease in the density of chromophores. However, the use thermally removable solubilizing groups has been shown to cause an enhancement in the photocurrent of photovoltaic devices.[2] Also, a general drawback with heterojunction devices made from polymer blends is that transport and collection of charges can be hindered by phase boundaries and discontinuities. One way to overcome this is to covalently bond donor and acceptor units into the same polymer chain.[3-5] The following research combines the benefits of a thermally removable solubilizing group onto alternating donor-acceptor copolymers with varying backbone structure.

5.1.2 Thermally Removable Solubilizing Groups

Liu *et al.* first took advantage of a thermally removable solubilizing group by synthesizing an ester-functionalized polythiophene (**Scheme 1**).[2] They were able to fabricate trilayer solar cells with the functionalized polythiophene as an interface material between poly(3-hexylthiophene) (P3HT) and titania layers and compare it to a bilayer device of P3HT and titania. A 3-fold increase in photocurrent was seen upon introduction of the ester-functionalized polythiophene. Further study into this material focused on the stability of solar cells fabricated with **1a**.[6] It was reported that **1a** behaved significantly different from any material previously tested and was estimated to have an operational lifetime in excess of

20,000 h. Analysis of this system showed that an increase in the rigidity, through more efficient packing and the formation of a hydrogen-bonded network, and self-doping in an oxidized state increased the stability of the system in a solar cell device.[7]

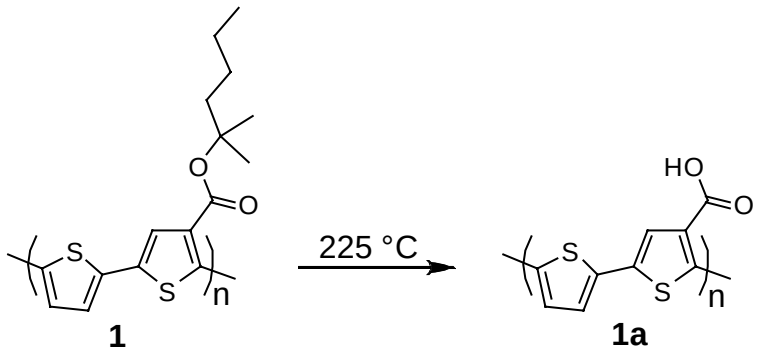

1 **1a**

Scheme 5.1. Ester-functionalized polythiophene before (**1**) and after (**1a**) thermolysis

Native polythiophene was produced from this same ester-functionalized polythiophene by heating the material to 300 °C. Bulk heterojunction solar cells were fabricated with the functionalized polymer mixed with PCBM. Thermal annealing/cleavage led to a bulk heterojunction device with native polythiophene as the matrix for the active layer with efficiencies of 1.5%.[8] Native polyparaphenylene was produced incorporating similar techniques with an observed decrease in bandgap upon cleavage of the ester group and again upon cleavage of the acid.[9] While these are promising materials, no research has been conducted on the further functionalization of this class of materials to control the bandgap.

In this work, we present the synthesis of solution processable alternating donor-acceptor conjugated polymers that undergo chemical conversions through thermal processing. The effects of this conversion on the bandgap of thin films of these materials are presented.

5.2 Experimental

5.2.1 Materials. All reagents were purchased from Aldrich and used without further purification unless otherwise noted. Tetrahydrofuran (THF) was refluxed over sodium and benzophenone and then distilled. *N*,*N*-Dimethylformamide (DMF) was dried over 4A molecular sieves, filtered and distilled. Toluene was dried by distillation after stirring over calcium hydride. 1,4-Dibromo-2,5-dimethoxybenzene (99%) and copper(I) iodide (98%) were purchased from Fisher and used without further purification.

5.2.2 Instrumentation. ^{1}H and ^{13}C NMR spectra were acquired in deuterated solvents on a Bruker 400 AVANCE spectrometer. Molecular weights, relative to narrow polystyrene standards, were measured using a Waters GPC system using RI detection. The measurements were taken at 35 °C with THF as the mobile phase on three columns (Waters Styragel HR2, HR4, HR5). Thermal transitions were measured with a Seiko 220C DSC on the second heat with a heating rate of 10 °C/min. Thermogravimetric analysis was carried out using a Perkin Elmer TGA with a heating rate of 10 °C/min in a N_2 atmosphere. UV-vis spectra were recorded using a Shimadzu UV-2401PC spectrophotometer. For the measurements of thin films, polymers were spin-coated onto precleaned quartz slides from 10 mg/mL polymer solutions in chlorobenzene.

5.2.3 Monomer Synthesis

2,5-Dibromothiophene-3-carboxylic acid. To a mixture of thiophene-3-carboxylic acid (5.0 g, 39.0 mmol) and 60 mL acetic acid 10 mL of Br_2 was added dropwise and stirred at 60 °C for 8 h. The mixture was allowed to cool and precipitated into 300 mL of cold water and Na_2SO_3 was added to decolorize. After filtering a yellow precipitate was collected and

recrystallized from water and ethanol (2:1) to afford off-white crystals (6.92 g, 62% recovery). ^{1}H-NMR ($CDCl_3$): δ (ppm) = 7.40 (s, 1H).

2-Methyl-2-hexyl-2,5-dibromothiophene-3-carboxylate. To a mixture of 2,5-dibromothiophene-3-carboxylic acid (3.0 g, 10.5 mmol) and 2-methyl-2-hexanol (1.6 g, 13.7 mmol) in pyridine (15 mL) was added 2-chloro-3,5-dinitropyridine (2.1 g, 10.5 mmol). The mixture was stirred at 115 °C for 30 min. The reaction mixture was allowed to cool to room temperature and poured into 6% aqueous $NaHCO_3$ (300 mL) and extracted with diethyl ether. The combined organic phases were washed with water then dried over anhydrous Na_2SO_4. The solvent was removed and the residue was purified by column chromatography (SiO_2) using ethyl acetate/hexane (1:7) as eluent. The desired product was obtained as a light yellow oil (1.1 g, 27% recovery). ^{1}H-NMR (CD_2Cl_2): δ (ppm) = 0.91 (t, 3H), 1.34 (m, 4H), 1.52 (s, 6H), 1,84 (t, 2H), 7.29 (s, 1H).

2-Methyl-2-hexyl-1,4-dibromobenzene-2-carboxylate. The same procedure as the synthesis of 2,methyl-2-hexyl-2,5-dibromothiophene-3-carboxylate was employed using 2,5-dibromobenzoic acid (3.0 g, 10.0 mmol) resulting in a light yellow oil (1.9 g, 50% recovery). ^{1}H-NMR (CD_2Cl_2): δ (ppm) = 0.91 (t, 3H), 1.35 (m, 4H), 1.56 (s, 6H), 1.88 (t, 2H), 7.42 (dd, 1H), 7.49 (d, 1H), 7.77 (d, 1H).

2,5-Dibromobenzoyl chloride. To a mixture of 2,5-dibromobenzoic acid (4.3 g, 15.3 mmol) and 1,2-dichloroethane (50 mL) was added dropwise thionyl chloride (20 mL). The solution was allowed to reflux for 4 h then allowed to cool to room temperature. The excess solvent was distilled resulting in a yellow solid (4.5 g, 100% recovery). ^{1}H-NMR (CD_2Cl_2): δ (ppm) = 7.59 (m, 2H), 8.17 (dd, 1H)

2,5-Dibromobenzophenone. To a solution of 2,5-dibromobenzoylchloride (4.3 g, 14.4 mmol) in benzene (10 mL) in NO_2CH_3 (10 mL) in an ice bath was added $AlCl_3$ (1.9 g, 14.4 mmol). The ice bath was removed and the solution was allowed to stir for 18 h at room temperature. The mixture was precipitated into cold acidic water and a light yellow powder was collected by filtration. The resulting solid was recrystallized from ethanol to give white crystals (2.6 g, 53% recovery). ^{1}H-NMR (CD_2Cl_2): δ (ppm) = 7.48-7.53 (overlap of peaks, 5H), 7.64 (tt, 1H), 7.78 (dd, 2H).

1,4-Bis-trimethylstannanyl-2,5-dimethoxybenzene. To a solution of 1,4-dibromo-2,5-dimethoxybenzene (5.0 g, 16.9 mmol) in THF (50 mL) at -78 °C was added butyllithium (25.5 mL of 2.0M in cyclohexane) and the mixture was warmed to 0 °C and allowed to stir for 1 h. The reaction mixture was cooled to -78 °C and $SnCl(CH_3)_3$ was added (51 mL of 1.0M in THF) and the solution was allowed to warm to room temperature and stir for 16 h. The reaction mixture was poured into water, extracted with diethyl ether, dried over $MgSO_4$, and the solvent was removed. The crude product was recrystallized from ethanol to afford the desired product as white crystals (2.7 g, 35% recovery). ^{1}H-NMR (CD_2Cl_2): δ (ppm) = 0.24 (t, 18H), 3.75 (s, 6H), 6.85 (s, 2H).

2,5-Bis-trimethylstannanyl-3,4-ethylenedioxythiophene. To a solution of 3,4-ethylenedioxythiophene (2.0 g, 17.5 mmol) in THF (50 mL) at -78 °C was added butyllithium (25.5 mL of 2.0M in cyclohexane) and the mixture was warmed to 0 °C and allowed to stir for 15 min. The reaction mixture was cooled to -78 °C and $SnCl(CH_3)_3$ was added (51 mL of 1.0M in THF) and the solution was allowed to warm to room temperature and stir for 1 h. The reaction mixture was poured into water, extracted with diethyl ether, dried over $MgSO_4$, and the solvent was removed. The crude product had a melting point near

room temperature and some mono-stannylated product was present, but the product was used without further purification. ^{1}H-NMR (CD_2Cl_2): δ (ppm) = 0.30 (t, 16H), 4.1 (t, 4H).

5.2.4 Polymer Synthesis. The following is a general procedure for the polymerization of the above monomers via Stille coupling. A solution of distannylated monomer (1 equiv.), dibrominated monomer (1 equiv.), $Pd(PPh_3)_4$ (0.05 equiv.), and Cu(I)I (2.1 equiv.) in toluene (30 mL) and DMF (10 mL) was stirred at 120 °C for 24 h. The solution was allowed to cool to room temperature and precipitated in 300 mL of methanol and filtered. The polymer was washed by Soxhlet extraction with hexane for 10 h and subsequently by THF for 10 h. The extracted fraction was concentrated and precipitated into methanol, filtered, and dried in a vacuum oven overnight.

5.3 Results and Discussion

5.3.1 Monomer Synthesis and Characterization. The monomers in **Figure 1** were chosen to allow for the study of the effect of polymer backbone structure on bandgap while also looking at how different solubilizing groups affect the packing of the polymer chains.

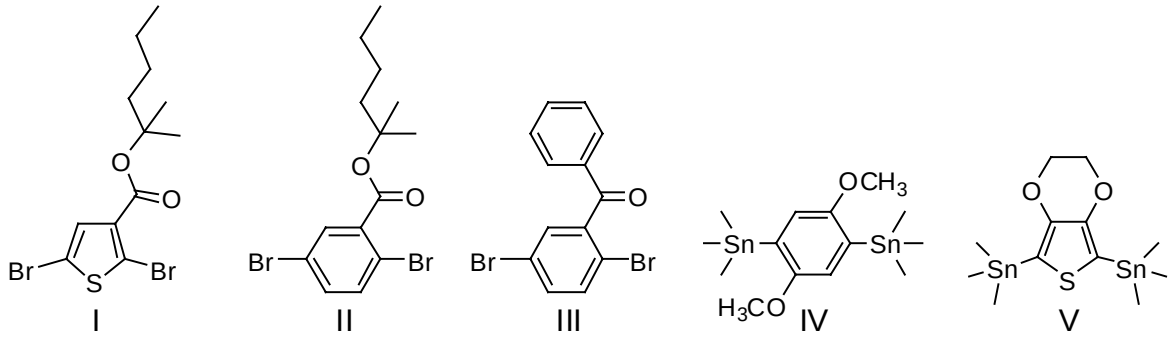

Figure 5.1. Monomers used for Stille coupling with pendant electron-withdrawing groups (I-III) and electron-donating groups (IV-V)

To achieve the synthesis of monomer **I,** thiophene-3-carboxylic acid first was brominated by slowly adding Br_2 to acetic acid and thiophene-3-carboxylic acid, resulting in off-white crystals with a melting point of 180 °C.

The esterification of the respective carboxylic acids to afford monomers I and II was carried out using 2-chloro-3,5-dinitropyridine as a condensing agent in pyridine at 115 °C for 30 minutes to afford **I** and **II** as light yellow oils (**Figure 2**).[9] The structure of monomers I and II was selected for a variety of reasons. The tertiary ester group allows for thermal cleavage at a relatively low temperature, the branched nature of the ester group contributes to higher solubility of the polymer, and a carboxylic acid π-conjugated to the polymer backbone remains after thermal cleavage of the ester group with further cleavage of the acid group occuring at higher temperatures.[2,8,9]

Monomer **III** was synthesized via Friedel-Crafts acylation of 2,5-dibromobenzoyl chloride and benzene in nitromethane with $AlCl_3$ catalyst. After recrystallization from ethanol, white crystals were obtained which exhibited a sharp melting peak at 104 °C. The structure of monomer **III** was chosen to allow for the comparison of alkyl solubilizing groups versus aromatic solubilizing groups and how they affect the packing of the polymer chains.

Monomer **IV** was synthesized via lithiation followed by stannylation of 1,4-dibromo-2,5-dimethoxybenzene to yield white needle-like crystals after recrystallization from ethanol.

Monomer **V** was synthesized via lithiation followed by stannylation of 3,4-ethylenedioxythiophene, in a similar method as monomer **IV**, to yield low melting orange-red crystals.

Monomers **IV** and **V** are the donor monomers in the copolymer due to the methoxy groups present on them. They will allow for the study of whether having the donating group

on a phenyl ring or a thiophene ring will affect the electronic properties of the polymer more significantly.

Since Stille coupling was going to be the method of polymerization, the acceptor monomers were dibrominated while the donor monomers were distannylated. This should allow for the most reactive system as the oxidative addition of the aryl halide is consistent with an aromatic nucleophilic substitution and the presence of an electron-withdrawing substituent leads to rate acceleration.[11]

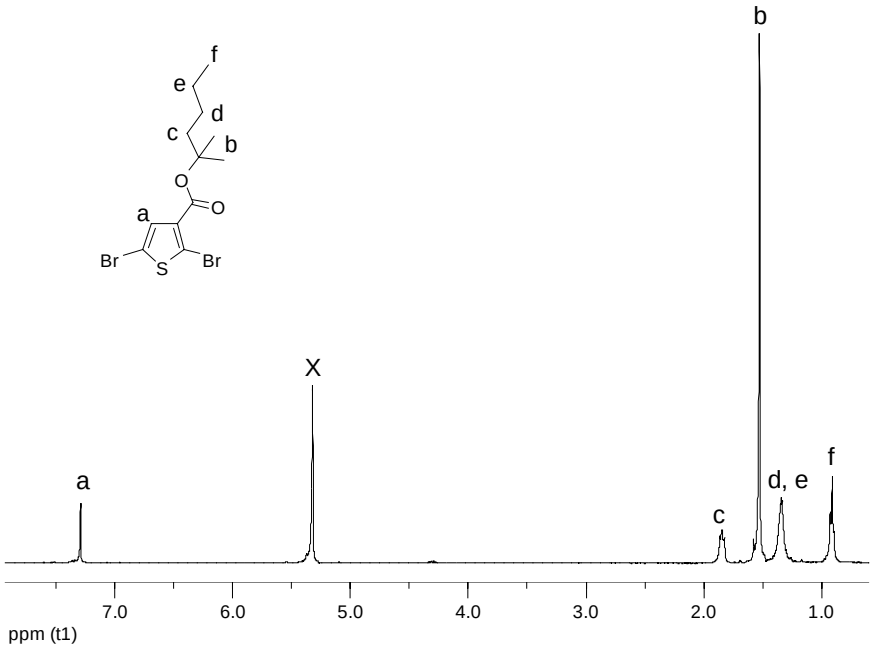

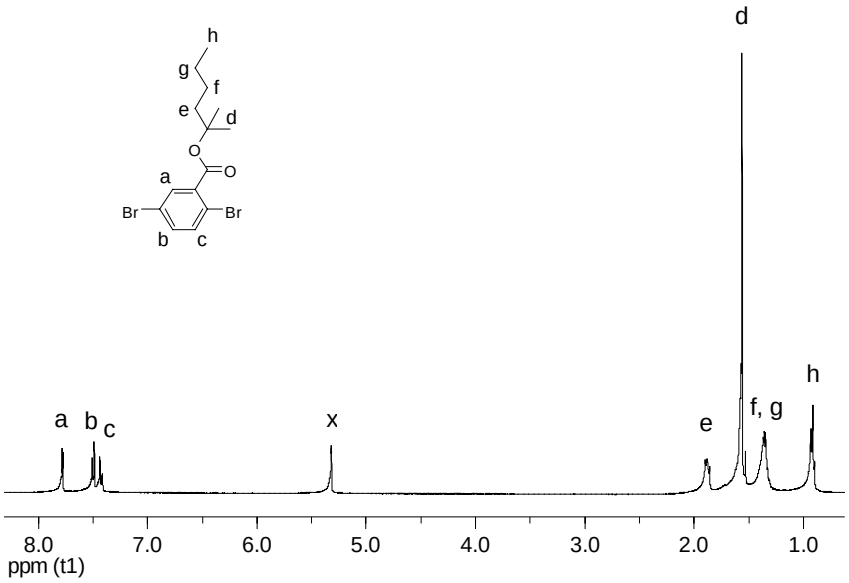

Figure 5.2. ^{1}H NMR spectrum and structural assignments of monomer I (top) and monomer II (bottom) in CD_2Cl_2

5.3.2 Polymer Synthesis and Characterization

A series of polymers were synthesized via Stille coupling (**Figure 3**). The polymer structures allowed for the study of how alternating donor and acceptor groups along the backbone of the polymer affect the bandgap of the polymeric system. **PI** is the only polymer in this series that does not possess a thermally cleavable ester on the acceptor monomer. Instead, a thermally stable benzophenone monomer is used to allow a comparison to be made with the cleavable polymer systems. **PII-PIV** contain ester solubilizing groups that can be removed thermally after device fabrication leaving carboxylic acid groups along the backbone which should allow for the polymer chains to pack in a more orderly fashion.

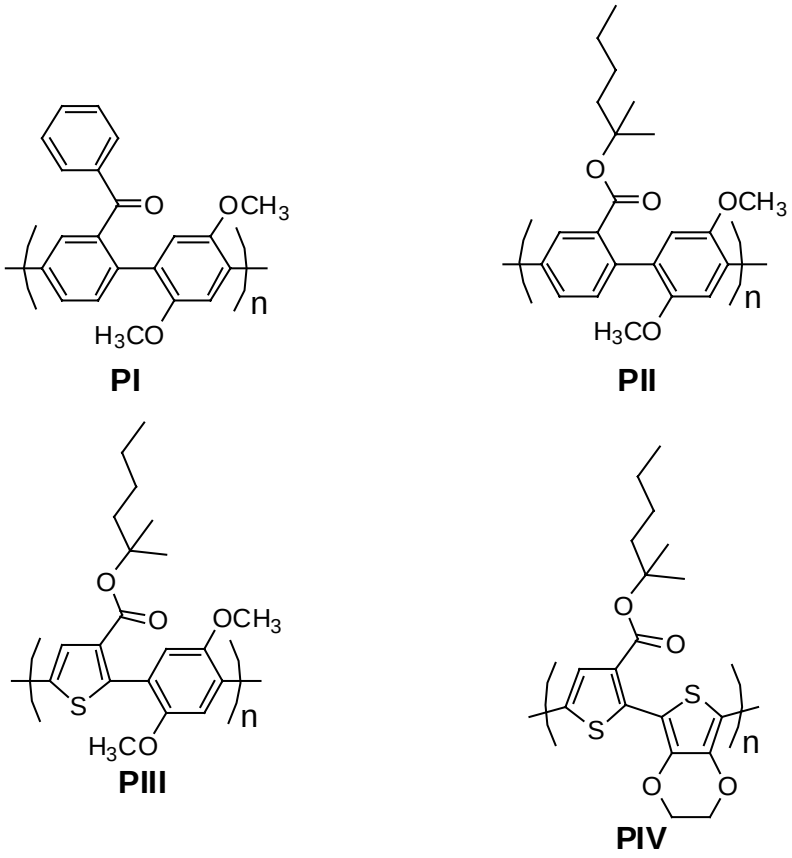

Figure 5.3. Alternating donor-acceptor copolymers synthesized from monomers I-V

First attempts to synthesize **PI** were unsuccessful and no product was able to be isolated. The addition of CuI in subsequent reactions led to polymer formation, and CuI was used in all other polymerizations. It has been suggested that the "copper effect" occurs due to the fact that CuI is able to scavenge free PPh_3 ligand which is known to slow the reaction.[11] After purification, **PI** was collected as a yellow powder in 36 % yield.

Polymers **PII-PIV** were synthesized in a similar manner as **PI**. The polymers produced were low molecular weight. It was expected that the system for **PIII** would achieve higher molecular weight than **PI** or **PII** since thiophene halides tend to be more reactive than phenyl halides. We believe **PIV** was unable to achieve higher molecular weights due to the difficulty of purifying monomer **V**. All polymers were powders that were soluble in common organic solvents such as THF, toluene, and chlorobenzene. Properties of

the polymers are summarized in **Table 1**. While the polymerizations failed to produce high molecular weight materials, they are sufficient to allow the study of structural variability on the bandgap of these polymers.

Sample	$<M_n>^a$ x 10^{-3}	PDI[a]	Yield (%)	T_g[b] (°C)
PI	1.6	1.3	36	127
PII	1.2	1.5	30	160
PIII	5.6	1.3	38	155
PIV	1.7	1.7	15	--[c]

Table 5.1. Properties of alternating donor-acceptor copolymers, a) determined by GPC with THF mobile phase, b) determined by DSC with heating rate of 10 °C/min, c) no thermal transitions observed by DSC

5.3.3 Photophysics

To test the bandgaps of the materials, thin films were spin coated from 10 wt % solutions with chlorobenzene. The samples were then left unannealed or annealed at 225 °C, 300 °C (for thioesters), or 400 °C (for phenyl esters) for 5 min. After the annealing step, UV-vis spectroscopy was conducted to determine the optical bandgaps of the materials. Annealing the samples at 225 °C was conducted to cleave the ester group and leave carboxylic acid functionalized polymers. A sample of **PII** was also annealed at 400 °C to cleave the carboxylic acid (**Figure 4**). Thin films of **PIII** and **PIV** were annealed at 300 °C to cleave the carboxylic acid the thiophene ring **(Figure 5**).

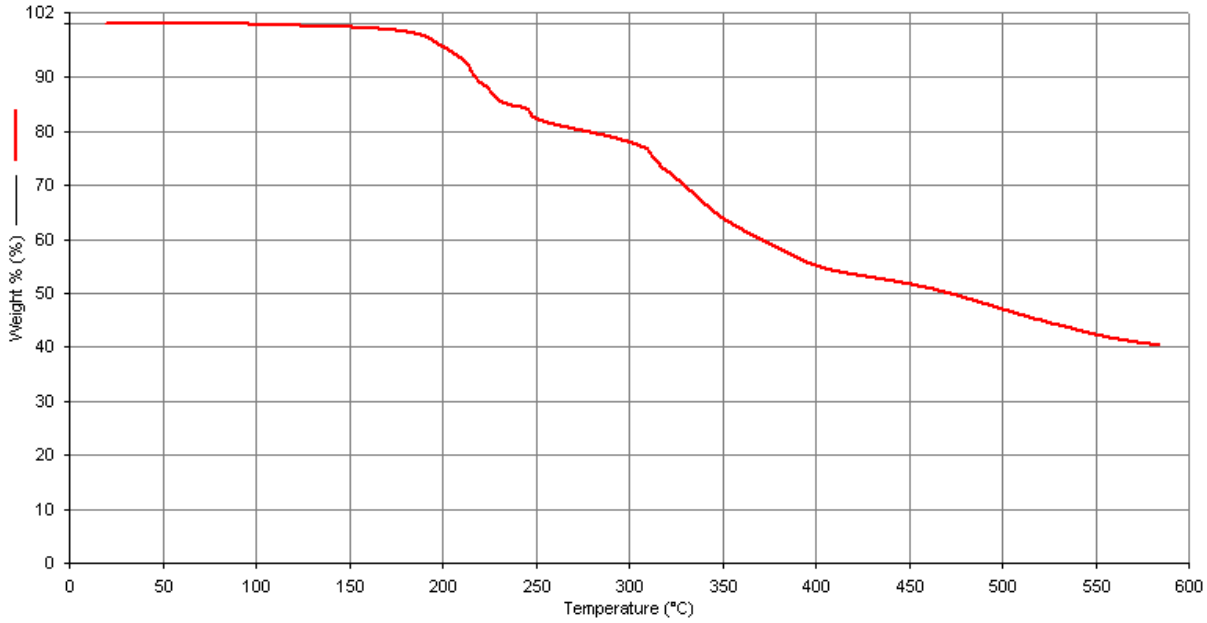

Figure 5.4. TGA curve of **PII**

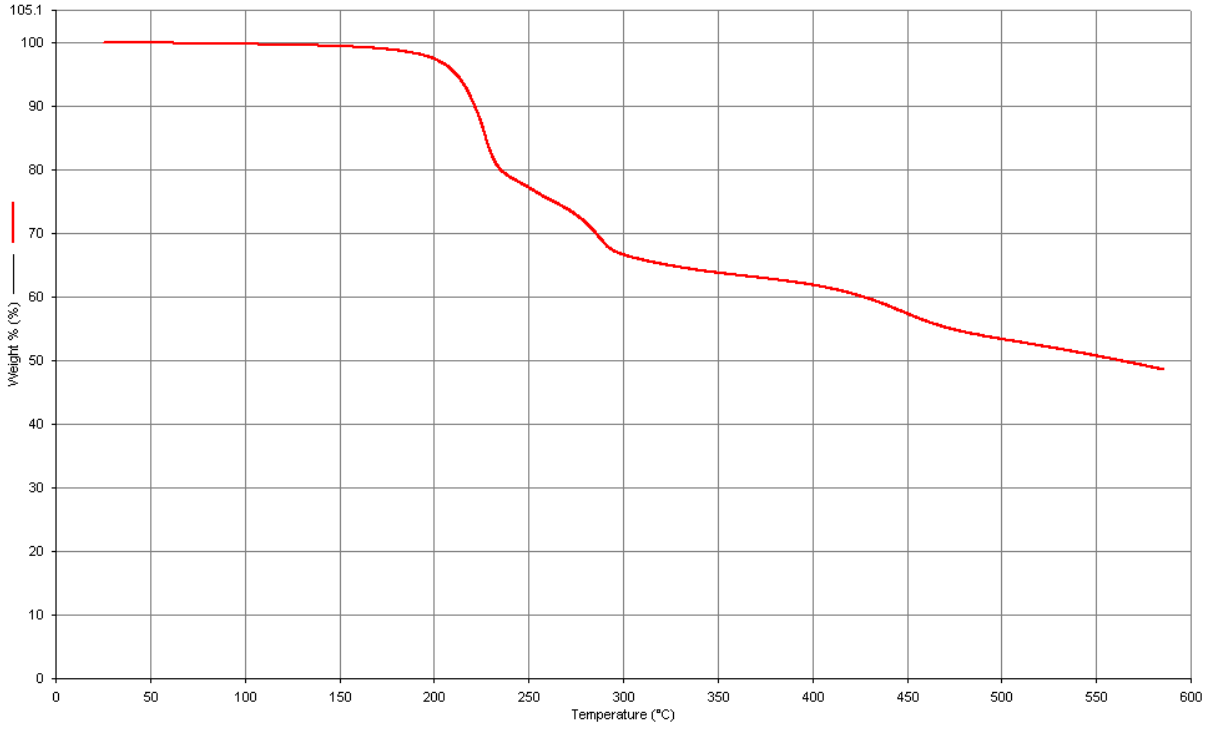

Figure 5.5. TGA curve of **PIII**

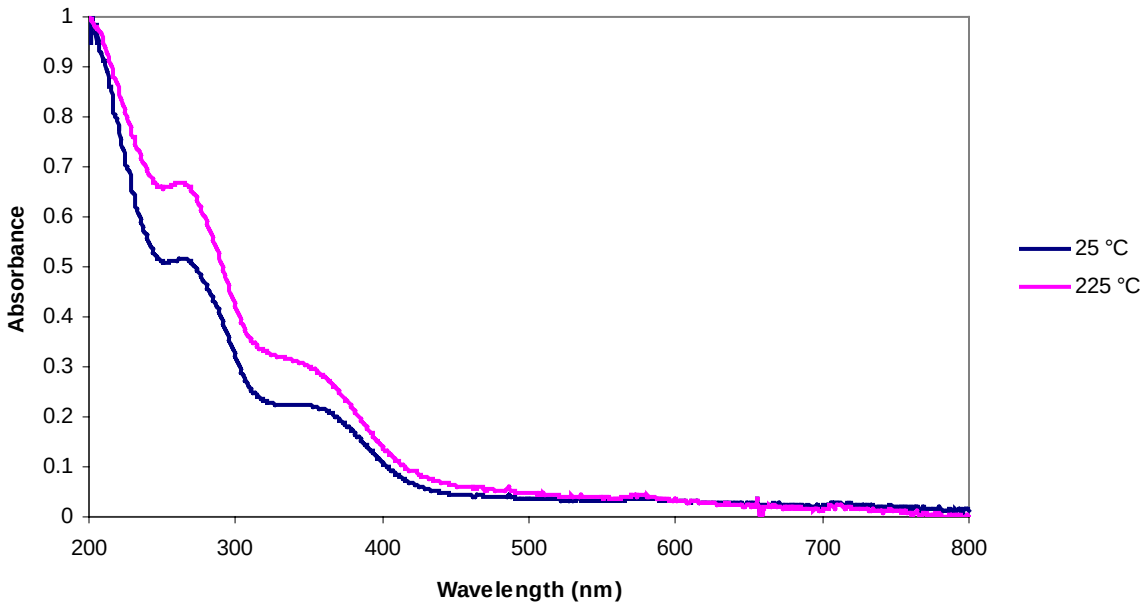

Figure 5.6. Normalized UV-vis of **PI** unannealed (blue) and annealed at 225 °C (pink)

As expected, annealing of **PI** had little effect on the bandgap of the material. The UV-vis spectra for the unannealed sample and the sample annealed at 225 °C both showed absorbance onsets of ~425 nm, corresponding with an optical bandgap of ~2.9 eV (**Figure 6**). This bandgap is too high for this material to be useful in a solar cell device. The bulky benzophenone most likely prevents the phenyl rings along the backbone from adopting a planar geometry, thereby reducing conjugation length. Also, annealing would most likely have little effect due to the fact that the benzophenone unit is thermally stable and does not undergo thermal cleavage at this low of a temperature.

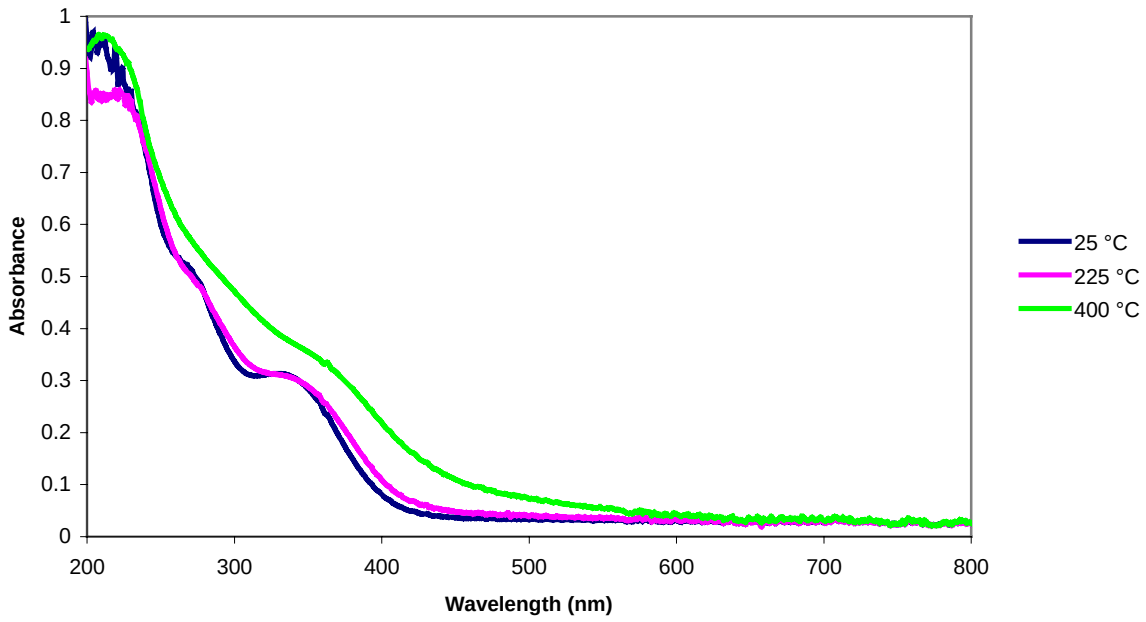

Figure 5.7. Normalized UV-vis of **PII** unannealed (blue), annealed at 225 °C (pink), and annealed at 400 °C (green)

The unannealed sample of **PII** showed very similar absorption to **PI** with an onset of absorbance at ~425 nm (**Figure 7**). Annealing the sample at 225 °C caused a very slight red shift in the absorbance. Annealing at 400 °C provided a significant shift in the absorption. With an onset of absorption ~500 nm the bandgap for **PII** is able to be reduced by ~0.4 eV through thermal cleavage of the solubilizing group. The bandgap for this material, even the sample annealed at 400 °C, is still on the high end of materials used for solar cell applications.

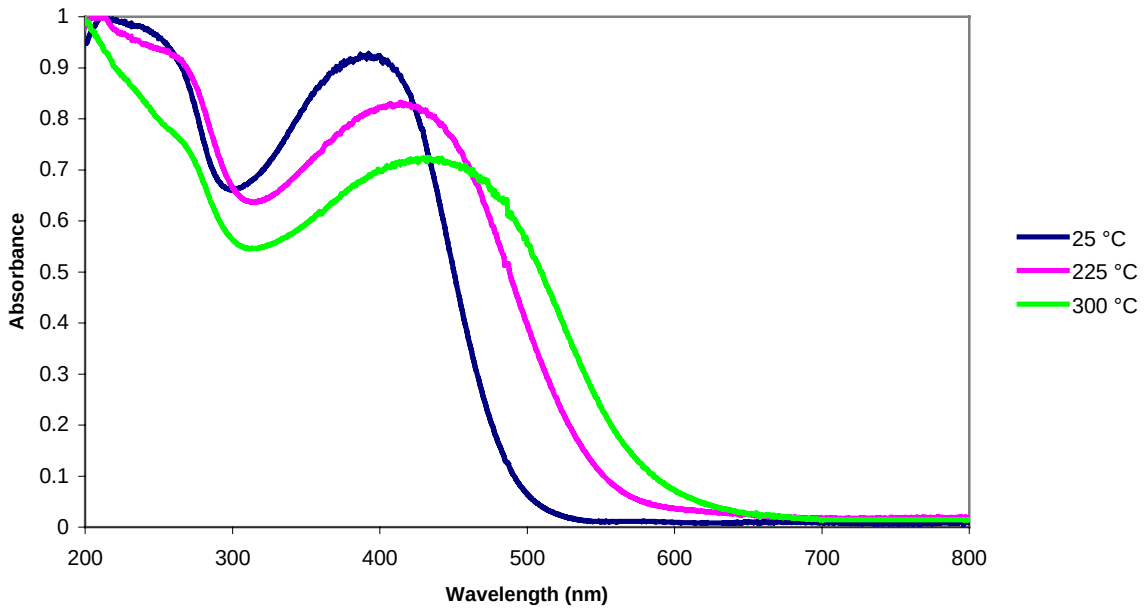

Figure 5.8. Normalized UV-vis of **PIII** unannealed (blue), annealed at 225 °C (pink), and annealed at 300 °C (green)

PI and **PII** both possessed bandgaps too high for use in solar cells. Even with the cleavage of the ester-solubilizing group, the polyparaphenylene backbone is still unable to adopt a planar geometry. In order to increase planarity along the backbone and, thus, produce a lower bandgap material, the phenyl ester (monomer **II**) was replaced with a thioester (monomer **I**). Absorption spectra of the thin films produced from **PIII** are shown in **Figure 8**. The unannealed sample of **PIII** showed a lower bandgap than any of the **PI** and **PII** samples with an onset of absorption ~530 nm, corresponding with a bandgap of ~2.3 eV. The sample annealed at 225 °C showed a significant red shift with the λ_{max} shifting from 395 nm for the unannealed sample to 415 nm and the onset shifting to ~575 nm, giving a bandgap of ~2.2 eV. The sample of **PIII** annealed at 300 °C was even more red-shifted. Its λ_{max} of 435 nm and onset of 630 nm starts to get into the range of the most commonly used polymers (P3HT and MDMO-PPV) for solar cell devices.

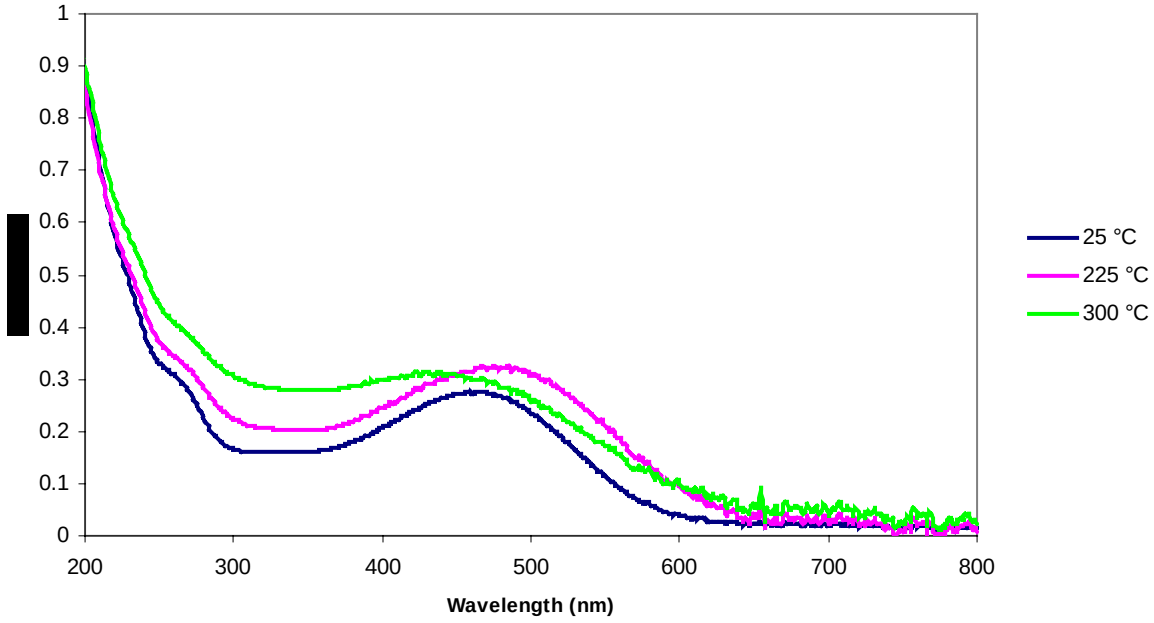

Figure 5.9. Normalized UV-vis of **PIV** unannealed (blue), annealed at 225 °C (pink), and annealed at 300 °C (green)

In order to attempt to lower the bandgap of these polymers even further, EDOT was used as the donor monomer for **PIV**. Many EDOT based polymers have been synthesized with low bandgaps (≤ 1.5 eV).[12-17] As expected, the bandgap of **PIV** was lower than those of **PI-PIII**. The onset of absorption for the unannealed film was ~600 nm, corresponding to a bandgap of ~2.1 eV and a λ_{max} ~445 nm (**Figure 9**). Annealing at 225 °C led to a similar absorption spectra that was red shifted with an onset of ~640 nm (bandgap of ~1.9 eV) and λ_{max} of ~480 nm. The sample annealed at 300 °C had a similar spectrum to the other **PIV** samples. Its onset of absorption was the same as the sample annealed at 225 °C, but the λ_{max} blue-shifted to ~465 nm.

Polymers **PI-PIV** showed a wide range of bandgaps that could, in the cases of **PII-PIV**, be reduced through a simple thermolysis of the solubilizing side groups. **Table 2** shows the bandgaps of all the films, and it is apparent that the use of thermally-cleavable

solubilizing groups leads to materials with good bandgap control as well as the expected result that increasing thiophene content versus phenylene content leads to lower bandgap materials.

Sample-Annealing Temp.	Bandgap[a] (eV)
PI-25 °C	2.9
PI-225 °C	2.9
PII-25 °C	2.9
PII-225 °C	2.9
PII-400 °C	2.5
PIII-25 °C	2.3
PIII-225 °C	2.2
PIII-300 °C	2.0
PIV-25 °C	2.1
PIV-225 °C	1.9
PIV-300 °C	1.9

Table 5.2. The effects of annealing temperature on the bandgap of the polymer, a) calculated from the onset of absorbance from UV-vis spectra

Figure 10 shows 4 mg/mL solutions of **PI-PIV** in THF being exposed to 365 nm excitation. **PI** does not show any visible fluorescence, but samples of **PII-PIV** show a wide range of fluorescence. The blue emission of **PII** is of special interest due to the lack of blue emitting materials compared with green and orange emitting materials.[18] The fluorescent properties of these materials is another useful area these polymers could be used and warrants further investigation.

Figure 5.10. Flourescence of (left to right) **P1, PII, PIII, PIV** when exposed to 365 nm light in THF solutions

5.4 Conclusions

A series of aromatic monomers containing electron-withdrawing groups (I-III) or electron-donating groups (IV-V) have been synthesized. Monomer **I** contains an aromatic solubilizing group and monomers **II** and **III** contain thermally cleavable solubilizing groups. A series of amorphous alternating donor-acceptor copolymers (**PI-PIV**) were synthesized via Stille coupling with bandgaps ranging from 1.9-2.9 eV. Incorporation of more thiophene rings versus phenylene rings led to lower bandgap materials with **PIV** showing the lowest bandgap of all materials. Thermal cleavage of the ester group in **PI-PIV** led to lowered bandgaps with **PII**, **PIII**, and **PIV** decreasing by 0.1, 0.1, and 0.2 eV, respectively. Further cleavage of the remaining acid moiety led to a further lowering of the bandgap with **PII** and **PIII** decreasing by 0.4 and 0.3 eV, respectively, versus the uncleaved polymer. **PIII** and **PIV** appear to be promising materials for use in layered or bulk heterojunction solar cells due

to their low bandgaps and solubility switch. **PII** is of interest for further study as a light emitting diode after preliminary investigation showed blue light emission.

5.5 Acknowledgements. This work is based on research funded by the ACS PRF. We would like to thank Dr. Wei You for discussions regarding synthesis and Stuart Williams for help with film preparation.

5.6 References

1. Padinger, F.; Rittberger, R. S.; Sariciftci, N. S. *Adv. Funct. Mater.* **2003**, 85.
2. Liu, J.; Kadnikova, E. N.; Liu, Y.; McGehee, M. D.; Frechet, J. M. J.; *J. Am. Chem. Soc.* **2004**, *126*, 9486.
3. Zhang, M.; Yang, C.; Mishra, A. K.; Pisula, W.; Zhou, G.; Schmaltz, B.; Baumgarten, M.; Mullen, K. *Chem. Comm.* **2007**, *17*, 1704.
4. Liu, J. S.; Sheina, E.; Kowalewski, T.; McCullough, R. D. *Angew. Chem., Int. Ed.* **2002**, *41*, 329.
5. Wang, H. B.; Wang, H. H.; Urban, V. S.; Littrell, K. C.; Thiyagarajan, P.; Yu, L. P. *J. Am. Chem. Soc.* **2000**, *122*, 6855.
6. Krebs, F. C. and Spanggaard, H. *Chem. Mater.* **2005**, *17*, 5235.
7. Bjerring, M.; Nielsen, J. S.; Siu, A.; Nielsen, N. C.; Krebs, F. C. *Solar Energy Materials & Solar Cells* **2008**, *92*, 772.
8. Gevorgyan, S. A. and Krebs, F. C. *Chem. Mater.* **2008**, *20*, 4386.
9. Chapter 4 of this dissertation.
10. Takimoto, S.; Abe, N.; Kodera, Y.; Ohta, H. *Bull. Chem. Soc. Jpn.* **1983**, *56*, 639.
11. Espinet, P. and Echavarren, A. M. *Angew. Chem. Int. Ed.* **2004**, *43*, 4704.
12. Zhu, S. S. and Swager, T. M. *J. Am. Chem. Soc.* **1997**, *119*, 12568-12577.
13. Berlin, A. and Zanelli, A. *Chem. Mater.* **2004**, *14*, 3667-3676.
14. Perepichka, I. F.; Levillain, E.; Roncali, J. *J. Mater. Chem.* **2004**, *14*, 1679-1681.

15. Raimundo, J. M.; Blanchard, P.; Brisset, H.; Akoudad, S.; Roncali, J. *Chem. Commun.* **2000**, *11*, 939-940.

16. Meng, H.; Tucker, D.; Chaffins, S.; Chen, Y.; Helgeson, R.; Dunn, B.; Wudl, F. *Adv. Mater.* **2003**, *15*, 146-149.

17. Nguyen, L. H.; Günes, S.; Neugebauer, H.; Sariciftci, N. S.; Colladet, K.; Fourier, S.; Cleij, T. J.; Lutsen, L.; Gelan, J.; Vanderzande, D. *Eur. Phys. J. Appl. Phys.* **2007**, *36*, 219-223.

18. Wang, E.; Li, C.; Mo, Y.; Zhang, Y.; Ma, G.: Shi, W.; Peng, J.; Yang, W.; Cao, Y. *J. Mater. Chem.* **2006**, *16*, 4133.

Chapter 6

GENERAL CONCLUSIONS AND FUTURE RESEARCH DIRECTIONS

6.1 General Conclusions

This dissertation focused on the synthesis and characterization of novel conjugated polymers and copolymers synthesized via Ni(0)-catalyzed coupling or Stille coupling. Chapter 2 discussed the synthesis of polylactide-*b*-poly(2,5-benzophenone)-*b*-polylactide triblock copolymers. Hydroxy-terminated poly(2,5-benzophenenone) macroinitiators with a range of molecular weights (2.0 – 12.3 kg/mol) were synthesized from the nucleophilic aromatic substitution of fluorine-terminated poly(2,5-benzophenone) synthesized via Ni(0)-catalyzed coupling. These macroinitiators were used as initiation sites for the ring-opening polymerization of L- and D-lactide to synthesize a variety of ABA triblock copolymers.

Chapter 3 described an investigation into the effects of reaction conditions on the Ni(0)-catalyzed coupling of 2-benzenesulfonyl-1,4-dichlorobenzene. Eleven polymers were synthesized while varying the ligand type, solvent type, reaction temperature and reaction time. It was shown that the addition of electron-donating groups onto the bipyridine ligand had little to no effect on the molecular weight of poly(2-benzenesulfonyl-1,4-benzene). Altering the solvent, temperature and reaction times also had no effect on the molecular weight of the final product as only oligomeric material with $<M_n>$ up to 1450 g/mol was observed. It appears that the structure of the monomer is the dominating factor in the ability to achieve high molecular weight material in this system. Materials synthesized in THF versus those synthesized in DMAc showed higher T_gs and thermal stability. Also, all polymerizations produced insoluble fractions that were similar in appearance to the soluble portions and showed similar thermal stability but no apparent thermal transitions.

In Chapter 4 a simple method was shown for synthesizing a soluble ester-functionalized PPP derivative that can be processed into carboxylic acid-functionalized PPP

and native PPP through a simple thermal treatment. Upon heating the bulk material, it goes from a soluble, soft and malleable material to an intractable powdery solid. A significant change in the photophysical properties was observed in the spin-coated films upon annealing with a decrease in the measured bandgap of 1.2 eV from the ester-functionalized PPP to native PPP. The fact that these polymers have tunable solubility and electronic properties makes them promising interface materials in solution-processed multiplayer solar cells. Also, the fact that the ester-functionalized polymer is easily malleable could lead it to be used as a precursor for molding shapes that could then be heated to produce molded poly(paraphenylene).

Chapter 5 described the synthesis of a series of aromatic monomers containing either electron-withdrawing groups or electron-donating groups. Two of the acceptor monomers contained thermally removable solubilizing groups. A series of amorphous alternating donor-acceptor copolymers were synthesized via Stille coupling with bandgaps ranging from 1.9-2.9 eV. Incorporation of more thiophene rings verses phenylenes rings led to lower bandgap materials. Thermal cleavage of the ester group in led to lowered bandgaps and further cleavage of the remaining acid moiety led to a further lowering of the bandgap versus the uncleaved polymers. **PIII** and **PIV** appear to be promising materials for use in layered or bulk heterojunction solar cells due to their low bandgaps and solubility switch. **PII** is of interest for further study as a light emitting diode after preliminary investigation showed blue light emission.

6.2 Research Directions

As previously mentioned, conjugated polymers can be used in a wide array of applications from high-strength plastics and composites to light-emitting diodes and solar

cells. The ester-functionalized poly(paraphenylene) synthesized in Chapter 3 shows a unique combination of properties. It is a soft, tacky material that is readily soluble in common organic solvents allowing it to be solvent-cast and spin-coated with ease. Removal of the solubilizing group by thermal cleavage yields an insoluble material with a reduced bandgap. Flourescence study of thin films of this material following along with the two thermolysis steps would provide good insight as to whether this material could be of interest for use in a light-emitting diode. Also, studying different fabrication techniques to allow for the molding of the ester-functionalized material followed by thermal cleavage without fracture of the molded sample occurring could provide a route to moldable poly(paraphenylene) or even conjugated nanoparticles. The ester group along the backbone of the polymer allows for the use of post polymerization reactions to add further functionality. Fluorescent conjugated polymers have been used to amplify sensing of chemical and biological analytes.[1] Hydrolysis of the ester in a basic solution followed by the addition of salt, such as sodium perchlorate, would lead to water-soluble polymer that could be studied as a fluorescence quencher.[2] Solid state NMR as well as IR need to be performed to confirm the chemical structure after cleavage.

Improvements on the materials synthesized in Chapter 5 are also desirable. Polymers with higher molecular weights would be beneficial with regards to film formation and increasing conjugation length. Suzuki coupling is usually preferred over Stille coupling for the synthesis of phenylene containing materials. A thiophene donor other than EDOT might also be required. EDOT is very difficult to purify and the monomer will oxidize over time. A simple alkyl or ether chain as the donor moiety on the 3 and/or 4 positions of the thiophene ring could provide for easier purification and higher molecular weight polymers.

Finally, another type of chemistry that could be useful for the synthesis of conjugated polymers that have a thermal solubility switch is poly(hydrazide)s.[3] Poly(hydrazide)s undergo cyclodehydration to poly(1,3,4-oxadiazole)s. Poly(1,3,4-thiadiazole) can also be prepared by dehydrosulfurization of poly(dithiahydrazide).[4] As the synthesis of the poly(hydrazide) is a step-growth polymerization between a diacid and a dihydrazide, many variations to monomer structure can be made to accomplish control over the optoelectronic properties of the materials.

5.3 References

1. Harrison, B. S.; Ramey, M. B.; Reynolds, J. R.; Schanze, K. S. *J. Am. Chem. Soc.* **2000**, *122*, 8561.

2. Zhao, X.; Jiang, H.; Schanze, K. S. *Macromolecules*, **2008**, *41*, 3422.

3. Liou, G. –S.; Hsiao, S. –H.; Fang, Y. –K. *J. Polym. Sci. Part A: Polym. Chem.* **2006**, *44*, 6466.

4. Stevens, M. P. *Polymer Chemistry: An Introduction 3rd Ed.* **1999**, New York, Oxford University Press.

Appendix A

SUPPLEMENTAL MATERIAL FOR CHAPTER 2

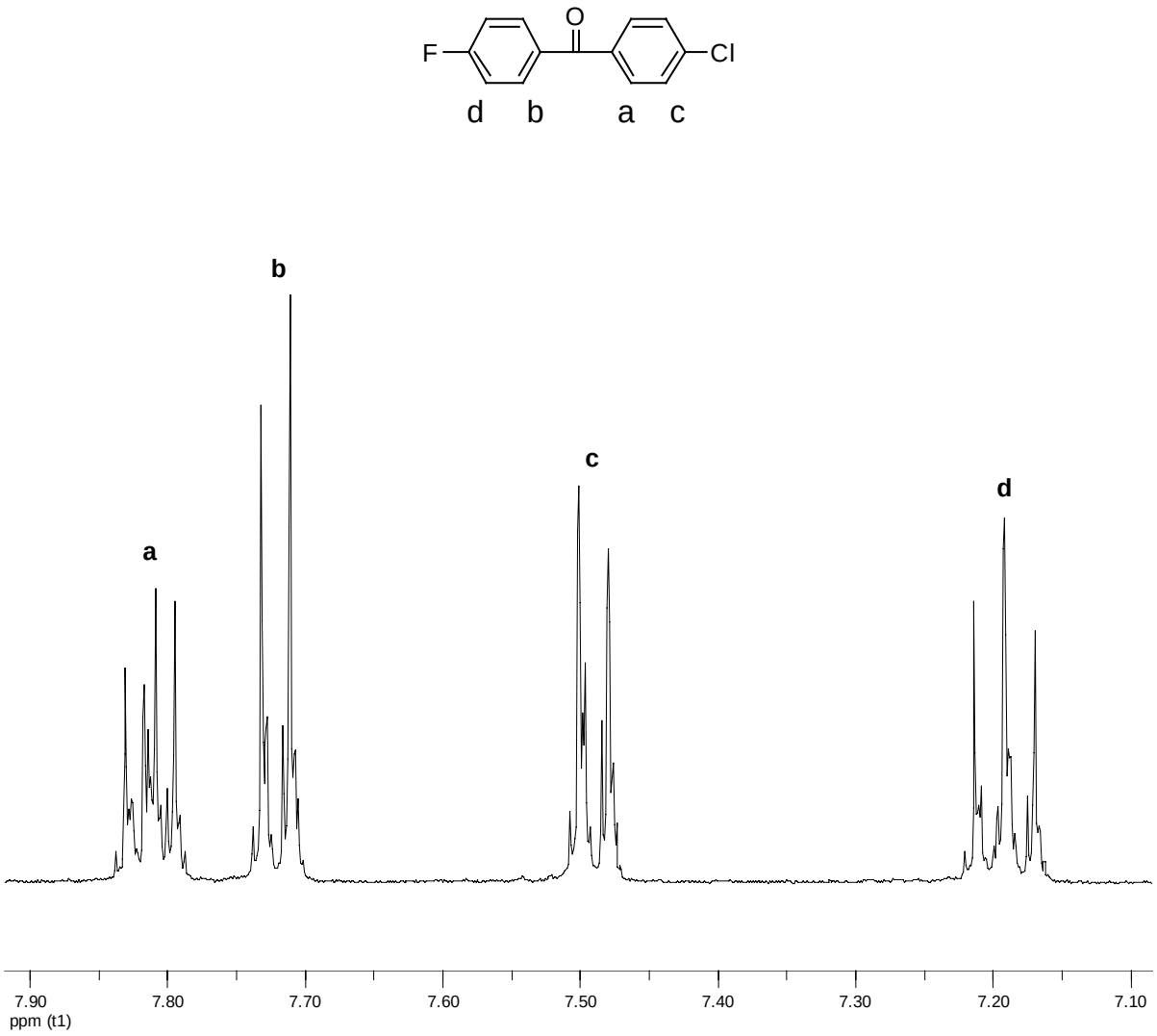

^{1}H-NMR of 4-chloro-4'-fluorobenzophenone in CD_2Cl_2

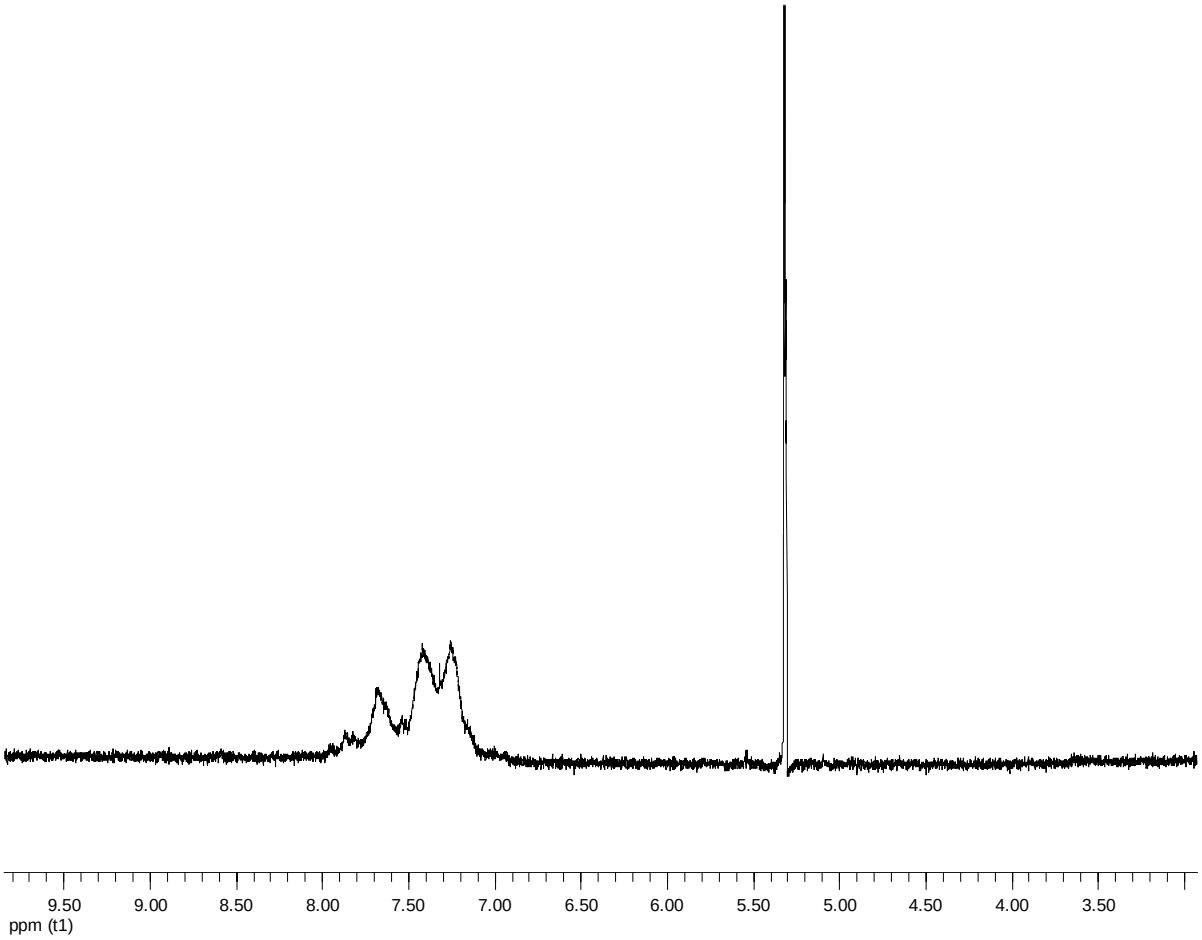

^{1}H-NMR of PBP-F

Ashby GPC Report

Reported by User: System Project Name: GPC4

Ashby Group GPC

SAMPLE INFORMATION

Sample Name:	M-27	Acquired By:	System
Sample Type:	Broad Unknown	Date Acquired:	10/7/04 10:57:37 PM
Vial:	68	Acq. Method Set:	GPCMTHSET
Injection #:	1	Date Processed:	10/11/04 10:23:08 AM
Injection Volume:	150.00 ul	Processing Method:	PM_040302
Run Time:	45.0 Minutes	Channel Name:	410
Sample Set Name:	Run_Samples_0410007	Proc. Chnl. Descr.:	

Auto-Scaled Chromatogram

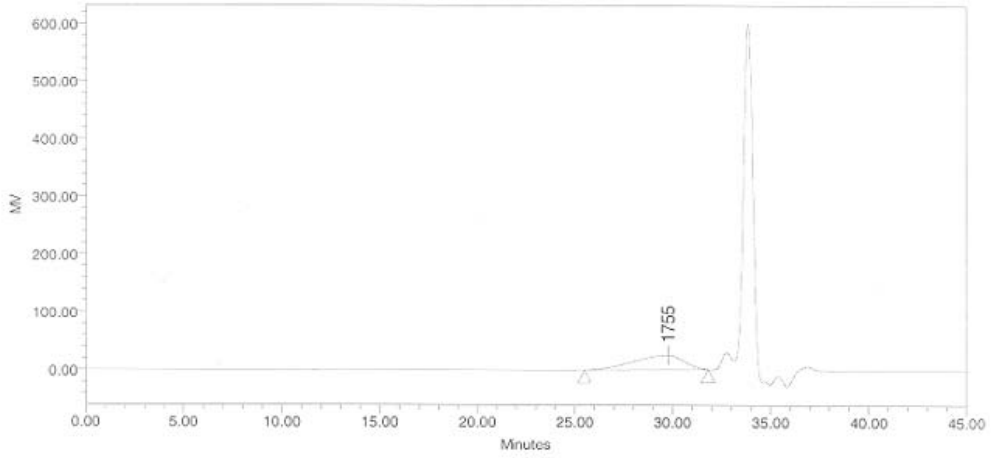

GPC Results

	Dist Name	Mn	Mw	Mv	MP	Mz	Mz+1	Polydispersity	K	alpha
1										
2		2057	3181		1755	5097	7538	1.546907		

Report Method: Ashby GPC Printed 7:48:49 PM 7/16/08 Page: 1 of 1

GPC curve for polymer **1**

Ashby GPC Report

Reported by User: System Project Name: GPC4

Ashby Group GPC

SAMPLE INFORMATION

Sample Name:	m01-47	Acquired By:	System
Sample Type:	Broad Unknown	Date Acquired:	2/4/05 1:23:43 AM
Vial:	62	Acq. Method Set:	GPCMTHSET
Injection #:	1	Date Processed:	2/4/05 10:56:53 AM
Injection Volume:	150.00 ul	Processing Method:	PM_040302
Run Time:	45.0 Minutes	Channel Name:	410
Sample Set Name:	Run_Samples_050203	Proc. Chnl. Descr.:	

Auto-Scaled Chromatogram

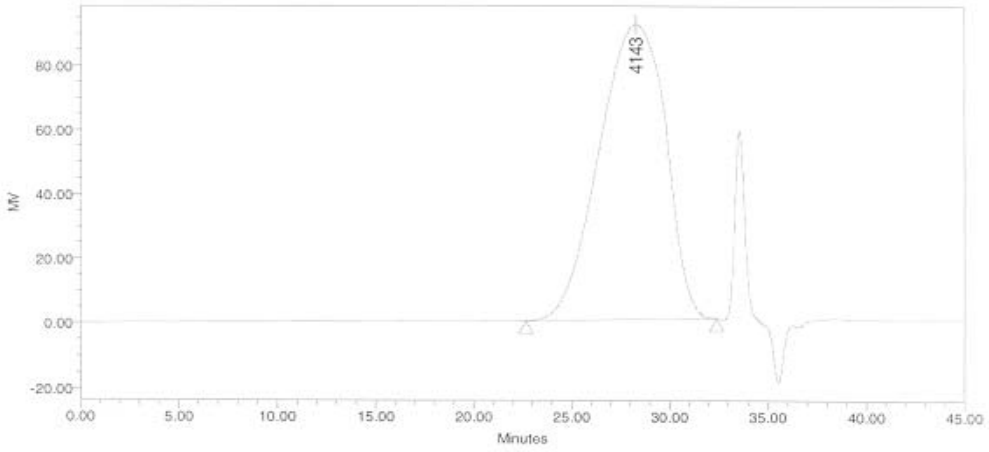

GPC Results

	Dist Name	Mn	Mw	Mv	MP	Mz	Mz+1	Polydispersity	K	alpha
1										
2		3500	7087		4143	14592	25670	2.024866		

Report Method: Ashby GPC Printed 7:48:43 PM 7/16/08 Page: 1 of 1

GPC curve for polymer **2**

Ashby GPC Report

Reported by User: System Project Name: GPC4

Ashby Group GPC

SAMPLE INFORMATION

Sample Name:	MO1-53	Acquired By:	System
Sample Type:	Broad Unknown	Date Acquired:	3/8/05 9:29:59 AM
Vial:	62	Acq. Method Set:	GPCMTHSET
Injection #:	1	Date Processed:	3/8/05 12:56:06 PM
Injection Volume:	150.00 ul	Processing Method:	PM_040302
Run Time:	45.0 Minutes	Channel Name:	410
Sample Set Name:	Run_Samples_050307	Proc. Chnl. Descr.:	

Auto-Scaled Chromatogram

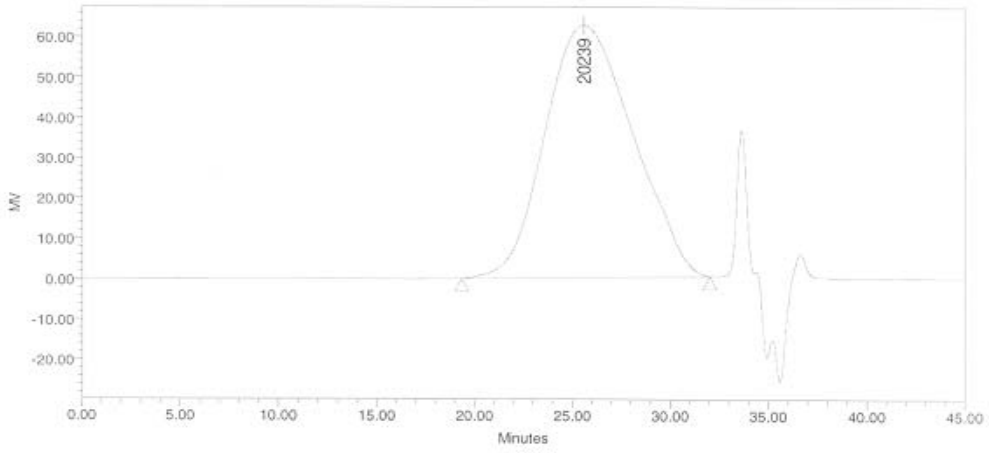

GPC Results

	Dist Name	Mn	Mw	Mv	MP	Mz	Mz+1	Polydispersity	K	alpha
1										
2		8068	30358		20239	89178	197865	3.763030		
3										

Report Method: Ashby GPC Printed 7:48:53 PM 7/16/08 Page: 1 of 1

GPC curve for polymer **3**

Ashby GPC Report

Reported by User: System Project Name: GPC4

Ashby Group GPC

SAMPLE INFORMATION

Sample Name:	m01-59	Acquired By:	System
Sample Type:	Broad Unknown	Date Acquired:	4/6/05 2:23:51 PM
Vial:	27	Acq. Method Set:	GPCMTHSET
Injection #:	1	Date Processed:	4/6/05 3:42:53 PM
Injection Volume:	150.00 ul	Processing Method:	PM_050405
Run Time:	45.0 Minutes	Channel Name:	410
Sample Set Name:	run_samples_050405	Proc. Chnl. Descr.:	

Auto-Scaled Chromatogram

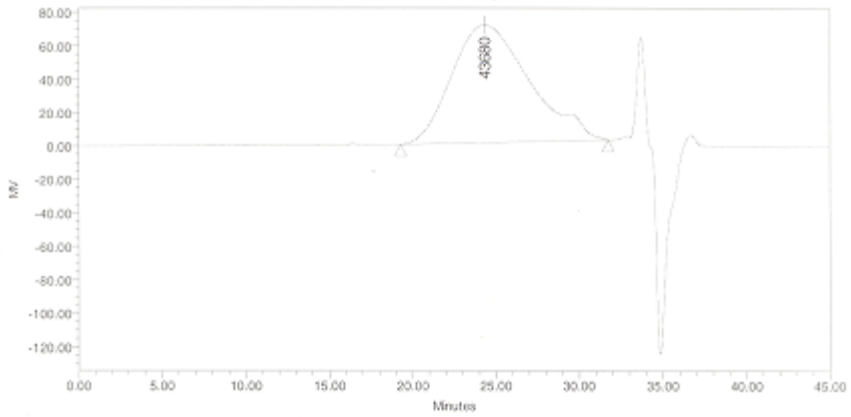

GPC Results

	Dist Name	Mn	Mw	Mv	MP	Mz	Mz+1	Polydispersity	K	alpha
1										
2		12370	58971		43680	147982	251100	4.767144		
3										

Report Method: Ashby GPC Printed 7:49:01 PM 7/16/08 Page: 1 of 1

GPC curve for polymer **4**

Ashby GPC Report

Reported by User: System Project Name: GPC3

Ashby Group GPC

SAMPLE INFORMATION

Sample Name:	M01-43	Acquired By:	System
Sample Type:	Broad Unknown	Date Acquired:	12/1/04 4:52:34 PM
Vial:	74	Acq. Method Set:	GPCMTHSET
Injection #:	1	Date Processed:	12/2/04 2:07:18 PM
Injection Volume:	150.00 ul	Processing Method:	PM_040302
Run Time:	45.0 Minutes	Channel Name:	410
Sample Set Name:	Run_Samples_041201	Proc. Chnl. Descr.:	

Auto-Scaled Chromatogram

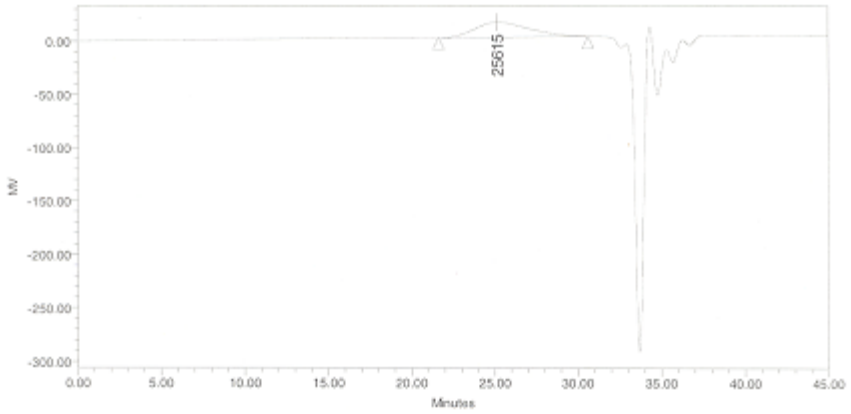

GPC Results

	Dist Name	Mn	Mw	Mv	MP	Mz	Mz+1	Polydispersity	K	alpha
1		12290	26724		25615	45171	64139	2.174441		

Report Method: Ashby GPC Printed 9:34:38 PM 7/16/08 Page: 1 of 1

GPC curve for polymer **5**

Ashby GPC Report

Reported by User: System Project Name: GPC4

Ashby Group GPC

SAMPLE INFORMATION

Sample Name:	M01-50	Acquired By:	System
Sample Type:	Broad Unknown	Date Acquired:	2/14/05 6:46:58 PM
Vial:	74	Acq. Method Set:	GPCMTHSET
Injection #:	1	Date Processed:	2/15/05 11:10:39 AM
Injection Volume:	150.00 ul	Processing Method:	PM_040302
Run Time:	45.0 Minutes	Channel Name:	410
Sample Set Name:	Run_Samples_050214	Proc. Chnl. Descr.:	

Auto-Scaled Chromatogram

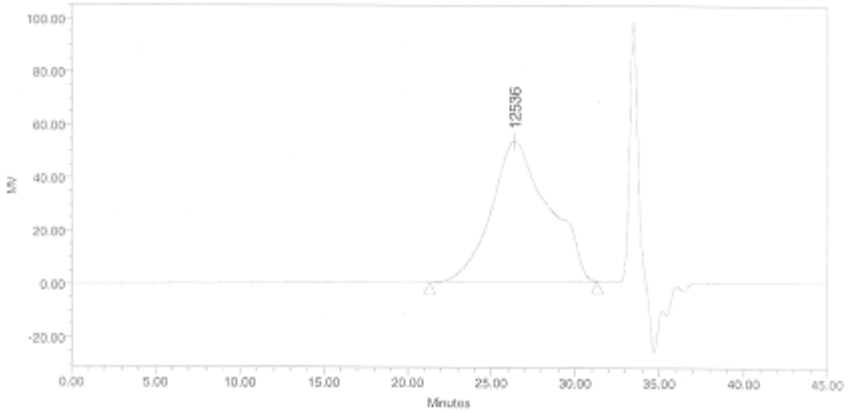

GPC Results

	Dist Name	Mn	Mw	Mv	MP	Mz	Mz+1	Polydispersity	K	alpha
1										
2		5962	15193		12536	34261	63156	2.548329		
3										

Report Method: Ashby GPC Printed 7:49:11 PM 7/16/08 Page: 1 of 1

GPC curve for polymer **6**

Ashby GPC Report

Reported by User: System Project Name: GPC4

Ashby Group GPC

SAMPLE INFORMATION

Sample Name:	M01-84	Acquired By:	System
Sample Type:	Broad Unknown	Date Acquired:	5/28/05 10:27:49 PM
Vial:	29	Acq. Method Set:	GPCMTHSET
Injection #:	1	Date Processed:	5/29/05 10:02:13 AM
Injection Volume:	150.00 ul	Processing Method:	PM_050528
Run Time:	45.0 Minutes	Channel Name:	410
Sample Set Name:	Run_Samples_050528	Proc. Chnl. Descr.:	

Auto-Scaled Chromatogram

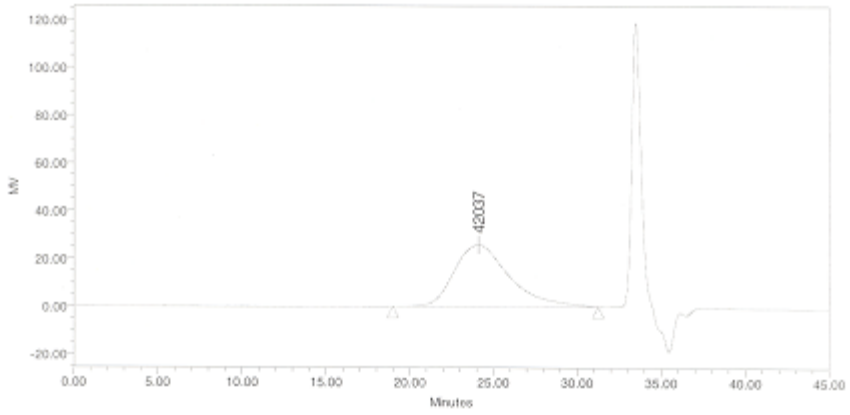

GPC Results

	Dst Name	Mn	Mw	Mv	MP	Mz	Mz+1	Polydispersity	K	alpha
1		20306	45796		42037	75019	117653	2.255363		

Report Method: Ashby GPC Printed 7:49:06 PM 7/16/08 Page: 1 of 1

GPC curve for polymer **7**

Ashby GPC Report

Reported by User: System Project Name: GPC4

Ashby Group GPC

SAMPLE INFORMATION

Sample Name:	M03-04c	Acquired By:	System
Sample Type:	Broad Unknown	Date Acquired:	4/12/06 4:49:16 PM
Vial:	28	Acq. Method Set:	GPCMTHSET
Injection #:	1	Date Processed:	4/13/06 9:06:40 AM
Injection Volume:	150.00 ul	Processing Method:	PM_060228
Run Time:	45.0 Minutes	Channel Name:	410
Sample Set Name:	Run_Samples_060412	Proc. Chnl. Descr.:	

Auto-Scaled Chromatogram

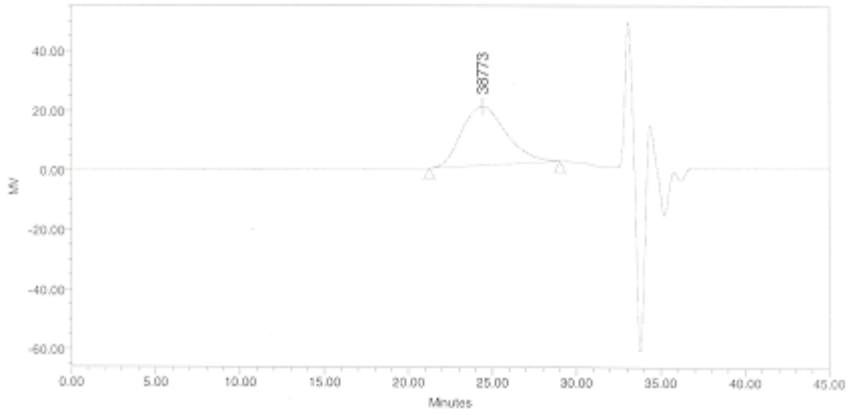

GPC Results

	Dist Name	Mn	Mw	Mv	MP	Mz	Mz+1	Polydispersity	K	alpha
1		26423	42394		38773	59619	76665	1.604427		

Report Method: Ashby GPC Printed 7:49:23 PM 7/16/08 Page: 1 of 1

GPC curve for polymer **8**

Ashby GPC Report

Reported by User: System Project Name: GPC4

Ashby Group GPC

SAMPLE INFORMATION

Sample Name:	M02-91b	Acquired By:	System
Sample Type:	Broad Unknown	Date Acquired:	3/21/06 2:30:41 PM
Vial:	51	Acq. Method Set:	GPCMTHSET
Injection #:	1	Date Processed:	3/22/06 9:55:31 AM
Injection Volume:	150.00 ul	Processing Method:	PM_060228
Run Time:	45.0 Minutes	Channel Name:	410
Sample Set Name:	Run_Samples_060321	Proc. Chnl. Descr.:	

Auto-Scaled Chromatogram

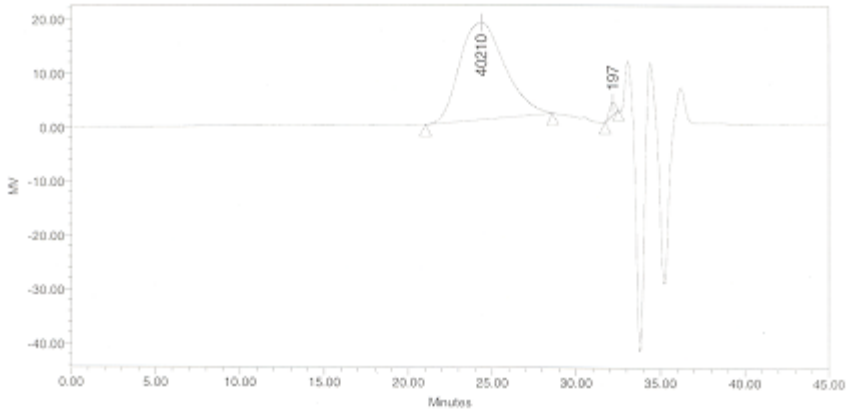

GPC Results

	Dist Name	Mn	Mw	Mv	MP	Mz	Mz+1	Polydispersity	K	alpha
1		28077	44469		40210	62458	80399	1.583838		
2					197					

Report Method: Ashby GPC Printed 7:49:25 PM 7/16/08 Page: 1 of 1

GPC curve for polymer **9**

Ashby GPC Report

Reported by User: System Project Name: GPC4

Ashby Group GPC

SAMPLE INFORMATION

Sample Name:	M03-01b	Acquired By:	System
Sample Type:	Broad Unknown	Date Acquired:	4/26/06 7:32:38 PM
Vial:	101	Acq. Method Set:	GPCMTHSET
Injection #:	1	Date Processed:	5/2/06 4:31:16 PM
Injection Volume:	150.00 ul	Processing Method:	PM_060228
Run Time:	45.0 Minutes	Channel Name:	410
Sample Set Name:	Run_Samples_060426	Proc. Chnl. Descr.:	

Auto-Scaled Chromatogram

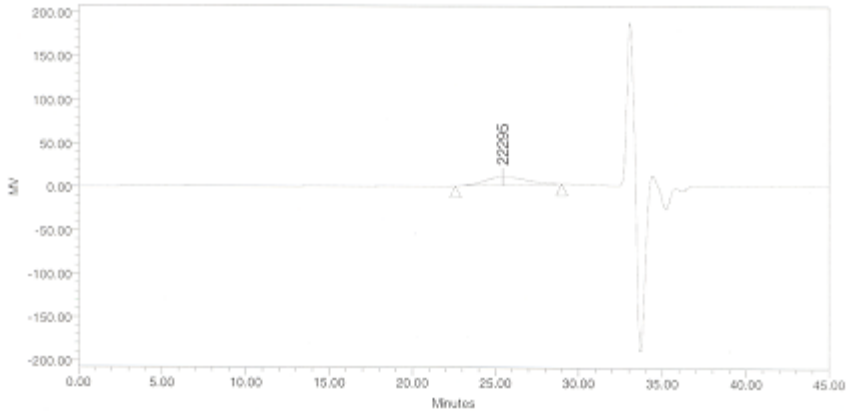

GPC Results

	Dist Name	Mn	Mw	Mv	MP	Mz	Mz+1	Polydispersity	K	alpha
1		15822	23071		22295	31146	39148	1.458158		

Report Method: Ashby GPC Printed 7:49:31 PM 7/16/08 Page: 1 of 1

GPC curve for polymer **10**

Ashby GPC Report

Reported by User: System Project Name: GPC4

Ashby Group GPC

SAMPLE INFORMATION

Sample Name:	m03-22	Acquired By:	System
Sample Type:	Broad Unknown	Date Acquired:	6/15/06 1:30:44 AM
Vial:	58	Acq. Method Set:	GPCMTHSET
Injection #:	1	Date Processed:	6/15/06 9:02:45 AM
Injection Volume:	150.00 ul	Processing Method:	PM_060614
Run Time:	45.0 Minutes	Channel Name:	410
Sample Set Name:	run samples 060615	Proc. Chnl. Descr.:	

Auto-Scaled Chromatogram

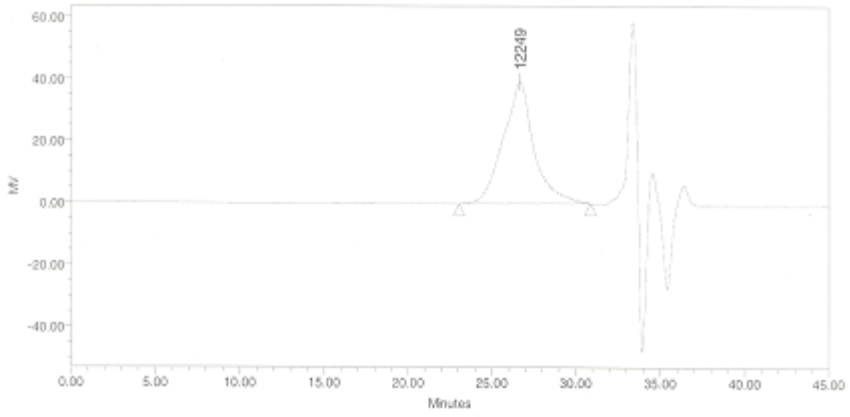

GPC Results

	Dist Name	Mn	Mw	Mv	MP	Mz	Mz+1	Polydispersity	K	alpha
1		9767	14599		12249	19574	25248	1.494747		

Report Method: Ashby GPC Printed 7:49:38 PM 7/16/06 Page: 1 of 1

GPC curve for polymer **11**

Ashby GPC Report

Reported by User: System Project Name: GPC4

Ashby Group GPC

SAMPLE INFORMATION

Sample Name:	M03-16c	Acquired By:	System
Sample Type:	Broad Unknown	Date Acquired:	7/11/06 11:16:13 PM
Vial:	26	Acq. Method Set:	GPCMTHSET
Injection #:	1	Date Processed:	7/12/06 9:56:00 AM
Injection Volume:	150.00 ul	Processing Method:	PM_060614
Run Time:	45.0 Minutes	Channel Name:	410
Sample Set Name:	run samples 060711	Proc. Chnl. Descr.:	

Auto-Scaled Chromatogram

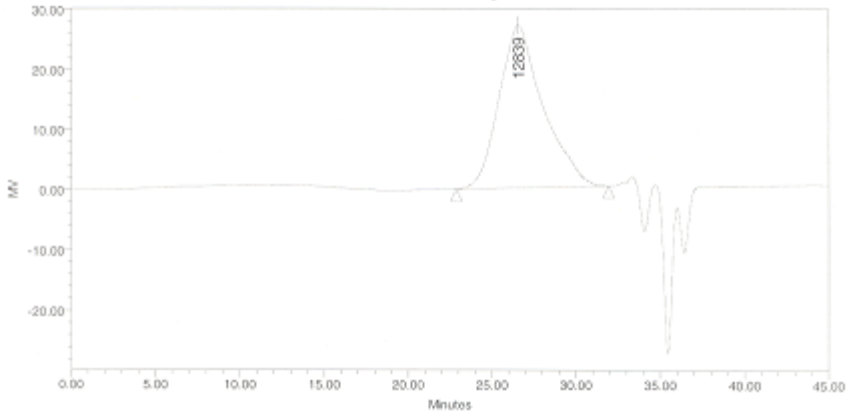

GPC Results

	Dist Name	Mn	Mw	Mv	MP	Mz	Mz+1	Polydispersity	K	alpha
1		6803	13472		12839	20751	28437	1.980149		

Report Method: Ashby GPC Printed 7:49:40 PM 7/16/08 Page: 1 of 1

GPC curve for polymer **12**

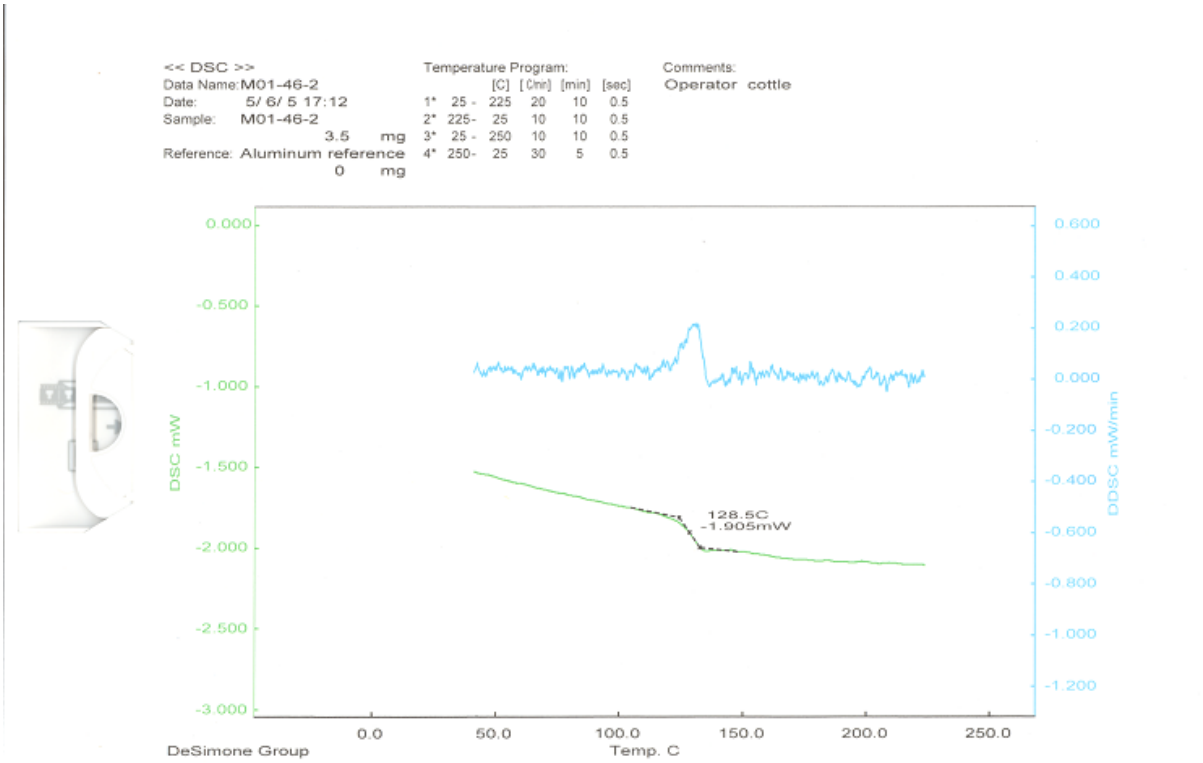

DSC curve for polymer **1**

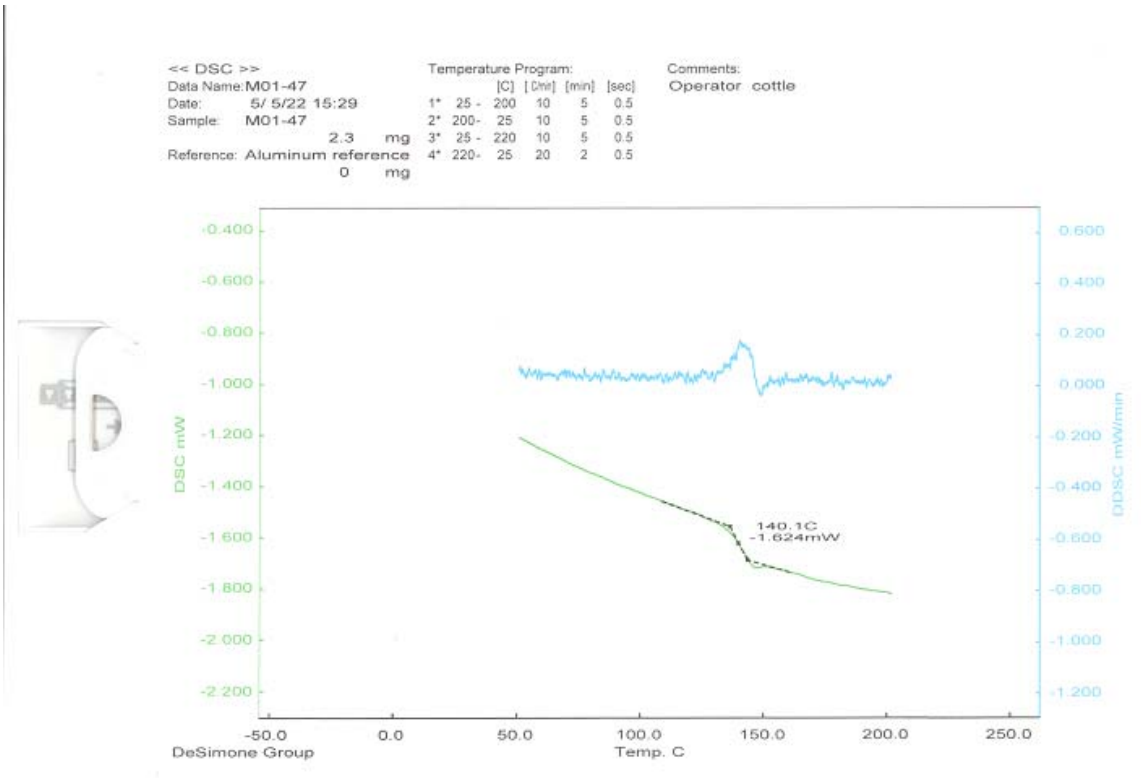

DSC curve for polymer **2**

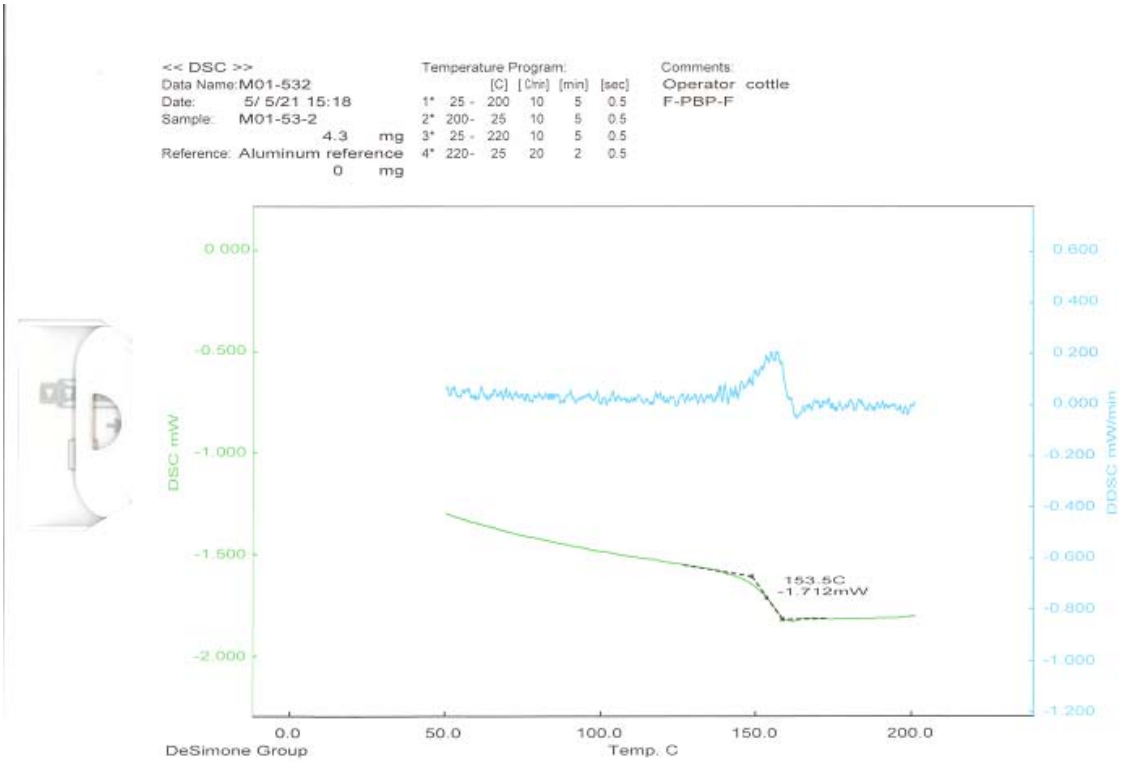

DSC curve for polymer **3**

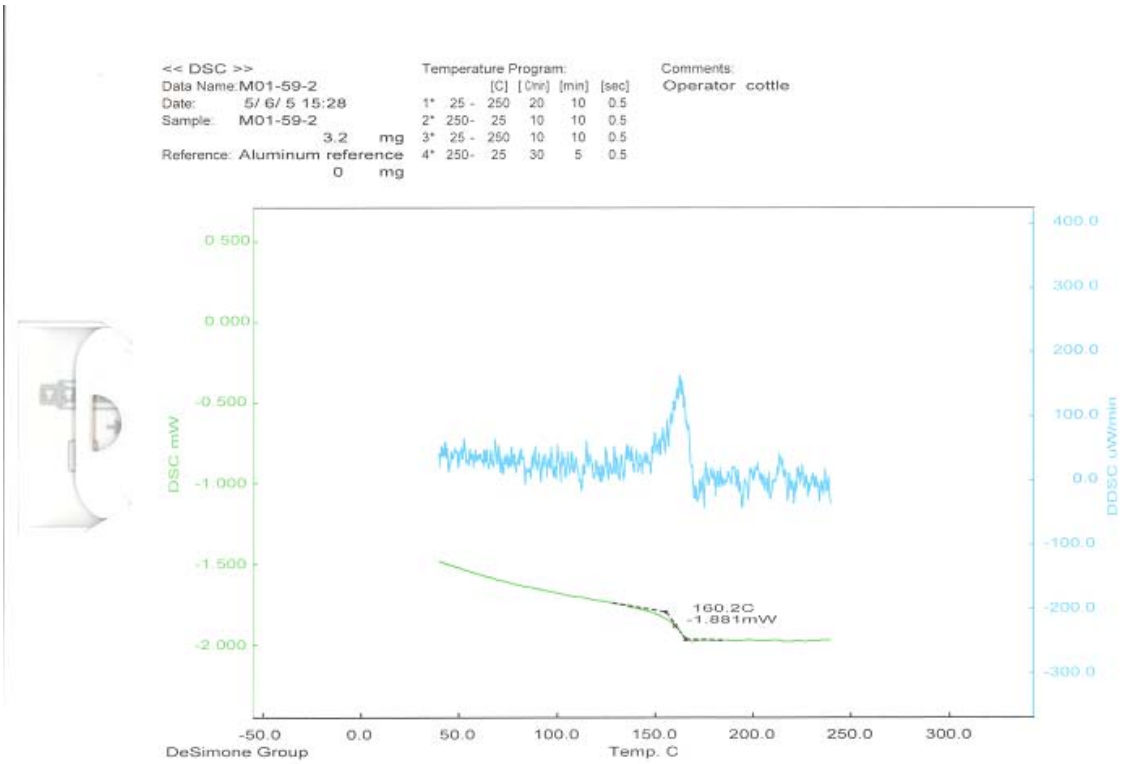

DSC curve for polymer **4**

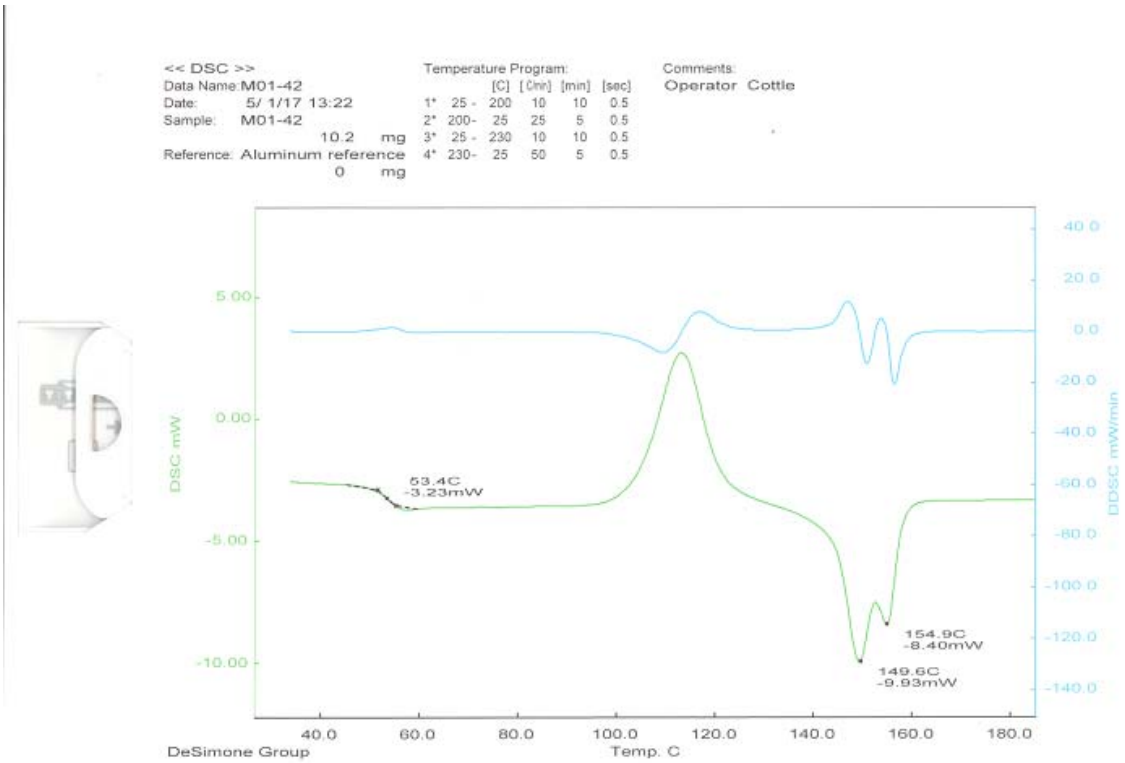

DSC curve for polymer **5**

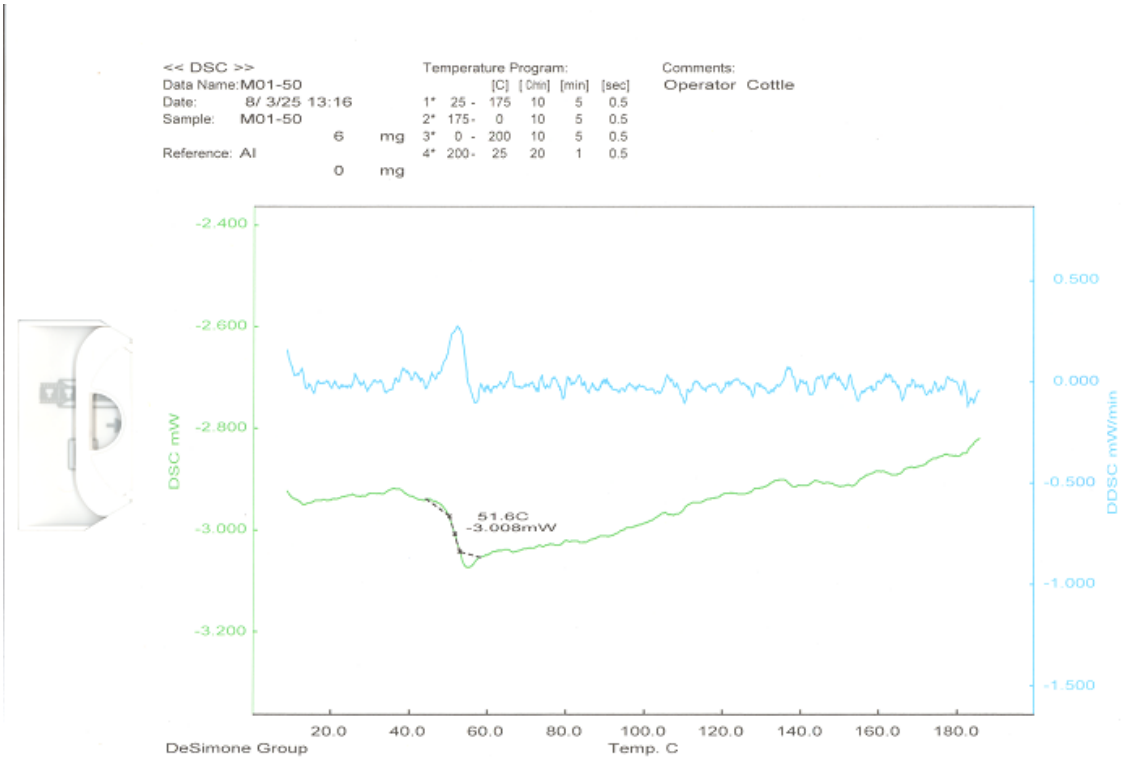

DSC curve for polymer **6**

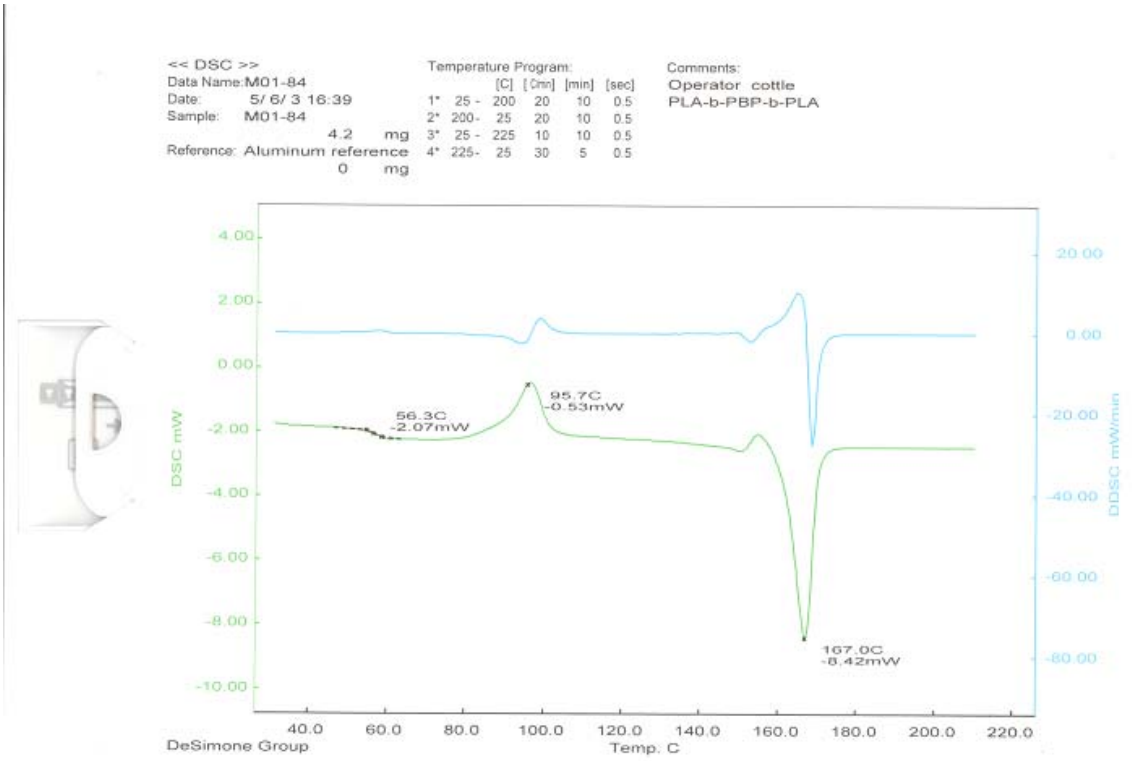

DSC curve for polymer **7**

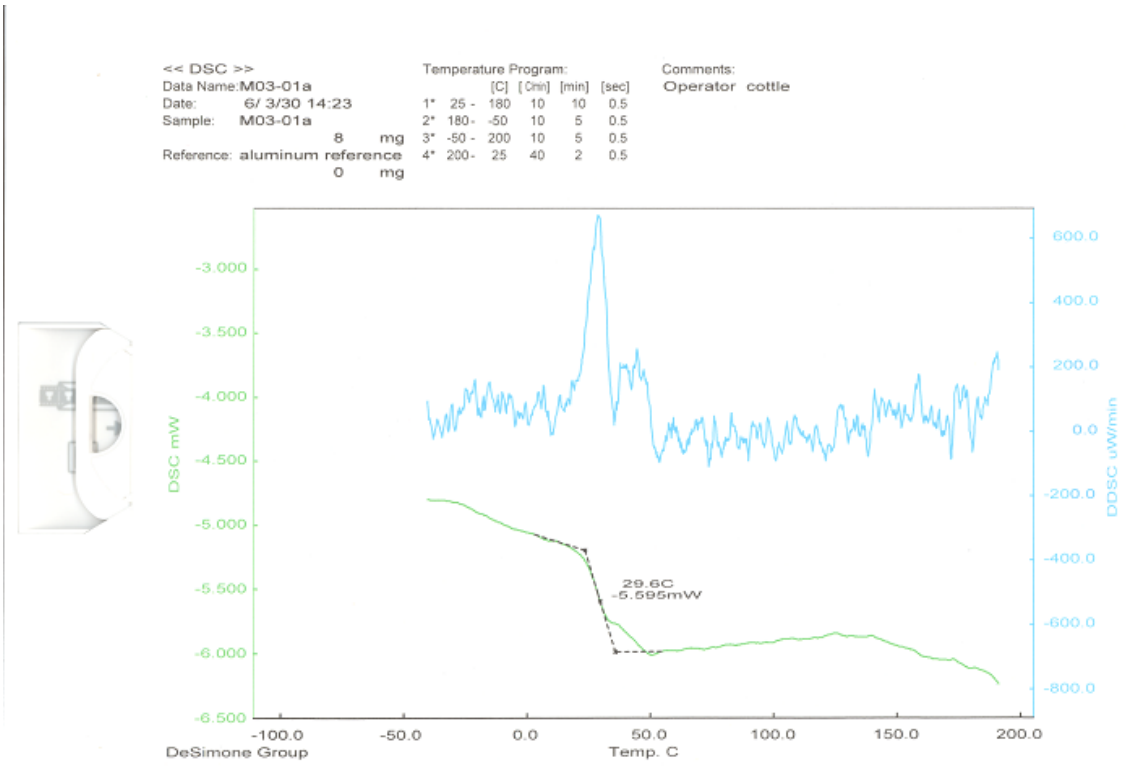

DSC curve for polymer **10**

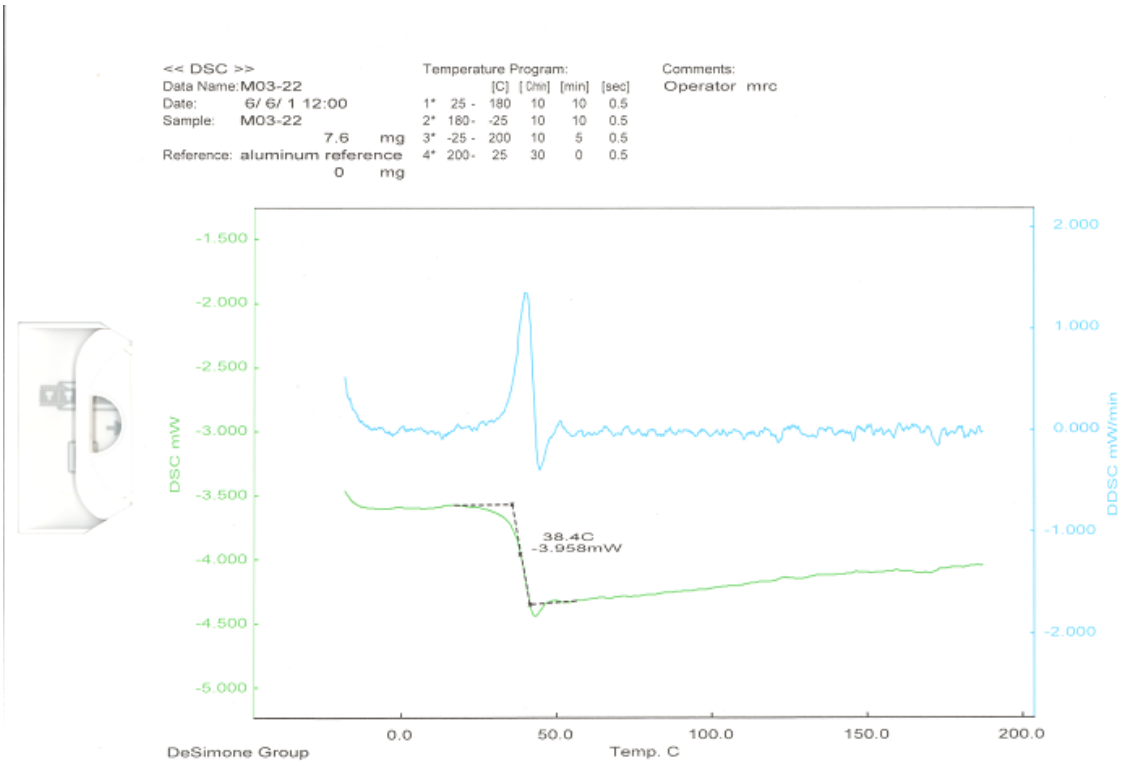

DSC curve for polymer **11**

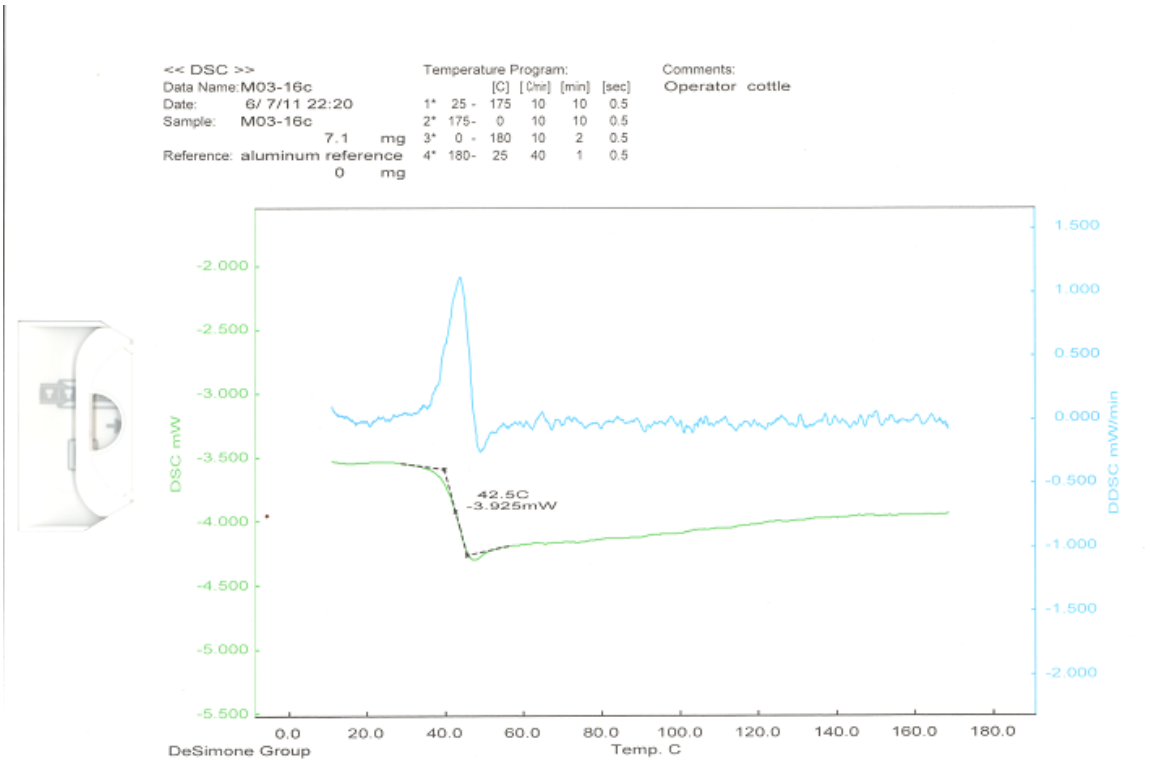

DSC curve for polymer **12**

Appendix B

SUPPLEMENTAL MATERIAL FOR CHAPTER 3

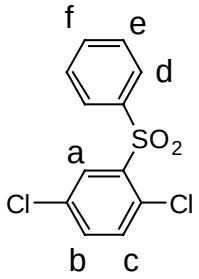

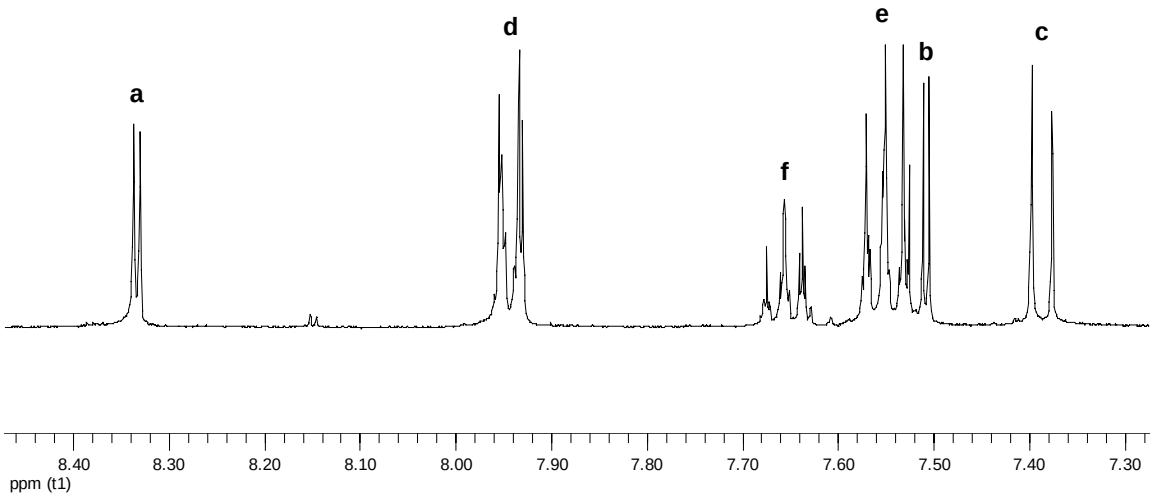

^{1}H-NMR of 2-benzenesulfonyl-1,4-dichlorobenzene in CD_2Cl_2

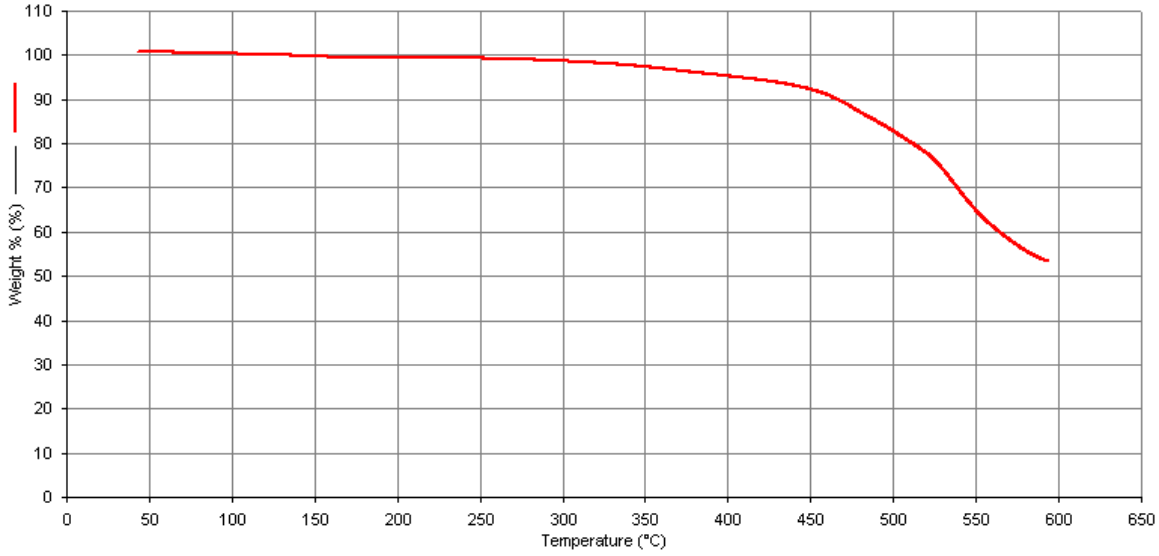

TGA data for polymer **1**

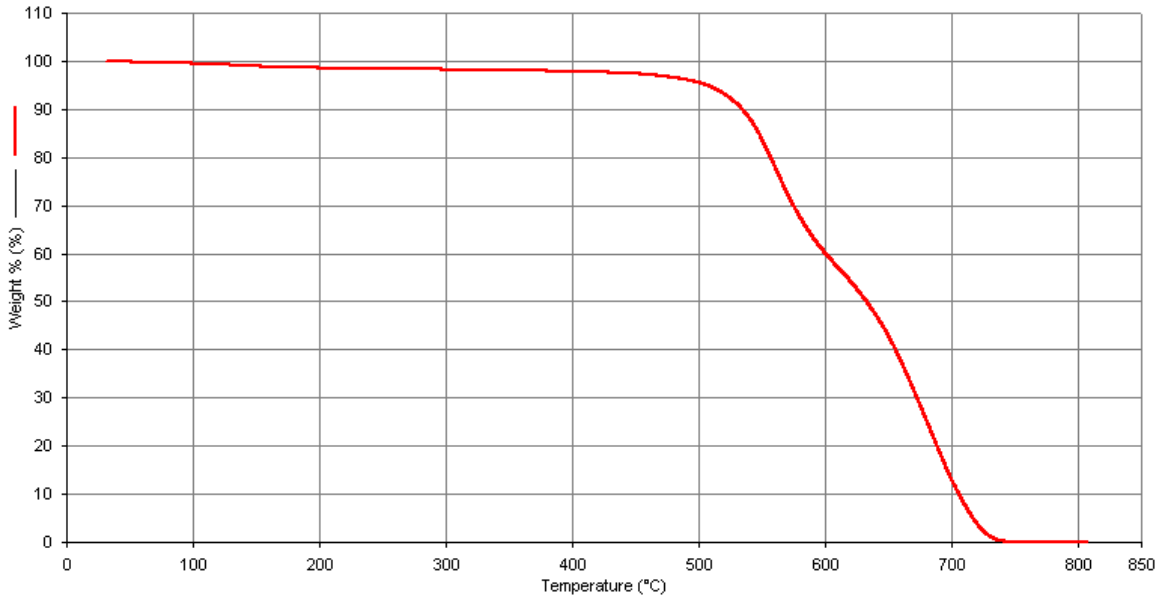

TGA data for polymer **2a**

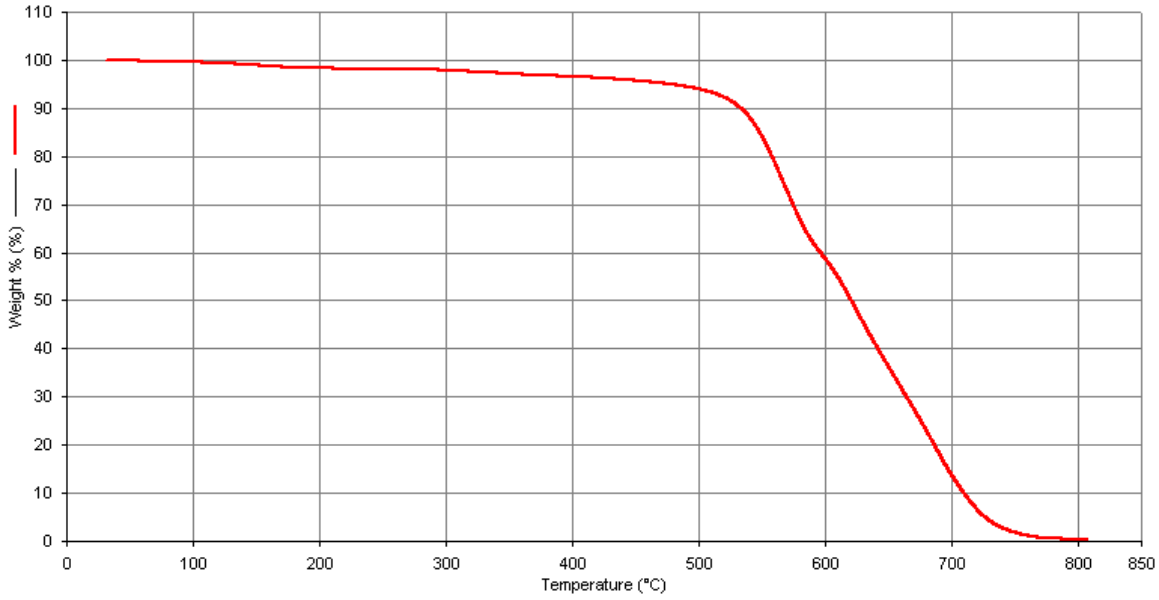

TGA data for polymer **2b**

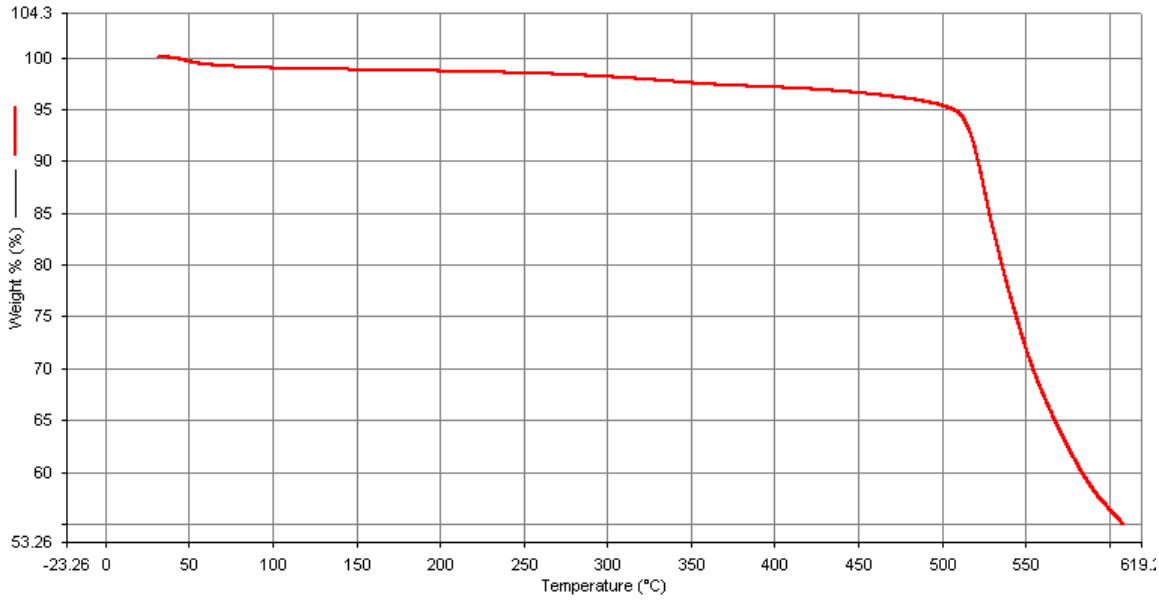

TGA data for polymer **3**

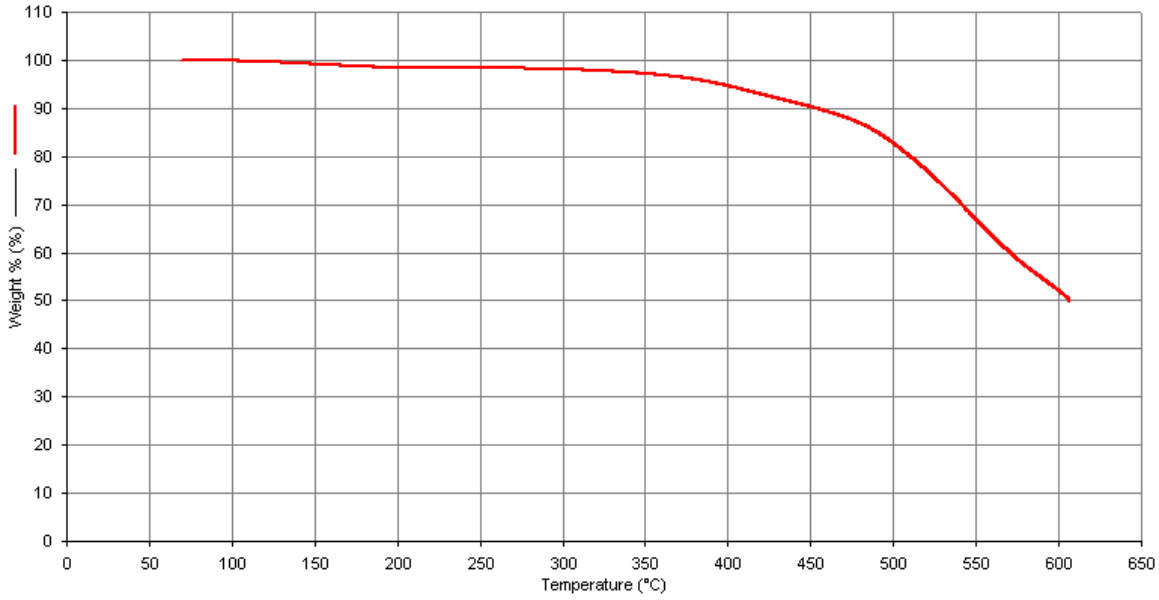

TGA data for polymer **4**

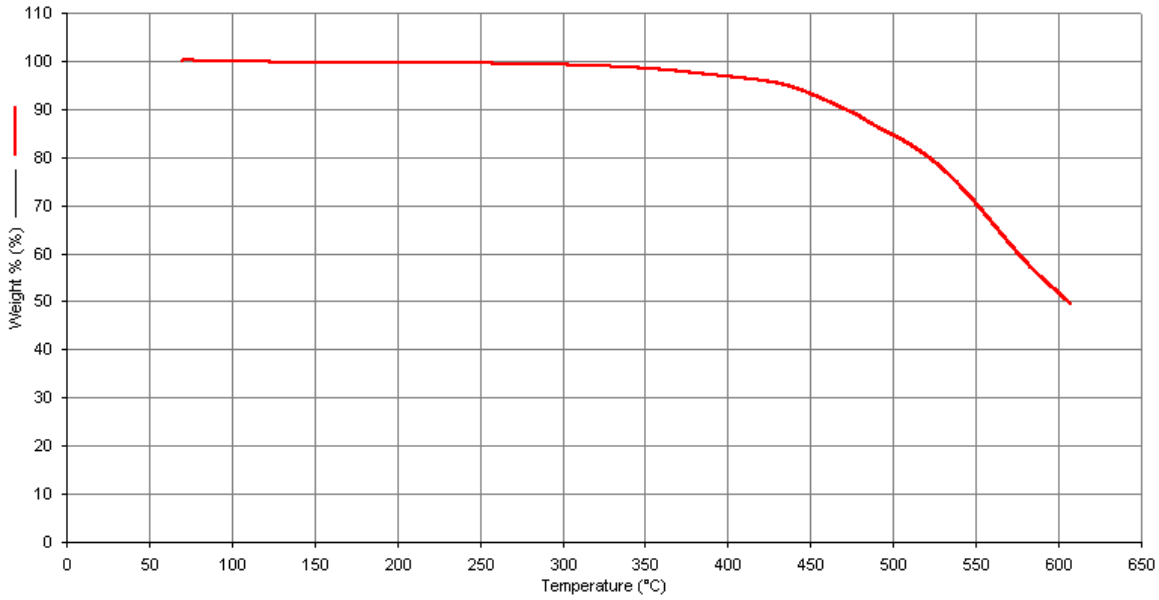

TGA data for polymer **5**

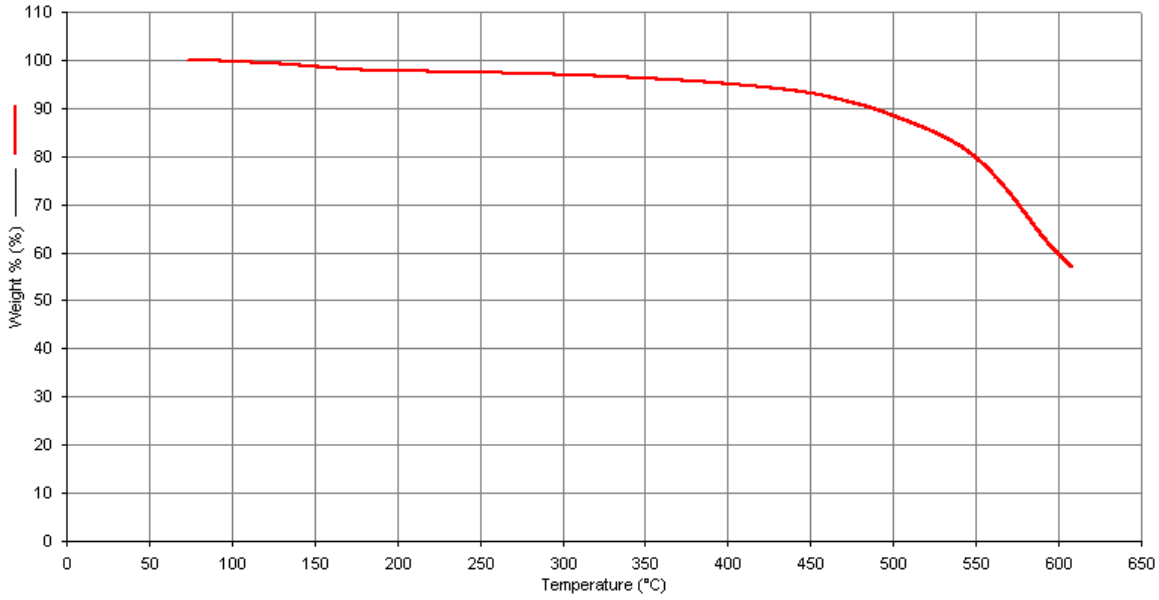

TGA data for polymer **6**

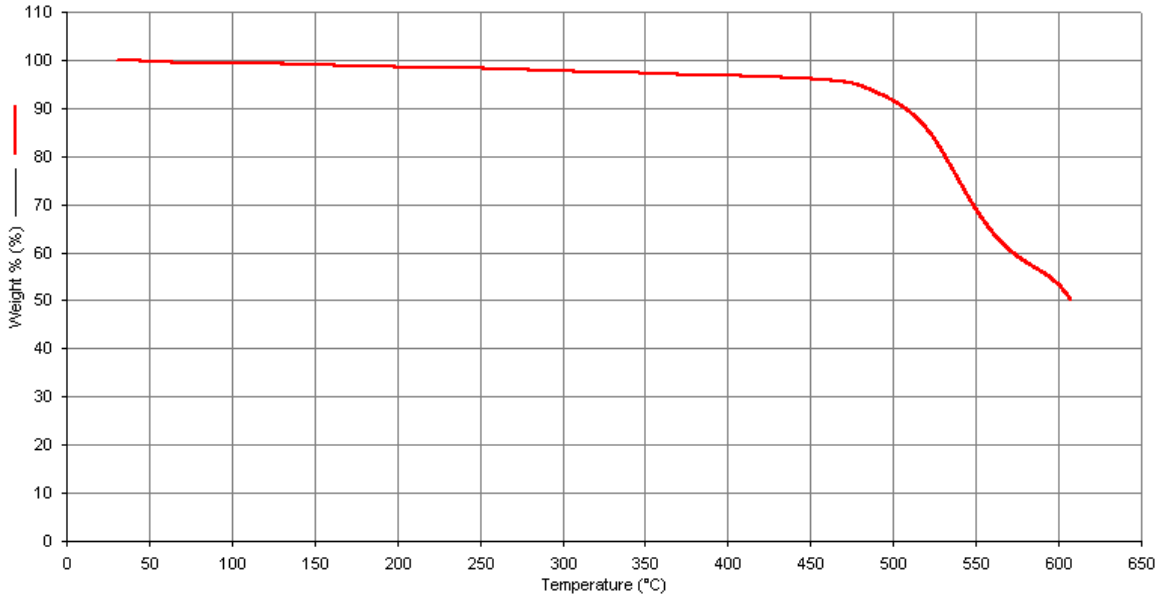

TGA data for polymer **7**

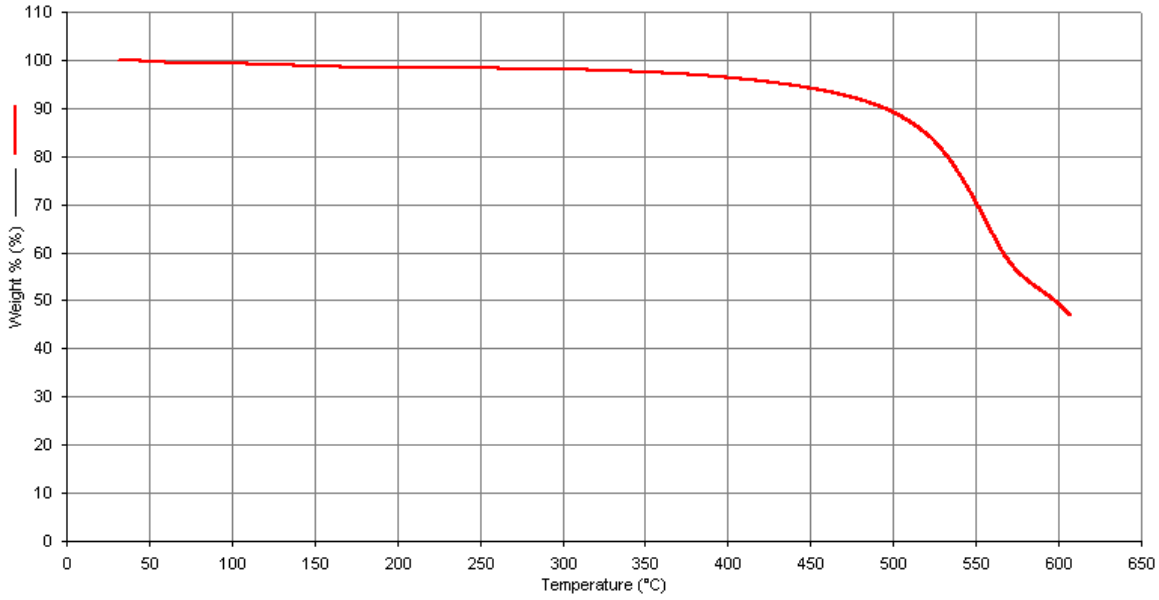

TGA data for polymer **8**

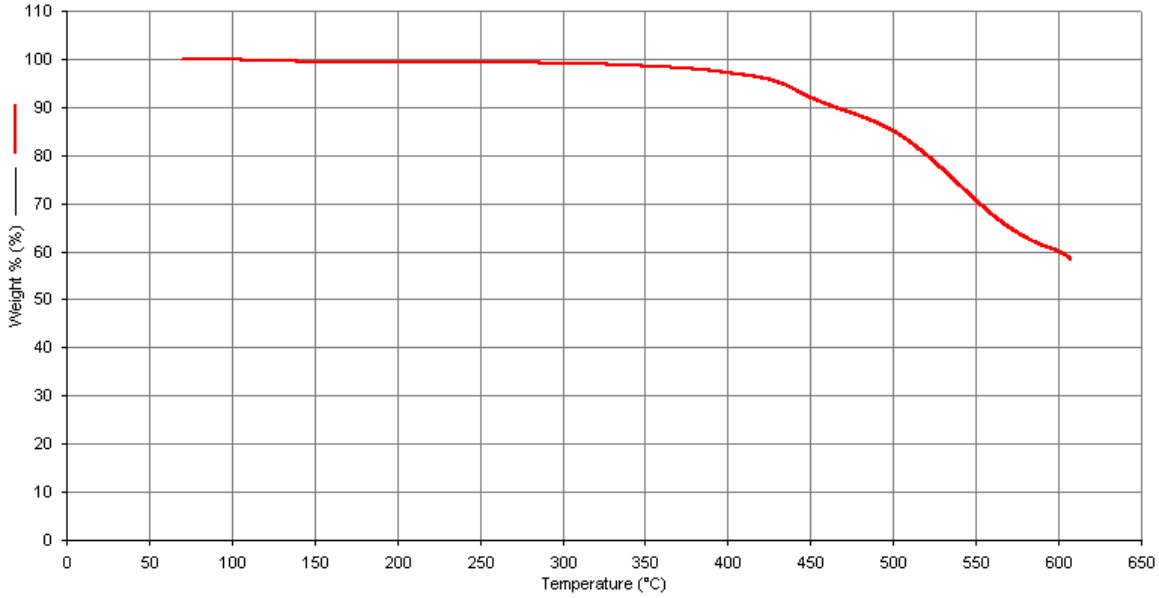

TGA data for polymer **9**

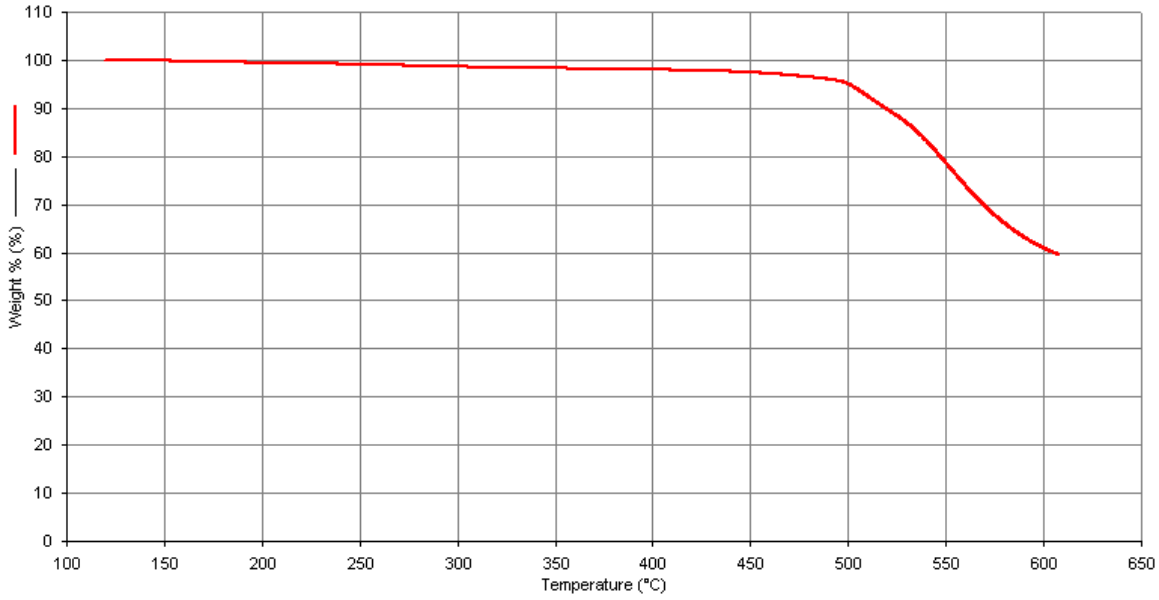

TGA data for polymer **10**

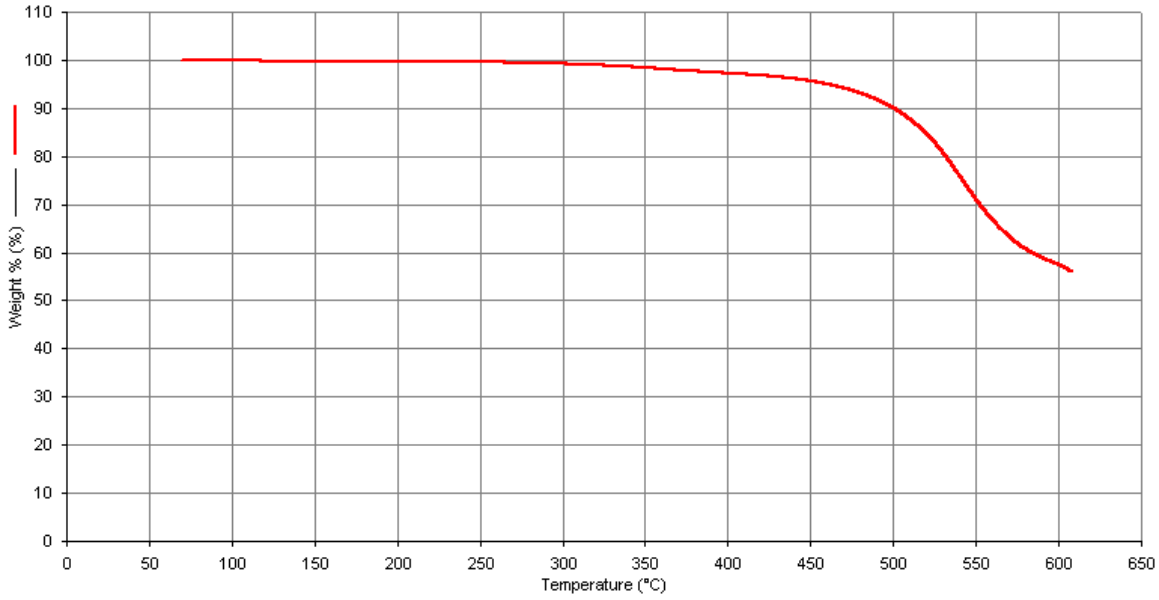

TGA data for polymer **11**

Ashby GPC Report

Reported by User: System Project Name: GPC4

Ashby Group GPC

SAMPLE INFORMATION

Sample Name:	M02-21	Acquired By:	System
Sample Type:	Broad Unknown	Date Acquired:	8/23/05 9:29:04 PM
Vial:	23	Acq. Method Set:	GPCMTHSET
Injection #:	1	Date Processed:	8/24/05 9:37:07 AM
Injection Volume:	150.00 ul	Processing Method:	PM_050614
Run Time:	45.0 Minutes	Channel Name:	410
Sample Set Name:	run samples 050823	Proc. Chnl. Descr.:	

Auto-Scaled Chromatogram

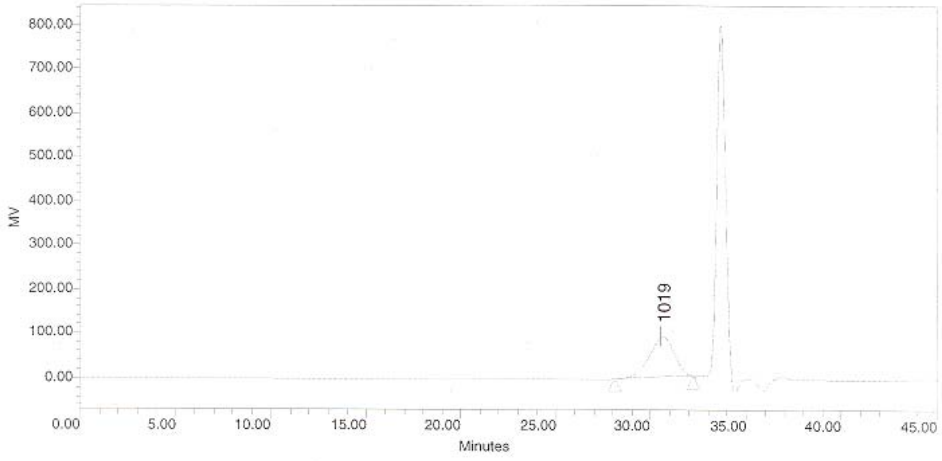

GPC Results

	Dist Name	Mn	Mw	Mv	MP	Mz	Mz+1	Polydispersity	K	alpha
1										
2		975	1200		1019	1488	1836	1.230360		

Report Method: Ashby GPC Printed 3:41:47 PM 7/16/08 Page: 1 of 1

GPC curve for polymer **1**

Ashby GPC Report

Reported by User: System Project Name: GPC4

Ashby Group GPC

SAMPLE INFORMATION

Sample Name:	M01-88s	Acquired By:	System
Sample Type:	Broad Unknown	Date Acquired:	8/23/05 7:52:22 PM
Vial:	21	Acq. Method Set:	GPCMTHSET
Injection #:	1	Date Processed:	8/24/05 9:36:26 AM
Injection Volume:	150.00 ul	Processing Method:	PM_050614
Run Time:	45.0 Minutes	Channel Name:	410
Sample Set Name:	run samples 050823	Proc. Chnl. Descr.:	

Auto-Scaled Chromatogram

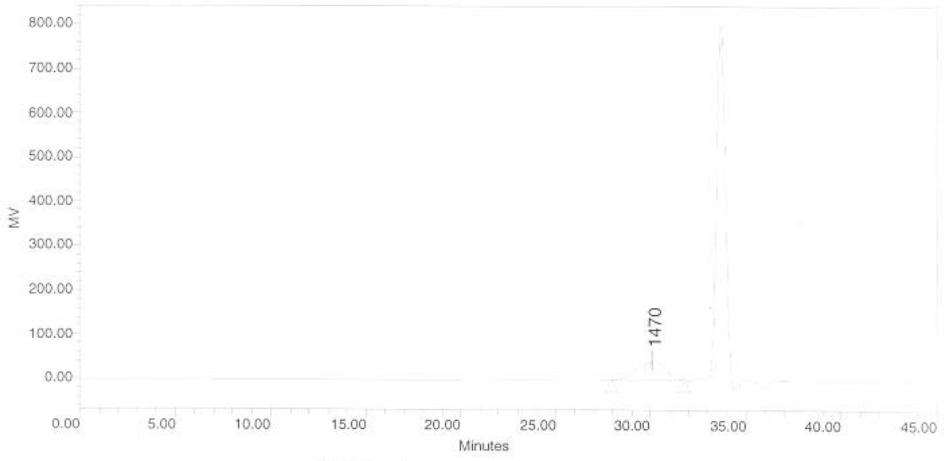

GPC Results

	Dist Name	Mn	Mw	Mv	MP	Mz	Mz+1	Polydispersity	K	alpha
1										
2		1454	1790		1470	2190	2619	1.231182		

Report Method: Ashby GPC Printed 3:41:26 PM 7/16/08 Page: 1 of 1

GPC curve for polymer **2b**

Empower 2 software

Ashby GPC Report

SAMPLE INFORMATION

Sample Name:	M02-26	Acquired By:	System
Sample Type:	Broad Unknown	Sample Set Name:	Run_Samples_080624
Vial:	103	Acq. Method Set:	GPC PDA Off
Injection #:	1	Processing Method:	070412 THF
Injection Volume:	100.00 ul	Channel Name:	410
Run Time:	50.0 Minutes	Proc. Chnl. Descr.:	
Date Acquired:	6/24/2008 6:19:38 PM EDT		
Date Processed:	7/16/2008 4:59:14 PM EDT		

Auto-Scaled Chromatogram

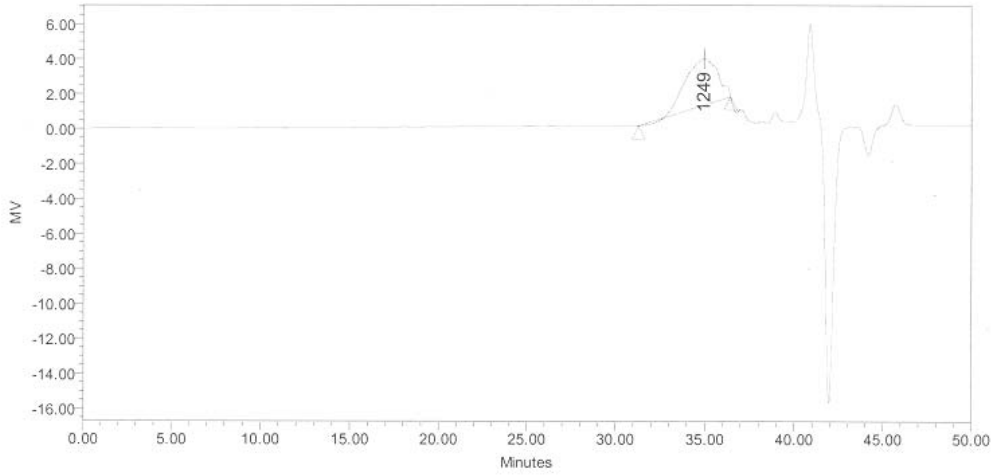

GPC Results

	Dist Name	Mn	Mw	Mv	MP	Mz	Mz+1	Poly dispersity	K	alpha
1		1295	1527		1249	1790	2058	1.179022		

Reported by User: System
Report Method: Ashby GPC Report
Report Method ID: 1111
Page: 1 of 1

Project Name: GPC
Date Printed:
7/16/2008
5:00:02 PM US/Eastern

GPC curve for polymer **3**

Ashby GPC Report

Reported by User: System Project Name: GPC4

Ashby Group GPC

SAMPLE INFORMATION

Sample Name:	M02-14	Acquired By:	System
Sample Type:	Broad Unknown	Date Acquired:	8/7/05 7:28:21 AM
Vial:	86	Acq. Method Set:	GPCMTHSET
Injection #:	1	Date Processed:	8/16/05 10:25:34 AM
Injection Volume:	150.00 ul	Processing Method:	PM_050614
Run Time:	45.0 Minutes	Channel Name:	410
Sample Set Name:	Run_Samples_050806	Proc. Chnl. Descr.:	

Auto-Scaled Chromatogram

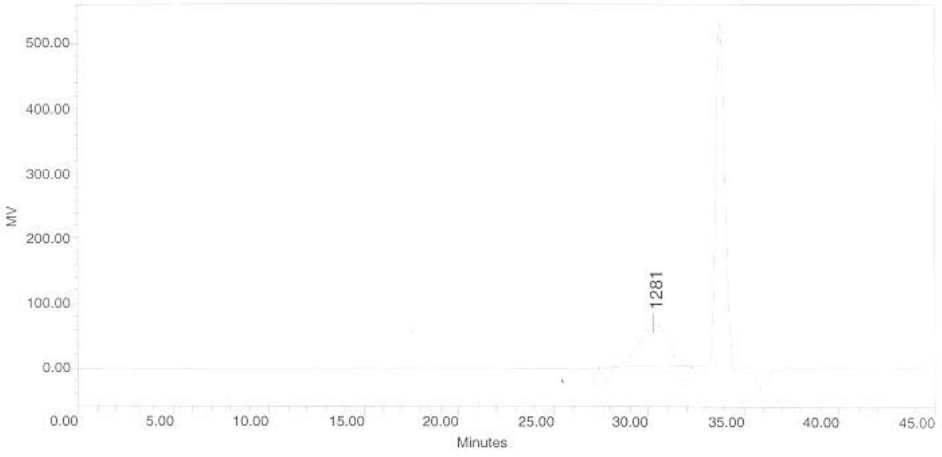

GPC Results

	Dist Name	Mn	Mw	Mv	MP	Mz	Mz+1	Polydispersity	K	alpha
1										
2		1189	1561		1281	2062	2682	1.313433		

Report Method: Ashby GPC Printed 3:41:34 PM 7/16/08 Page: 1 of 1

GPC curve for polymer **4**

Reported by User: System Project Name: GPC4

Ashby Group GPC

SAMPLE INFORMATION

Sample Name:	M02-17	Acquired By:	System
Sample Type:	Broad Unknown	Date Acquired:	8/7/05 9:05:08 AM
Vial:	88	Acq. Method Set:	GPCMTHSET
Injection #:	1	Date Processed:	8/16/05 10:25:33 AM
Injection Volume:	150.00 ul	Processing Method:	PM_050614
Run Time:	45.0 Minutes	Channel Name:	410
Sample Set Name:	Run_Samples_050806	Proc. Chnl. Descr.:	

Auto-Scaled Chromatogram

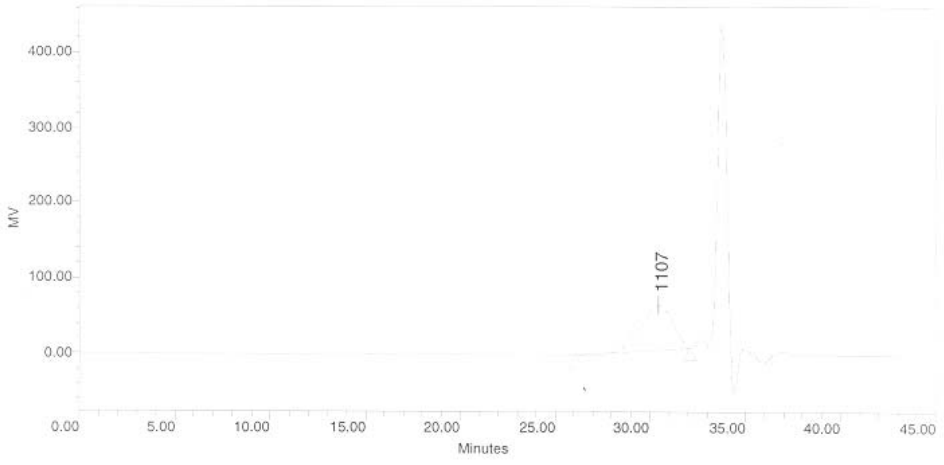

GPC Results

	Dist Name	Mn	Mw	Mv	MP	Mz	Mz+1	Polydispersity	K	alpha
1										
2		1113	1484		1107	1980	2540	1.333296		

Report Method: Ashby GPC Printed 3:41:44 PM 7/16/08 Page: 1 of 1

GPC curve for polymer **5**

Ashby GPC Report

Reported by User: System Project Name: GPC4

Ashby Group GPC

SAMPLE INFORMATION

Sample Name:	M02-19	Acquired By:	System
Sample Type:	Broad Unknown	Date Acquired:	8/23/05 8:40:43 PM
Vial:	22	Acq. Method Set:	GPCMTHSET
Injection #:	1	Date Processed:	8/24/05 9:36:26 AM
Injection Volume:	150.00 ul	Processing Method:	PM_050614
Run Time:	45.0 Minutes	Channel Name:	410
Sample Set Name:	run samples 050823	Proc. Chnl. Descr.:	

Auto-Scaled Chromatogram

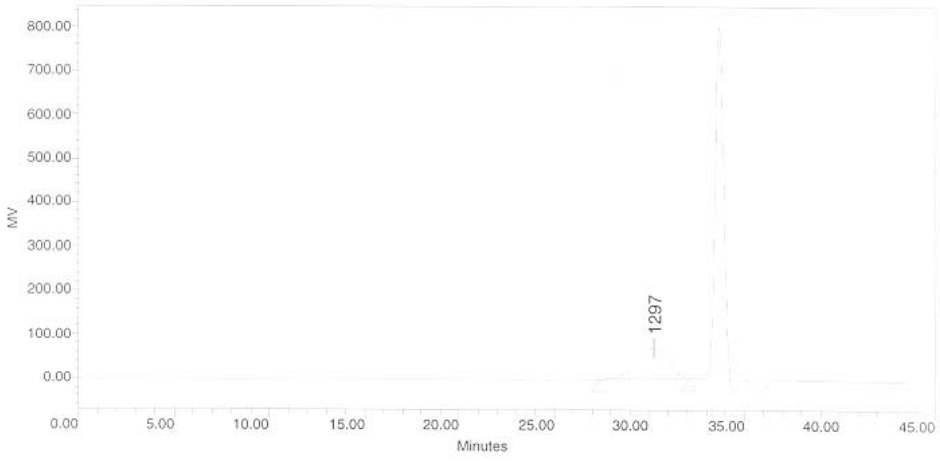

GPC Results

	Dist Name	Mn	Mw	Mv	MP	Mz	Mz+1	Polydispersity	K	alpha
1										
2		1246	1665		1297	2246	2964	1.336037		

Report Method: Ashby GPC Printed 3:41:45 PM 7/16/08 Page: 1 of 1

GPC curve for polymer **6**

Ashby GPC Report

Reported by User: System Project Name: GPC4

Ashby Group GPC

SAMPLE INFORMATION

Sample Name:	M02-09	Acquired By:	System
Sample Type:	Broad Unknown	Date Acquired:	8/7/05 5:51:37 AM
Vial:	84	Acq. Method Set:	GPCMTHSET
Injection #:	1	Date Processed:	8/16/05 10:25:35 AM
Injection Volume:	150.00 ul	Processing Method:	PM_050614
Run Time:	45.0 Minutes	Channel Name:	410
Sample Set Name:	Run_Samples_050806	Proc. Chnl. Descr.:	

Auto-Scaled Chromatogram

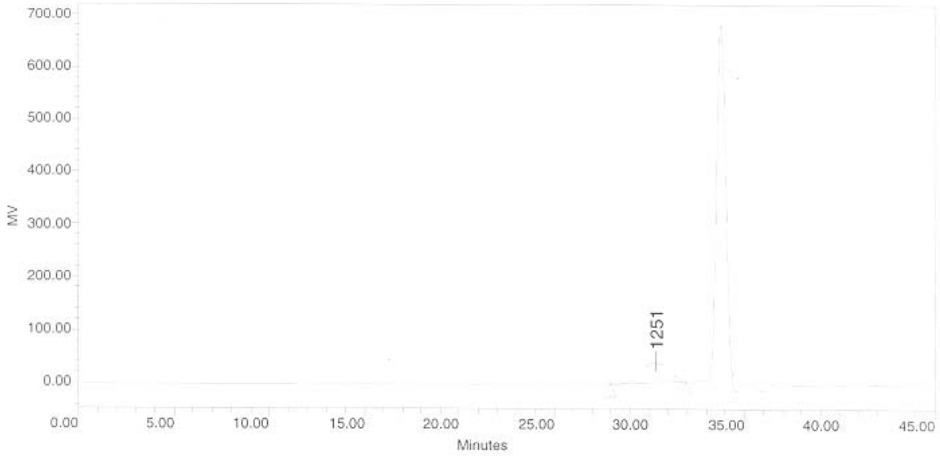

GPC Results

	Dist Name	Mn	Mw	Mv	MP	Mz	Mz+1	Polydispersity	K	alpha
1										
2		1133	1403		1251	1721	2071	1.237666		

Report Method: Ashby GPC Printed 3:41:31 PM 7/16/08 Page: 1 of 1

GPC curve for polymer **7**

Ashby GPC Report

Reported by User: System Project Name: GPC4

Ashby Group GPC

SAMPLE INFORMATION

Sample Name:	M02-13	Acquired By:	System
Sample Type:	Broad Unknown	Date Acquired:	8/7/05 6:40:00 AM
Vial:	85	Acq. Method Set:	GPCMTHSET
Injection #:	1	Date Processed:	8/16/05 10:25:34 AM
Injection Volume:	150.00 ul	Processing Method:	PM_050614
Run Time:	45.0 Minutes	Channel Name:	410
Sample Set Name:	Run_Samples_050806	Proc. Chnl. Descr.:	

Auto-Scaled Chromatogram

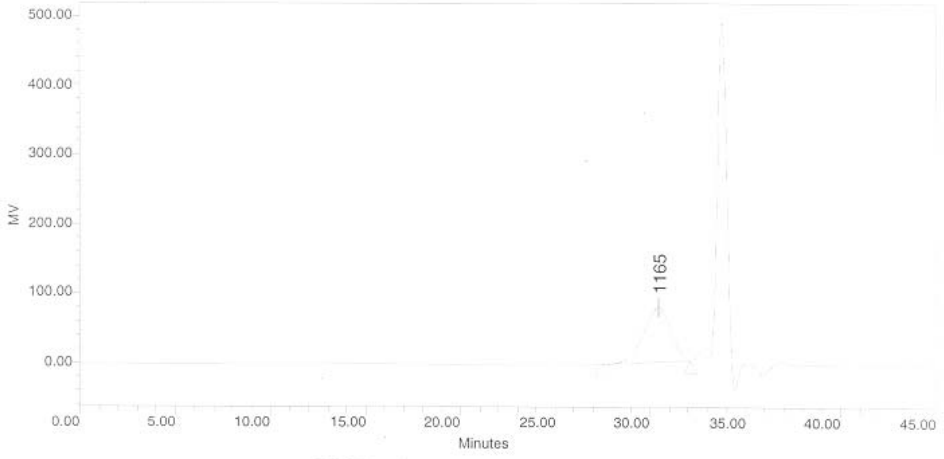

GPC Results

	Dist Name	Mn	Mw	Mv	MP	Mz	Mz+1	Polydispersity	K	alpha
1										
2		1115	1411		1165	1800	2271	1.266030		

Report Method: Ashby GPC Printed 3:41:32 PM 7/16/08 Page: 1 of 1

GPC curve for polymer **8**

Ashby GPC Report

Reported by User: System Project Name: GPC4

Ashby Group GPC

SAMPLE INFORMATION

Sample Name:	M02-15	Acquired By:	System
Sample Type:	Broad Unknown	Date Acquired:	8/7/05 8:16:46 AM
Vial:	87	Acq. Method Set:	GPCMTHSET
Injection #:	1	Date Processed:	8/16/05 10:25:34 AM
Injection Volume:	150.00 ul	Processing Method:	PM_050614
Run Time:	45.0 Minutes	Channel Name:	410
Sample Set Name:	Run_Samples_050806	Proc. Chnl. Descr.:	

Auto-Scaled Chromatogram

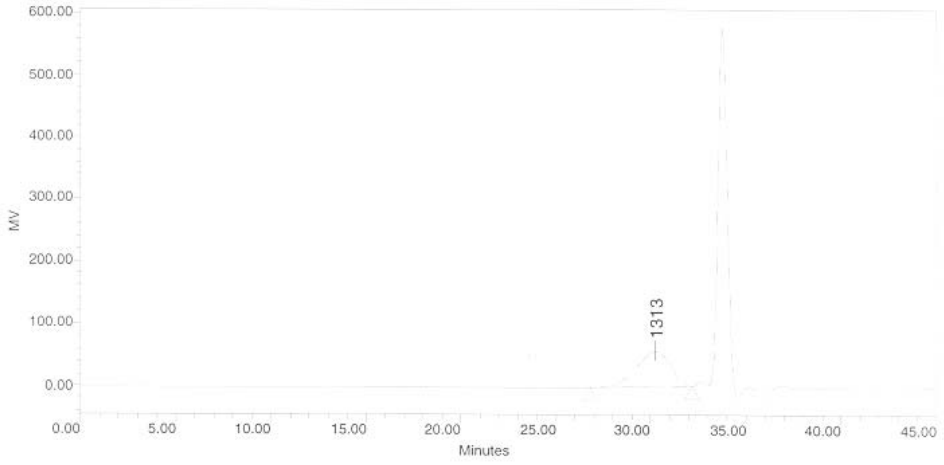

GPC Results

	Dist Name	Mn	Mw	Mv	MP	Mz	Mz+1	Polydispersity	K	alpha
1										
2		1281	1788		1313	2521	3438	1.395734		

Report Method: Ashby GPC Printed 3:41:38 PM 7/16/08 Page: 1 of 1

GPC curve for polymer **9**

Empower 2 software

Ashby GPC Report

SAMPLE INFORMATION

Sample Name:	M02-24	Acquired By:	System
Sample Type:	Broad Unknown	Sample Set Name:	Run_Samples_080624
Vial:	102	Acq. Method Set:	GPC PDA Off
Injection #:	1	Processing Method:	070412 THF
Injection Volume:	100.00 ul	Channel Name:	410
Run Time:	50.0 Minutes	Proc. Chnl. Descr.:	
Date Acquired:	6/24/2008 5:28:11 PM EDT		
Date Processed:	7/16/2008 4:58:41 PM EDT		

Auto-Scaled Chromatogram

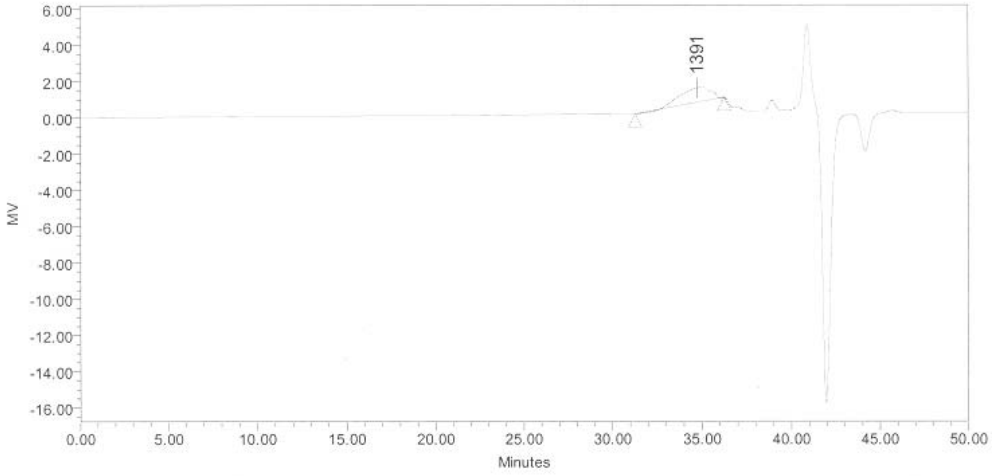

GPC Results

	Dist Name	Mn	Mw	Mv	MP	Mz	Mz+1	Poly dispersity	K	alpha
1		1482	1703		1391	1955	2215	1.148503		

Reported by User: System
Report Method: Ashby GPC Report
Report Method ID: 1111
Page: 1 of 1

Project Name: GPC
Date Printed:
7/16/2008
5:00:03 PM US/Eastern

GPC curve for polymer **10**

Ashby GPC Report

Reported by User: System Project Name: GPC4

Ashby Group GPC

SAMPLE INFORMATION

Sample Name:	M02-22	Acquired By:	System
Sample Type:	Broad Unknown	Date Acquired:	8/23/05 10:17:26 PM
Vial:	24	Acq. Method Set:	GPCMTHSET
Injection #:	1	Date Processed:	8/24/05 9:36:26 AM
Injection Volume:	150.00 ul	Processing Method:	PM_050614
Run Time:	45.0 Minutes	Channel Name:	410
Sample Set Name:	run samples 050823	Proc. Chnl. Descr.:	

Auto-Scaled Chromatogram

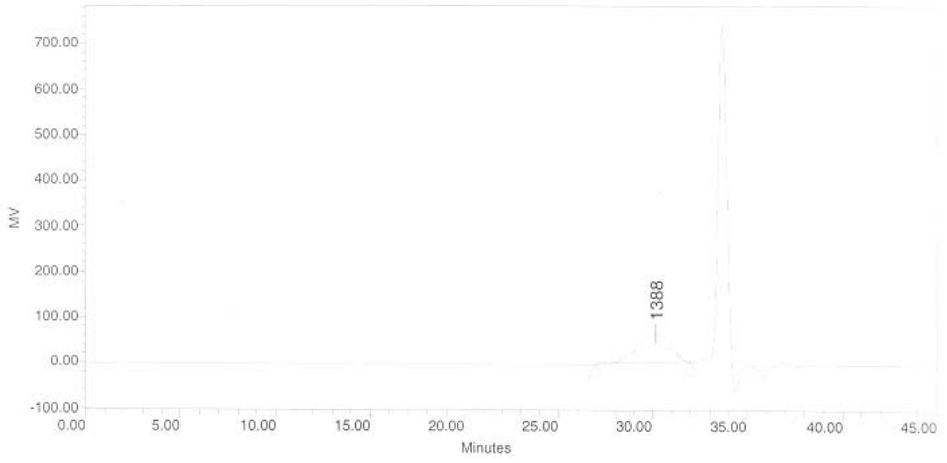

GPC Results

	Dist Name	Mn	Mw	Mv	MP	Mz	Mz+1	Polydispersity	K	alpha
1										
2		1351	1861		1388	2586	3477	1.377502		

Report Method: Ashby GPC Printed 3:41:49 PM 7/16/08 Page: 1 of 1

GPC curve for polymer **11**

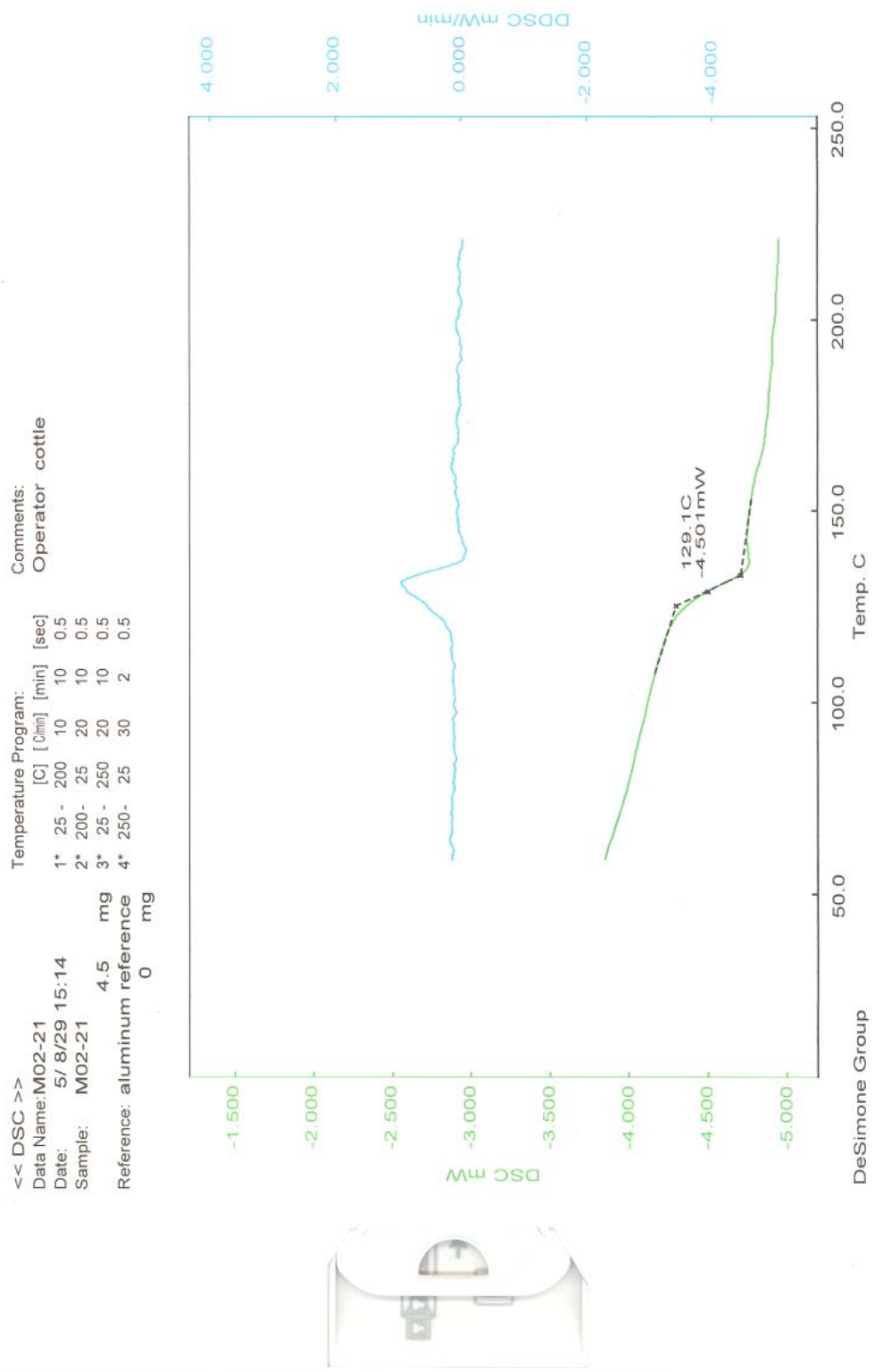

DSC curve for polymer **1**

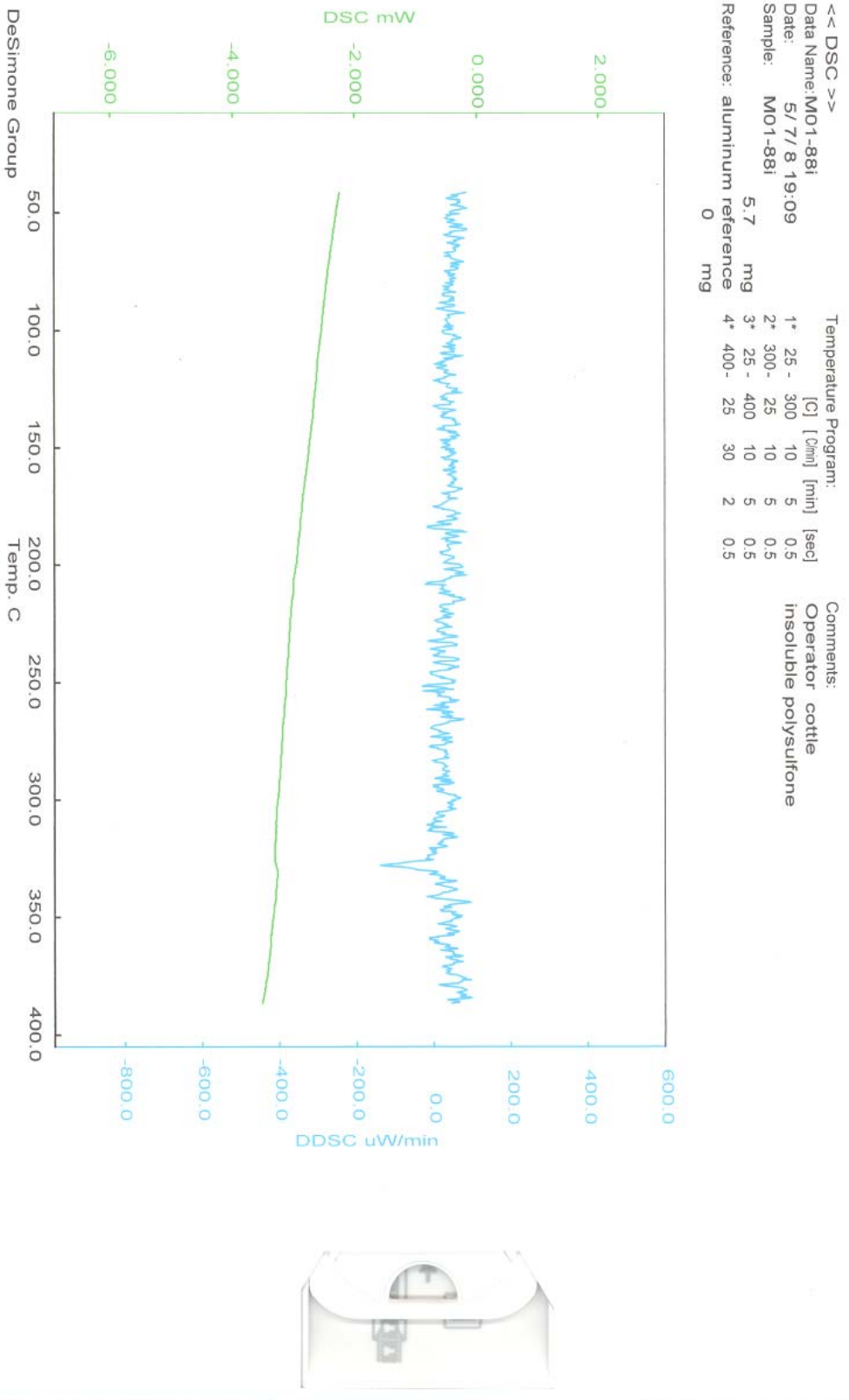

DSC curve for polymer **2a**

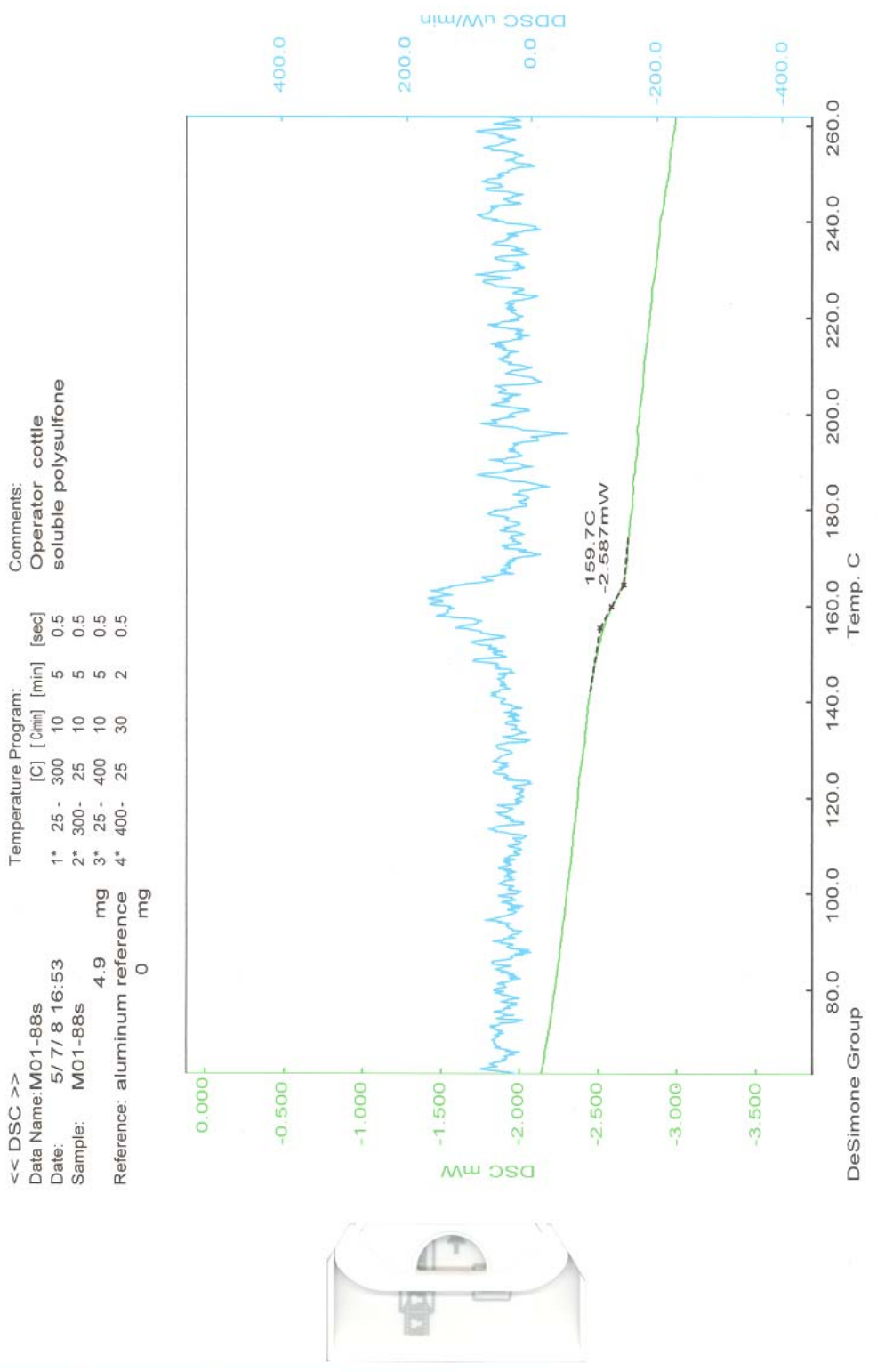

DSC curve for polymer **2b**

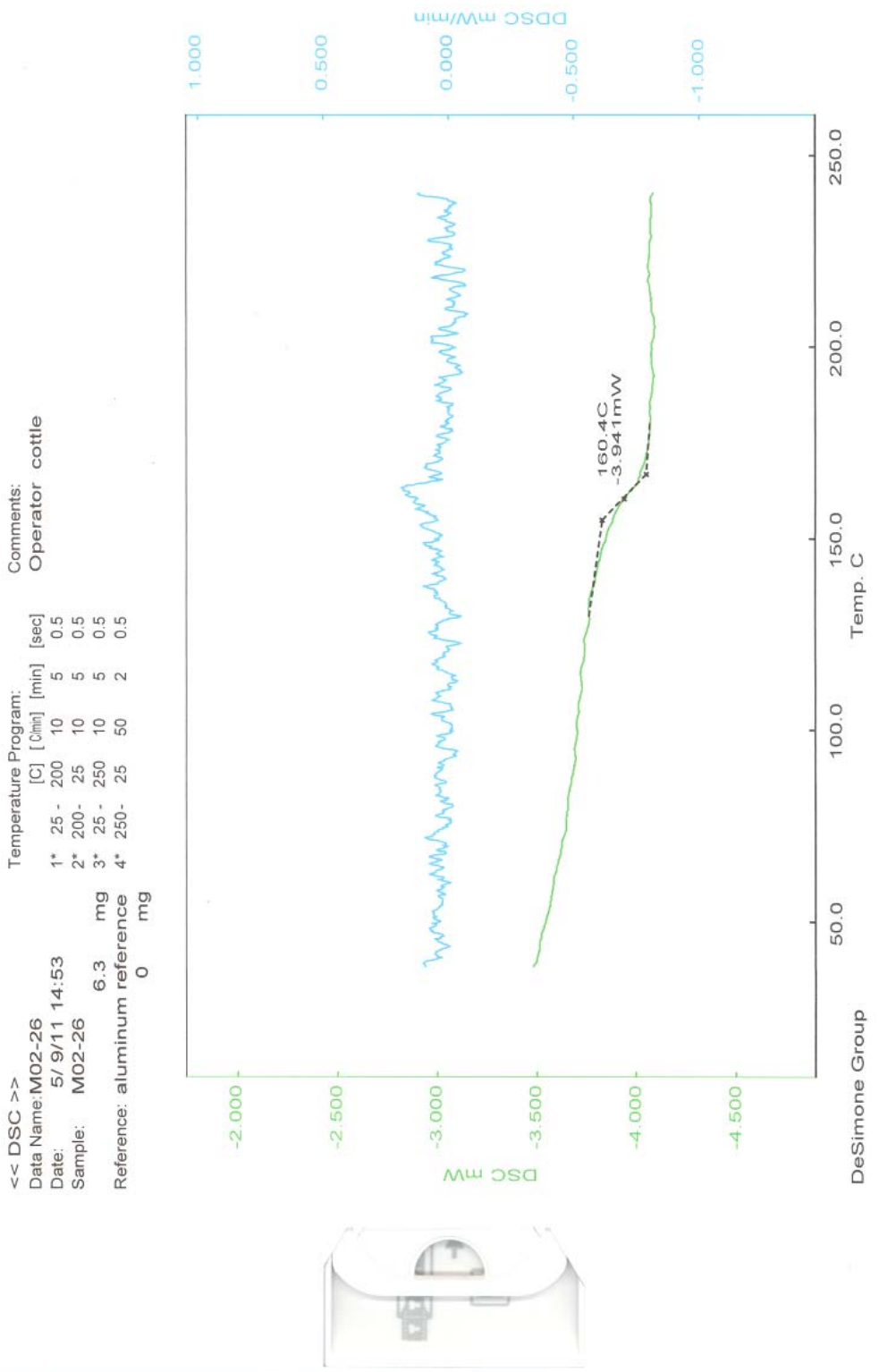

DSC curve for polymer **3**

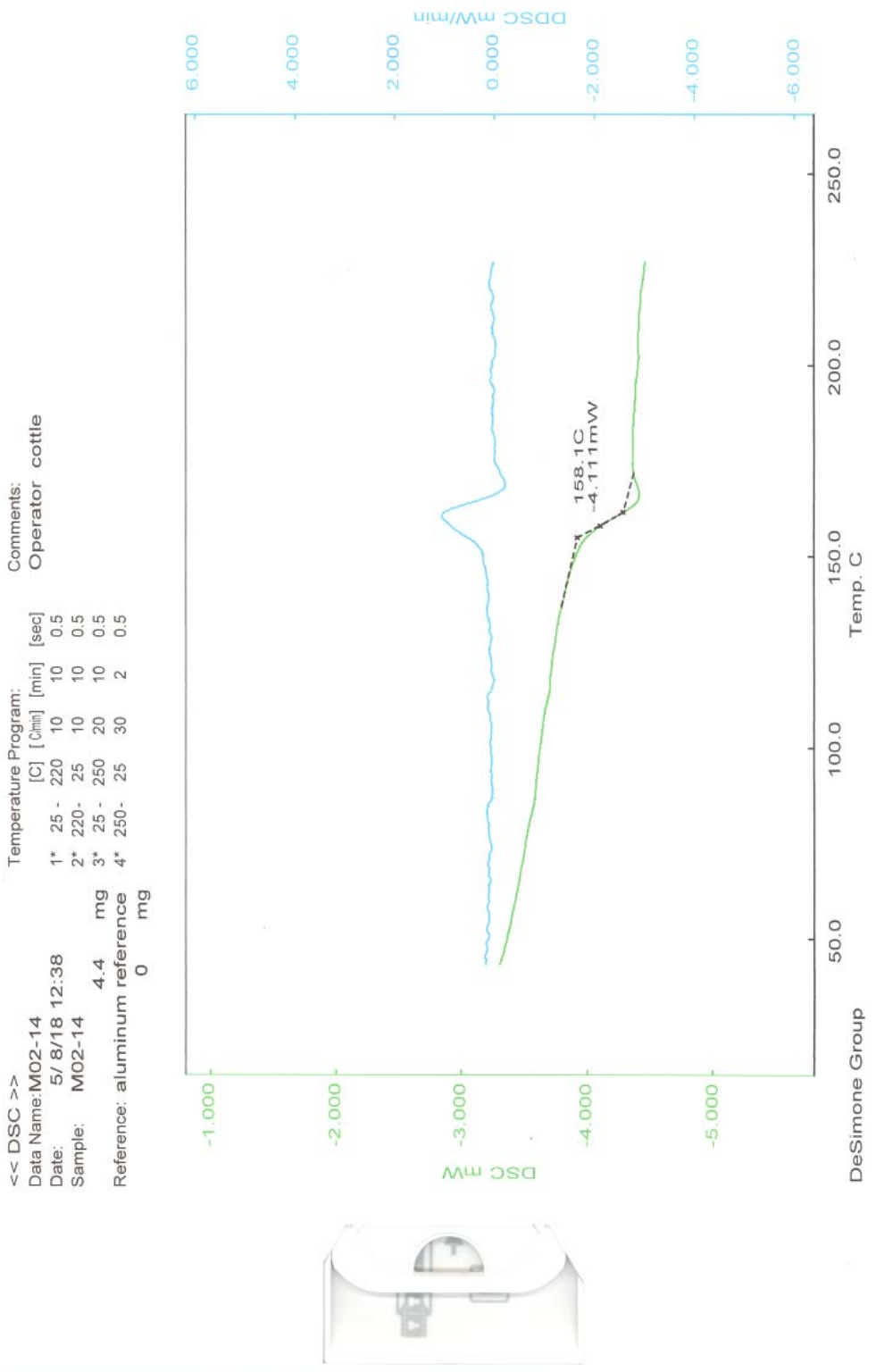

DSC curve for polymer **4**

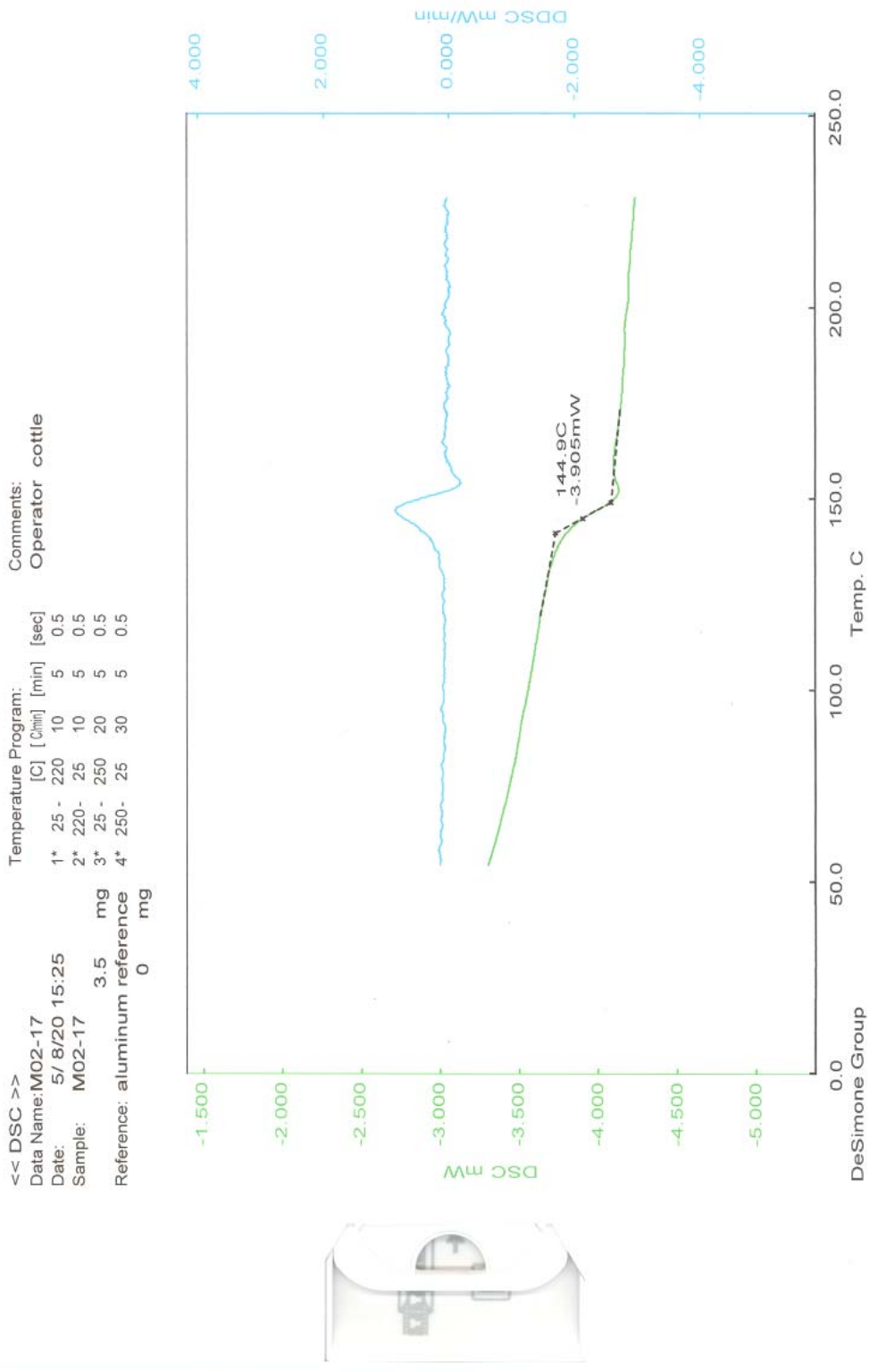

DSC curve for polymer **5**

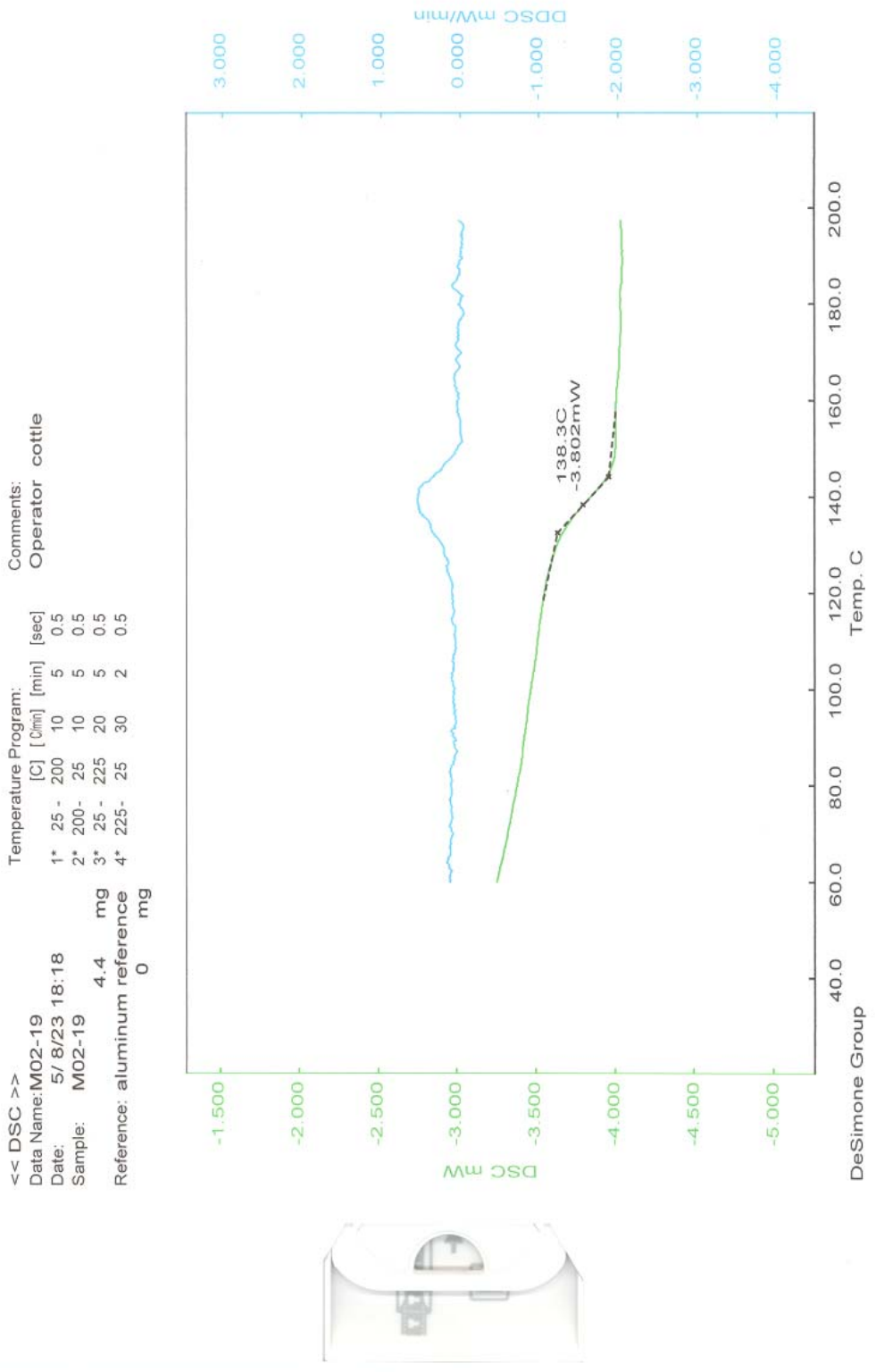

DSC curve for polymer **6**

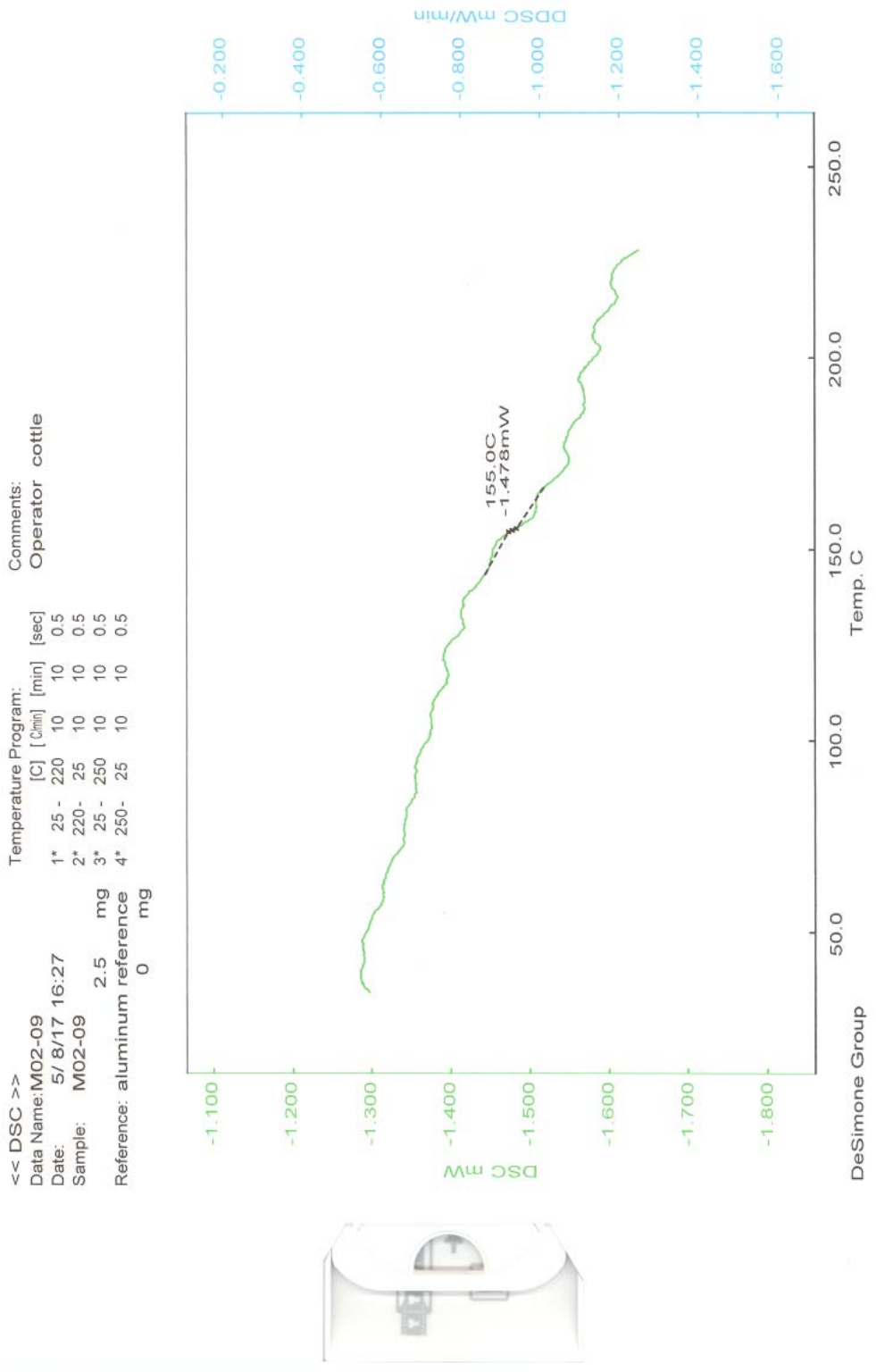

DSC curve for polymer **7**

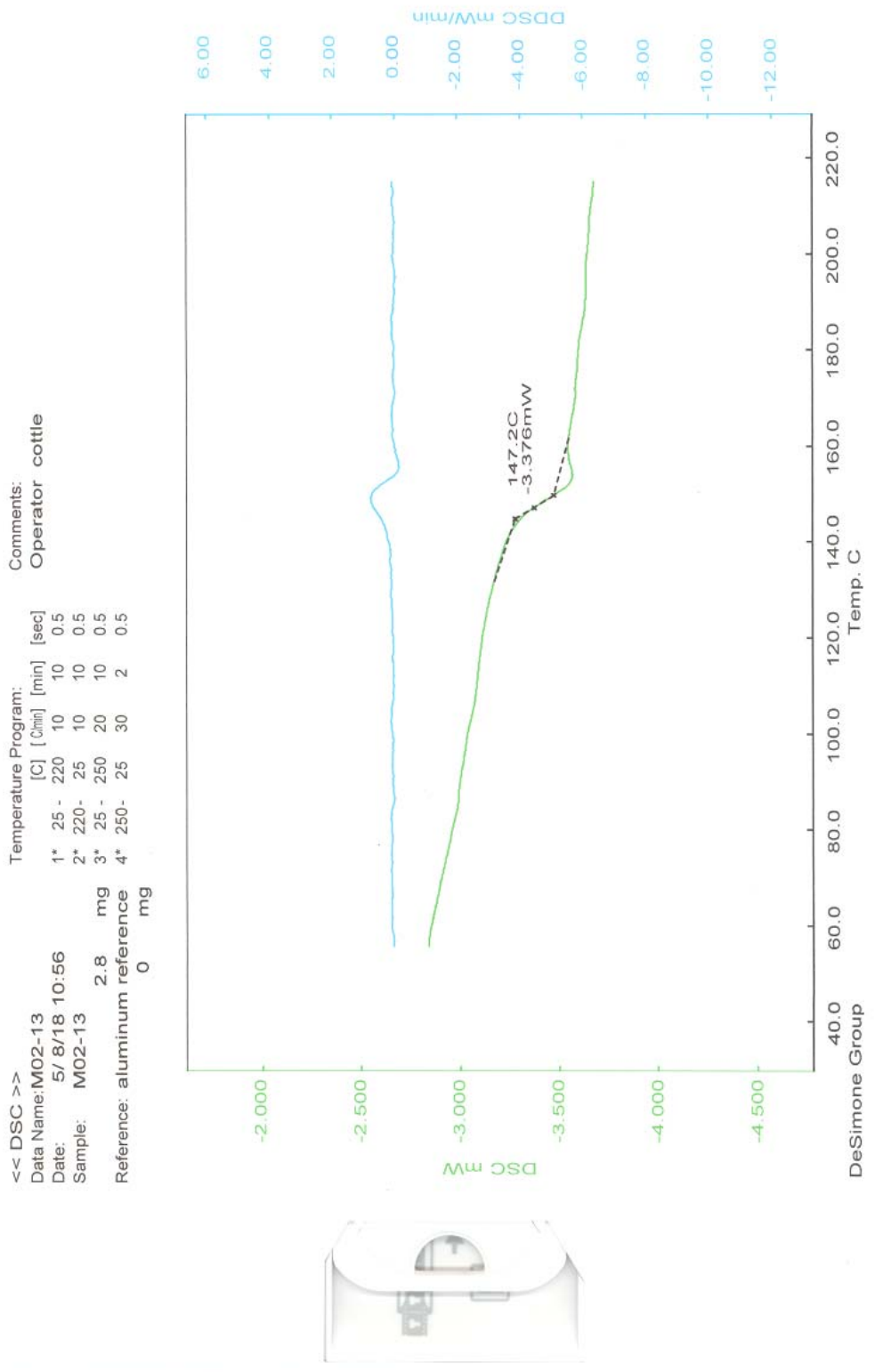

DSC curve for polymer **8**

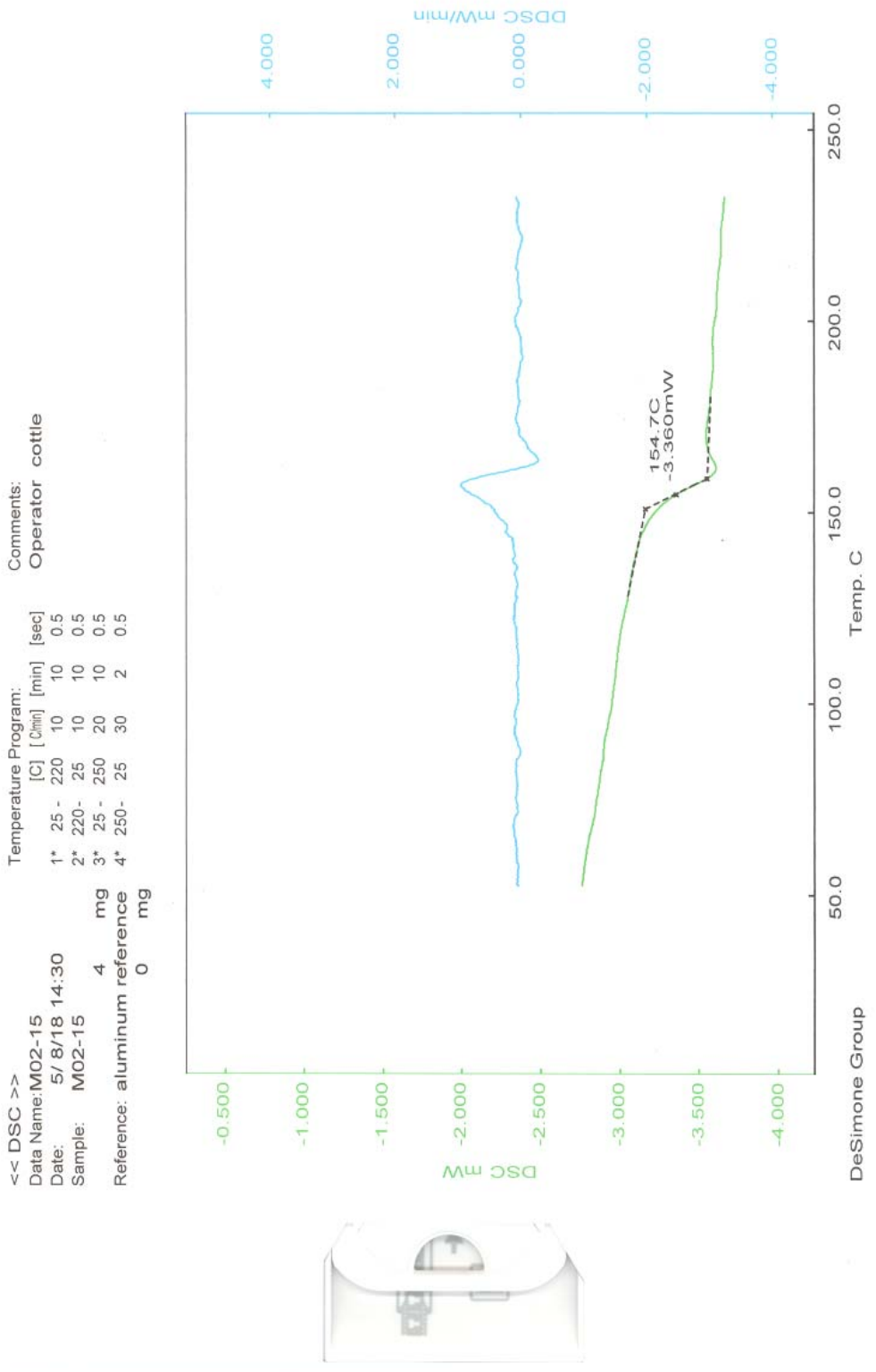

DSC curve for polymer **9**

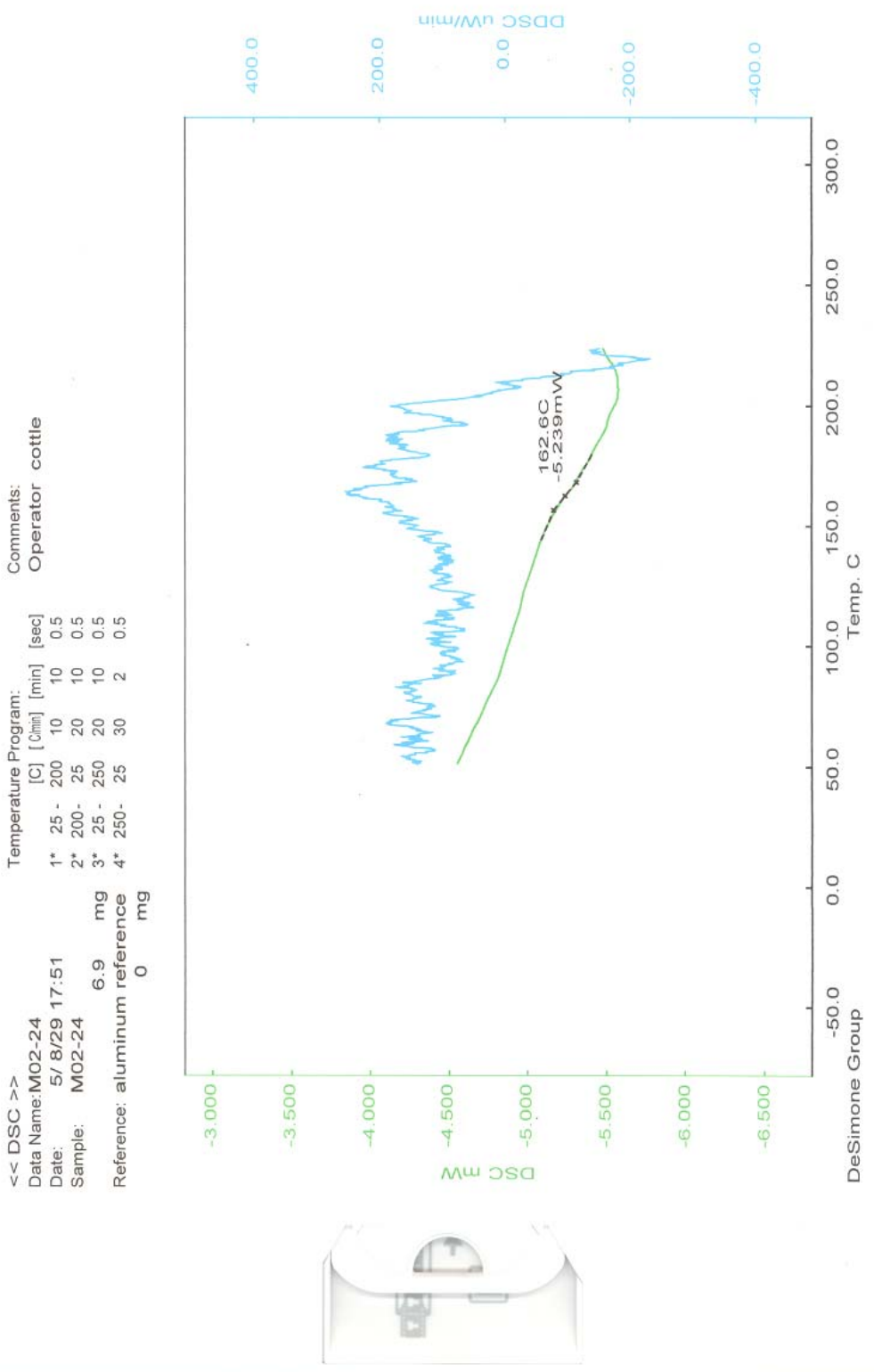

DSC curve for polymer **10**

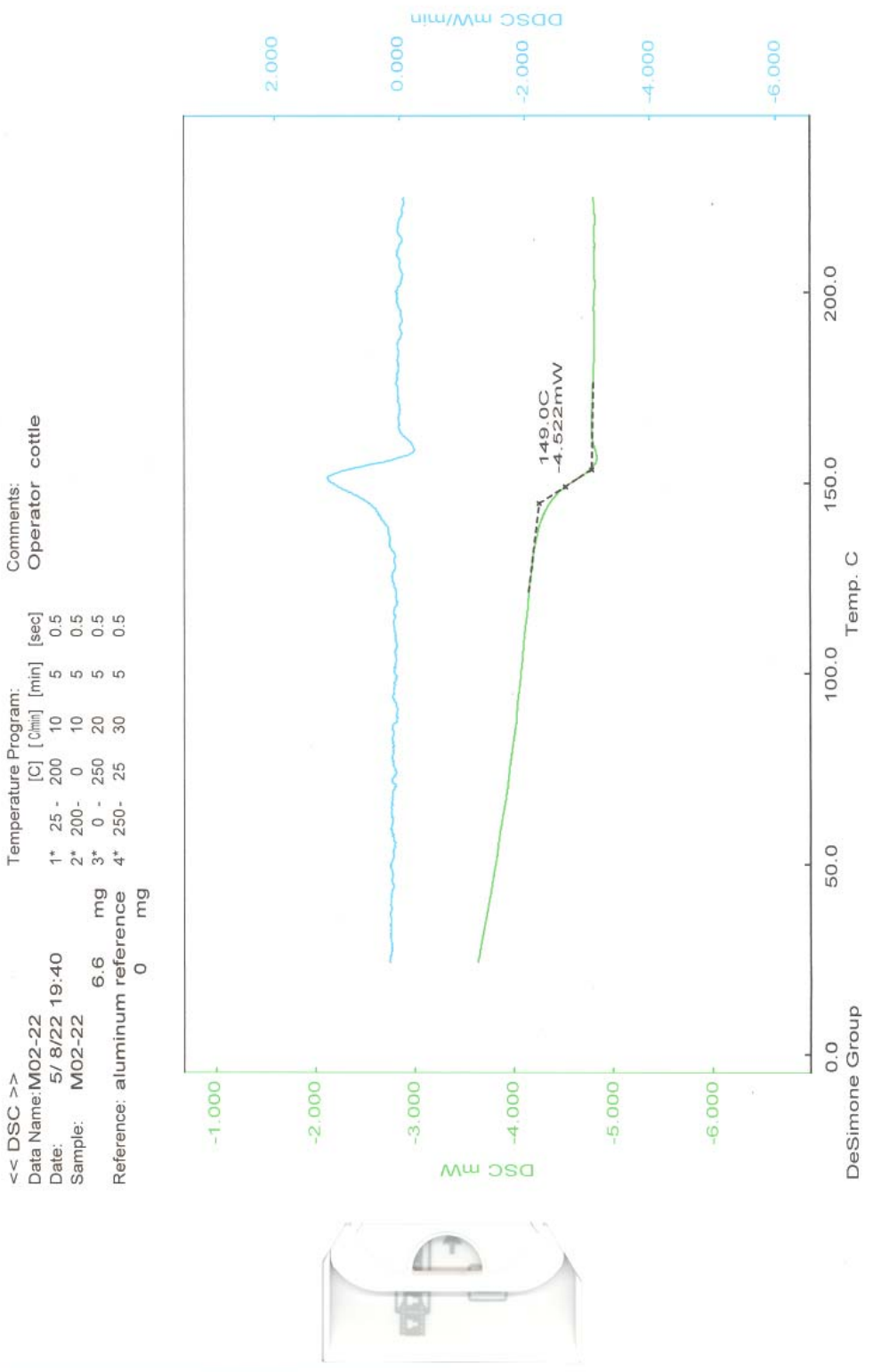

DSC curve for polymer **11**

Appendix C

SUPPLEMENTAL MATERIALS FOR CHAPTER 4

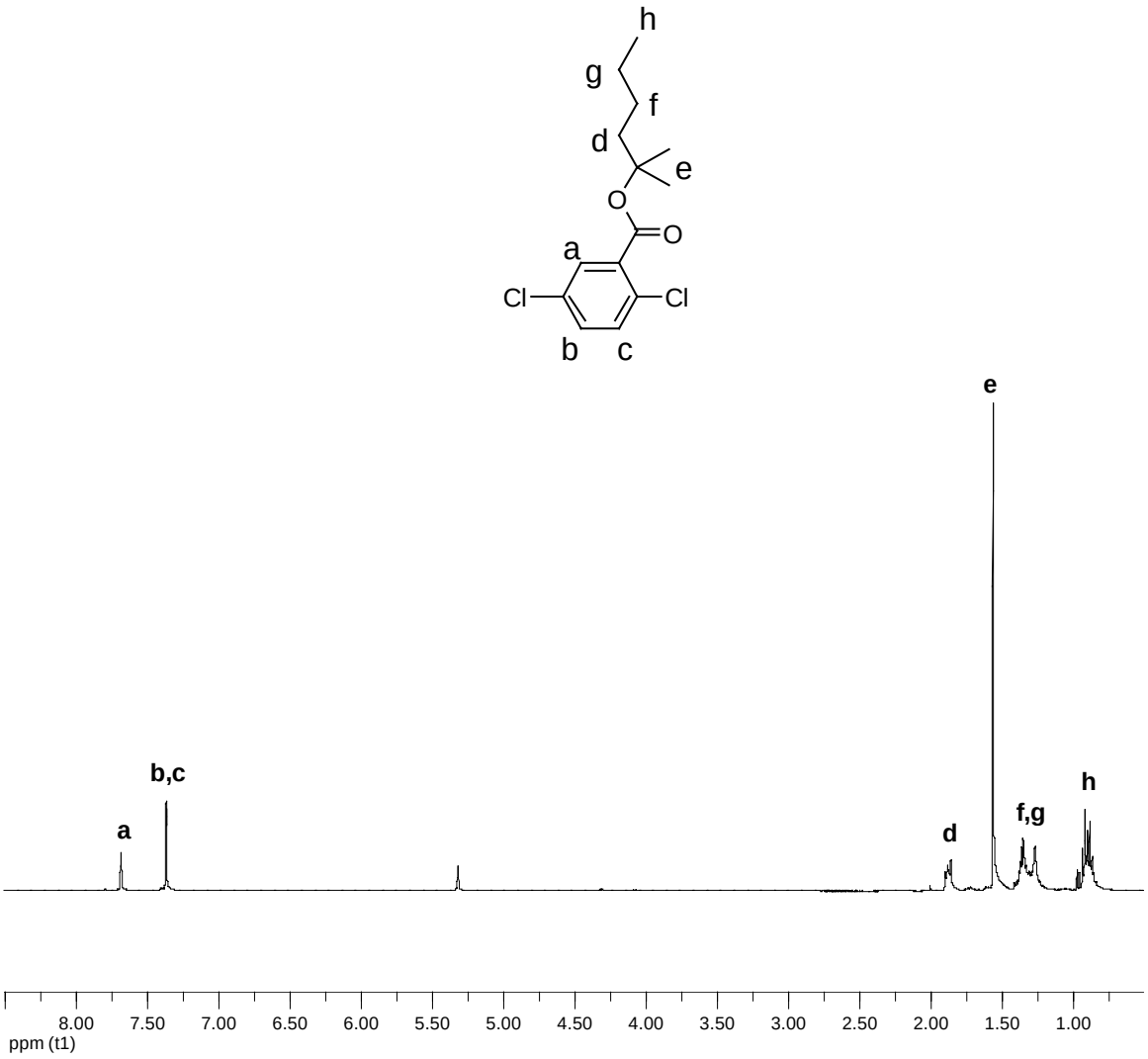

[1]H-NMR of 2-Methyl-2-hexyl-2,5-dichlorobenzene-2-carboxylate

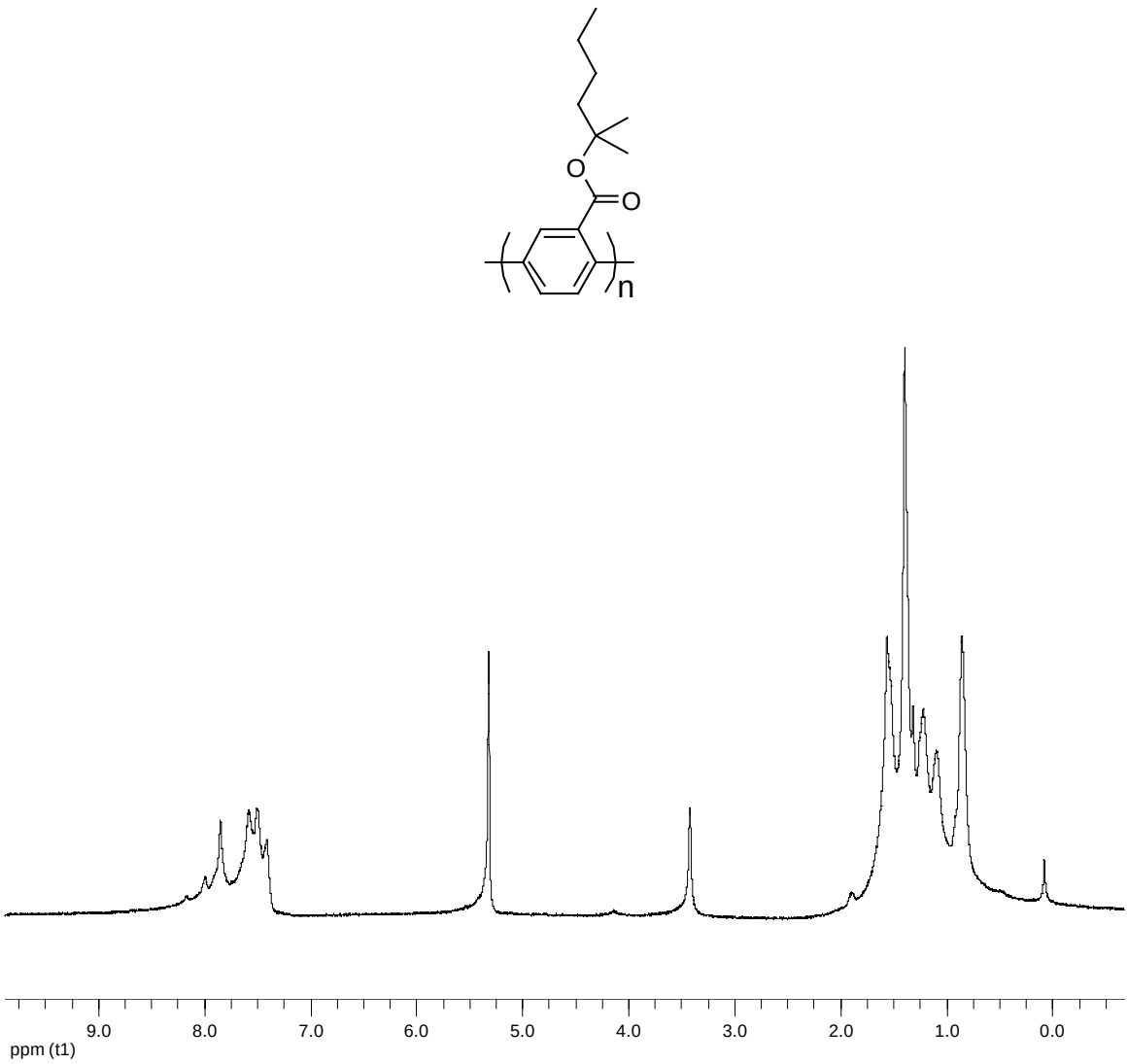

^{1}H-NMR of ester-functionalized poly(paraphenylene)

Empower 2 software

Ashby GPC Report

SAMPLE INFORMATION

Sample Name:	M05-77	Acquired By:	System
Sample Type:	Broad Unknow n	Sample Set Name:	Run_Samples_080530
Vial:	117	Acq. Method Set:	GPC PDA Off
Injection #:	1	Processing Method:	070412 THF
Injection Volume:	100.00 ul	Channel Name:	410
Run Time:	50.0 Minutes	Proc. Chnl. Descr.:	
Date Acquired:	5/30/2008 1:06:25 PM EDT		
Date Processed:	5/30/2008 3:55:33 PM EDT		

Auto-Scaled Chromatogram

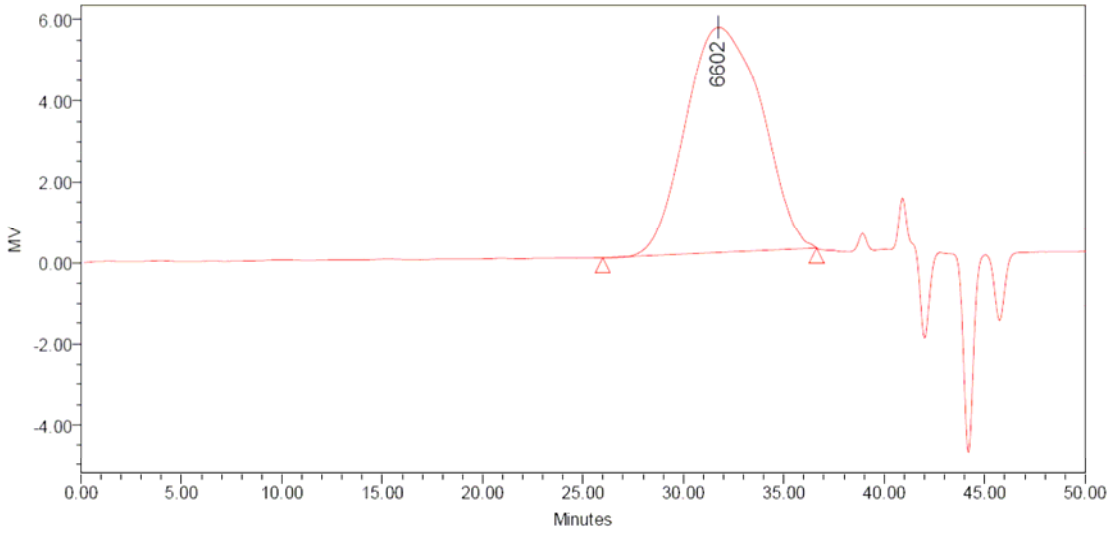

GPC Results

	Dist Name	Mn	Mw	Mv	MP	Mz	Mz+1	Poly dispersity	K	alpha
1		4015	7546		6602	12808	18854	1.879540		

Reported by User: System
Report Method: Ashby GPC Report
Report Method ID: 1111
Page: 1 of 1

Project Name: GPC
Date Printed:
7/13/2008
11:01:01 AM US/Eastern

GPC data for ester-functionalized poly(paraphenylene)

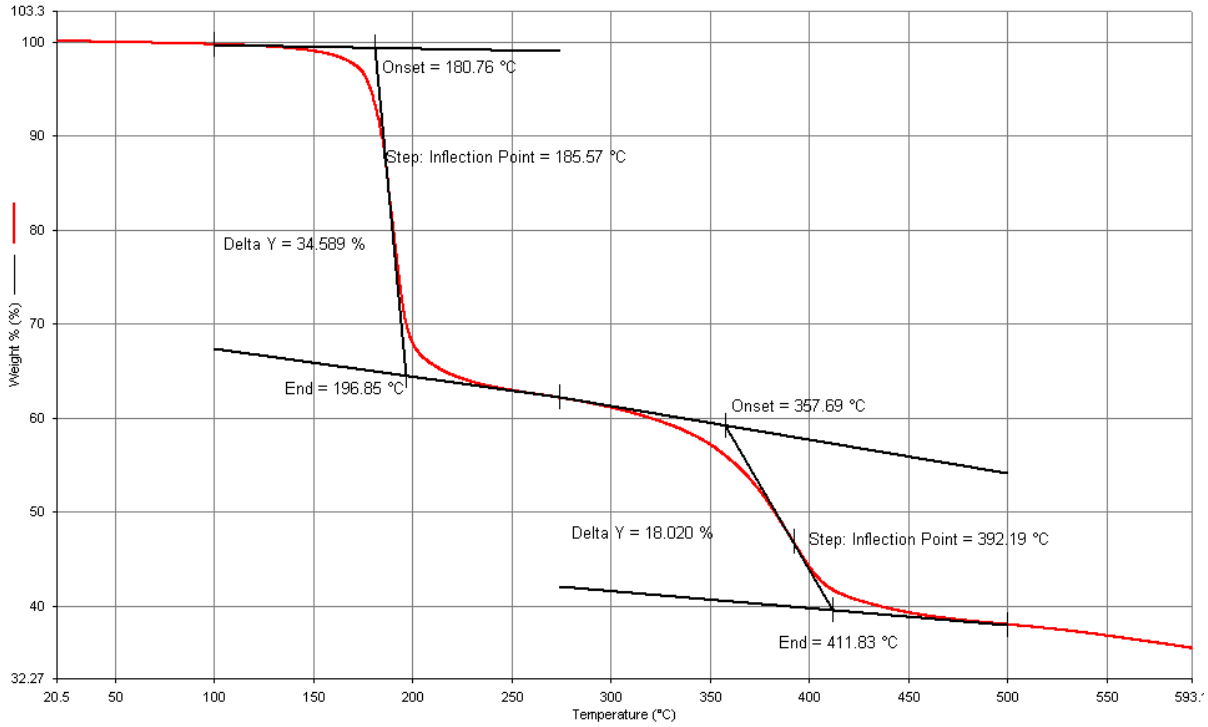

TGA data for ester-functionalized PPP with a heating rate of 10 °C/min

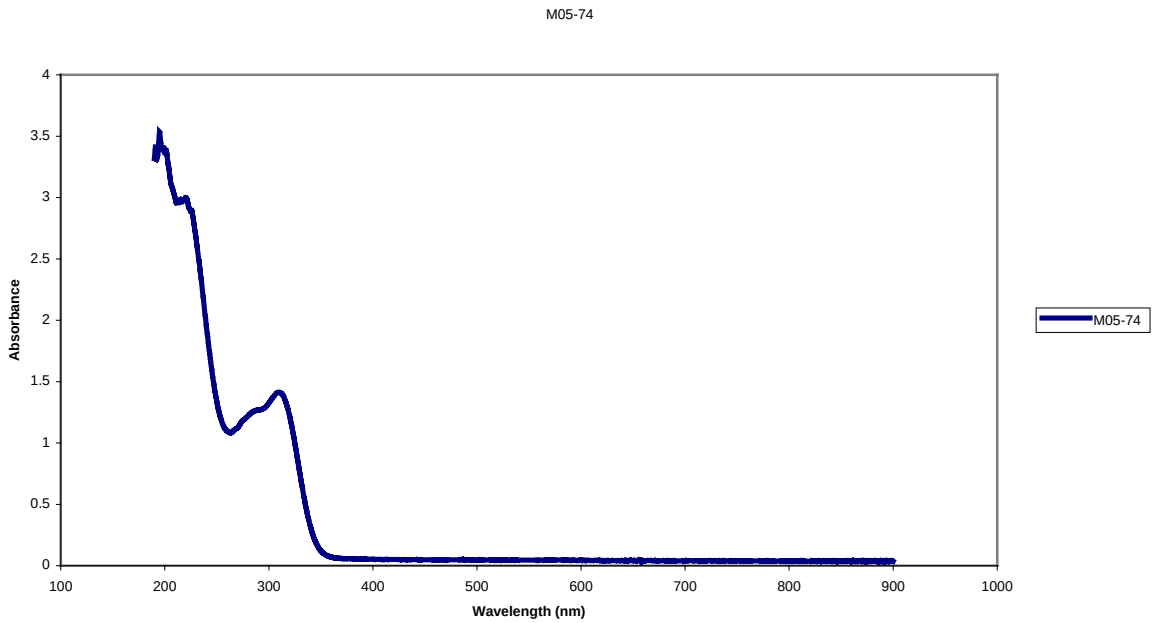

UV-vis spectra for ester-functionalized PPP unannealed

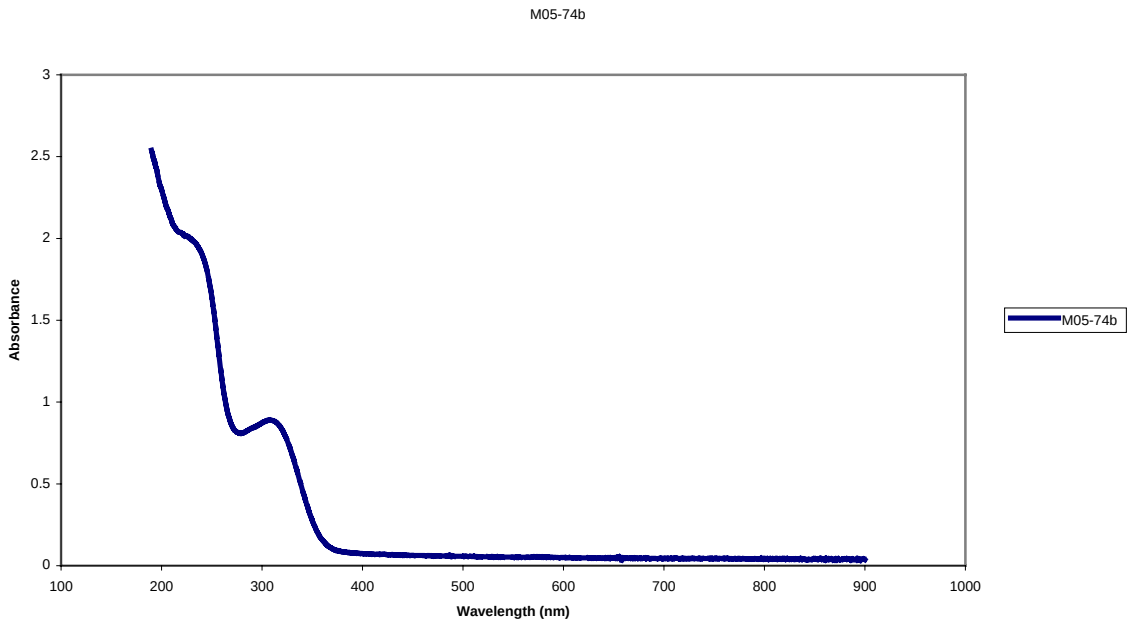

UV-vis spectra for ester-functionalized PPP annealed at 225 °C for 5 min

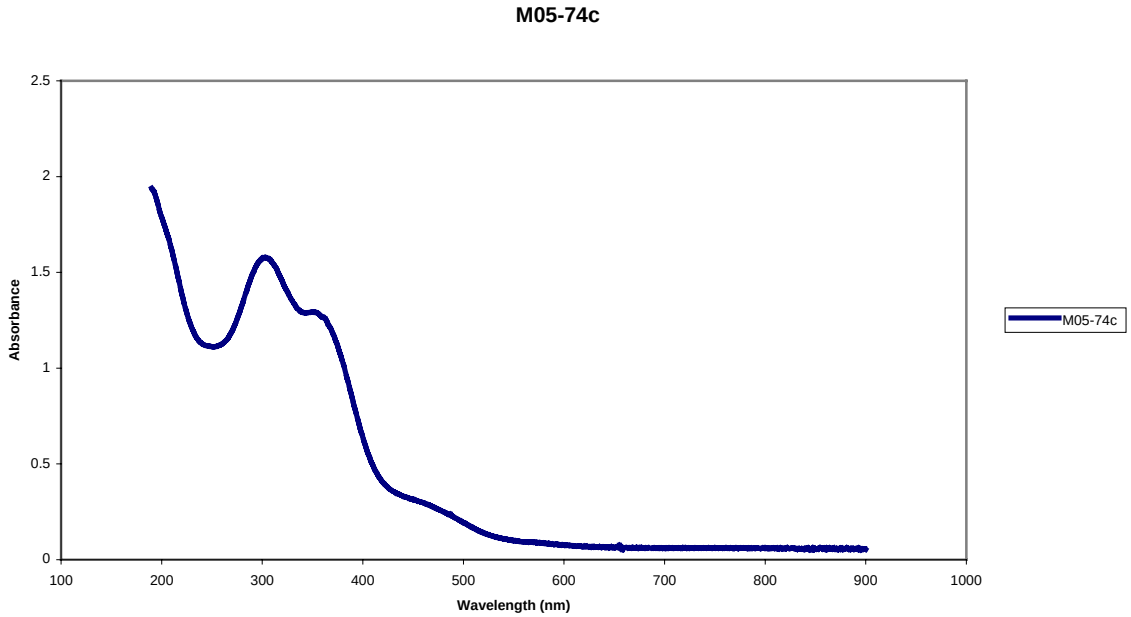

UV-vis spectrum for ester-functionalized PPP annealed at 400 °C for 5 min

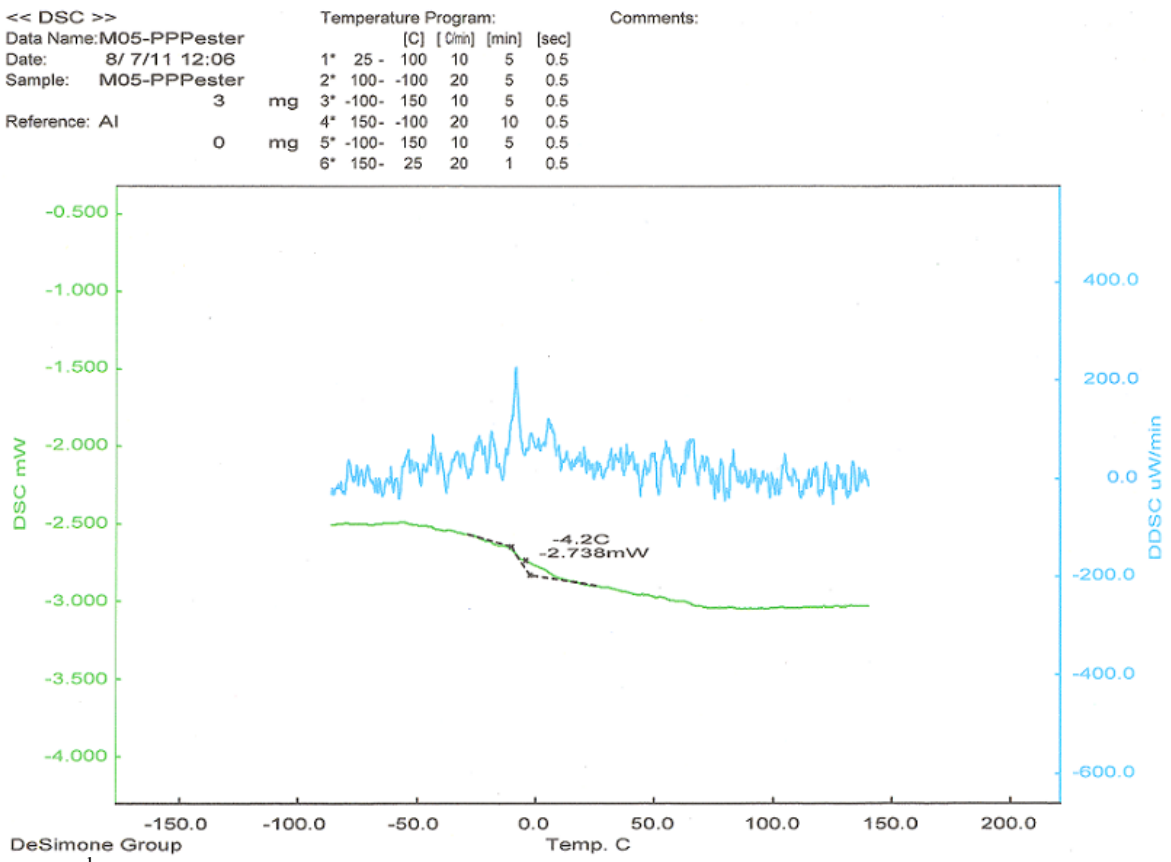

DSC (3rd heat) for ester-functionalized PPP over a temperature range of –100-150 °C

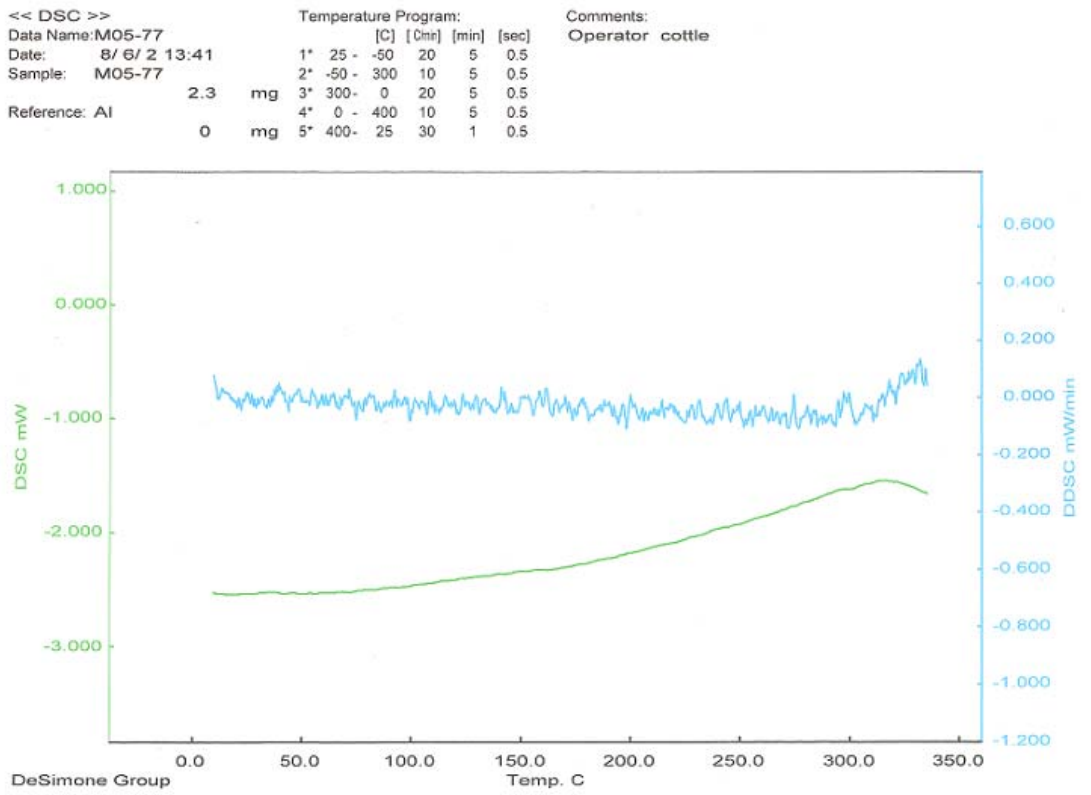

DSC (2nd heat) of ester-functionalized PPP over a temperature range of 0-400 °C

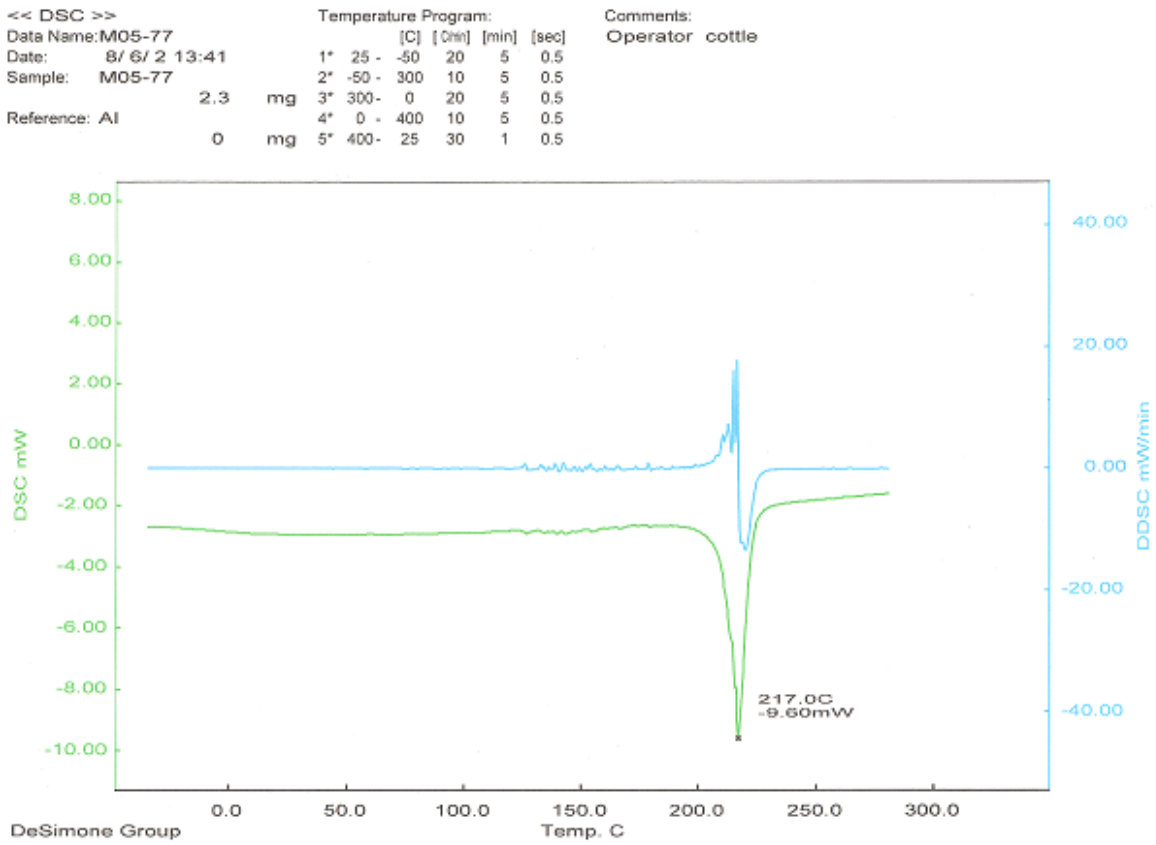

DSC (1st heat) of ester-functionalized PPP over a temperature range of –50-300 °C

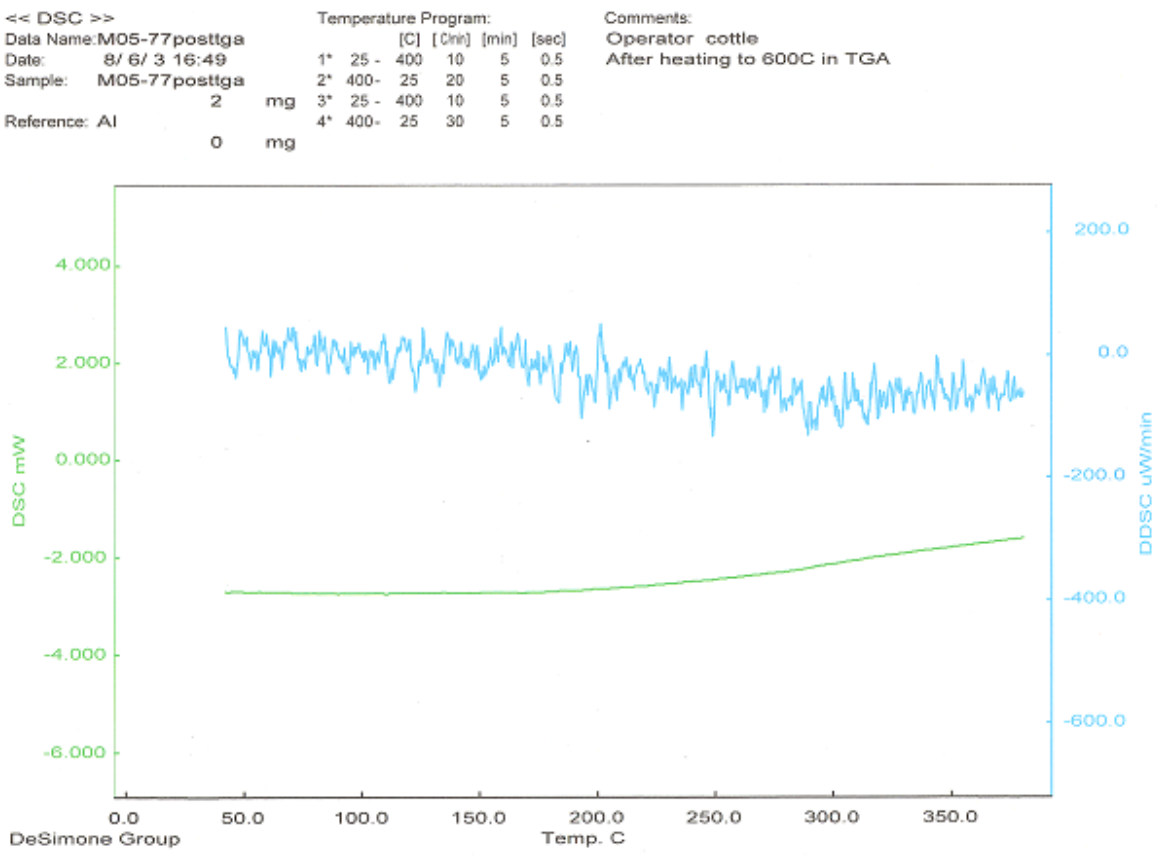

DSC (2nd heat) of ester-functionalized PPP over a temperature range of 25-400 °C after heating sample in TGA to 600 °C

Appendix D

SUPPLEMENTAL MATERIALS FOR CHAPTER 5

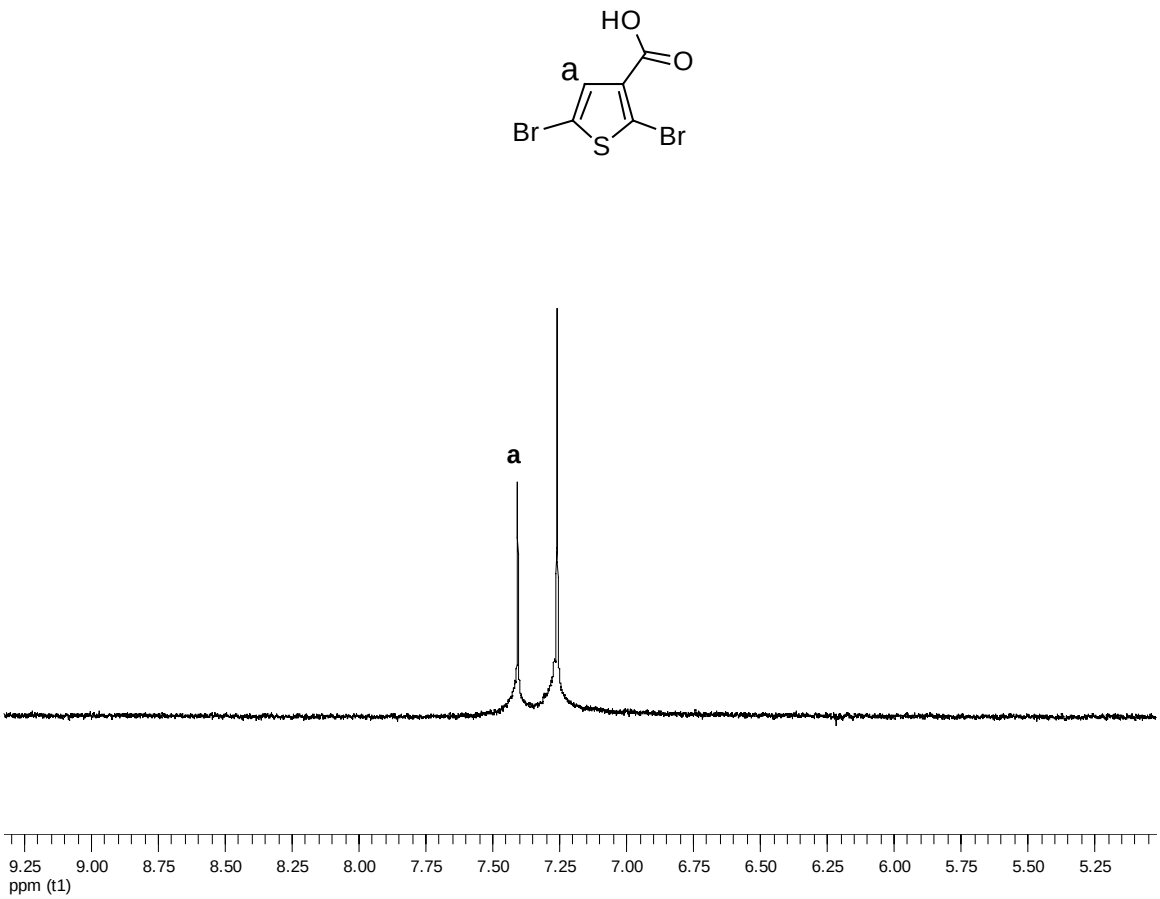

^{1}H-NMR of 2,5-dibromothiophene-3-carboxylic acid in $CDCl_3$

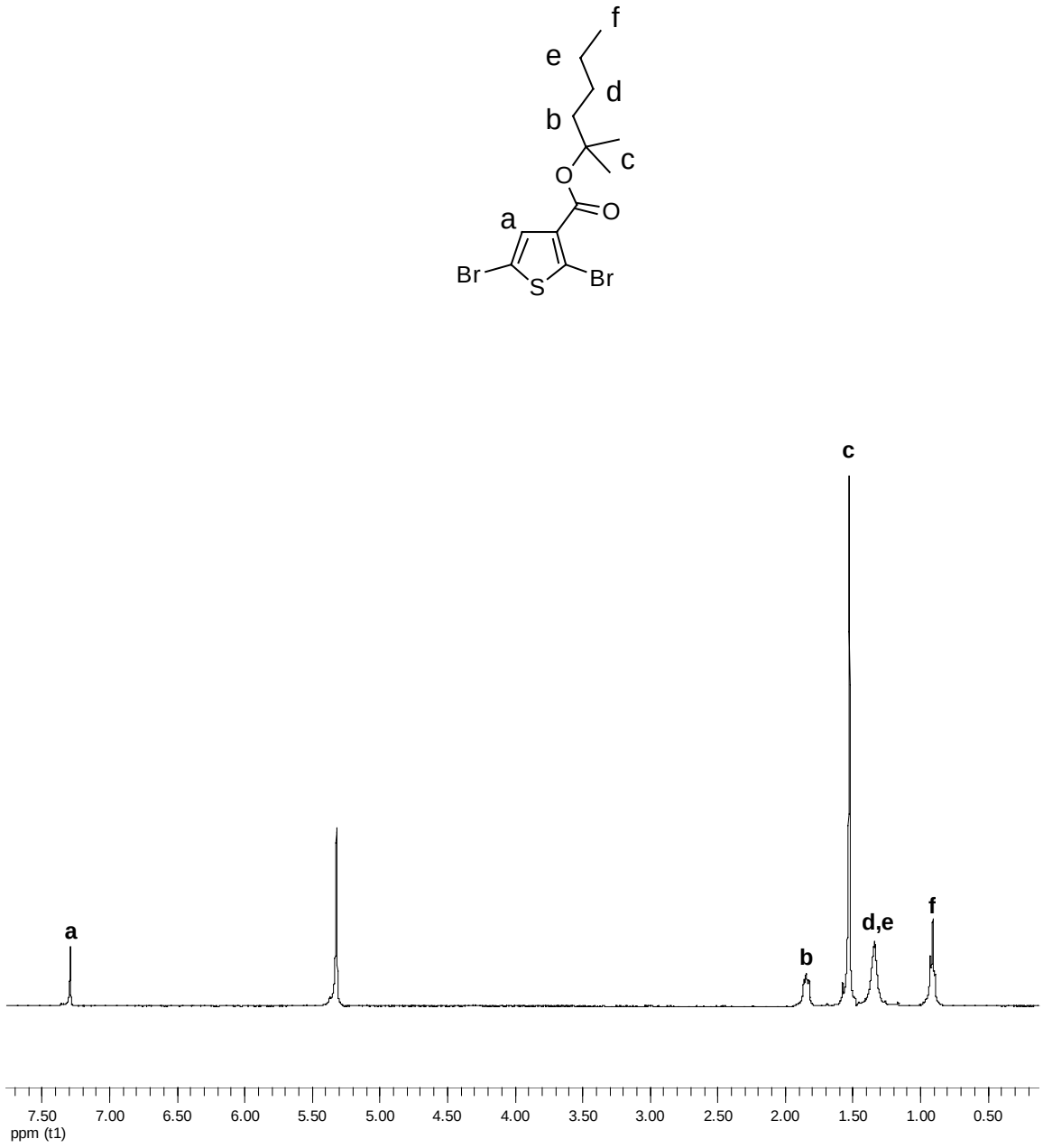

^{1}H-NMR of 2-methyl-2-hexyl-2,5-dibromothiophene-3-carboxylate in CD_2Cl_2

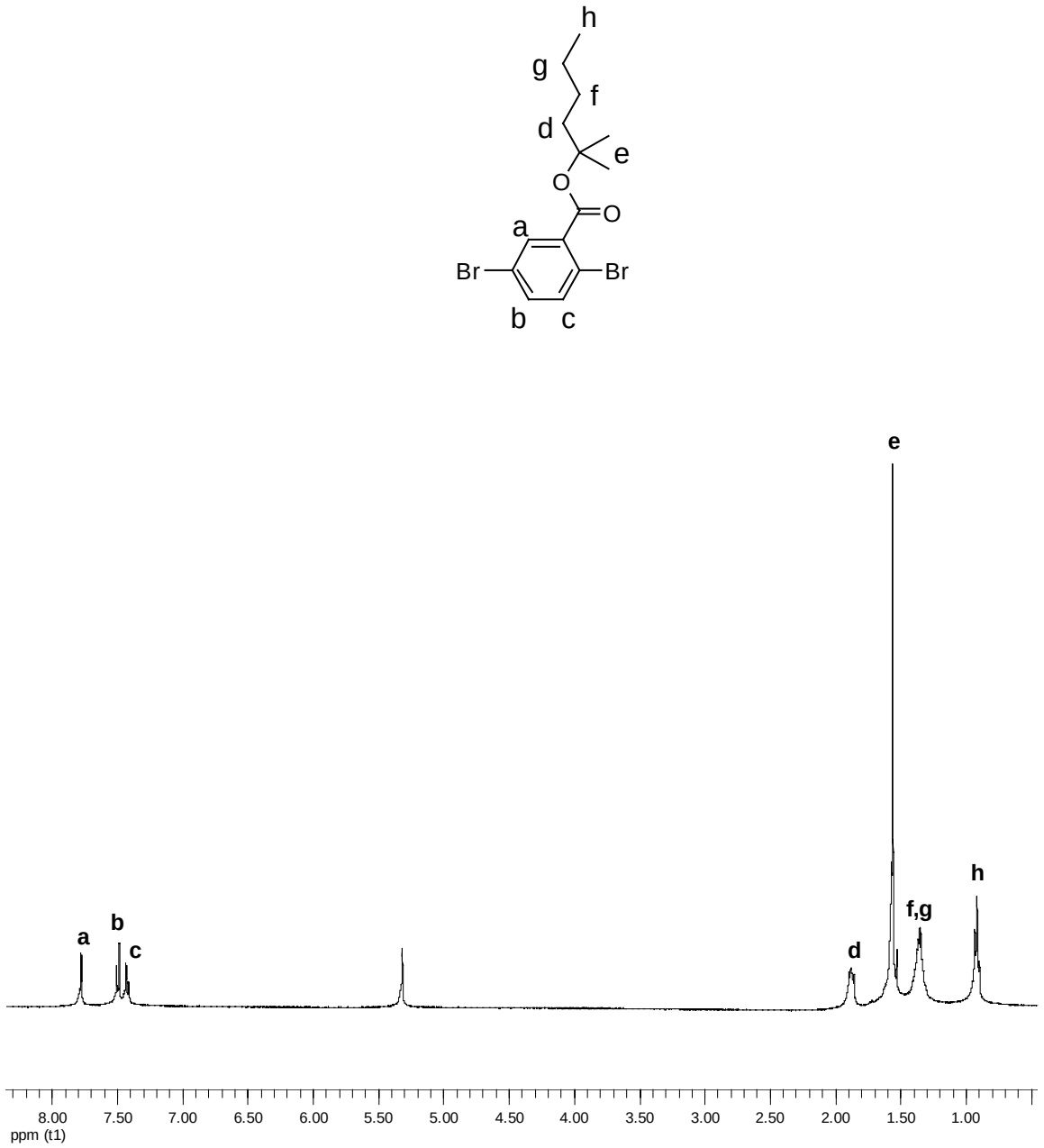

^{1}H-NMR of 2-methyl-2-hexyl-1,4-dibromobenzene-2-carboxylate in CD_2Cl_2

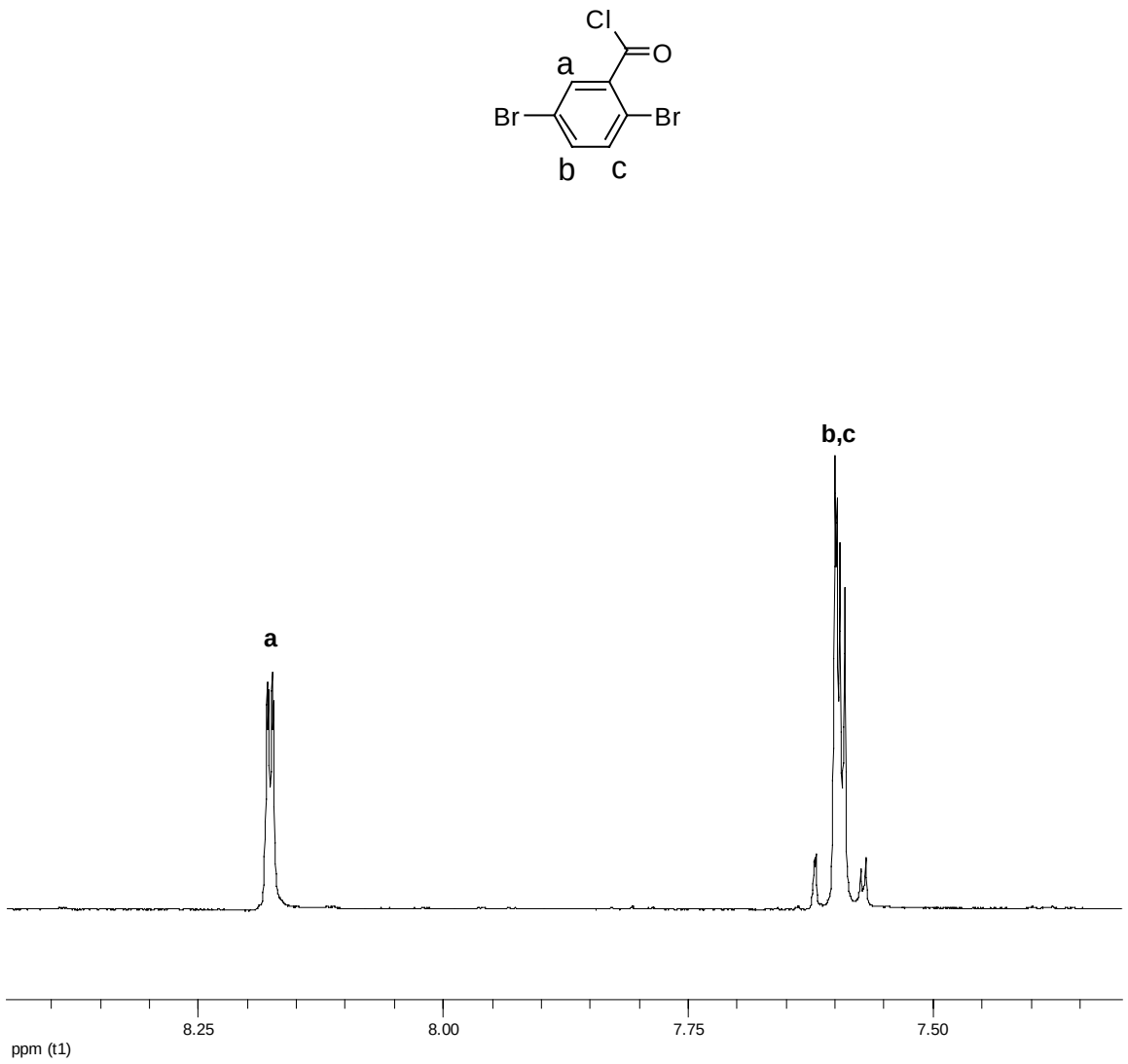

^{1}H-NMR of 2,5-dibromobenzoic acid in CD_2Cl_2

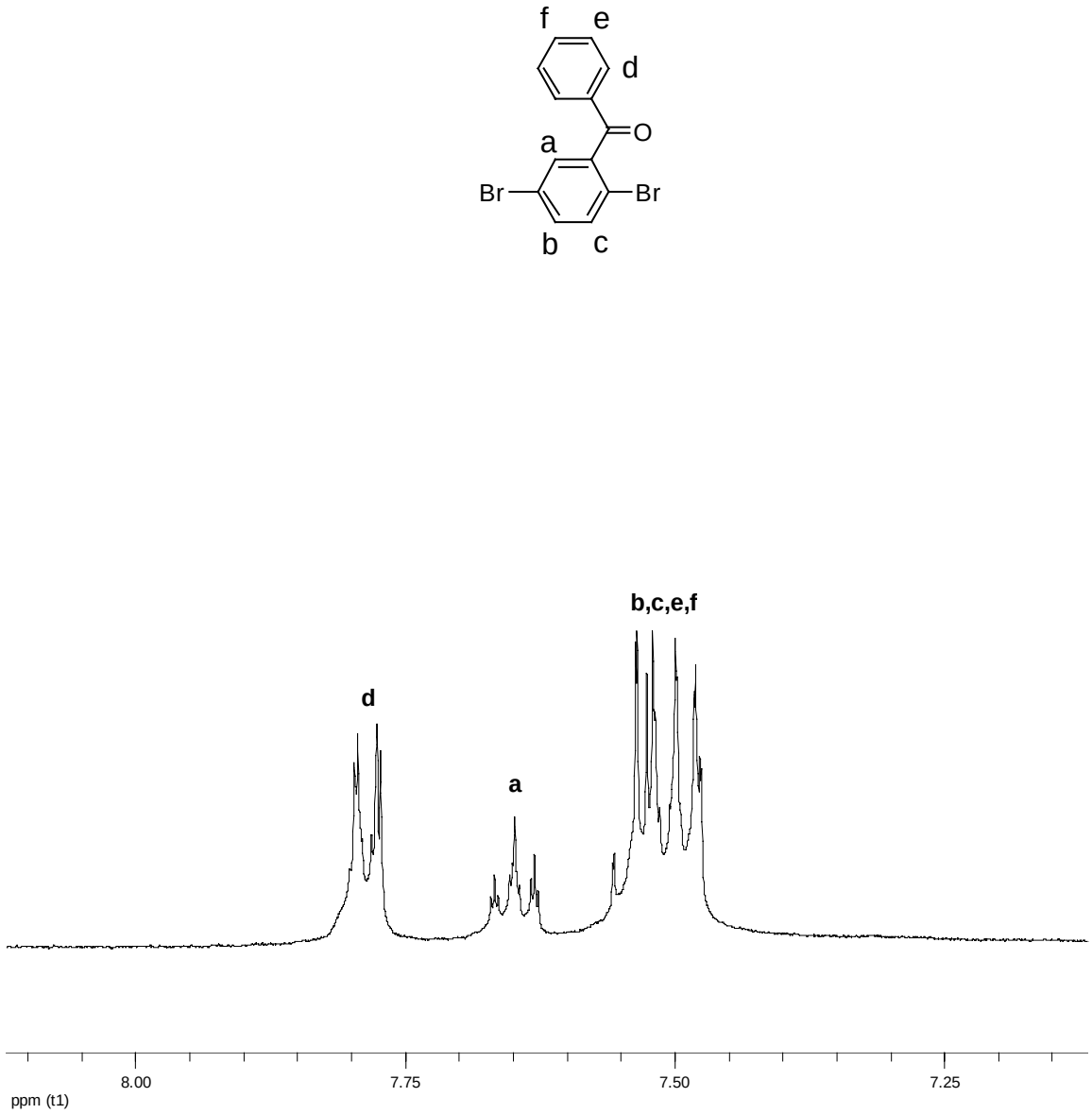

^{1}H-NMR of 2,5-dibromobenzophenone in CD_2Cl_2

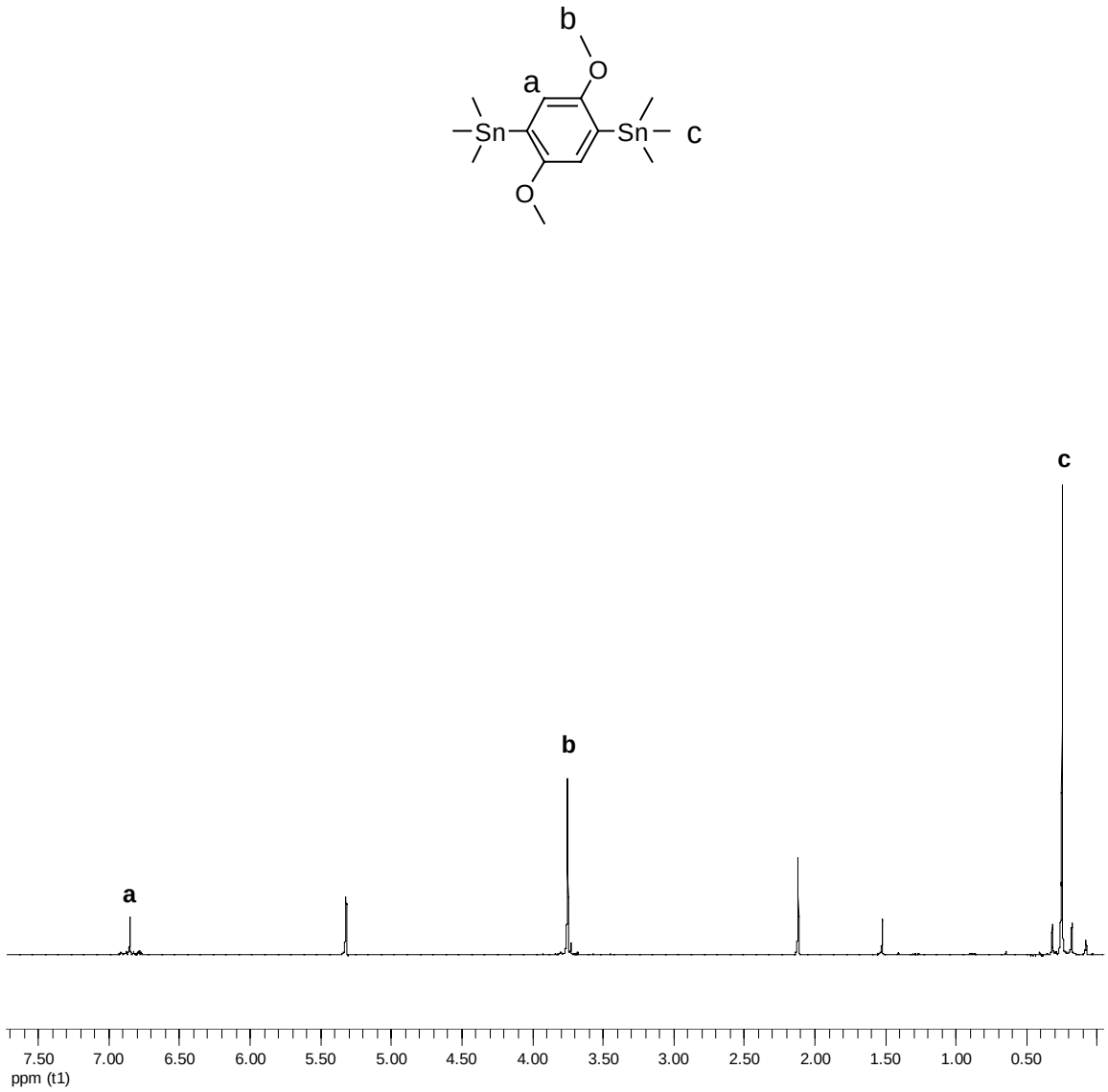

^{1}H-NMR of 1,4-Bis-trimethylstannanyl-2,5-dimethoxybenzene in CD_2Cl_2

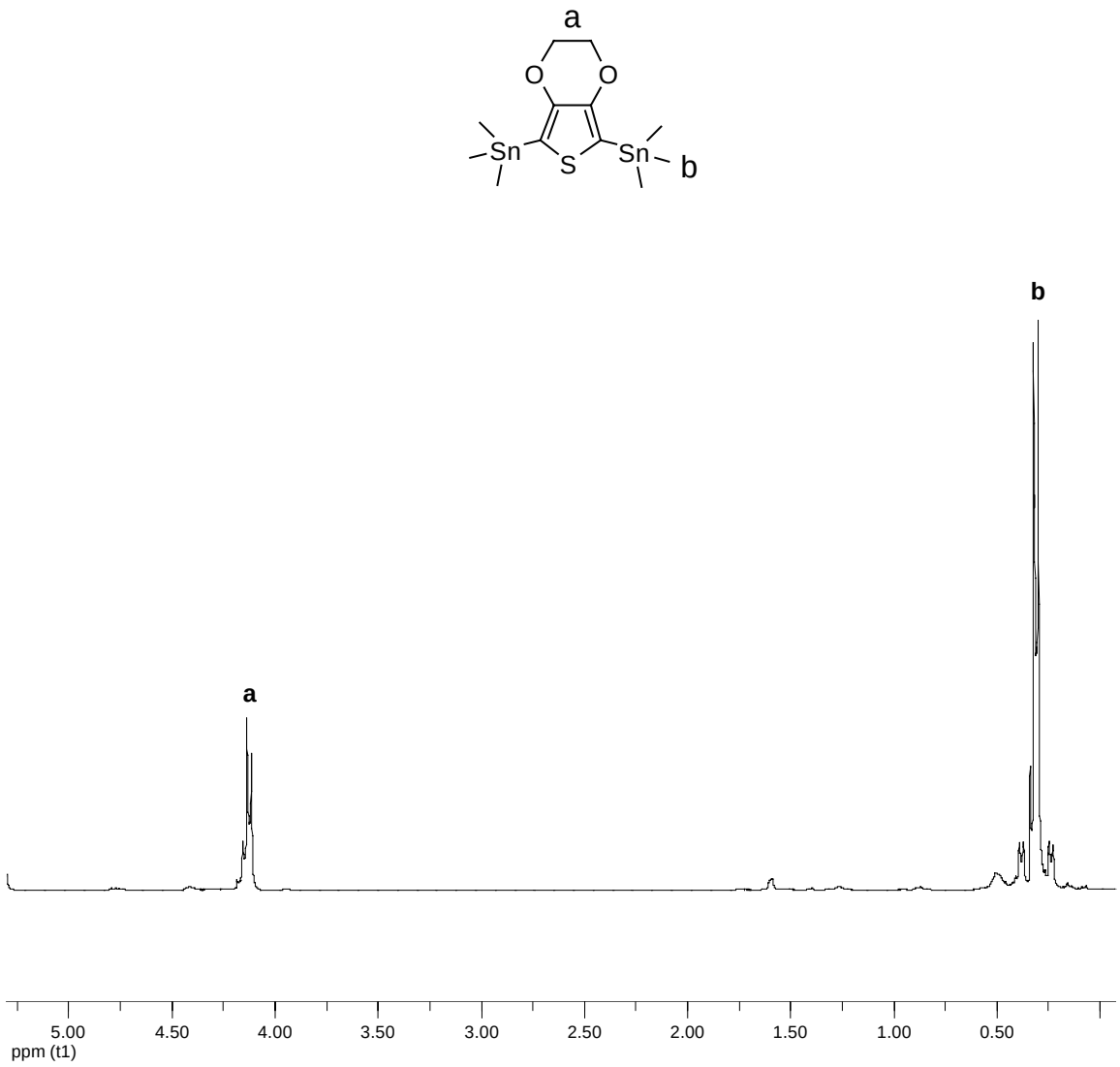

^{1}H-NMR of 2,5-bis-trimethylstannanyl-3,4-ethylenedioxythiophene in CD_2Cl_2

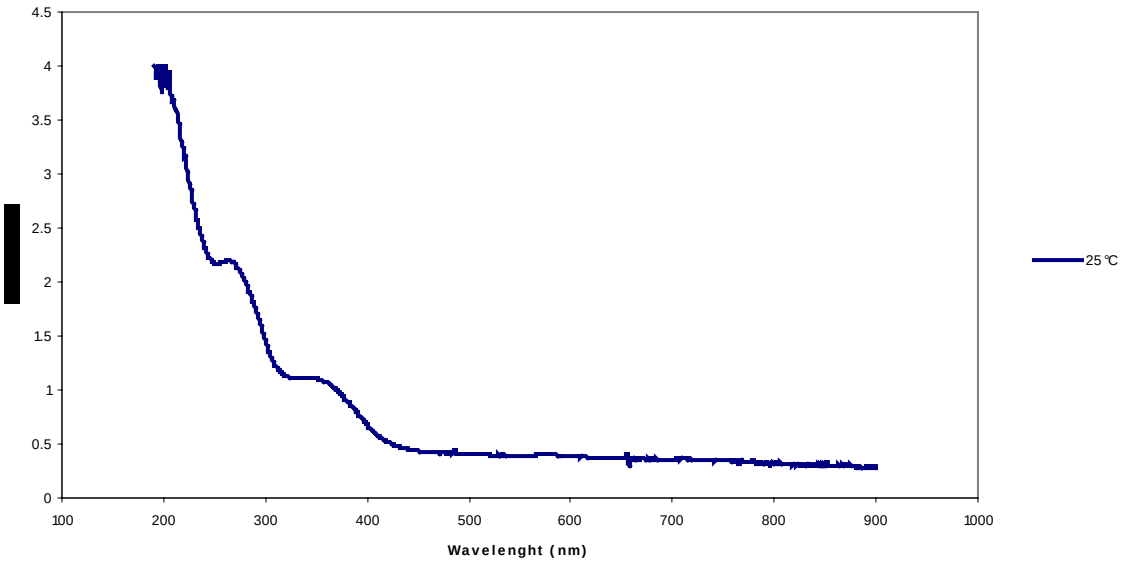

UV-vis spectrum for unannealed **PI**

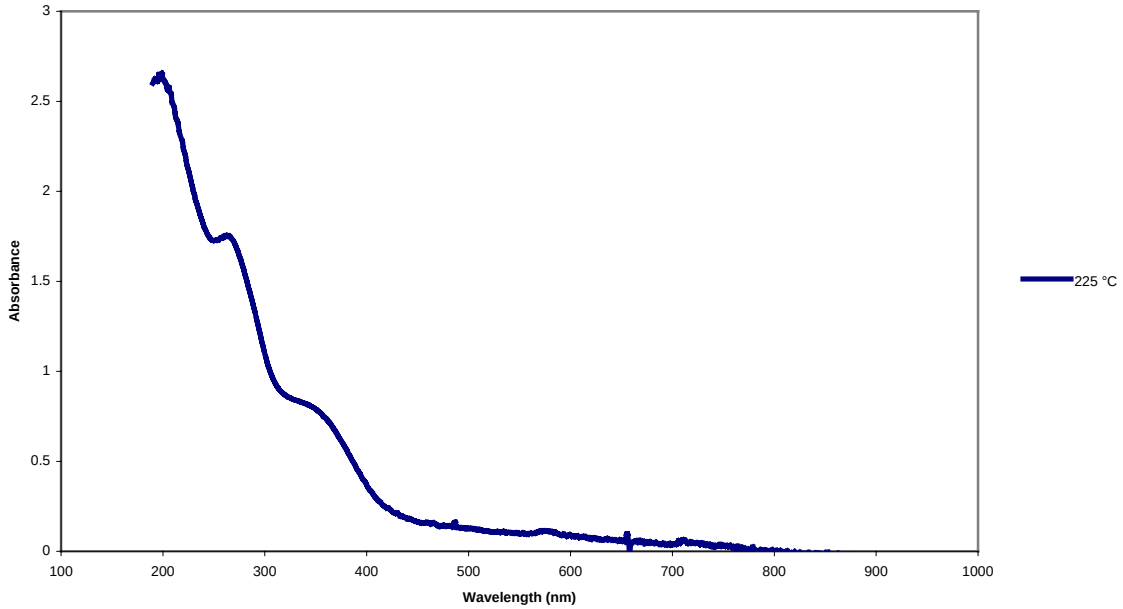

UV-vis spectrum for **PI** annealed at 225 °C

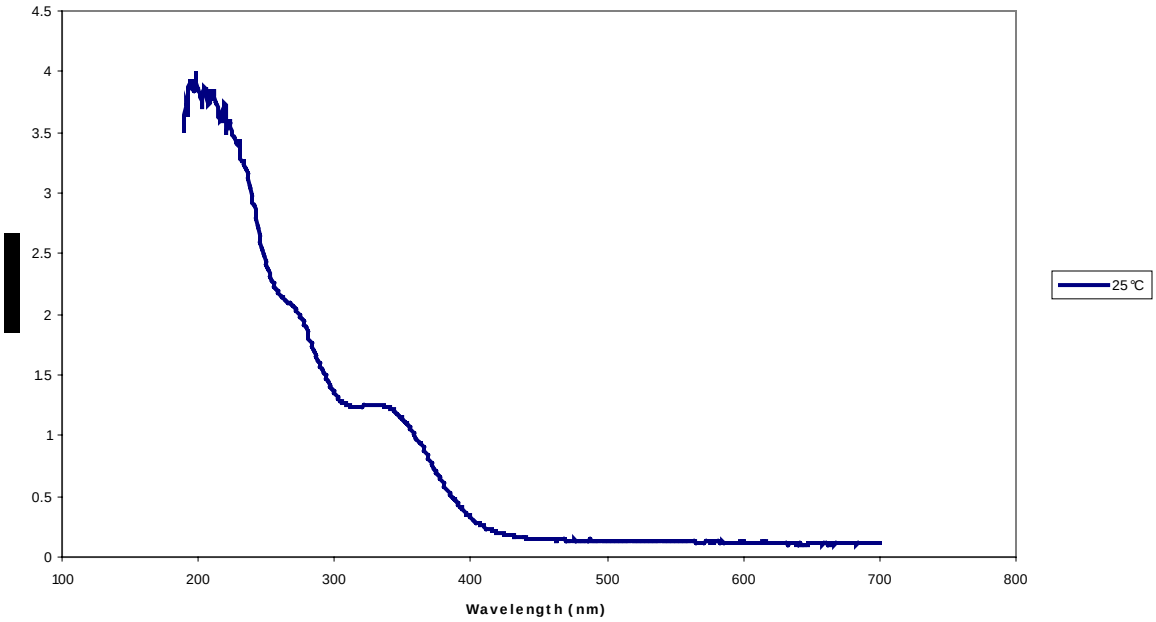

UV-vis spectrum for unannealed **PII**

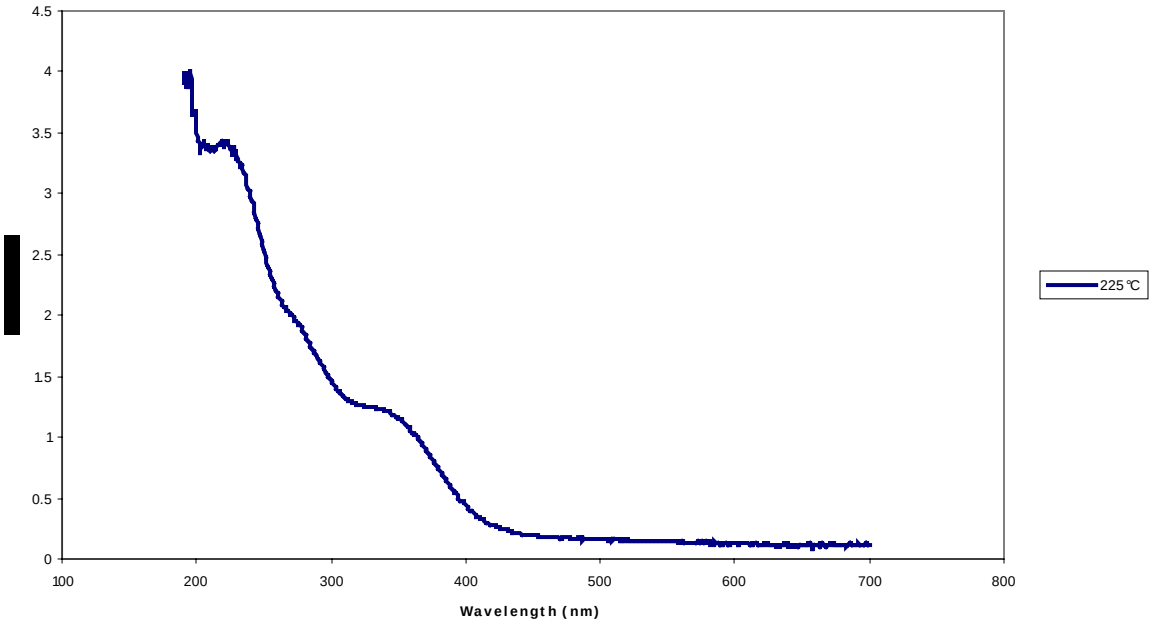

UV-vis spectrum for **PII** annealed at 225 °C

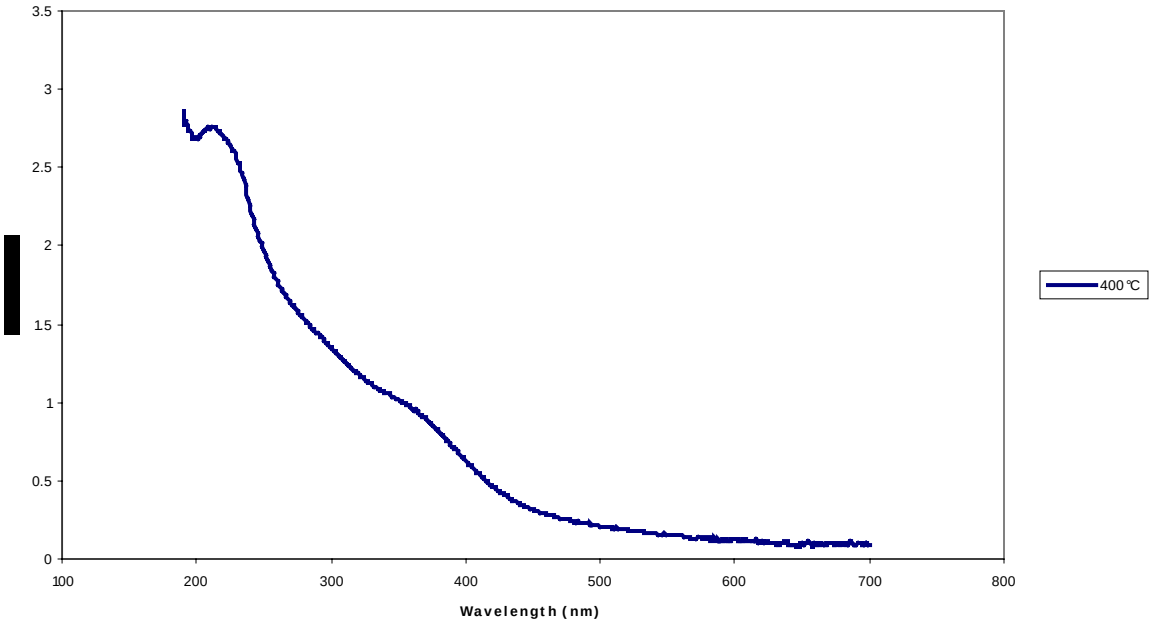

UV-vis spectrum for **PII** annealed at 400 °C

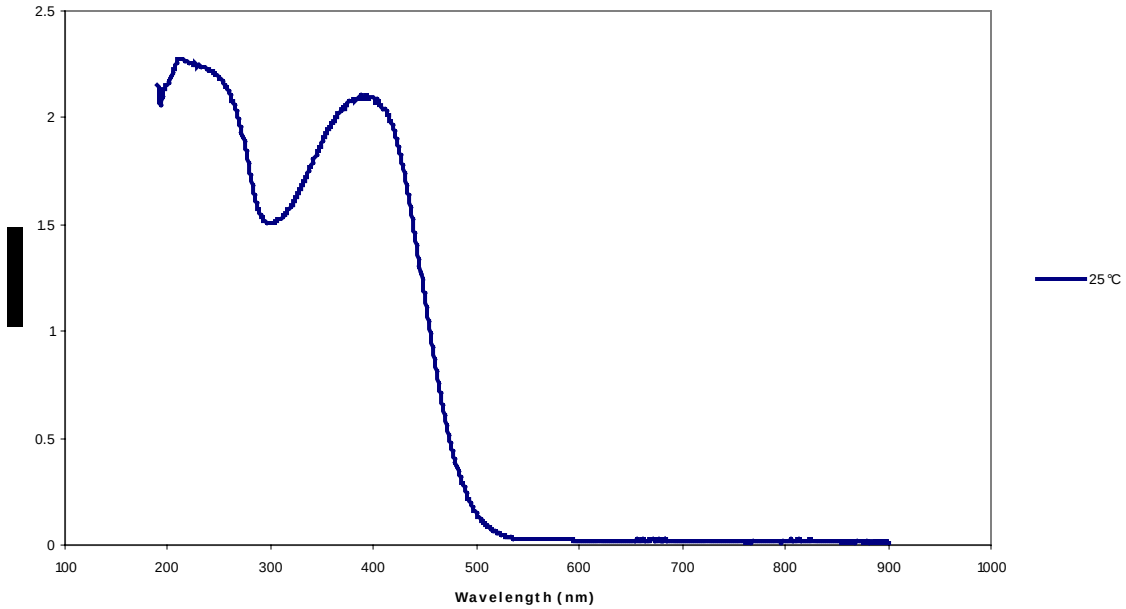

UV-vis spectrum for unannealed **PIII**

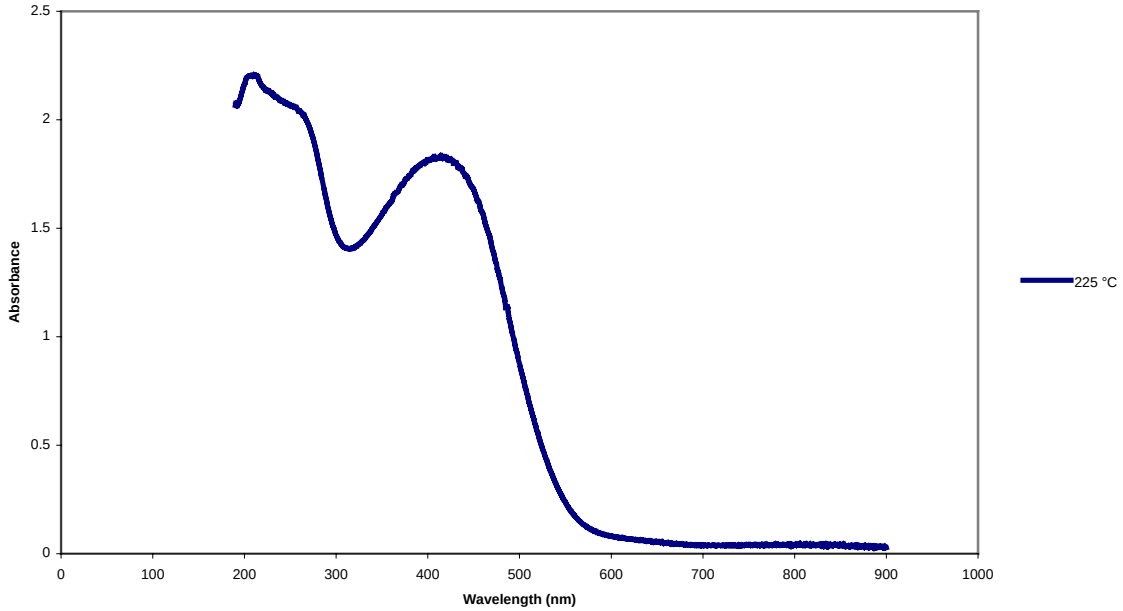

UV-vis spectrum for **PIII** annealed at 225 °C

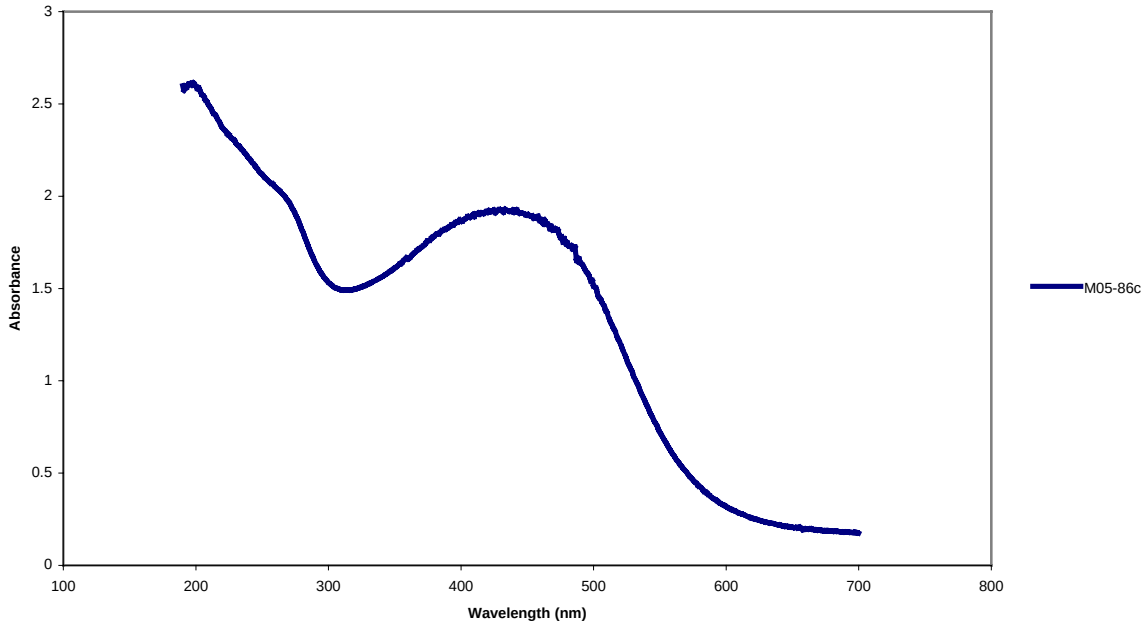

UV-vis spectrum for **PIII** annealed at 300 °C

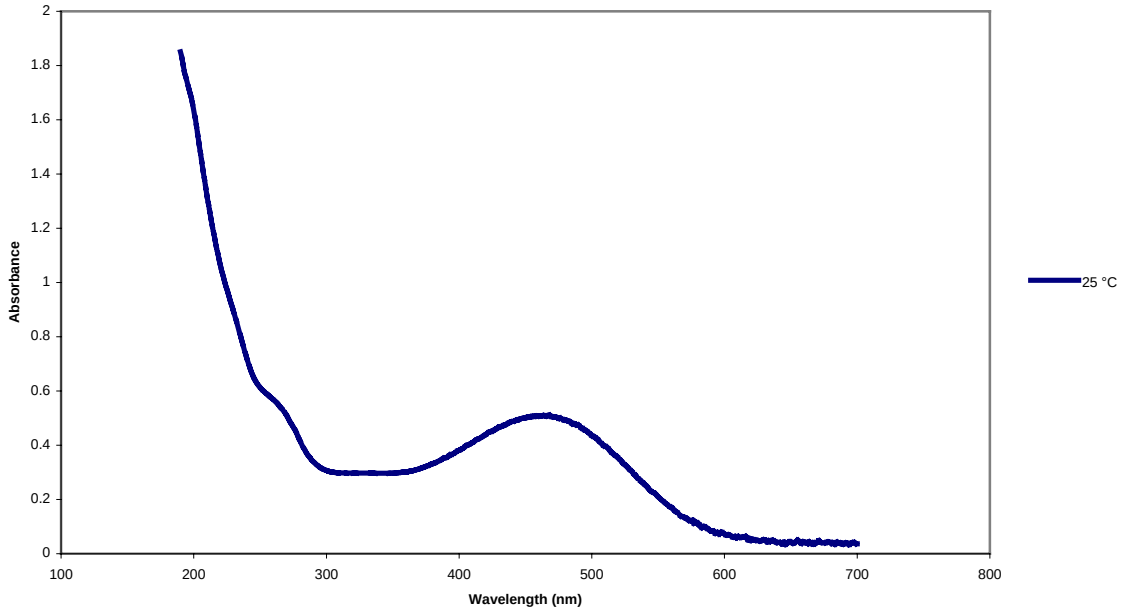

UV-vis spectrum for unannealed **PIV**

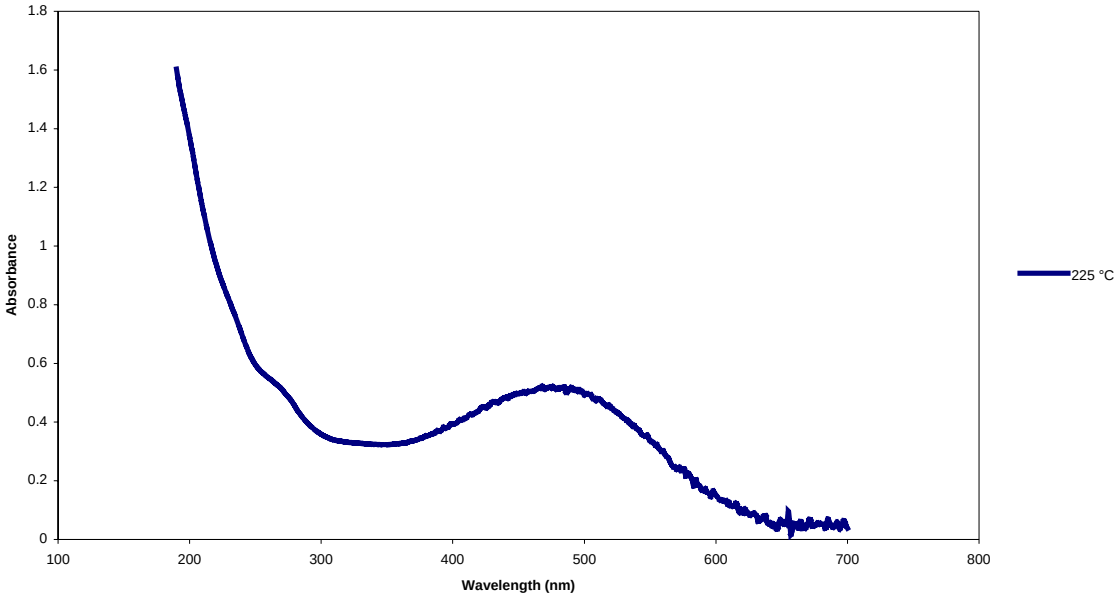

UV-vis spectrum for **PIV** annealed at 225 °C

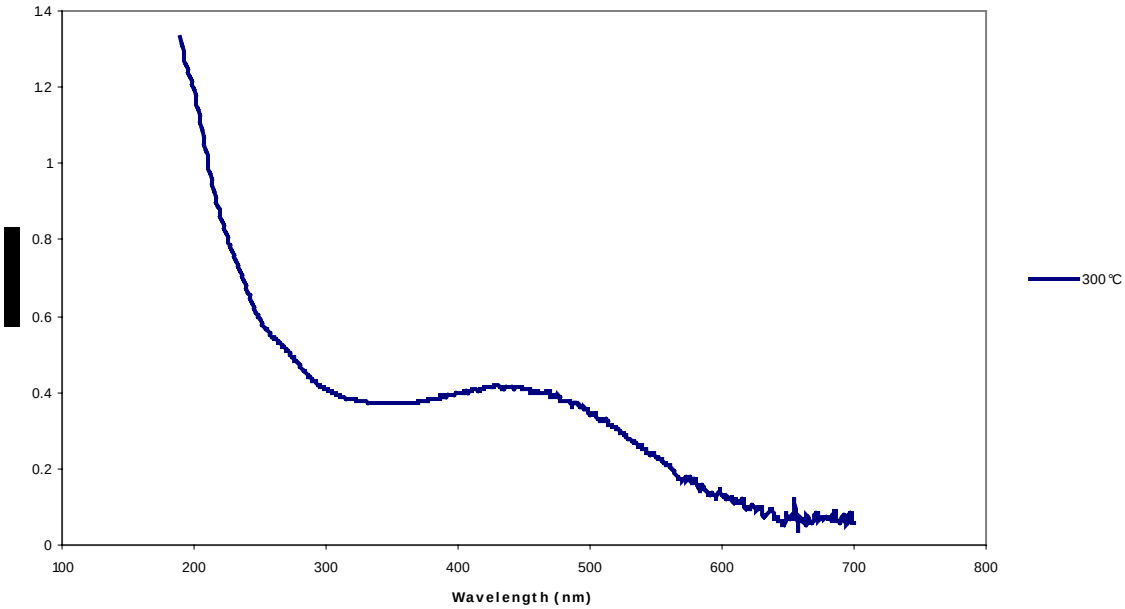

UV-vis spectrum for **PIV** annealed at 300 °C

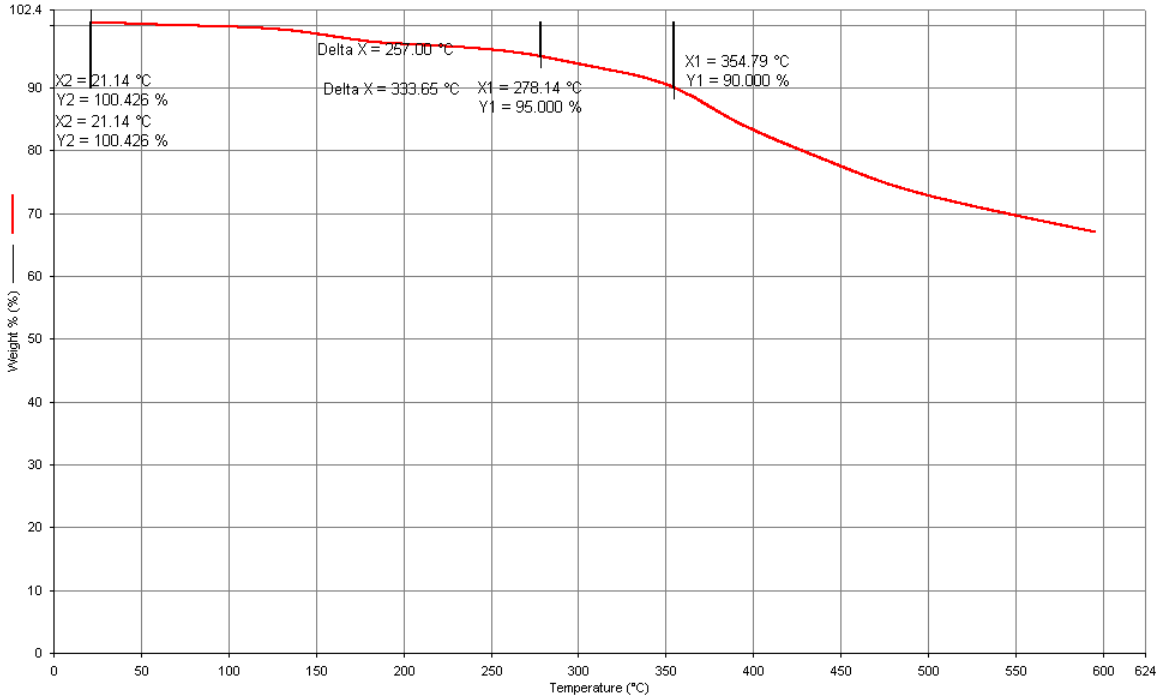

TGA curve for **PI**

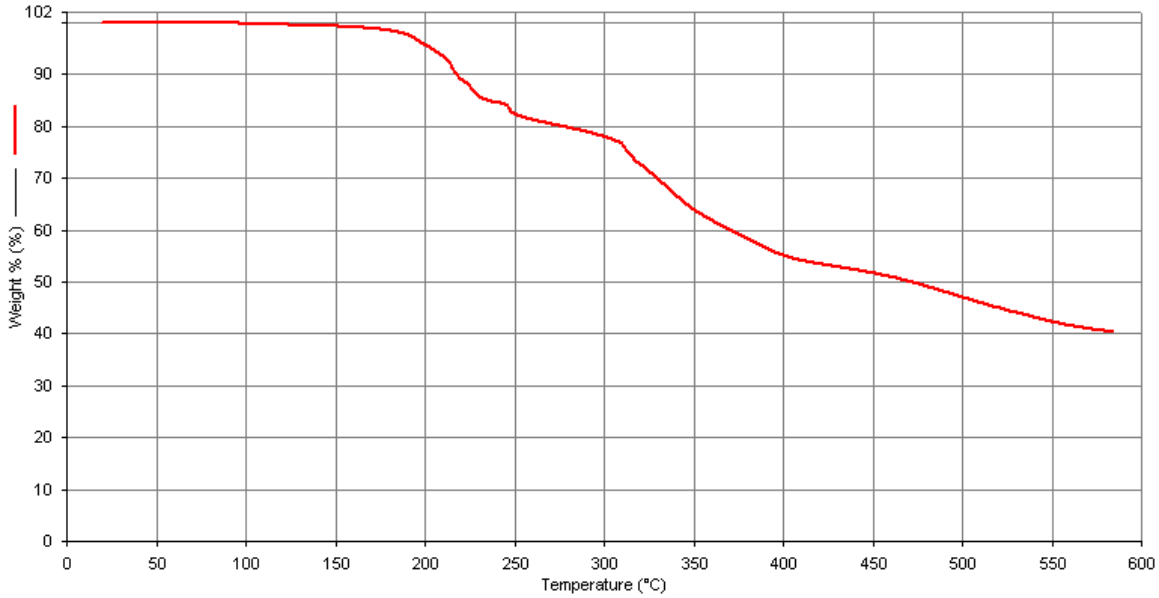

TGA curve for **PII**

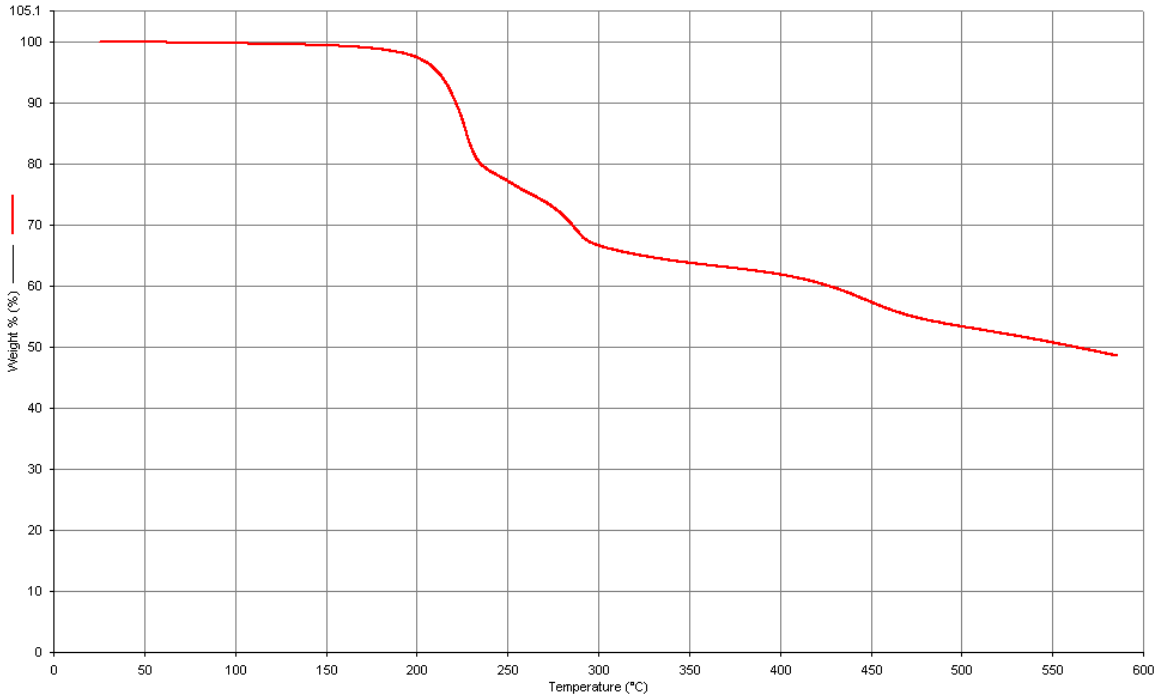

TGA curve for **PIII**

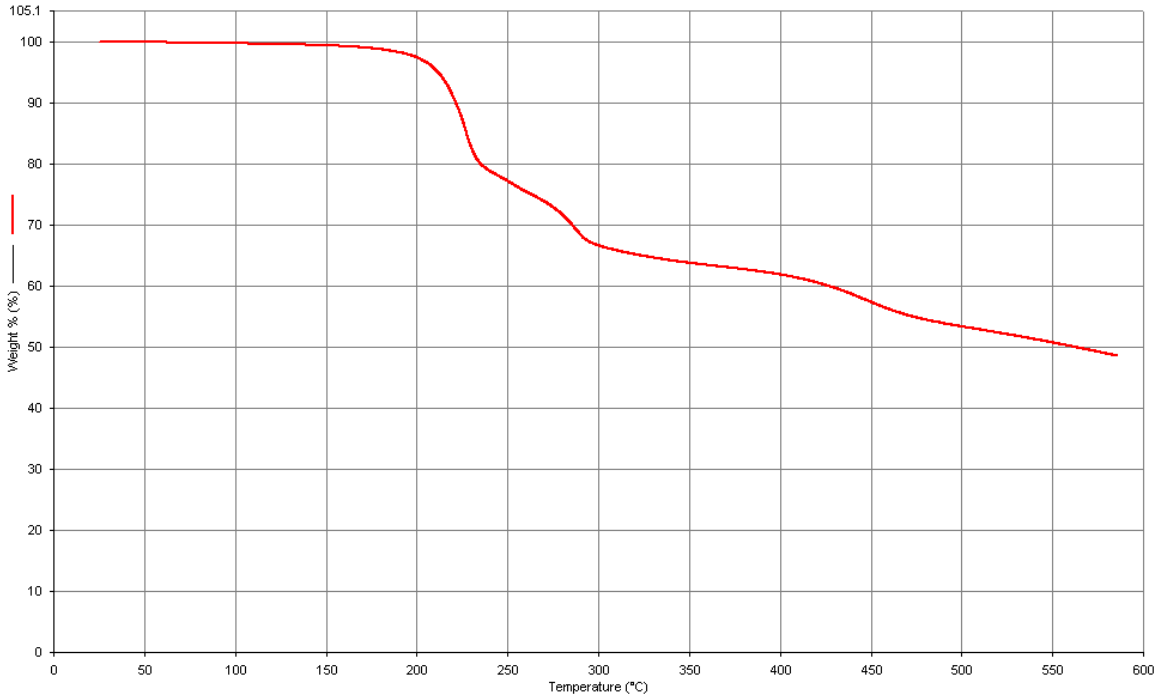

TGA curve for **PIV**

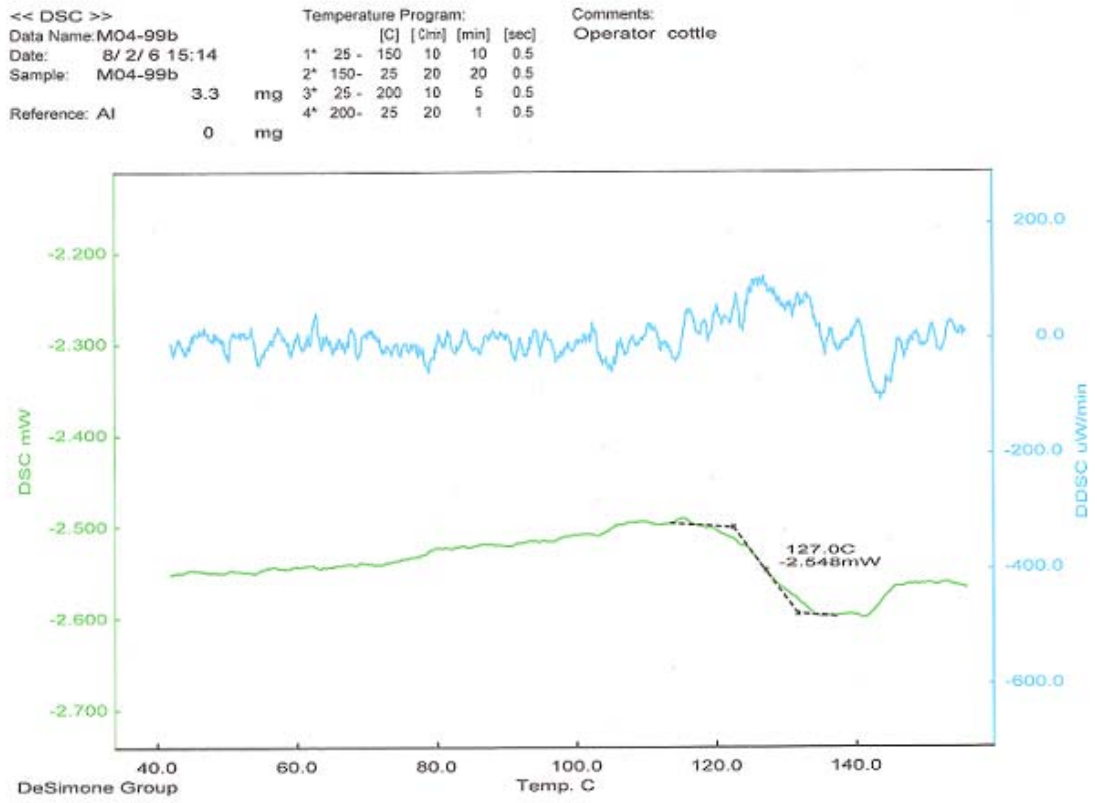

DSC curve for **PI**

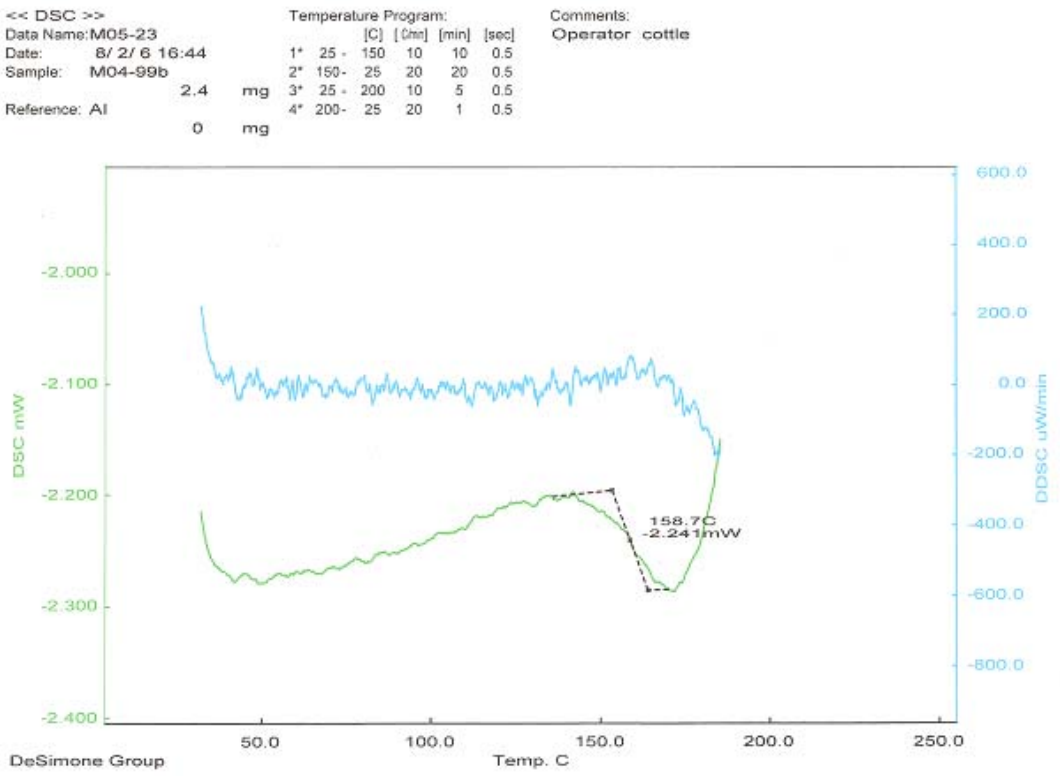

DSC curve for **PII**

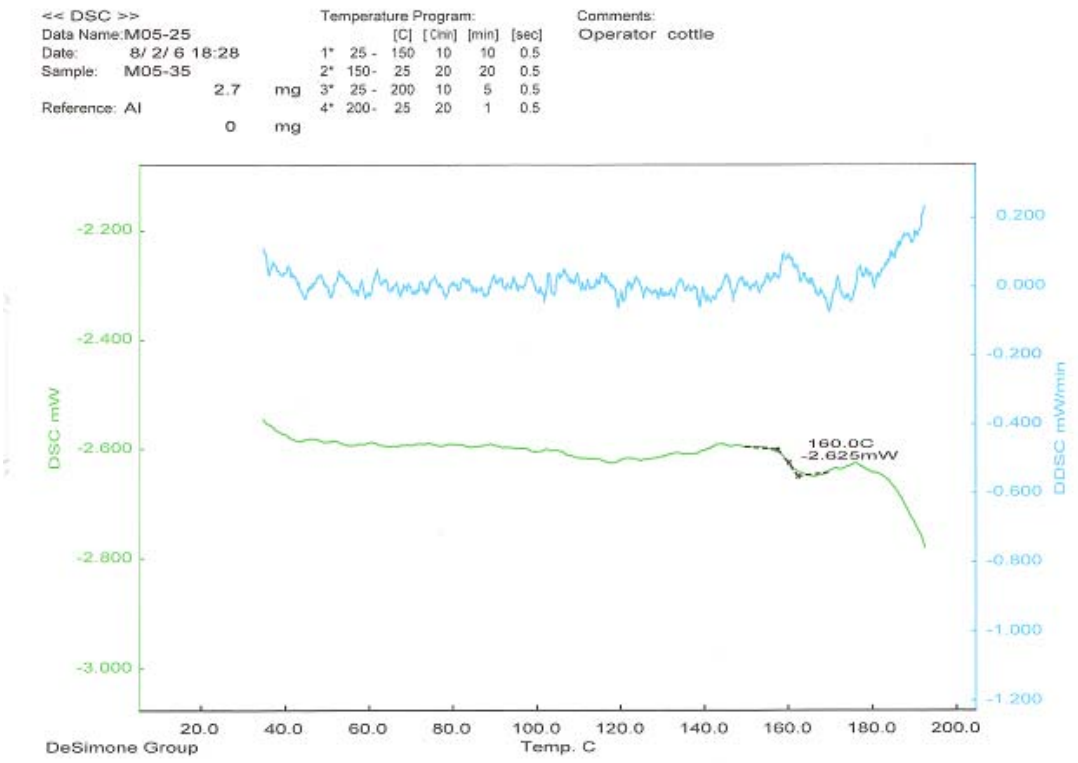

DSC curve for **PIII**

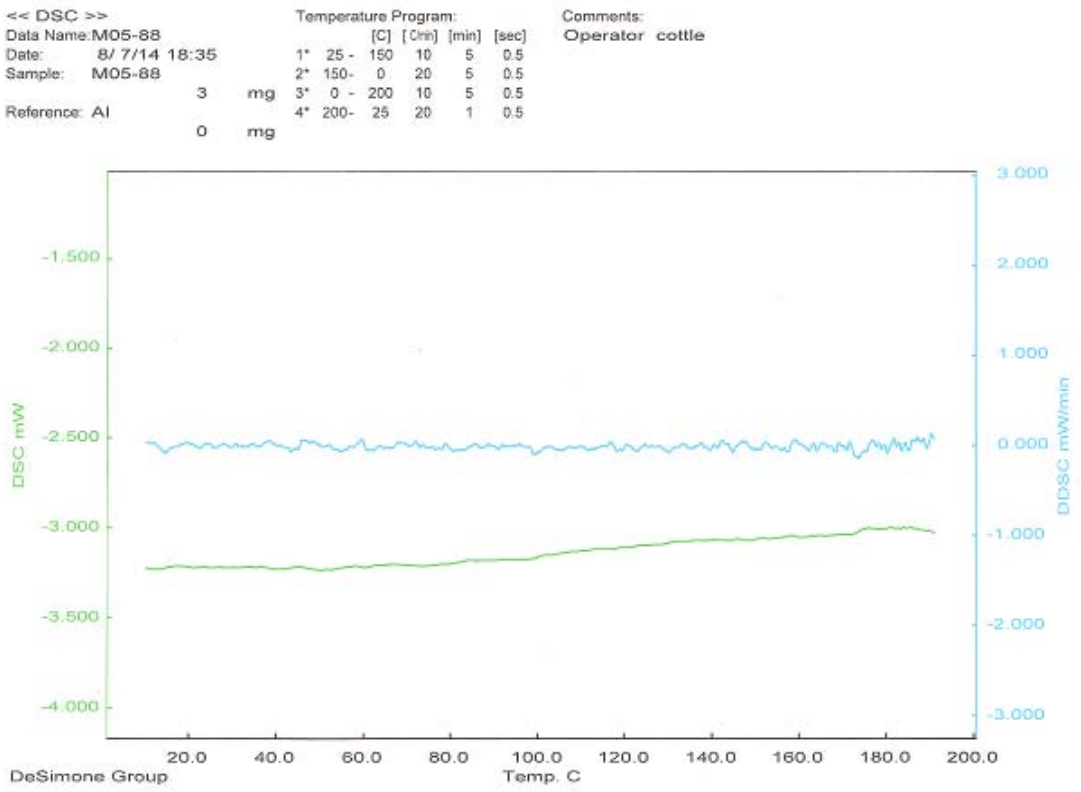

DSC curve for **PIV**

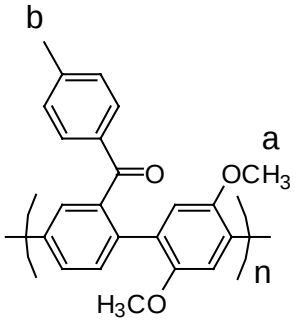

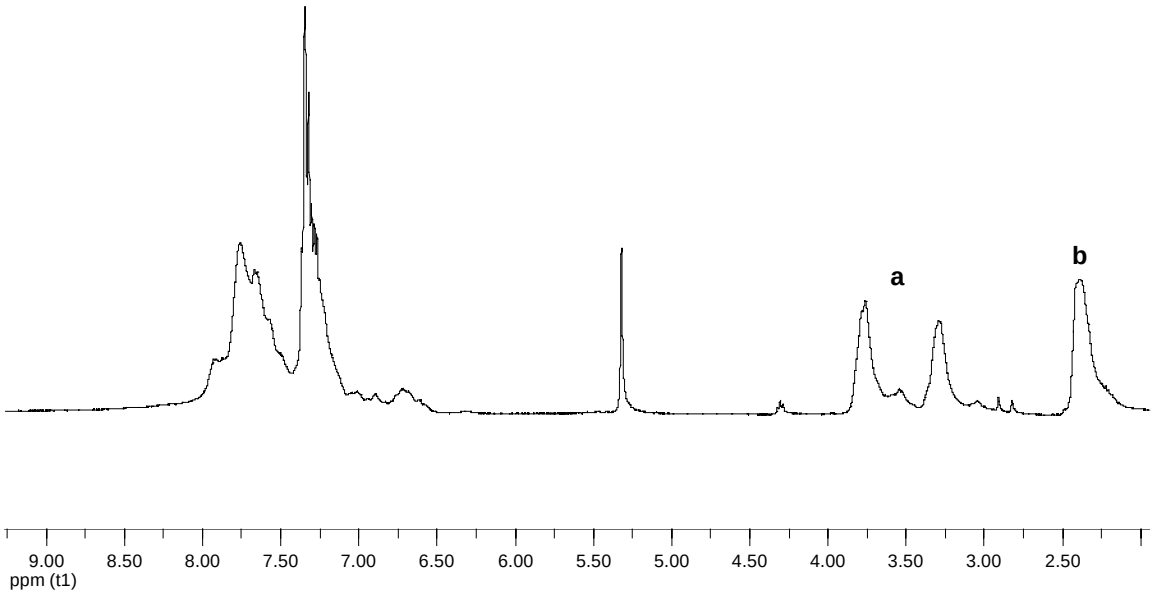

^{1}H-NMR of **PI** in CD_2Cl_2

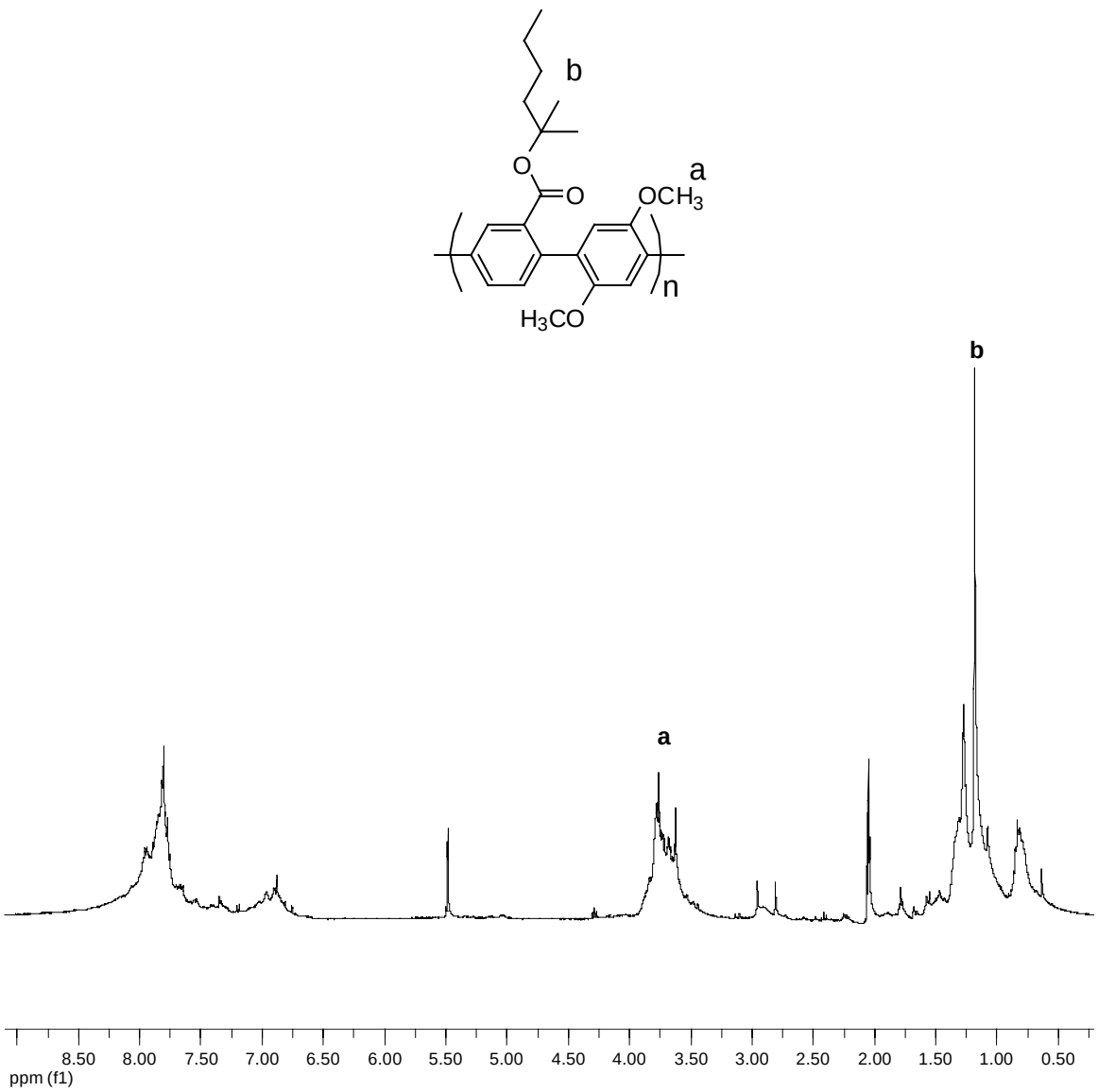

^{1}H-NMR of **PII** in CD_2Cl_2 and acetone-d_6

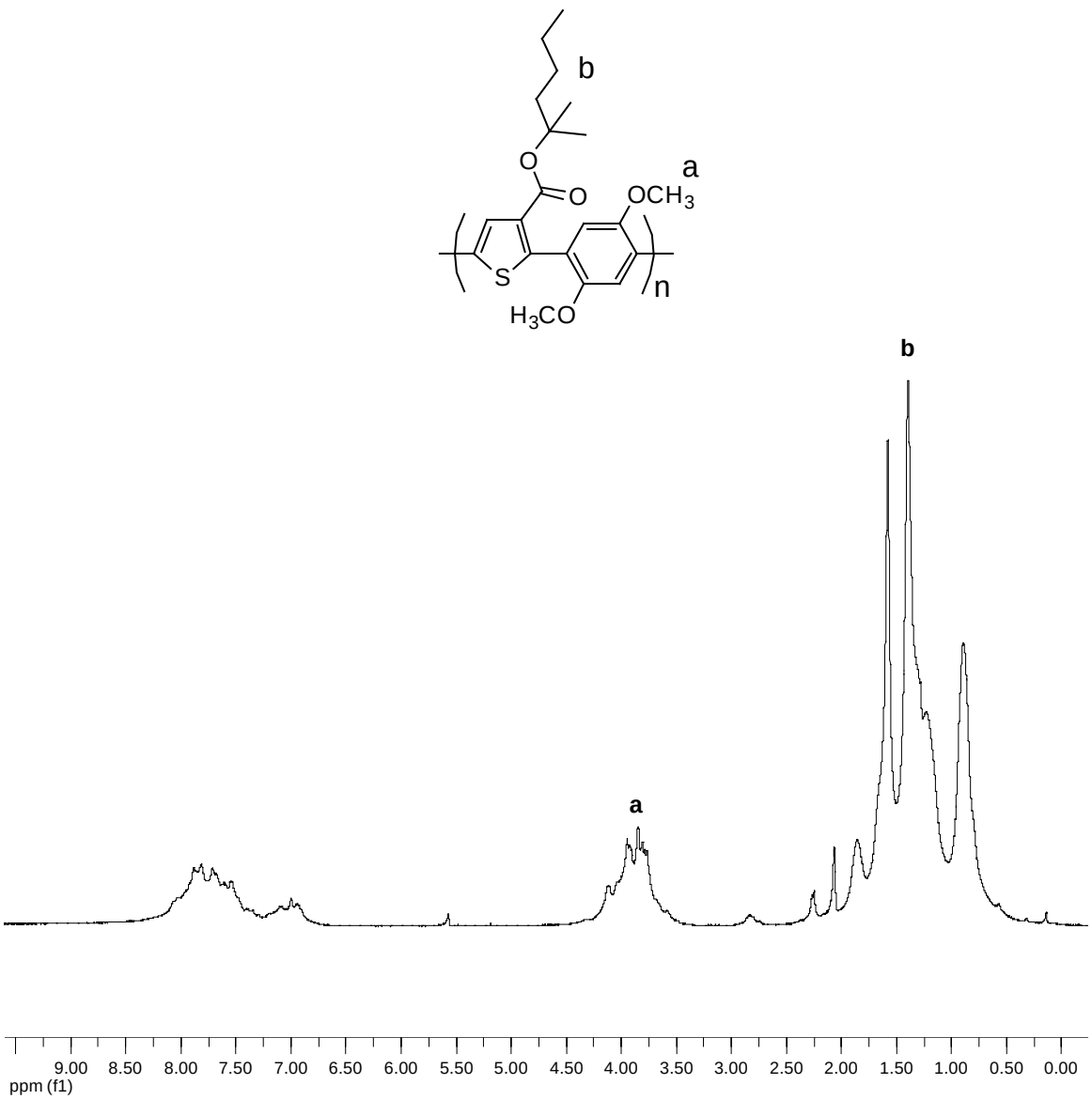

^{1}H-NMR of **PIII** in CD_2Cl_2 and acetone-d_6

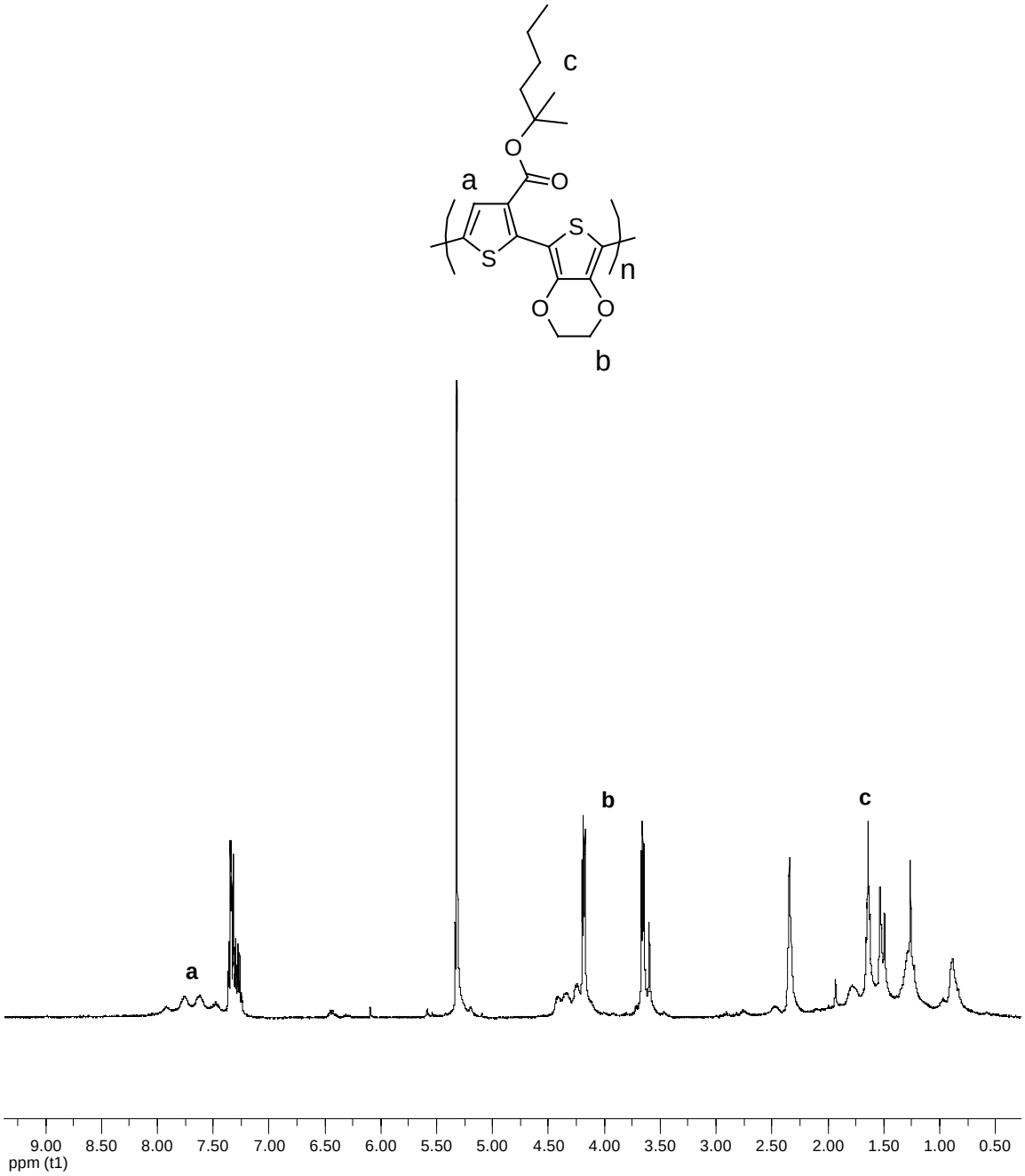

^{1}H-NMR of **PIV** in CD_2Cl_2